University of Canterbury

Master's Thesis

Controlled Damage Rocking Systems for Accelerated Bridge Construction

Author:
Samuel White

Supervisor:
Dr. Alessandro Palermo

Co-supervisor: Dr. Allan Scott

A thesis submitted in fulfilment of the requirements for the degree of Master of Engineering

in the

Department of Civil and Natural Resource Engineering

March 2014

UNIVERSITY OF CANTERBURY

Abstract

College of Engineering
Department of Civil and Natural Resource Engineering

Master of Engineering

Controlled Damage Rocking Systems for Accelerated Bridge Construction

by Samuel White

Bridge substructures are generally constructed using cast-in-place concrete and designed to undergo inelastic deformation in earthquake events. Although this construction approach has proven to be economical and provides adequate seismic performance through the formation of ductile plastic hinges, there are downsides relating to construction speed and quality, and post-earthquake repairability.

This thesis explores two categories of Accelerated Bridge Construction (ABC) connection types, which use precast concrete instead of cast-in-place concrete to offer advantages including increased construction speed and quality. High Damage (HD) ABC connection types emulate the seismic behaviour of cast-in-place construction through the formation of ductile plastic hinges.

Controlled Damage (CD) ABC connection types use unbonded post-tensioned precast connections to offer additional advantages including reduced residual drifts, limited and controlled damage and simple repair options. Novel buckling-restrained, fused mild steel energy dissipators suitable for use in CD connections are also developed and tested. These designs utilise 'dry' fabrication to simplify the fabrication process and minimise cost.

Half-scale experimental testing is carried out to demonstrate both the assembly processes and behaviour under reversed cyclic uniaxial and biaxial loading representing an earthquake event. Following benchmark testing, repair strategies are applied to the CD connection types and the columns are tested again, representing a subsequent earthquake event. Good results are obtained from all cases with relatively straightforward construction and repair processes. With further developments and testing, the connection types proposed can provide competitive alternatives to conventional bridge pier design with regard to seismic performance and life cycle costs, with the additional benefits associated with precast construction.

Acknowledgements

I first wish to thank my primary supervisor, Dr. Alessandro Palermo. His enthusiasm, extensive knowledge, creative ideas and constant support and encouragement throughout both my undergraduate and postgraduate studies is greatly appreciated and has made this research what it is.

I also would like to acknowledge and thank my co-supervisor Dr. Allan Scott for his technical support throughout the project.

Thanks to all members of the Canterbury bridge team for their support and companionship. In particular, I would like to greatly thank Mustafa Mashal. He has provided assistance throughout this research in its entirety, and was a primary contributor to the testing of the High Damage specimens.

Many challenges were encountered during experimental testing throughout this research and without the technical support, patience and unique sense of humour of the lab technicians, in particular Gavin Keats and Russell McConchie, these challenges would not have been overcome.

I wish to acknowledge also the New Zealand Natural Hazards Research Platform (NHRP) who provided funding for this project as part of the wider research programme titled Advanced Bridge Construction and Design (ABCD) co-ordinated by Dr. Alessandro Palermo at the University of Canterbury. I would also like to thank Ancon Building Products and Fletcher Reinforcement for providing reinforcement, anchorage and coupling products for the research.

Finally, I am immensely appreciative of the continuous support and encouragement provided by my friends and family throughout all of my studies.

Contents

List of Figures

List of Tables

Abbreviations

ABC	**A**ccelerated **B**ridge **C**onstruction
ABCD	**A**dvanced **B**ridge **C**onstruction and **D**esign
ADRS	**A**cceleration-**D**isplacement **R**esponse **S**pectrum
BRB	**B**uckling-**R**estrained **B**race
BRF	**B**uckling-**R**estrained **F**used
CBC	**C**oupled **B**ar **C**onnection
CD	**C**ontrolled **D**amage
CDC	**C**ontrolled **D**amage **C**ircular (test column)
CDS	**C**ontrolled **D**amage **S**quare (test column)
DCR	**D**issipative **C**ontrolled **R**ocking
FRP	**F**ibre **R**einforced **P**olymer
GDC	**G**routed **D**uct **C**onnection
HD	**H**igh **D**amage
HDC	**H**igh **D**amage **C**ircular (test column)
HDS	**H**igh **D**amage **S**quare (test column)
LD	**L**ow **D**amage
MCE	**M**aximum **C**onsidered **E**earthquake
MSC	**M**ember **S**ocket **C**onnection
PRESSS	**PRE**cast **S**eismic **S**tructural **S**ystem
SLS	**S**erviceability **L**imit **S**tate
ULS	**U**ltimate **L**imit **S**tate

Chapter 1

Introduction and Scope

1.1 Introduction

Bridge substructures have historically been constructed using cast-in-place concrete. Although this construction approach has proven to be effective at achieving the base goal of achieving life safety and collapse prevention of the structure in severe earthquake events, there are downsides with this approach relating to construction speed and quality, and post-earthquake repairability.

Current seismic design codes accept ductile, inelastic behaviour of structures when subjected to design level earthquakes. When using conventional monolithic construction, this results in the formation of ductile plastic hinges in reinforced concrete elements in a design level earthquake. While this design philosophy is economical and prevents collapse of the structure, it can result in significant levels of damage which lead to high repair costs and possible closure of the structure following earthquake events. Interruption of the operation of bridge structures, especially those located on state highways, can impact significantly on both regular commuters and the freight industry leading to economic losses [NZ Transport Agency, 2010].

Expectations of the public, industry and infrastructure owners regarding the seismic resilience of structures are changing. There is a move towards low damage technologies to minimise repair costs and downtime and rapid construction techniques to minimise the disturbance associated with the construction of new structures.

This thesis explores HD and CD connections for precast bridge substructures. HD connection types emulate the behaviour of conventional construction systems through the formation of ductile plastic hinges during severe earthquake events. This plastic hinging involves spalling of concrete and yielding (and potentially buckling or rupture) of internal reinforcement, hence the name 'High Damage'. CD connection types limit and control damage in the connection, with simple repair strategies developed to quickly repair any damage that does occur, hence the name 'Controlled Damage'. The solutions presented in this research are the HD Grouted Duct Connection, the HD Member Socket Connection, the CD Member Socket Connection and the CD Coupled Bar Connection.

These solutions build upon the concepts of Accelerated Bridge Construction (ABC) [Billington et al., 1999, Marsh et al., 2011] and Dissipative Controlled Rocking (DCR) [Palermo, 2004; Palermo et al. 2005, 2007, 2008 and Marriott, 2009] to form precast connection types which offer advantages over conventional construction methods. These advantages include increased construction speed, reduced damage and residual drifts during earthquake events and simple repair strategies, while being competitive with conventional systems when considering life cycle costs.

1.2 Research Motivation

The essential goal of bridges is to provide passage over obstacles. This passage may be for pedestrians, motor vehicles, or even boats. The obstacle may be any number of things - including land, waterways, roads, train lines or buildings. Any disruption to this service means the bridge is no longer achieving the goal it was designed for with varying degrees of consequence. There are a number of causes of disruption including construction or replacement of the bridge, maintenance or improving of the bridge, repair of the bridge following an earthquake, and finally deconstruction of the bridge at the end of its service life. Minimising these disruptions through improving construction speed, reducing maintenance requirements, reducing the need for repair or increasing repair speed, and increasing the service life of the bridge all contribute to maximising the service of the bridge, while minimising life cycle costs of the structure.

Conventional cast-in-place methods have proven themselves to be economical when it comes to initial construction cost however are relatively time consuming to erect and can

be difficult to repair following a significant earthquake event. This is due to the connections in cast-in-place undergoing significant inelastic deformation resulting in spalling of concrete in the plastic hinge region, along with yielding, buckling or fracture of reinforcing bars [Kawashima, 2000, Priestley et al., 1996]. Also, the bridge is often left with residual drifts following an earthquake event offering further difficulties with the repair of the structure. Residual drifts also have a significant effect of the immediate use of bridge structures following earthquake events [Christopoulos et al., 2002, Kawashima et al., 1998, Lee and Billington, 2011, Mackie and Stojadinovic, 2004, Pampanin et al., 2003]. Quality control can also be an issue with cast-in-place structures as the casting of concrete occurs on-site where the casting environment is less controlled than in precast construction. This can lead to poorer material quality leading to increased levels of required maintenance throughout the life of the bridge. These factors all lead to increased construction time and maintenance requirements, along with increased costs and downtime associated with repair.

Accelerated Bridge Construction (ABC) involves the use of precast concrete instead of cast-in-place concrete for construction of bridge superstructures and substructures. This addresses some of the issues of conventional construction through increasing construction speed and quality which in turn reduce construction and maintenance costs which is a step in the right direction. However, ABC connections are generally designed to emulate the behaviour of conventional monolithic construction. This means that concrete spalling, yielding of reinforcing bars and residual drifts in the structure can be expected during a design level seismic event when ABC is applied to bridge substructure systems.

One alternative to emulation of conventional behaviour is the use of Dissipative Controlled Rocking (DCR) or Hybrid PRESSS connections [Palermo, 2004; Palermo et al. 2005, 2007, 2008 and Marriott, 2009]. The DCR solution features a jointed connection that combines post-tensioning components to recenter the structure with easily replaceable energy dissipation devices. Typically, these types of connections are designed to achieve low or no damage to concrete components, with repair involving replacement of external energy dissipators.

This type of connection is well suited to the concepts of ABC processes resulting in increased construction speed and quality with simple repair options and little of no

residual drift, minimising the downtime to serviceability of the bridge. The main downside to Low Damage DCR connections is the initial construction cost, with the need for fabrication of external dissipators, provisions for mounting of dissipators and armouring of precast components.

In many cases, it is unlikely that repair of a bridge structure will be required during its life, making it hard for infrastructure owners to justify the increased construction costs associated with low damage technologies. They understand however, that the consequences of a significant earthquake event can be severe, including significant downtime in the serviceability of bridge structures along with the need for costly repair or replacement of the bridge. This risk can be quantified using loss modelling, which has been researched extensively with notable contributions from Bradley et al. [2010], Christopoulos et al. [2003], Dhakal and Mander [2006], Lee and Billington [2011], Mander et al. [2007], Marriott et al. [2009], Pampanin et al. [2003], Solberg et al. [2008], Uma et al. [2006, 2010]. A balance between initial construction costs, probability of bridge damage in its lifetime, consequences of bridge damage and downtime, and cost and downtime associated with repair or replacement of bridge structures needs to found.

This purpose of this research is to develop Controlled Damage connection types which offer a compromise between the relatively low initial costs of ABC High Damage (HD) and monolithic solutions, and the ease of repair of Low Damage (LD) rocking systems. This is illustrated in Table 1.1 where a qualitative comparison of the systems is made. Red colour indicates a high value, orange indicates a moderate value and green indicates a low value.

To achieve relatively low initial construction costs, CD connections will generally feature conventional reinforcing as the energy dissipation component of the connection. Unlike the low damage DCR solution, some damage to the connection is permitted during earthquake loading, however this damage is controlled meaning it is limited and constrained to certain regions of the structure with little or no residual drifts present. Peak strains in the energy dissipation system are also controlled through debonding or necking of energy dissipation components. Specific repair strategies are developed at the design stage of each connection type, and appropriate detailing is provided to allow for straightforward application of the repair strategy following damage due to lateral

loading, reinstating strength and ductility to the connection. This significantly reduces the repair cost and downtime of the structure.

		Low	Moderate	High
Monolithic	Material / Fabrication Cost			
	Construction Time			
	Repair Cost and Time			
ABC High Damage	Material / Fabrication Cost			
	Construction Time			
	Repair Cost and Time			
ABC Controlled Damage	Material / Fabrication Cost			
	Construction Time			
	Repair Cost and Time			
ABC Low Damage	Material / Fabrication Cost			
	Construction Time			
	Repair Cost and Time			

Table 1.1: Comparison of connection types

1.3 Scope and Objectives

The main objective of this research is to develop Controlled Damage (CD) bridge pier systems based on the concepts of Dissipative Controlled Rocking (DCR) with rapid construction methodologies based on ABC concepts. Biaxial performance of CD systems under lateral loading will be investigated. Construction and repair methods of CD systems will be developed and demonstrated, with the effectiveness of the repair demonstrated through experimental testing. New types of buckling restrained dissipator will also be developed and tested which are suitable for use in CD connection types.

The specific objectives of this research are as follows:

Objective 1

Development and Testing of High Damage (HD) Pier Systems

Chapter 4

- Explore existing precast connection types that are designed to emulate the behaviour of conventional methods of construction.
- Demonstrate the design, detailing and construction processes for precast bridge substructures using a selection of HD connection types in a half scale bridge pier.
- Test the performance of the HD connections under both uniaxial and biaxial loading regimes.

Objective 2

Development and Testing of Controlled Damage (CD) Pier Systems

Chapter 5

- Develop CD connection types and repair strategies that provide better performance than High Damage connections with straightforward, pre-determined methods of repair.
- Demonstrate the design, detailing and construction processes for precast bridge substructures using a selection of CD connection types in a half scale bridge pier.
- Demonstrate application of repair strategies for each connection type.
- Test the performance of the connections both before and after repair using the performance of HD connection types as a benchmark.
- Compare the performance of the CD solutions with that of the HD solutions.

Objective 3

Development of Buckling-Restrained, Fused Mild Steel Energy Dissipators

Chapter 3

- Explore current options for energy dissipation in structures utilising Dissipative Controlled Rocking (DCR).

- Develop and test new types of 'dry' buckling-restrained mild steel dissiptors.
- Compare the performance of these new dissipators with existing dissipator options.

1.4 Overview

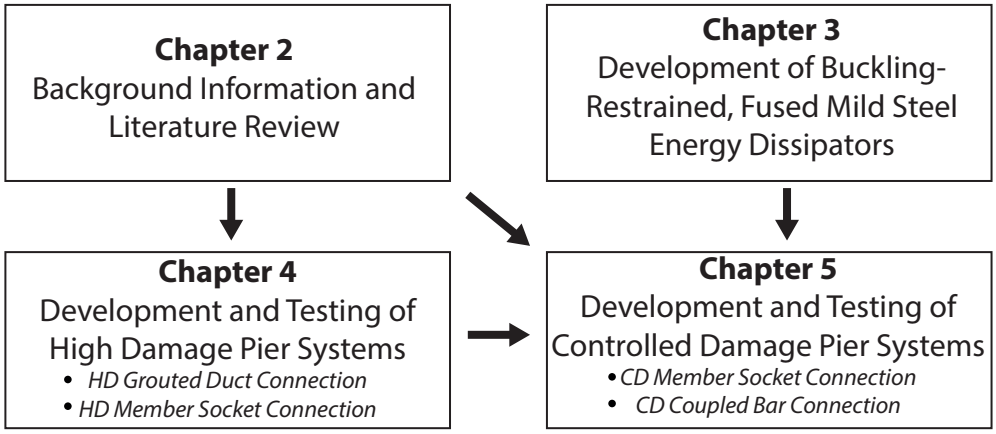

Figure 1.1: Thesis structure overview

Chapter 2 introduces the concepts of Accelerated Bridge Construction (ABC) and Dissipative Controlled Rocking (DCR) and presents relevant prior research into these topics. This is followed by a review of current energy dissipation devices for use in rocking structures in Chapter 3.

Chapter 3 also presents the findings of preliminary testing of new dissipator types at the University of Canterbury. These are buckling-restrained devices meaning they can be deformed in both tension and compression without buckling. They utilise 'dry' fabrication, meaning no grout or epoxy is required for fabrication of the dissipator.

Chapter 4 presents the prototype structure and testing arrangement adopted for the research. The design, detailing, construction and experimental testing of four half scale bridge piers featuring three types of High Damage ABC connection is then presented. The High Damage connections are designed and detailed to emulate the behaviour of conventional monolithic construction through the formation of plastic hinges in the column elements under lateral loading. The connection types tested were two variations of the Grouted Duct Connection (GDC) and one variation of the MSC. Both uniaxial and biaxial test regimes were undertaken on the four test columns.

Chapter 5 presents the design, detailing, construction and experimental testing of two half scale bridge piers featuring two types of Controlled Damage ABC connection. The connection types presented are the CD Member Socket Connection (MSC) and the CD Coupled Bar Connection (CBC). The Controlled Damage connections use unbonded post-tensioned rocking behaviour based on the concepts of Dissipative Controlled Rocking or PRESSS to control the amount of damage and residual drifts that the structure is subjected to during seismic loading. Repair strategies are developed and implemented, with their effectiveness demonstrated through experimental testing. Biaxial loading is used for the testing of the CD connection types. The performance of the CD connection types is evaluated using the HD results as a benchmark.

Chapter 6 summarises the results of the research and discusses further developments required for implementation of the presented technologies. A discussion of the suitability of each connection types will also be presented.

Chapter 2

Background Information and Literature Review

2.1 Accelerated Bridge Construction (ABC)

Bridge substructures in New Zealand and worldwide are typically constructed using cast-in-place concrete. Although this method of construction has proven to be effective at achieving the base goal of the structure, which is ensuring life safety, these types of structure are slow to construct and often face issues with quality control.

This is due to the fact that for each substructure component - whether it is a pile cap, pier, pier cap or abutment:

- Formwork fabrication, on-site assembly and bracing is required.
- Member reinforcement is cut and bent off-site by an external contractor, delivered to site and then tied on-site. Some parts of the reinforcing could be tied off-site and delivered to minimise the amount of on-site work required.
- Concrete is delivered by truck and poured on-site - often in sub-optimal conditions leading to the potential for problems with material quality control.
- The concrete is then left to cure before formwork is removed.
- The concrete then needs to cure further before achieving its design level of strength.

There has been recent interest from infrastructure asset owners as well as the public for bridge structures that can be rapidly constructed while achieving good construction

quality and seismic performance. Rapid construction means that there is limited disruption to traffic during the construction phase of the bridge while good quality leads to minimised maintenance costs and disruption. The use of precast concrete offers a number of advantages over cast-in-place construction including increased on-site construction speed, improved construction quality, increased on-site safety and minimal traffic disruption. Precast construction is particularly suited to regions of limited accessibility, as less equipment, labour and machinery is required for assembly [Billington et al., 1999, Marsh et al., 2011].

A typical precast construction sequence may proceed as follows:

- Formwork is fabricated and assembled off-site at the precast yard. There is a higher level of flexibility in the casting process as concrete members can be poured at any orientation. For example a pier column can be poured horizontally with reduced bracing requirements.
- Member reinforcement is bent and tied either at the precast yard or by an external contractor.
- Concrete is either mixed at the precast yard or supplied by an external contractor. It is then poured in conditions that are often much better than those on-site including improved shelter, control over casting and curing temperature and improved accessibility. This leads to a higher level of construction quality.
- The concrete member is removed from the mould after initial curing and can then be stored of-site to allow the concrete to cure further before being delivered to site for assembly of the bridge structure.
- The precast member is delivered to site for assembly as it is required.

Precast construction of bridge superstructures has proven to be economical with widespread use in Australia and New Zealand with the NZ Transport Agency producing guidelines for the use of standard precast bridge deck systems [NZ Transport Agency, 2008]. Generally, bridge superstructures are designed as capacity protected elements, meaning that they will remain elastic in an earthquake event with no inelastic behaviour. It should be noted, however, that a number of bridge superstructure collapses occurred in the Northridge earthquake of 1994 highlighting the need for robust precast connections, even in capacity protected elements.

It should be noted that precasting of bridge elements is most feasible when there are a

large number of regular elements to be cast. Long span structures will generally have a large number of elements which are repeated along the length of the bridge, such as deck segments, cap beams and pier segments. The use of precasting means that all similar elements can be cast using the same mould (with some adjustment if necessary). The other case where precasting is feasible is when standardised component designs are used, meaning the same elements are used in a number of bridges. An example of this is the standardised bridge deck systems presented in NZTA Research Report 364 [NZ Transport Agency, 2008].

Generally, assembly of precast components involves minimal 'wet work' - that is, on-site pouring of concrete or grout - leading to increased construction speed. Additionally, the column can be loaded to its design level as soon as it has been constructed as sufficient time can be provided between casting and assembly. Less labour, materials and equipment are required on-site for bridge assembly leading to a safer working environment.

Billington et al. [1999] presents a precast segmental system for standardisation of bridge substructures in regions of low seismicity. The system is made up of predominantly precast elements with four column sizes and one basic cap shape proposed. The system is segmental and suitable for varying heights and widths. The system features match-casting, where one precast element is used as formwork for the adjacent element, giving a perfect match between the two. It also features post-tensioning to clamp the segments together, with adjustable supports between key elements providing construction tolerance.

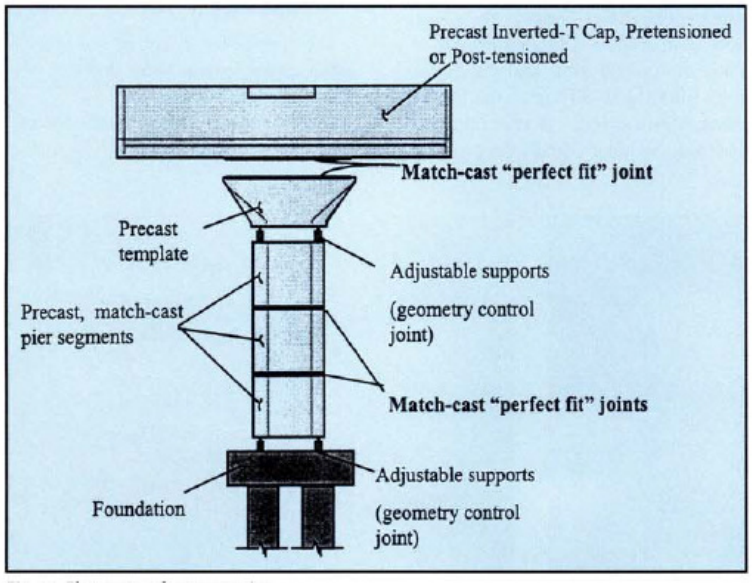

(a) Example assembly schematic

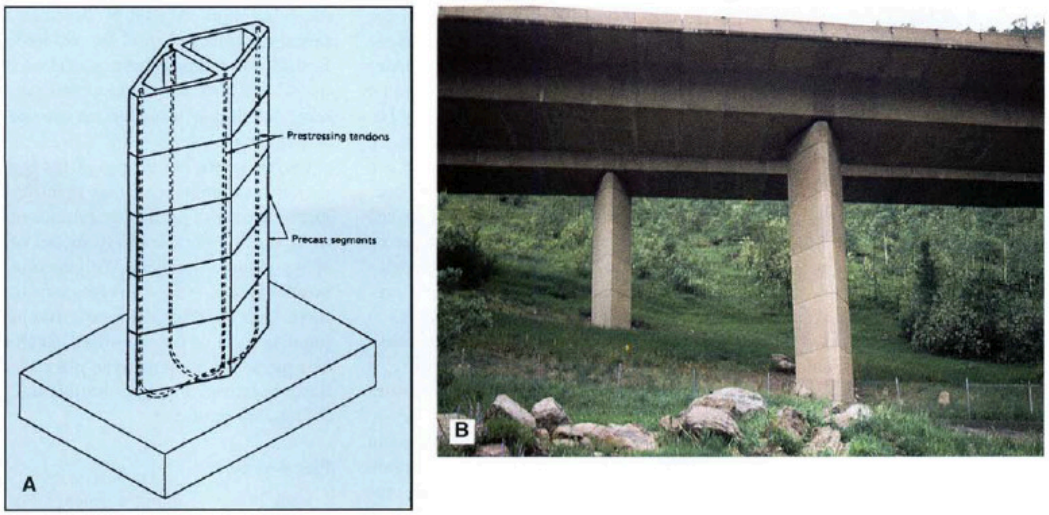

(b) Schematic drawing and as-built view of precast piers for Vail Pass in Colorado

Figure 2.1: Standardised precast substructure system [Billington et al., 1999]

There has also been significant interest in Accelerated Bridge Construction for bridge substructures by US Departments of Transportation including Washington [Hieber et al., 2005, Khaleghi, 2010], Texas [Ralls et al., 2004], Utah [Burkett et al., 2004, Utah DOT, 2008] and The Federal Highway Administration [U.S. Federal Highway Administration, 2011]. A number of successful applications of ABC to bridge substructures in regions of low seismicity exist including U.S. Highways 183 and 249, and Dacio Marin III at Lake Belton (Figure 2.2).

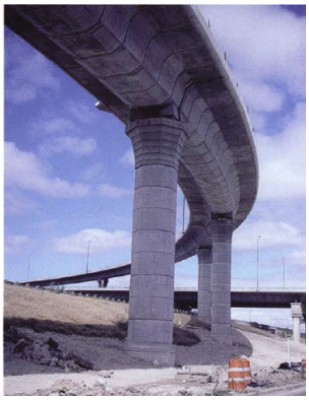

(a) U.S Highway 183 [Billington et al., 1999]

(b) U.S Highway 249 [Billington et al., 1999]

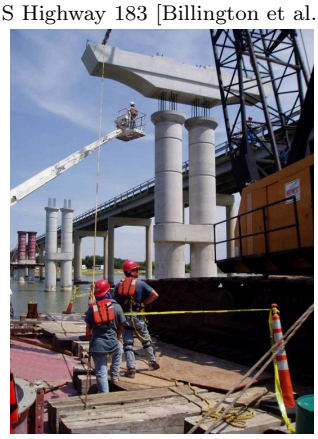

(c) Dacio Marin III at Lake Belton [Texas DOT, 2008]

Figure 2.2: Examples of application of ABC in the U.S.

The use of ABC substructures in moderate to high seismic regions has been limited due to concerns regarding the seismic performance of the connections between precast elements [Stanton et al., 1992]. The need for improved seismic performance of precast structures was highlighted in recent earthquakes such as the Loma Prieta earthquake in 1989 and the Northridge earthquake in 1994 [Buckle, 1994, Hawkins et al., 1994]. Since bridge substructures exhibit column sway behaviour during earthquake loading, there is little redundancy in the system. A single connection failure could lead to collapse of the bridge. For this reason, further investigation into the strength and ductility of precast connections is required before wide spread implementation of ABC substructures can proceed.

Marsh et al. [2011] presents a summary of a precast connections suitable for use in ABC applications in regions of moderate to high seismicity. A number of different connection types including bar coupler, grouted duct, pocket, socket, hybrid and integral connections are compared in terms of technological readiness, potential seismic performance

and time savings potential. The evaluation of these systems was based on literature review and a survey questionnaire that involved bridge owners, U.S. Departments of Transportation, U.S. and international universities and organisations, contractors, pre-cast producers, and vendors. Emerging technologies such as shape memory alloy or elastomeric bearing based connections were also investigated. The paper concludes that significant work is under way and more is needed to ensure that ABC connections can meet the required seismic performance, in addition to having the necessary non-seismic properties of constructability, cost effectiveness, durability and inspectability.

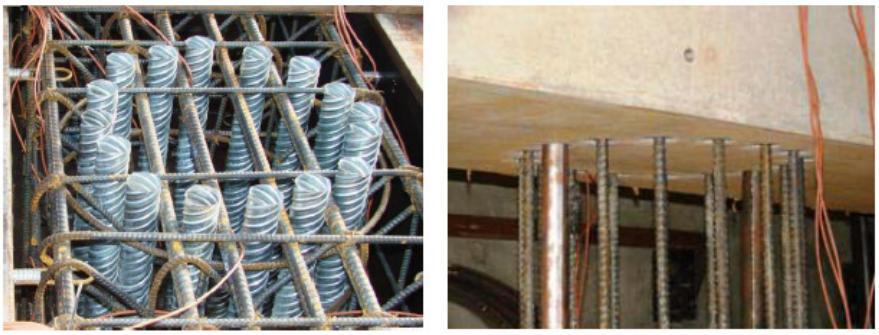

(a)

(b)

Figure 2.3: Examples of Grouted Duct Connection [Marsh et al., 2011]

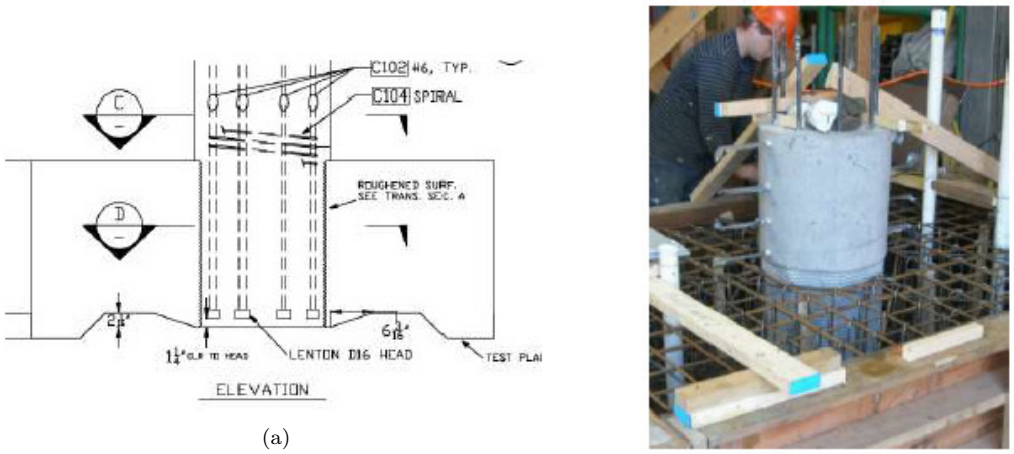

(a) (b)

Figure 2.4: Examples of Member Socket Connection [Marsh et al., 2011]

Ou et al. [2011] investigates the use of a post-tensioned pier system that combines segmental precast and cast-in-place construction. This system uses a cast-in-place section in the plastic hinge region at the base of the pier with segmental precast upper sections. The combination of cast-in-place and precast segmental construction allows for rapid pier construction, while emulating cast-in-place systems in terms of seismic performance, avoiding the issues associated with connection of precast elements in the plastic hinge region.

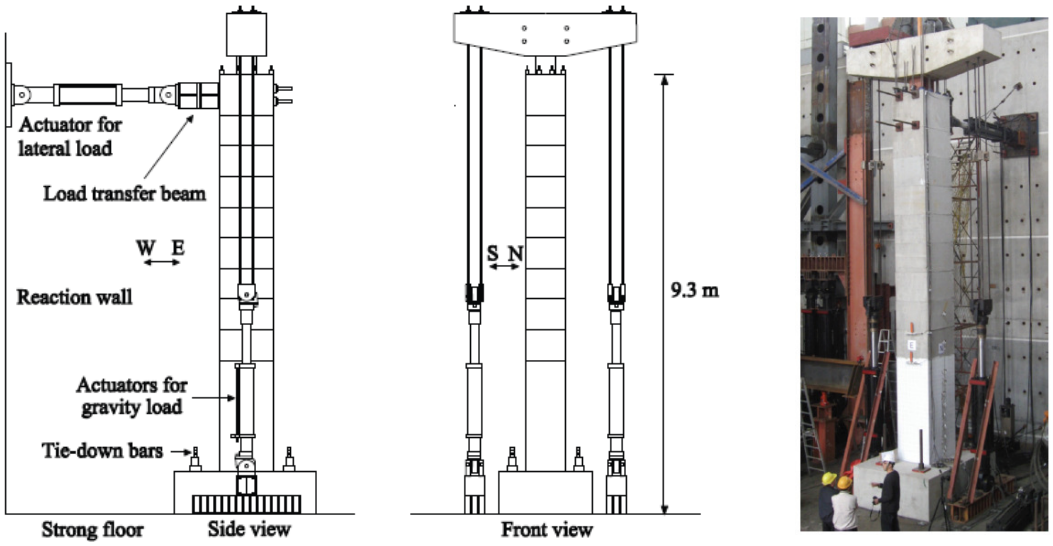

(a) (b)

Figure 2.5: Substructure system combining precast and cast-in-place construction [Ou et al., 2011]

2.2 Rocking Pier Systems

Dissipative Controlled Rocking (DCR) connections [Palermo, 2004] combine unbonded post-tensioning with energy dissipation components to provide a system with minimal residual drifts following a seismic event and good energy dissipation properties. This system is particularly applicable to ABC substructure systems which often utilise post-tensioning for clamping of precast elements [Billington et al., 1999], but have limitations in terms of application in regions of moderate to high seismicity. The development of rocking connections and their application to bridge substructures is presented in this section.

Housner [1963] first introduced the concept of pure rocking of structures and since then there have been a number of bridges to which the concept has been applied. The purpose of pure rocking is to extend the period of the bridge acting as a form of seismic isolation. The concept of pure rocking was extended to form the hybrid system, giving more control over the performance of the structure and a more favourable response during seismic loading.

Beck and Skinner [1974] adapted the concept for use in the South Rangitikei Viaduct (Figure 2.6) which was constructed in New Zealand in 1981. The bridge features a 'stepping pier' behaviour where lateral displacement of the bridge is accommodated by rocking between the two pier columns, avoiding the formation of plastic hinges in the bridge piers. The bridge features a shear pin system with torsional dampers to dissipate energy.

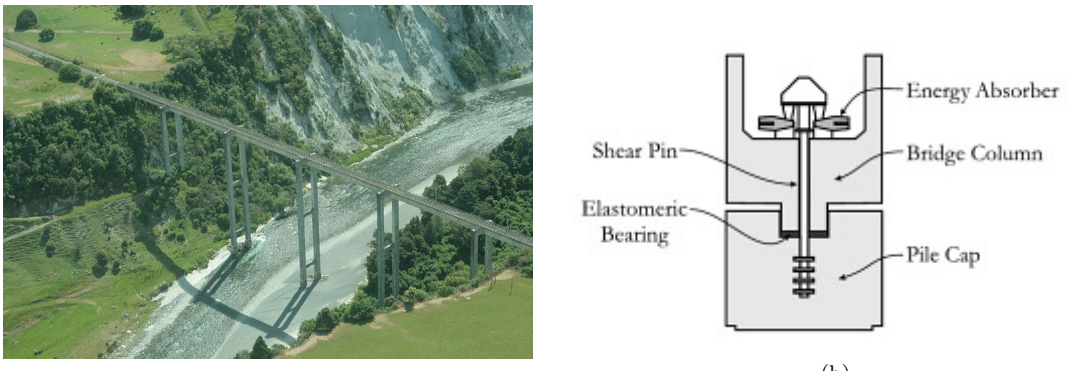

(a) (b)

Figure 2.6: South Ranitikei Viaduct with energy dissipation schematic [Beck and Skinner, 1974]

The hybrid system for building structures was developed as part of the US-PRESSS (PREcast Seismic Structural Systems) program co-ordinated by the University of California, San Diego [Priestley, 1991, 1996, Priestley et al., 1999, Stanton et al., 1991, 1997, Stone et al., 1995]. The hybrid system combines unbonded post-tensioned tendons/bars with longitudinal mild steel or supplemental dissipation devices. The post-tensioned tendons provide self-centering capability to the system while the mild steel or dissipation devices provide additional energy dissipation. The result is a system that can undergo large deformations with little or no damage or residual displacement. The combination of self-centering and energy dissipation capabilities leads to a hysteresis behaviour typically referred to as flag-shaped (Figure 2.8). Research into both hybrid frame and wall systems was conducted [Kurama, 1997, Kurama et al., 1999, Restrepo et al., 2001]. Guidelines for the design of PRESSS buildings are given in the PRESSS Design Handbook [Pampanin et al., 2010].

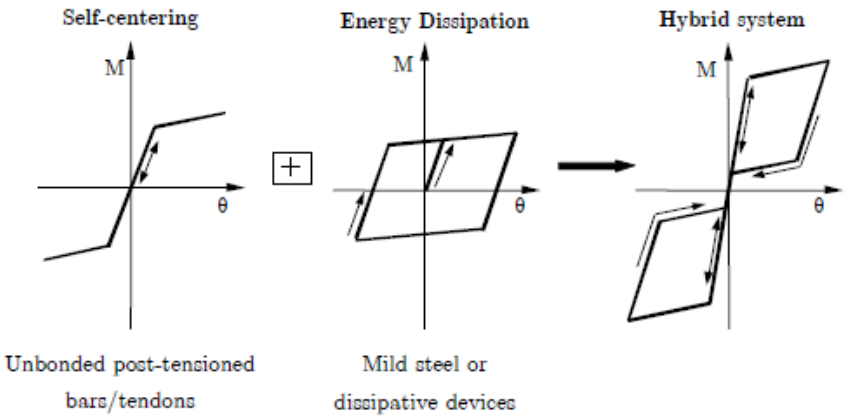

Figure 2.7: Flag-shaped hysteretic behaviour of hybrid connection [Priestley et al., 1999]

Mander and Cheng [1997] propose a modular precast bridge construcion system based on the concept of Damage Avoidance Design that is free to rock under large lateral loads. Special detailing is included to minimise damage to the structure. In this system, post-tensioning can be included to enhance the lateral strength if desired, but is not required. Damping of the structure is through impact alone, with a rubber interface also used in some cases to increase damping. To investigate the behaviour, testing of a near full scale specimen was carried out. As intended, the structure behaved in a bilinear

elastic fashion with no damage or degradation in strength or stiffness. A complete force-deformation model is presented, with good agreement between observed and theoretical behaviour.

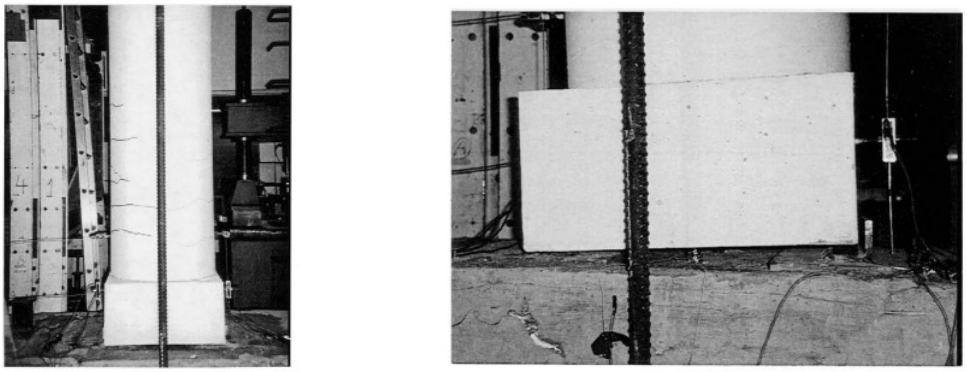

(a) (b)

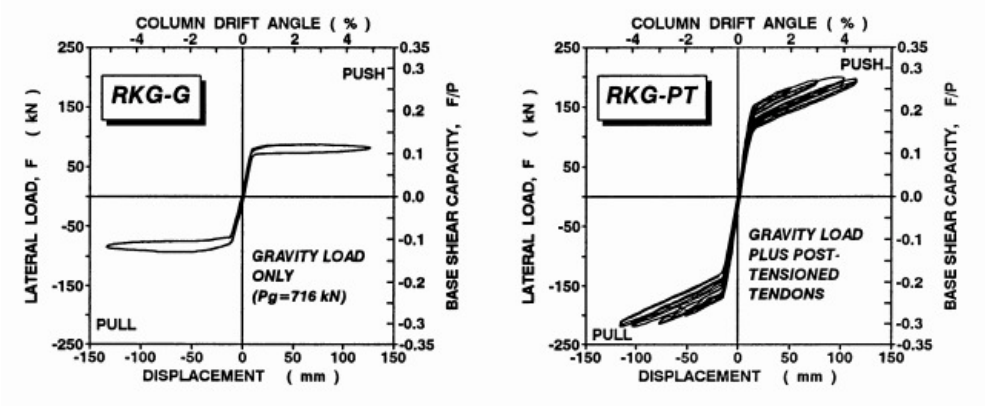

(c)

Figure 2.8: Testing of rocking column with force-displacement behaviour [Mander and Cheng, 1997]

Following on from the research of Mander and Cheng [1997], Hewes and Priestley [2002] investigated the seismic design and performance of precast segmental bridge columns with unbonded post-tensioned tendons but no additional energy dissipation devices. The specimens tested were two columns with a high aspect ratio and two with a low aspect ratio. The tests were conducted with circular pier sections with steel jacketing of varying thickness. It was found that with relatively low initial tendon stiffness, all specimens performed well. The columns underwent large nonlinear displacements of drifts in the order of 4.0% without experiencing significant or sudden loss of strength. Under large post-tensioning force, specimens with thicker steel jacketing performed better achieving drifts of 6.0% with only minimal capacity degradation. Overall, observed column damage was low, primarily consisting of minor concrete crushing at the base of the pier.

Palermo [2004], Stanton et al. [2005], Hieber2006 and Palermo et al. [2005, 2007, 2008] extended the concept of hybrid systems, with both self-centering and energy dissipation components, to bridge structures as a viable and efficient solution for improved seismic performance when compared with conventional monolithic systems (Figure 2.9). The concept is known as Dissipative Controlled Rocking or DCR. In bridge pier systems, the self-centering capability is not only provided by the unbonded post-tensioned tendons/bars, but also by the effects of axial load in the pier element.

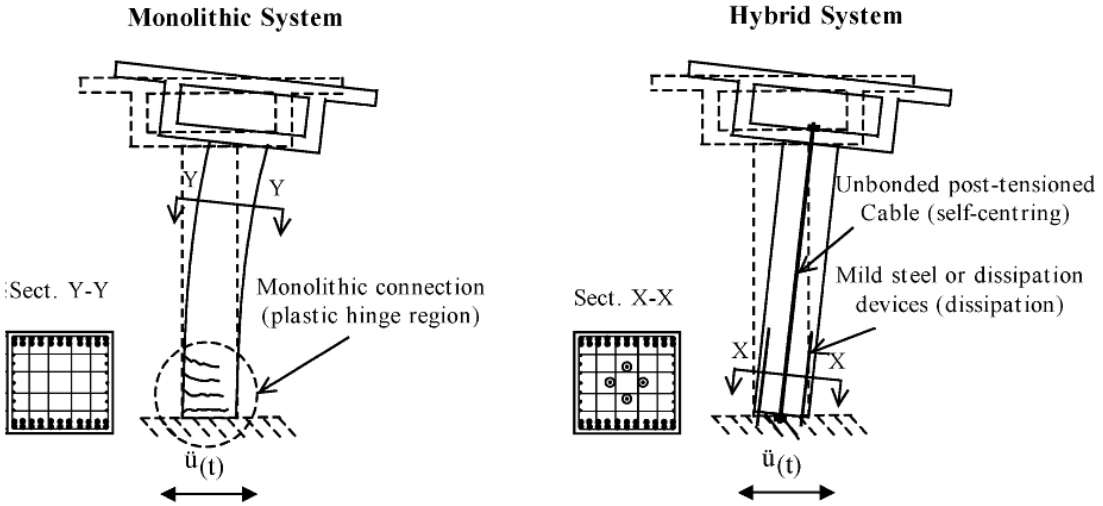

Figure 2.9: Monolithic and DCR pier systems [Palermo et al., 2005]

The total moment capacity of the joint is given by the combination of moment contributions from post-tensioning, axial load and mild steel or energy dissipators.

$$M_{TOT} = M_{PT} + M_N + M_S \tag{2.1}$$

The λ parameter represents the ratio of self-centering and energy dissipation moment contributions and dictates the overall energy dissipation and self-centering behaviour of the system.

$$\lambda = \frac{M_{PT} + M_N}{M_S} \tag{2.2}$$

It is suggested that a value of λ of 1.15 to 1.5 is adopted for design [New Zealand Standards, 2006a, Pampanin et al., 2010]. This range allows for adequate self-centering

and energy dissipation abilities which results in very small residual drifts and acceptable peak drifts when compared to a monolithic system.

Internal or external energy dissipation devices can be used in DCR systems. A typical internal dissipation system is the use of mild steel bars grouted into corrguated ducts in the precast pier element [Marriott, 2009]. The mild steel bars are unbonded for a certain length to prevent premature yielding of the bars under seismic loading. The bars may also be necked by reducing the diameter of the bar over a certain length in order to concentrate inelastic deformation to a certain area of the bar and to minimise strain penetration.

Christopoulos [2004] investigated dynamic behaviour of flag-shaped, single degree of freedom hysteretic systems. Little prior analysis of the nonlinear dynamic behaviour of such systems had been carried out. This research covered systems ranging from post-tensioning only ($\lambda = \infty$) to full bilinear elastoplastic systems ($\lambda = 0$). Results from this research suggest that self-centering, flag-shaped systems with a sufficient amount of energy dissipation capacity will sustain maximum displacement demands under seismic loading similar to those of conventional monolithic systems, despite the fact that they dissipate, at most, one half of the energy dissipated by elastoplastic systems per cycle.

Solberg et al. [2006] investigated the performance of a damage-protected highway bridge pier subjected to bi-directional earthquake loading. The research involved quasi-static and pseudo-dynamic test of 30% scale specimens. Both conventional monolithic and Damage Avoidance Design (or DCR) systems were tested. The DCR specimen consisted of a circular pier specimen with a square shoe block. The shoe block had no external armouring but was constructed using high strength concrete mix with 1% crimped-steel fibres per weight. The reinforcing of the pier was welded to that of the shoe block and wrapped in wire rope to improve confinement of the connection, forming a monolithic connection between the pier and shoe block.

It was concluded that owners can have a high confidence that damage will not be sustained in a design level earthquake. For a maximum credible earthquake (MCE) scenario, there should be at least 50% confidence that the DCR pier will not collapse. The chance of collapse of the monolithic system in an MCE scenario is about the same as the DCR system, but a higher level of damage can be expected in a design level earthquake. Minor damage was observed in the shoe block caused by concentrated axial forces under

bi-axial loading up to 5.5% drift in the pier. It appears that the use of fibre-reinforced concrete and sufficient confinement helped to minimise the damage to the shoe block. No stiffness degradation or residual displacement was observed. This was shown to be due to the rocking mechanism which resulted in bilinear elastic hysteretic behaviour of the pier. Thus, such piers can be used for immediate post-earthquake operational purposes.

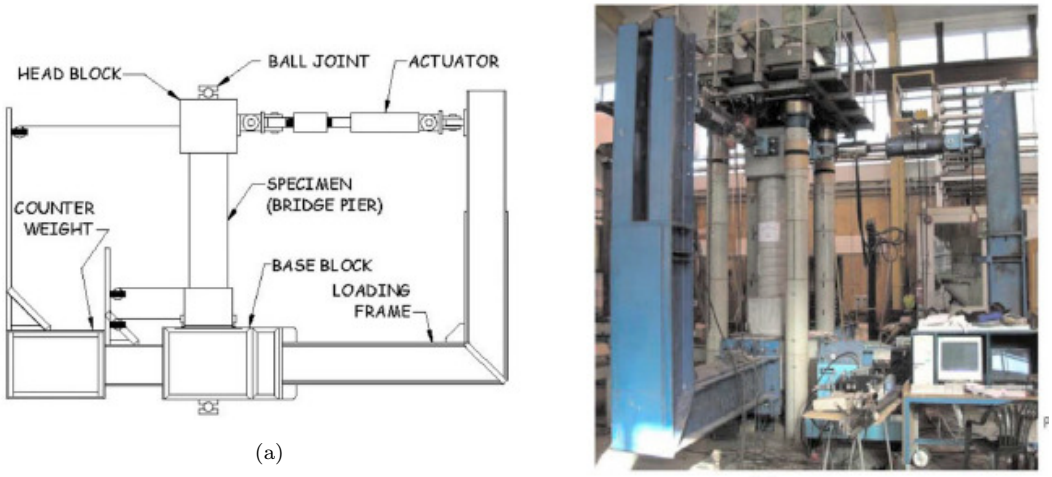

(a) (b)

Figure 2.10: Testing of rocking pier with shoe block [Solberg et al., 2006]

Billington and Yoon [2004] investigate the use of ductile fiber-reinforced concrete in the plastic hinge zones of unbonded post-tensioned segmental precast columns. These columns were designed to distribute damage throughout a ductile fiber-reinforced concrete segment rather than concentrating the column deformation to a single joint. The segments were connected without the use of mild steel bars as this provides a faster and less complex construction method. The columns utilising ductile fiber-reinforced concrete were compared to similar columns constructed using only normal concrete without fiber reinforcement. The columns were scaled to about 1/6th that of a typical bridge pier.

It was found that all of the test specimens reached drift levels of about 9% before yielding of the post-tensioning tendon occurred. All specimens exhibited residual displacements of less than 1%. The fibre-reinforced concrete specimens dissipated more energy and exhibited finer and more distributed cracking than the specimens constructed using ordinary concrete. The ductile fibre-reinforced concrete was also considerably better

at maintaining its integrity under high compressive loads without the use of transverse confinement steel beyond what was required for shear strength.

Marriott [2009] investigated the response of post-tensioned rocking bridge piers with internally and externally mounted mild steel bars (Figure 2.11). Post-tensioned piers without additional energy dissipation devices and monolithic piers were also tested for comparison. A series of 1/3 scale uni-axial and bi-axial cyclic tests were performed.

The internal dissipation system consisted of mild steel bars grouted into ducts in the precast pier element. In one case, the mild steel bars were connected to the foundation using threaded couplers. The bars in this case were not necked. In another case, the bars were cast into the foundation and were necked over a length of 50 mm. Shear across the rocking interface was primarily transferred through dowel action and the use of external shear keys located around the perimeter of the pier. A hemispherical shear key located at the center of the interface was also included to help recenter the pier and prevent sliding. Steel angles of 2mm wall thickness were cast into the pier to resist the concentrated stress that occurs during rocking as shown in Figure 2.11c.

In all cases, damage of the DCR systems was limited to flexural cracking up the height of the pier. The cracks were of hairline thickness following unloading of the pier. Some superficial spalling occurred at the rocking interface of the pier. In contrast, the monolithic equivalent pier sustained extensive cracking and spalling. It was found that both of the systems using internal bars showed very stable response, with large amounts of dependable energy dissipation capacity. Less cyclic stiffness degradation was present in the specimen with a necked region in the mild steel bars due to less strain penetration and bond deterioration. Bar buckling occurred in one of the tests using internal mild steel bars, this caused significant pinching and stiffness degradation. It was stated that little attempt was made to prevent buckling of the bars.

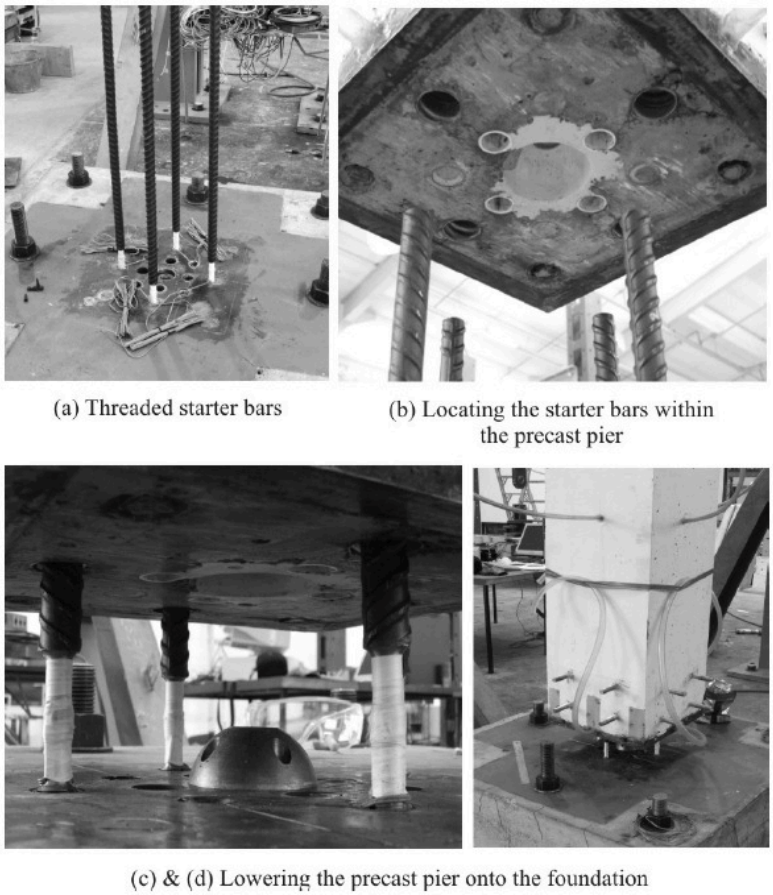

Figure 2.11: Assembly of pier with internal dissipation [Marriott, 2009]

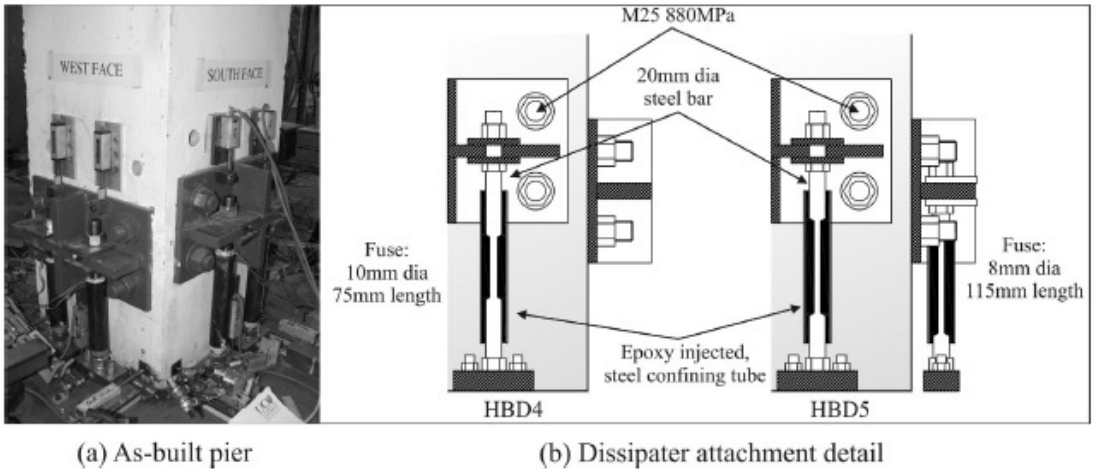

Figure 2.12: Rocking pier with external dissipation [Marriott, 2009]

Sideris et al. [2010] at the University at Buffalo SUNY/MCEER successfully tested a half scale fully precast segmental bridge (Figure 2.13). The bridge remained functional with no structural damage after undergoing three shake table tests in both vertical and horizontal directions. The system did not incorporate any supplemental source of

dissipation but relied on multi-rocking response and sliding friction. Sliding was allowed to occur between the pier segments providing multi-level seismic isolation with the post-tensioning providing a restoring force through dowel effect.

Figure 2.13: University at Buffalo experimental test setup [Sideris et al., 2010]

Prior research into DCR systems often focuses on damage avoidance through the use of armoured precast elements with external, replaceable dissipators Marriott [2009] or post-tensioning only with no energy dissipation systems. Although these systems offer good performance with good strength and ductility and minimal residual drifts, they are often considerable more expensive than conventional construction methods. Alternative solutions feature unbonded post-tensioning with internal reinforcing bars, but no reference is made into the residual ductility capacity of these bars following an earthquake or how replacement of the energy dissipation system would be carried out. There is a need for DCR systems that utilise conventional materials for energy dissipation such as internal mild steel reinforcing bars while still offering limited damage and straightforward options for repair. This research aims to address these needs with development of ABC Controlled Damage connection types.

Chapter 3

Development of Buckling-Restrained, Fused Energy Dissipators

3.1 Introduction

A number of options exist for energy dissipation in ABC precast pier systems. HD connection types tend to use conventional reinforcing bars for energy dissipation which are cost effective, but difficult to inspect, repair and replace. External dissipators are generally used for LD connection types allowing for straightforward inspection and replacement. CD system use a combination of internal and external dissipators (Figure 3.1).

This Chapter presents development and testing of novel 'dry' buckling-restrained fused type energy dissipators suitable for use in ABC Controlled Damage and LD systems. Buckling-restrained dissipators use a steel tube to provide buckling resistance to a fused mild steel bar which yields in compression and tension. Existing Buckling-Restrained Fused (BRF) dissipators use a filling material to close the gap between the bar and confining tube [Sarti et al., 2013]. The novel dissipators presented in this chapter are termed 'dry' dissipators as they do not require filling material, with buckling restraint provided through direct contact between bar and confining tube.

This chapter first presents existing options for energy dissipation in precast bridge piers. Four novel 'dry' buckling-restrained fused type dissipators are then presented along with testing arrangement, preliminary experimental test results and strain limits for design.

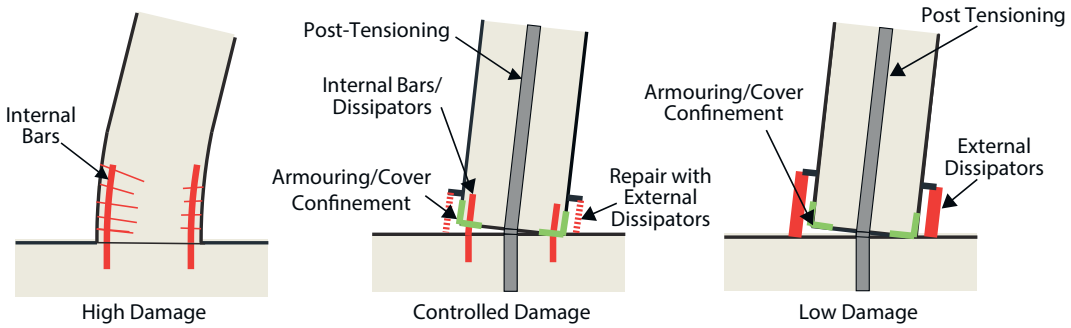

Figure 3.1: ABC connection types

3.2 Existing Options for Dissipation in Precast Bridge Piers

This section presents existing dissipation options for precast bridge pier systems, focussing primarily on mild steel dissipation systems designed to yield in tension and compression, in particular mild steel reinforcement, and buckling-restrained, fused-type (BRF) dissipators. A brief overview of other dissipation option is also given including other yielding type dissipators such as U-shaped flexural plates, lead extrusion dampers and torsion dampers. Non-yielding dissipators types such as friction and viscous dampers are then presented.

3.2.1 Mild Steel Reinforcing Bars

Yielding of steel reinforcing bars is the typical method of energy dissipation in reinforced concrete structures. This is due to steel reinforcement being readily available, cheap and ductile. Grade 300 steel is generally preferred for use in energy dissipation systems due to it having a higher strain capcity, although Grade 500 can be used if desired, provided the appropriate material limit states are satisfied [Pampanin et al., 2010].

The main limitation of steel reinforcement as the energy dissipation system in reinforced concrete structures is the difficulty and cost of replacement of the bars following earthquake damage. Tests have indicated that spalling of cover concrete and yielding either longitudinal or transverse reinforcement should not be considered to militate

against retrofitting. However, if reinforcement has been fractured, buckled, or deformed signficantly out of straight, column replacement should be adopted rather than repair [Priestley et al., 1996]. For bars that have yielded, it is difficult to determine the levels of strain and residual strength and ductility that remains [Coffin, 1954, Mander et al., 1994, Manson, 1953, Momtahan et al., 2009]. The use of replaceable dissipators offer the advantage of relatively straightforward inspection and replacement in any case of uncertainty into strength or ductility of components of the energy dissipation system.

The use of couplers with replaceable segments of reinforcement is an option to allow for replacement of sections of reinforcing bar following earthquake loading. This type of approach is used in the development of the Controlled Damage Coupled Bar Connection as presented in Chapter 5. It should be noted, however, that the use of couplers in the plastic hinge regions of structures is generally not permitted by design codes [Kirkcaldie and Lloyd, 2013, New Zealand Standards, 2006b].

In order to reduce strain concentrations, debonding of bars may be used (Figure 3.2). This is particularly important in rocking type connections where a single gap opens, limiting distribution of inelastic deformation. Debonding can be achieved by applying tape to the reinforcing bars, achieving a smooth bar profile to prevent interlock between deformations and surrounding concrete, along with preventing friction or chemical adhesion of concrete to the bars. Grease tape is useful for this application as it is thick and mouldable, allowing a smooth profile to be easily obtained.

The length of debonding required is generally that which reduces peak strains in the bars to below a 5% threshold at the design level of structure drift. The allowable design strain of 5% accounts for the expected reduction in strain capacity due to reversed cyclic loading and the susceptibility to bar buckling causing low cycle fatigue [Coffin, 1954, Manson, 1953, Pampanin et al., 2010].

From the PRESSS Design Handbook [Pampanin et al., 2010], the strain demand (ε_s) in the mild steel of a rocking connection is calculated using:

$$\varepsilon_s = \frac{\Delta_s + 2/3.l_{sp}.\varepsilon_y}{l_{ub} + 2l_{sp}} \tag{3.1}$$

Where,

ε_y is the yield strain of the steel.

Δ_s is the elongation of the mild steel bar (mm).

l_{sp} is the strain penetration length, equal to $0.022 f_y d_{bl}$ (mm).

f_y is the yield strength of the reinforcement (MPa).

d_{bl} is the diameter of the reinforcing bar (mm).

l_{ub} is the unbonded length of the mild steel reinforcement (mm).

Setting $\varepsilon_s = 0.05$ and rearranging for l_{ub} gives the required unbonded length of:

$$l_{ub} = 20(\Delta_{sd} + 2/3.l_{sp}.\varepsilon_y) - 2l_{sp}(mm) \tag{3.2}$$

Where

Δ_{sd} is the elongation of the mild steel bar at the design level of structure drift.

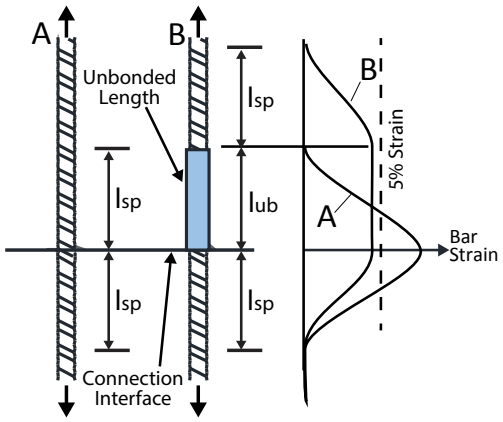

Figure 3.2: Effect of unbonded length on bar strain

Advantages:

- Very cost effective and readily available.
- Little to no fabrication required, other than rolling and bending of bars.
- Good hysteretic behaviour under tension and compression with high ductility.
- Good control over peak strain and concentration of yielding through the use of debonding.

Disadvantages:

- Limited repairability without the use of bar couplers in the initial construction. Removal of concrete is required to gain access to bars for inspection and/or repair.
- Buckling restraint is required, generally through the use of stirrups.

- Susceptible to low cycle fatigue, especially if inadequate buckling restraint is provided.

3.2.2 Buckling-Restrained Fused (BRF) Type Dissipators

BRF type dissipators (Figure 3.3) [Amaris Mesa, 2010, Christopoulos et al., 2002, Marriott, 2009, Sarti et al., 2013] have been implemented in a number of structures including Learning and Research Building at Victoria University in Wellington (-41.290139, 174.768465), and the Merrit building in Christchurch (-43.521897, 172.629237). BRF dissipators are based on Buckling-Restrained Brace (BRB) devices, commonly used in steel frame structures [Iwata and Murai, 2006].

The BRF type dissipator is made up of a plain bar with a turned down length of reduced diameter. The reduced diameter concentrates yielding of the bar and ensures that threaded regions of the dissipator remain elastic. Generally a reduction in cross sectional area of at least 20% is used, to prevent yielding of components outside the reduced length when strain hardening in the bar initiates. The length of reduced cross section is determined from the expected level of deformation of the dissipator and is chosen to limit strain in the dissipator during earthquake loading. A strain limit of 5% is generally assuming in design to limit low cycle fatigue issues in the dissipator [Pampanin et al., 2010].

A confining tube is placed over the dissipator. Grout or epoxy is poured to fill the gap between bar and tube. The bar and filling material provide confinement to the bar, reducing buckling effects while the dissipator is subjected to compressive deformation. Testing by Sarti et al. [2013] showed little difference in performance when using grout or epoxy.

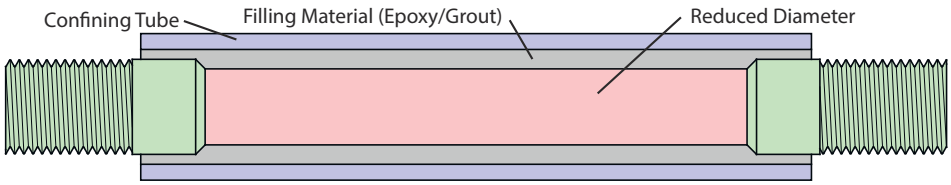

Figure 3.3: Buckling-Restrained Fused-type (BRF) dissipator

Testing by Amaris Mesa [2010] (Figure 3.4) shows that this dissipator behaves well under net positive deformation with no sign of buckling and stable hysteresis loops. Under net

negative deformation however there is a significant increase in stiffness of the dissipator with buckling occurring at low levels of negative strain. This is due to contact between at the bar and filling material at the ends of the reduced region of the bar. Under negative net deformation, some load from the bar is transferred to the grout causing an effective increase in cross sectional area (Figure 3.5).

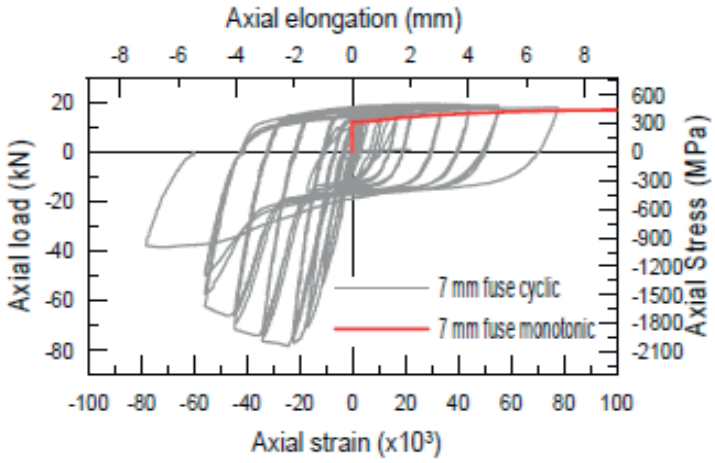

Figure 3.4: Test results of BRF type dissipator (Amaris Mesa, 2010)

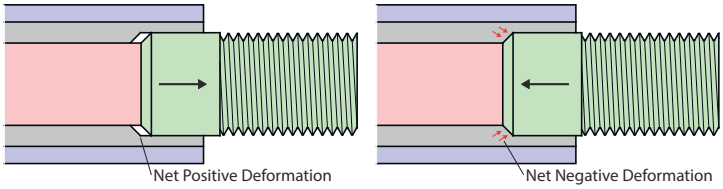

Figure 3.5: Effect of negative net strain

Advantages:

- Limited steel fabrication required. Can be turned down on lathe accurately to required dimensions. Regular tube required.
- Good hysteretic behaviour under tension and compression (while subject to net positive strains)
- Good buckling resistance. Continuous contact of filling material with bar.

Disadvantages:

- Requires pouring of grout or epoxy. Adds to fabrication difficulty and cost.
- Significant increase in stiffness under negative net strain.

3.2.3 Other Types of Yielding Dissipators

Lead extrusion dissipators use deformation of lead to dissipate energy. These types of dissipator generally don't suffer from buckling issues and offer very stable energy dissipation with little cyclic degradation. A notable example of a lead extrusion type damper is the High Force to Volume (HF2V) damper (Figure 3.6) developed at the University of Canterbury [Rodgers, 2009]. HF2V dissipators are able to achieve large resistive forces in a very compact package able to fit within structural connections with very little degradation in performance under large amounts of cyclic loading. These devices are cheaper than proprietary viscous dampers and provide equivalent or greater force capacity in a more compact unit.

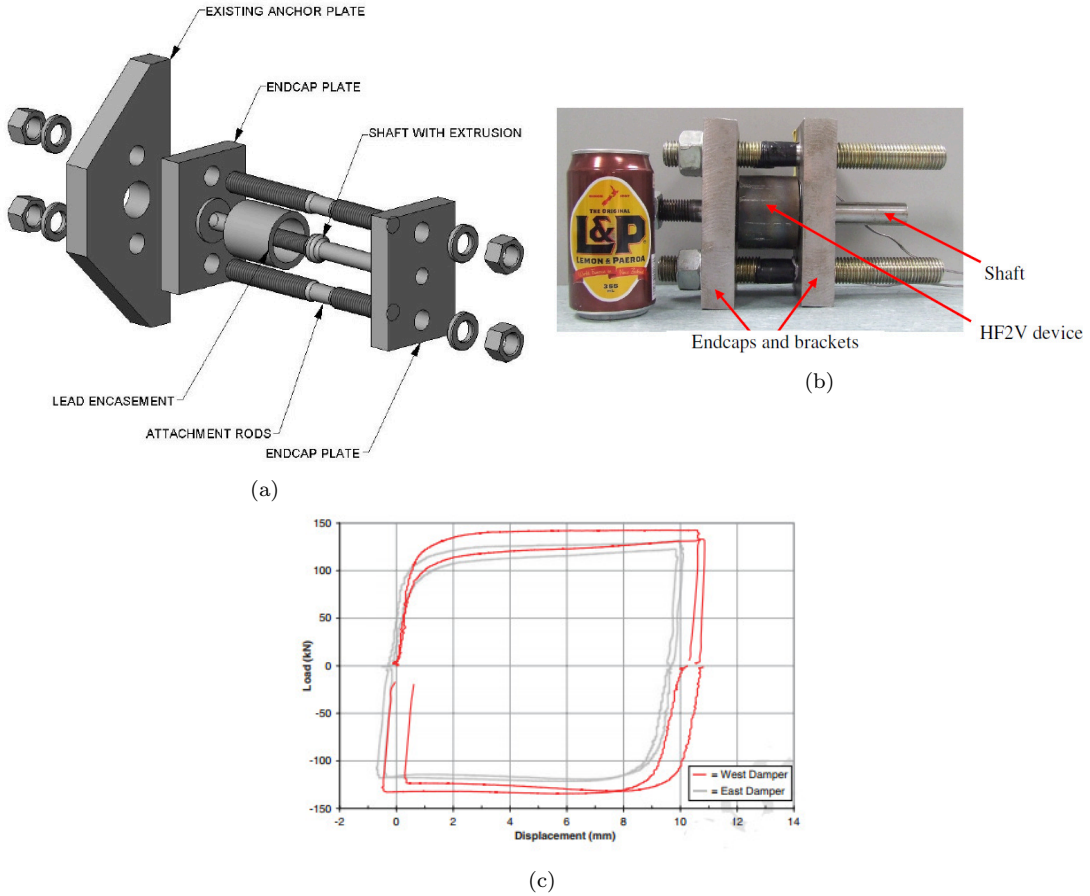

Figure 3.6: HF2V Damper and hysteretic behaviour [Rodgers, 2009]

Torsional dampers dissipate energy through torsional yielding of a steel bar as shown in Figure 3.7 [Kelly et al., 1972]. In the case of a column-footing connection, the centre plate may be mounted to the column, while the outer connections are mounted to the footing. Displacement of the column induces a torsional deformation in the bar connecting the

plates, with torsional yielding of the bar dissipating energy. This dissipator type was used in the South Rangitikei viaduct (-39.797452, 175.809161) spanning the Rangitikei River in 1981 (Figure 3.8) Testing is currently under way at the University of Canterbury into application of torsional dampers in precast column-footing connections.

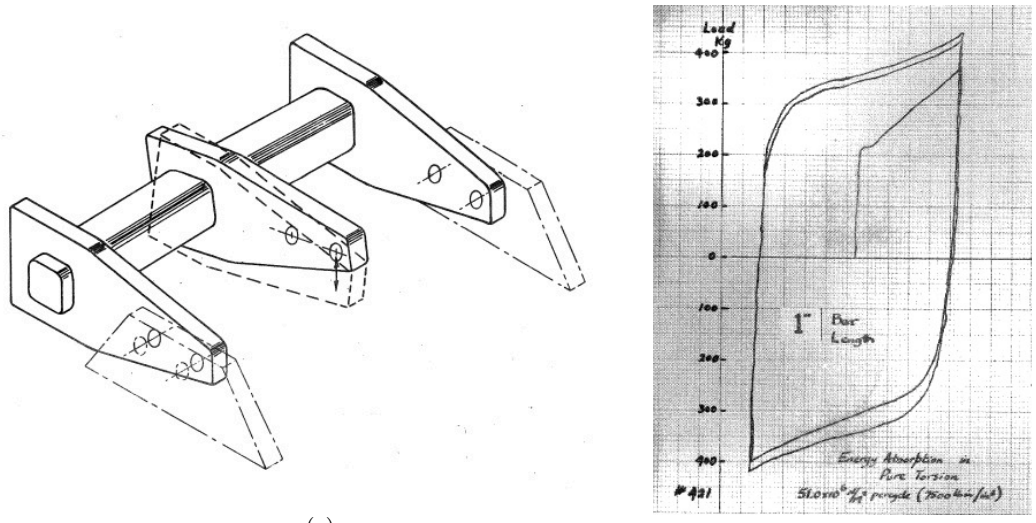

(a) (b)

Figure 3.7: Torsional damper with hysteretic response [Kelly et al., 1972]

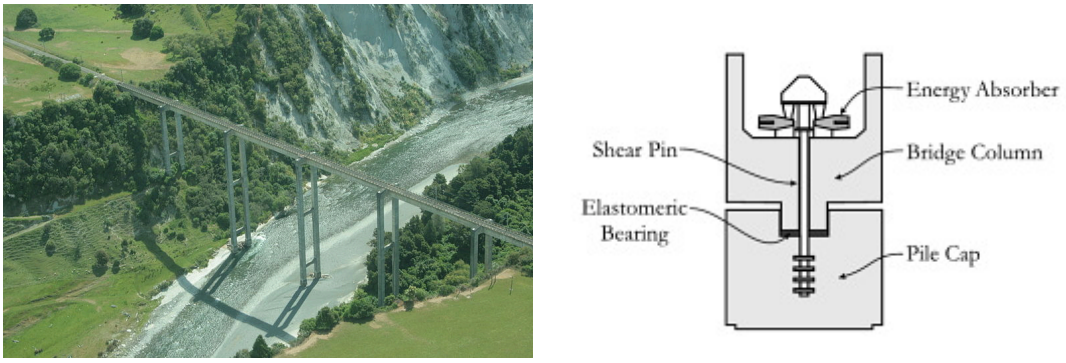

(a) (b)

Figure 3.8: South Ranitikei Viaduct with energy dissipation schematic [Filiatrault et al., 2013]

U-Shaped Flexural Plates (UFP) (Figure 3.9) were developed in New Zealand by Dr. Ivan Skinner [Kelly et al., 1972]. They consist of steel plate, bent into a U-shape. Relative movement of each side of the U-shape causes a rolling deformation in the steel, dissipating energy. UFPs are very effective at dissipating energy and can undergo many deformation cycles with little degradation in performance. These dissipators are typically used in rocking wall type structures, but can be adapted for use in rocking column systems.

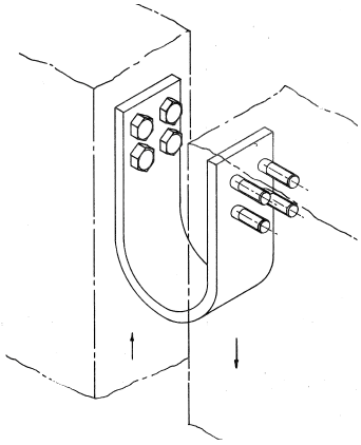

(a)

(b)

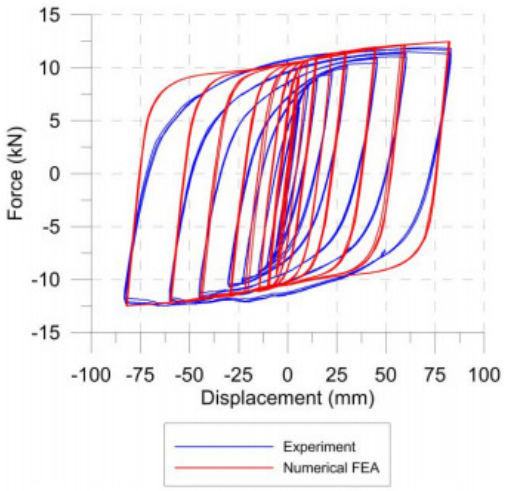

(c)

Figure 3.9: U-Shaped Flexural Plate (UFP) with hysteretic behaviour [Baird et al., 2013, Kelly et al., 1972]

3.2.4 Non-Yielding Dissipators

Viscous dampers (Figures 3.10 and 3.11) resist motion through viscous friction [Constantinou and Symans, 1992, Filiatrault et al., 2001, Kurama, 2000]. They consist of a piston that moves through a cylinder of fluid. Viscous dampers are primarily velocity dependant and so are particularly effective for near field earthquake situations, which can involve large velocity pulses. They are less effective, however, in far field events with little velocity components of motion. Viscous dampers are more expensive than yielding steel type dissipators, but can generally handle many cycles of loading with no damage or degradation of performance.

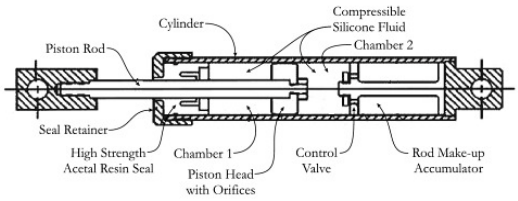

(a)

(b)

Figure 3.10: Viscous damper [Filiatrault et al., 2013]

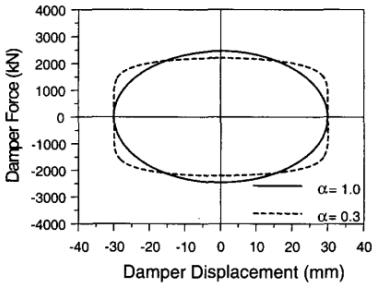

Figure 3.11: Hysteretic behavour of viscous dampers [Filiatrault et al., 2001]

Friction dampers dissipate energy through friction between a number of steel plates that move relative to one another as the structure deforms [Clifton, 2005, Kurama, 2004, Morgen and Kurama, 2004]. They are able to dissipate energy with little to no degradation or damage. Shims are typically used between the plates to improve the performance of the dissipator. A notable example is the Asymetrical Friction Connection (AFC) (Figure 3.12) developed by Clifton [2005].

Morgen and Kurama [2004] present a rotational type friction damper and demonstrate its performance in a hybrid beam column joint (Figure 3.13). Figures 3.13b and 3.13c show the results of hybrid testing, with a square hysteretic behaviour exhibited by the damper. When combined with unbonded post-tensioning, a clear flag shape is seen in the results with good energy dissipation and strong recentering behaviour.

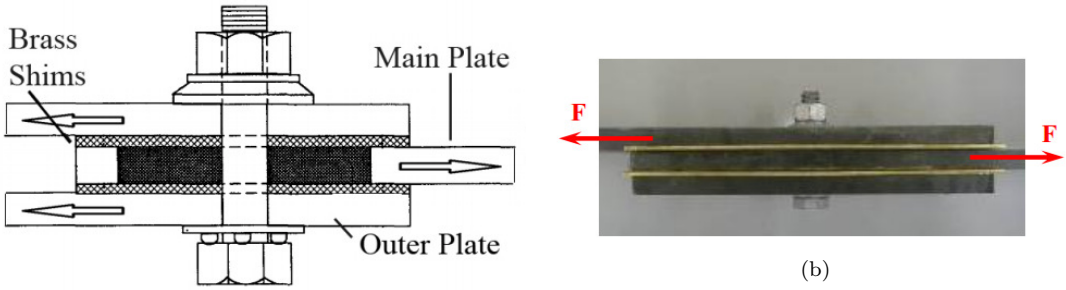

(a) (b)

Figure 3.12: Friction damper [Clifton, 2005]

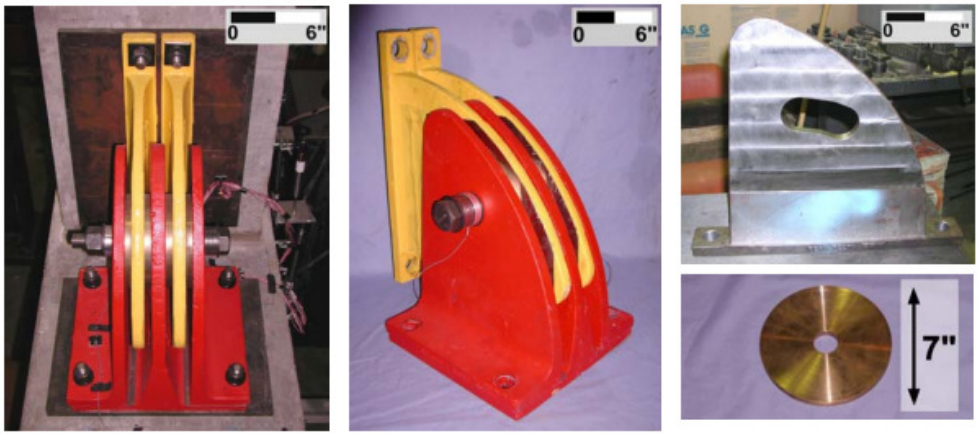

(a)

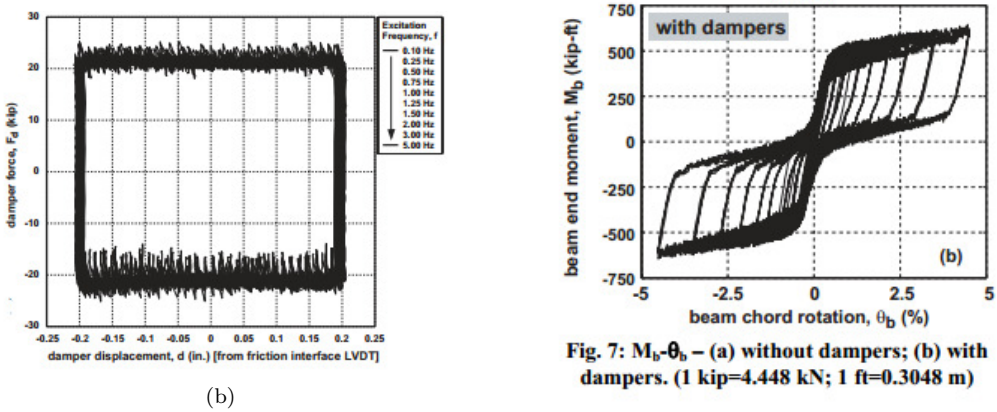

(b) (c)

Figure 3.13: Rotational-type friction damper in a hybrid precast connection [Morgen and Kurama, 2004]

A combination of dissipators can be used to achieve an Advanced Flag-shape System (AFS) system [Kam et al., 2010]. These systems combine velocity dependent dissipators with yielding or friction dissipators (which are generally velocity independent) to achieve high seismic performance for both far-fault and near-fault motions. This is particularly

applicable in situations like that of Wellington, where conventional dissipation methods may be insufficient to adequately handle velocity pulses associated with near field earthquakes.

3.3 Development and Testing of 'Dry' Buckling-Restrained Dissipators

This section presents the development and testing of four novel 'dry' buckling-restrained fused type dissipators. The BRF dissipators presented in Section 3.2.2 require a filling material such as epoxy or grout to fill the gap between the bar and confining tube. The dissipators in this section are termed 'dry' as they require no filling material, with buckling restraint provided through direct contact between bar and confining tube. This section outlines each of the new dissipator types and presents results of preliminary testing.

3.3.1 Dissipator Testing Arrangement

Preliminary experimental testing of four new dissipator types was carried out. This involved cyclic testing of each dissipator in compression and tension using the testing arrangement shown in Figure 3.14. The dissipators were subjected to increasing levels of cyclic strain until failure, with three cycles applied at each strain limit. The exception is the testing of the split tube type dissipator (Section 3.3.2) where the dissipator was subjected to cyclic loading up to 7.5% strain before monotonic loading to failure.

The test dissipators all feature a total length of 250mm, with a reduced cross section over the central 170mm of the dissipator. The full diameter of bar used was 24mm, with an effective reduced diameter of 17mm. Testing of the plain bar showed a yield strength of 350MPa. All dissipators featured a buckling restraint tube with a minimum wall thickness of 5mm.

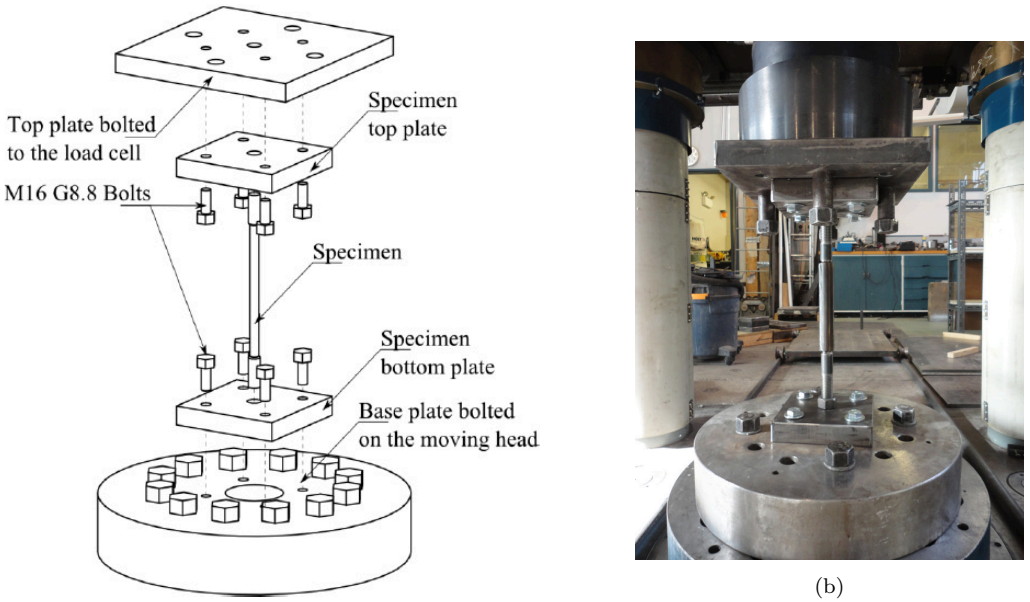

Figure 3.14: Dissipator testing arrangement [Sarti et al., 2013]

3.3.2 Split Tube Type

The split tube type dissipator (Figure 3.15) uses a turned down bar similar to that of the BRF dissipator. In this case, however, the confining tube maintains contact with the bar for the almost the full bar length with no filling material. For this reason, the dissipator is termed a 'dry' type dissipator with no grout or epoxy used in construction. The tube features two different inside diameters for the full diameter and reduced diameter lengths of the bar. The tube is cut lengthwise then placed around the bar and the two halves of the tube are welded together.

A small gap is left between bar and tube during fabrication to avoid friction, particularly under compressive loading where the bar undergoes an increase in diameter due to the Poisson effect. Friction between tube and bar may increase the stiffness of the dissipator or lead to strain concentrations in the bar, altering the hysteretic behaviour and potentially leading to premature failure. Welding of the tube may also cause a clamping effect of the tube onto the bar which should be sllowed for when determining required tube diameter.

A gap between bar and tube in the longitudinal direction is also provided at each end of the reduced length of bar, allowing for net negative strains of the bar without longitudinal loading of the confining tube. It is expected that this detail will avoid the

significant increase in stiffness under net negative deformation that occurs with BRF type dissipators. The length of gap provided depends on the expected amount of negative deformation of the dissipator. Provided the gap is relatively short in length, it is expected that no reduction in buckling resistance of the bar will occur.

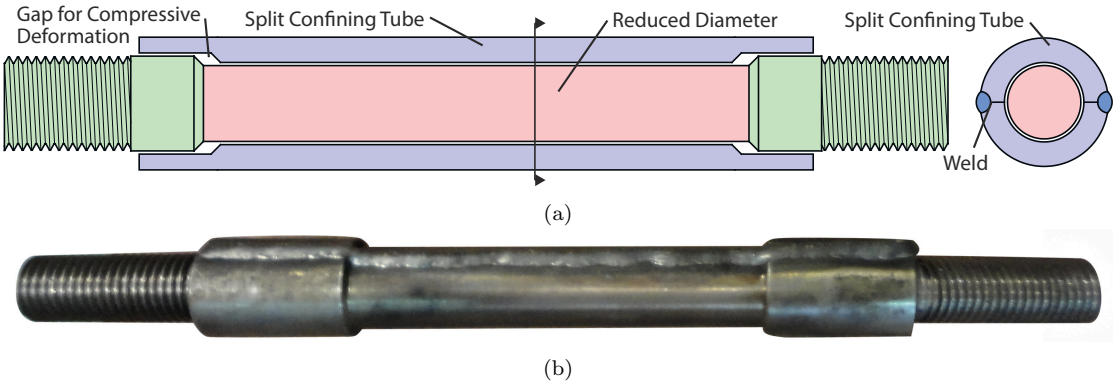

(a)

(b)

Figure 3.15: Split tube type dissipator

The split tube type dissipator was subjected to cyclic testing up to strains of 7.5% before being loaded monotonically until failure (Figure 3.16). This differs from subsequent tests, where the dissipator was loaded cyclically until failure. Under cyclic loading, the dissipator was subjected to three cycles at each strain limit.

The results show very stable hysteretic behaviour during the cyclic stage of loading with no sign of buckling occurring. Under monotonic loading, an ultimate strain of 18% was achieved before initiation of bar fracture in the reduced length of bar. It is expected that a lower ultimate strain would be achieved if the dissipator was subjected to further cyclic testing as seen in subsequent dissipator tests, rather than loading monotonically. The dissipator was not subjected to net negative strains, however it is expected that no significant increase in stiffness would be observed as discussed previously.

The maximum completed strain cycle, ε_{max}, was 7.8% with a yield strain, ε_y, of 1.3%. This corresponds to a strain ductility, μ_ε, of 5.8 using Equation 3.3. It is expected that the split tube type dissipator would have sucesssfully completed a maximum strain cycle of 9% had the same test regime as subsequent tests been used, which would increase the strain ductility obtained from the test.

$$\mu = \frac{\varepsilon_{max}}{\varepsilon_y} \tag{3.3}$$

Strain thresholds are imposed when designing structures using mild steel dissipators to account for the expected reduction in strain capacity due to reversed cyclic loading and the susceptibility to bar buckling causing low cycle fatigue. The PRESSS design handbook [Pampanin et al., 2010] assumes a strain threshold of 5% for mild steel energy dissipation components. Assuming strain limits of $70\%\epsilon_{max}$ for the Ultimate Limit State (ULS) case and $70\%\epsilon_{max}$ for the Maximum Credible Earthquake (MCE) case:

$$\varepsilon_{ULS} = 70\%\varepsilon_{max} = 5.3\% \tag{3.4}$$

$$\varepsilon_{MCE} = 90\%\varepsilon_{max} = 6.8\% \tag{3.5}$$

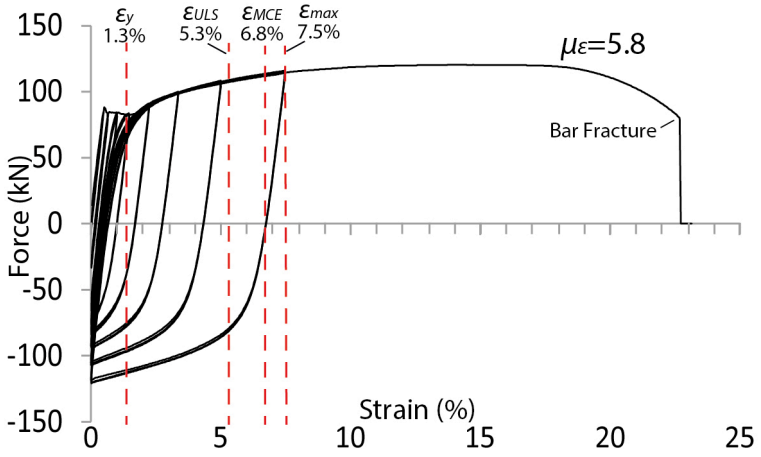

Figure 3.16: Preliminary test results of split tube type dissipator

Advantages:

- Dry connection - no epoxy or grout required.
- Good hysteretic behaviour under tension and compression.
- No significant increase in stiffness expected under negative net deformations.
- Good buckling restraint. Continuous contact between bar and tube.

Disadvantages:

- Complex tube fabrication with two different inside diameters and splitting and welding of tube required, although can still be manufactured without specialised equipment.

3.3.3 Deformed Tube Type

The deformed tube type dissipator (Figure 3.17) is similar to the split tube type dissipator with contact between bar and tube maintained for almost the full length of dissipator. Like the previous dissipator, this design uses a plain bar with a reduced cross section over a length of the bar to constrain yielding. In this case, a regular tube of a single inside diameter is used. After placement of the tube over the dissipator, the tube is deformed to reduce its diameter, closing the gap between bar and tube. This avoids the need for splitting and welding of the tube.

Like the split tube type dissipator, a gap is left at each end of the reduced section allowing for net negative deformations of the bar without longitudinal bearing of the bar on the confining tube causing an increase in stiffness.

To accurately deform the tube, specialised rolling machinery may be required. Too much deformation of the tube may lead to undesirable friction between the tube and bar, while too little may lead to insufficient confinement of the bar, allowing buckling to occur. Deformation of the tube used for the test dissipator was carried out through heating and beating of the tube around the bar. This method achieved the intended effect of closing the gap between bar and tube although the level of accuracy was less than if rolling equipment was used.

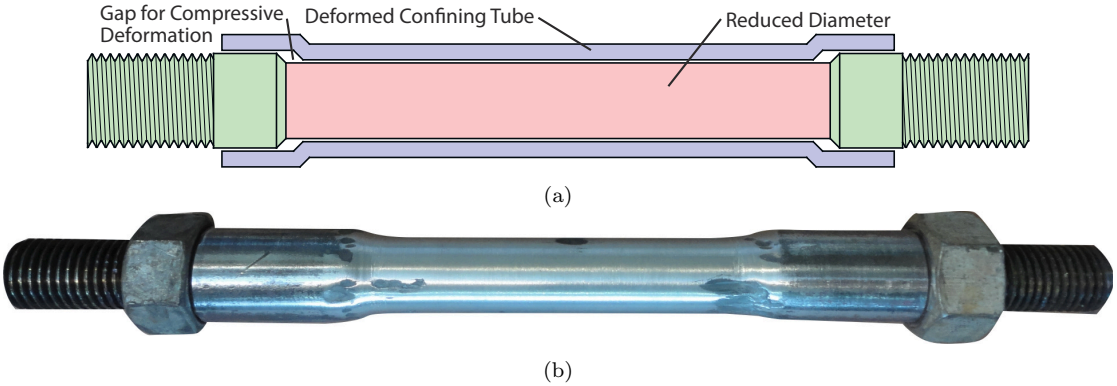

Figure 3.17: Deformed tube type dissipator

Figure 3.18 shows the results from preliminary testing of the deformed tube type dissipator. In this and subsequent tests, the dissipators were subjected to increasing cyclic displacements until failure.

Again, relatively stable hysteresis loops were oberserved. The dissipator completed all three cycles at 9% strain before failing due to buckling during the 13% strain cycle. An increase in stiffness can be seen while loading under compression as the dissipator approaches zero net deformation. It is thought that this is caused by contact between the bar and tube as the bar buckles. This may be due to the gap between the bar and tube being too large. No tube deformation was observed at this point indicating sufficient tube wall thickness was provided.

Since the tube was deformed through beating rather than rolling, it was difficult to control the amount of tube deformation and in turn, the amount of gap between tube and bar. With specialised rolling equipment, it is expected that a higher level of accuracy will be achieved, leading to better dissipator performance.

The maximum completed strain cycle, ε_{max}, was 9% with a yield strain, ε_y, of 1.7%. This corresponds to a strain ductility, μ_ε, of 5.3 using Equation 3.3. Using the strain limits from Equations 3.4 and 3.5, $\varepsilon_{ULS} = 6.3\%$ and $\varepsilon_{ULS} = 8.1\%$.

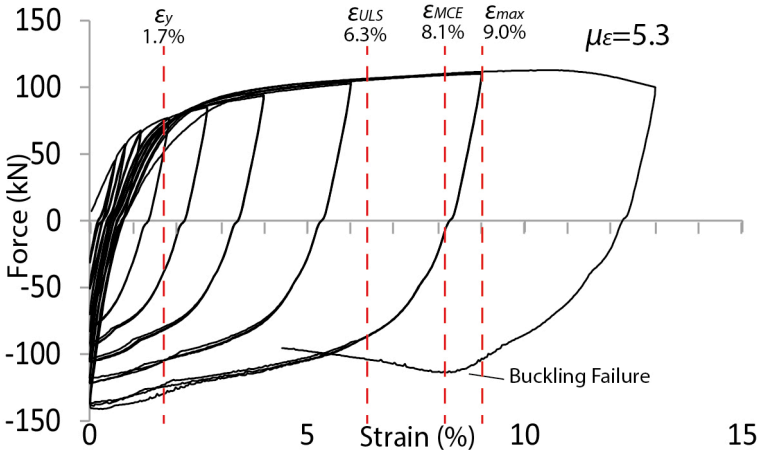

Figure 3.18: Preliminary test results of deformed tube type dissipator

Advantages:

- Dry connection - no epoxy or grout required.
- Good hysteretic behaviour under tension and compression.
- No significant increase in stiffness expected under negative net deformations.
- Good buckling restraint. Continuous contact between bar and tube.
- Conventional materials required with the used of a turned down bar and regular steel tube.
- Simple construction, provided the required machinery is available.

Disadvantages:

- Requires deformation of confining tube to close the gap between bar and tube.
- May require specialised machinery to accurately control amount of deformation.

3.3.4 Supported Bar Type

The supported bar type dissipator (Figure 3.19) features alternating lengths of reduced and full diameter bar along the length of the dissipator. Unlike the other dissipator types, full contact is not maintained along the length of the bar. The approach taken with this dissipator is to reduce the effective buckling length of the dissipator (when compared to a necked bar with no confining tube) through provision of supports along the length of the reduced region of the bar. These supports force a higher mode of buckling than would occur without supports, meaning a higher level of axial load in the dissipator is required to induce buckling. The number and dimensions of support points can be varied depending on the specific application.

Yielding of the bar is distributed between all of the lengths of reduced section, with the same total length of reduced cross section as previous dissipators. As a result, a larger overall length of dissipator is required to accommodate the support points.

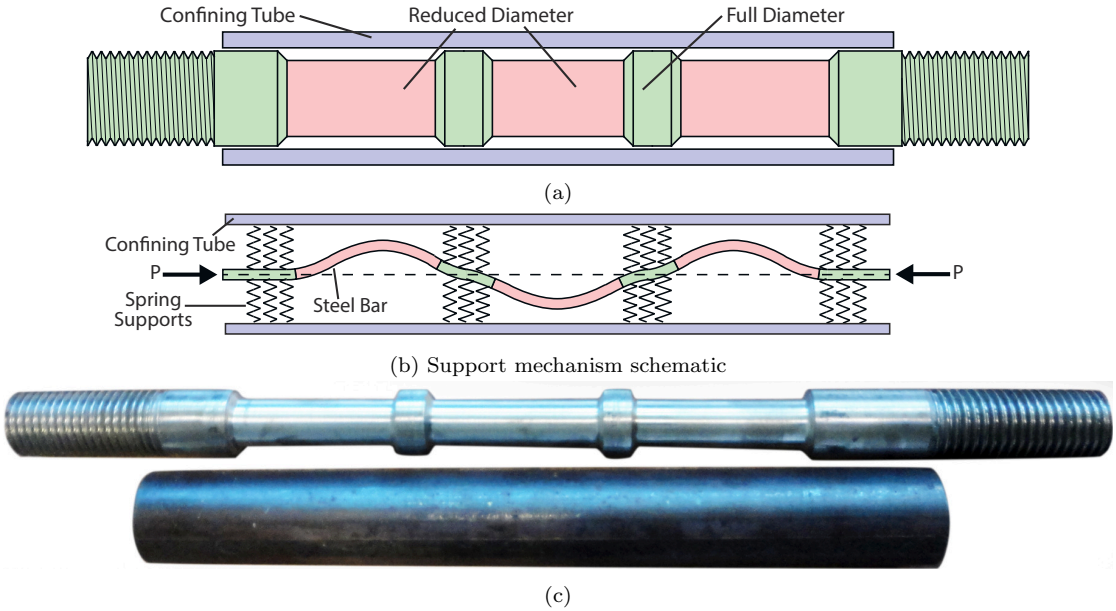

Figure 3.19: Supported bar type dissipator

Like the deformed tube type dissipator, the supported bar type dissipator completed the 9% strain cycle without failure as shown in Figure 3.20. There was however a more pronounced increase in stiffness under compressive loading during the 9% cycle due to buckling of the bar. More severe buckling of the bar occurred during the 13% strain cycle as shown by undulations in the hysteretic curve, with some deformation of the confining tube occurring. Bar rupture occurred during the third cycle of the 13% strain limit.

The maximum completed strain cycle, ε_{max}, was 9% with a yield strain, ε_y, of 1.4%. This corresponds to a strain ductility, μ_ε, of 6.4 using Equation 3.3. Using the strain limits from Equations 3.4 and 3.5, $\varepsilon_{ULS} = 6.3\%$ and $\varepsilon_{ULS} = 8.1\%$.

The test dissipator featured two support points along the reduced length of bar. It is expected that the behaviour of the dissipator would improve with an increase in the number of support points resulting in a reduction in effective buckling length. Increasing the number of supports, however, increases the required overall length of the dissipator.

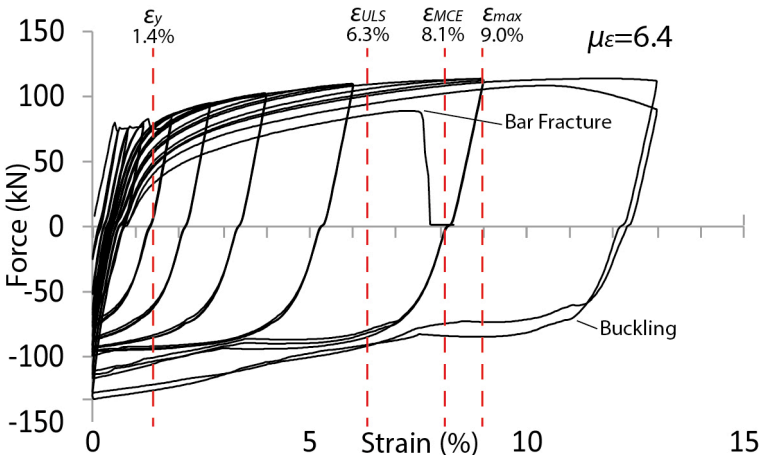

Figure 3.20: Preliminary test results of supported bar type dissipator

Advantages:

- Dry connection - no epoxy or grout required.
- Simple construction - similar to that of the BRF dissipators. Can be turned down on lathe accurately to required dimensions. Regular tube required.
- Good hysteretic behaviour under tension and compression.
- No significant increase in stiffness expected under negative net deformations, provided sufficient support points are provided.

Disadvantages:

- Non-continuous buckling restraint of bar. Higher buckling modes may occur although this can be avoided with sufficient support points.
- Larger overall length of dissipator required to achieve same total length of reduced section.

3.3.5 Groove Type

The groove type dissipator (Figure 3.21) is the last of the 'dry' type dissipators tested, and the selected dissipator for use in Controlled Damage testing (Chapter 5). It features a bar with a number of grooves milled along the length of the bar. A regular confining tube is placed over the grooved bar to provide continuous buckling restraint along the length of the bar.

The number and depth of grooves is such that the same net cross sectional area is achieved as in previous dissipators. The length of groove is also equal to the length of reduced cross section in previous dissipators. The number and depth of grooves can be altered depending on requirements as shown in Figure 3.22. If too deep a groove is required to achieve the desired net area, the overall bar diameter may be reduced or the number of grooves may be increased. Further investigation is required to determine the most effective cross sections arrangement, including maximum allowable groove depth for a given bar diameter.

A potential issue for this type of dissipator is low cycle fatigue of the steel, which may be more prevalent in this type of connection due to the sharp angles in the reduced section of the dissipator. This may be mitigated against by smoothing the cross sectional profile of the bar. Further investigation into low cycle fatigue and fracture mechanics of the dissipator is required to fully understand and mitigate against these potential issues.

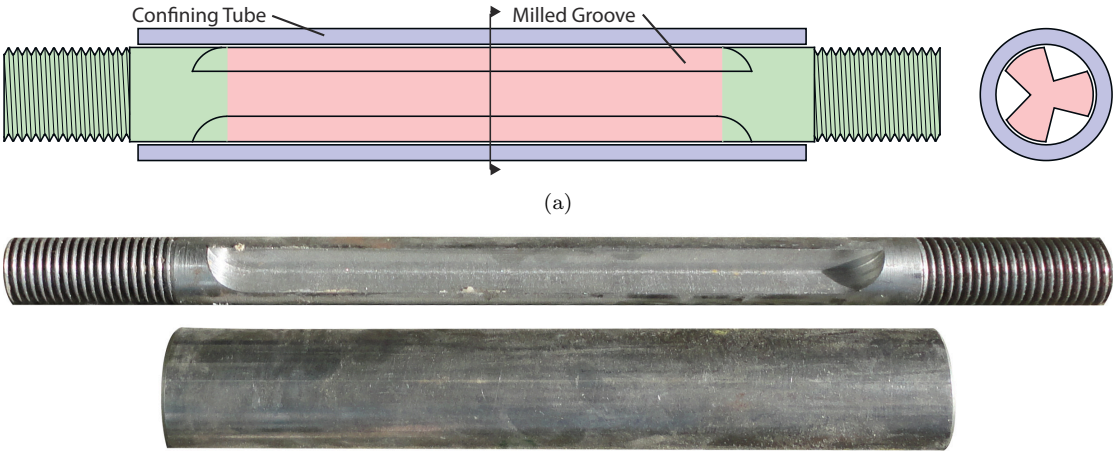

(a)

(b)

Figure 3.21: Grooved bar type dissipator

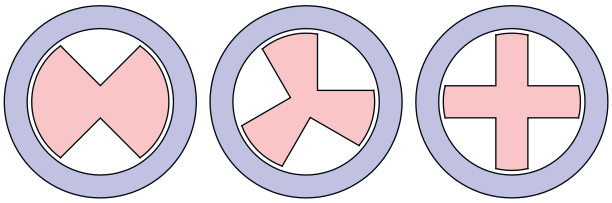

Figure 3.22: Variations to number and depth of grooves

Like previous tests, the grooved bar type dissipator completed the 9% strain cycle with no failure or sign of buckling as shown in Figure 3.23. Very stable hysteresis loops were observed before bar fracture occurred at the centre of the reduced length during the second cycle of the 13% strain limit. Like the previous 'dry' dissipator types, an increase in stiffness is not expected under negative net loading, especially since space for accomodation of the increase in cross sectional area due to the Poisson effect is provided in the grooves.

The maximum completed strain cycle, ε_{max}, was 9% with a yield strain, ε_y, of 1.3%. This corresponds to a strain ductility, μ_ε, of 6.9 using Equation 3.3. Using the strain limits from Equations 3.4 and 3.5, $\varepsilon_{_{ULS}} = 6.3\%$ and $\varepsilon_{_{ULS}} = 8.1\%$.

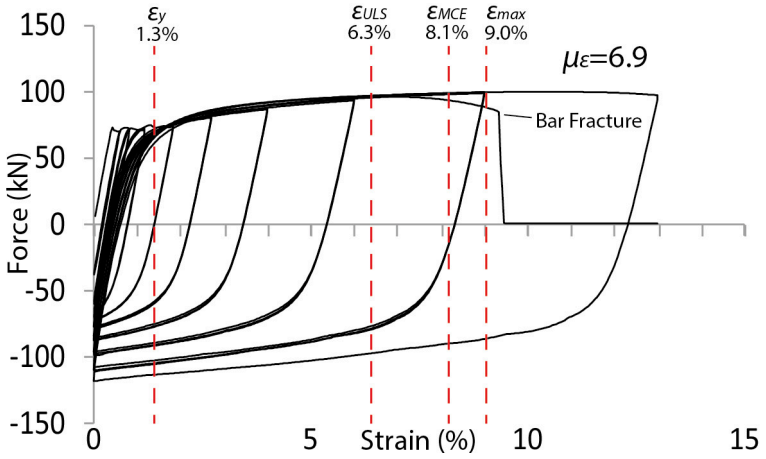

Figure 3.23: Preliminary test results of grooved bar type dissipator

In Controlled Damage testing (Section 5.3.5c), premature failure of grooved dissipators occurred due to a detailing error where there was an overlap of threaded and grooved lengths of the dissipator (Figure 3.24). Bar fracture occurred in this overlapped region. Therefore, it must be ensured that sufficient length of full diameter bar is provided between the threaded and grooved regions of the bar.

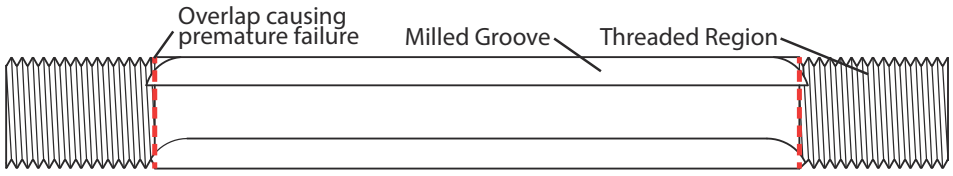

Figure 3.24: Overlap of grooved and threaded regions leading to premature failure

Advantages:

- Dry connection - no epoxy or grout required.
- Simple construction - Can be constructed on a mill with no specialised machinery.
- Regular tube required with no variation in diameter.
- Good hysteretic behaviour under tension and compression.
- No significant increase in stiffness expected under negative net deformations.
- Good buckling restraint. Continuous contact between bar and tube.

Disadvantages:

- Potential for low-cycle fatigue issues. This may be overcome with further research and optimisation of detailing.

3.4 Conclusions

Promising results were obtained in the testing of novel buckling-restrained fused mild steel energy dissipators. These dissipators feature a dissipating mild steel bar which yields in both tension and compression. Buckling restraint is provided through the use of a confining tube, which provides lateral support to the bar under compressive loading. The novel options presented were split tube, deformed tube, supported bar and grooved bar type dissipators. All four offered the advantage over conventional BRF type dissipator design of 'dry' fabrication, meaning no grout or epoxy filling material was required between the dissipating bar and confining tube. An additional advantage is the ability of the dissipator to undergo net negative displacements without significant increases in stiffness as occurs in BRF type dissipators [Sarti et al., 2013].

The dissipators were subjected to cyclic tension-compression loading until failure, with three cycles completed at each strain limit. The exception to this testing regime was the split tube type dissipator, which was cyclically loaded up to a strain of 7.5% before being subjected to monotonic loading until failure.

- The split tube dissipator successfully completed the 7.5% drift cycle and went onto achieve an ultimate strain capacity of 18% before bar rupture. It is expected that the dissipator would have successfully completed the 9% drift cycle, had it been applied.
- Based on the maximum achieved drift cycle of 7.8%, ϵ_{max} and the yield strain, ϵ_y of 1.3%, the dissipator achieved a strain ductility, μ_ϵ, of 5.8. Assuming strain limits of $70\%\epsilon_{max}$ for the ULS case and $70\%\epsilon_{max}$ for the MCE case, the strain limits assumed for design are 5.3% and 6.8%, respectively which is similar to values assumed in the design of PRESSS structures [Pampanin et al., 2010].
- The deformed tube, supported bar and grooved bar type dissipators all successfully completed the 9% strain cycle with strain ductilities, μ_ϵ, of 5.3, 6.4 and 6.9, respectively.
- Based on the maximum achieved drift cycle of 9%, the strain limits for these dissipators is assumed to be 6.3% for the ULS case and 8.1% for the MCE case.
- The reduced strain ductility of the deformed tube dissipator was caused by an increased yield strain. The yield strain of the dissipating bar may have been affected by the fabrication process used for the dissipator, which included heating and deformation of the confining tube.
- The supported bar type of dissipator exhibited good behaviour in the drift cycles

corresponding to the assumed ULS strain limits. However, buckling of the dissipating bar occurred during larger strain cycles. This buckling is undesirable as it can accelerate the initiation of low cycle fatigue failure in the bar. Increasing the number and width of supporting points along the length of the dissipating bar will limit this buckling effect by reducing the effective length of the dissipator.

- The grooved bar dissipator showed very good behaviour in both tension and compression with no signs of buckling. The main advantage of the grooved bar dissipator over the other designs is the continuous support of the dissipating bar along its length without the need for a confining tube of varying internal diameter, which greatly simplifies the fabrication process.

Further development and testing of each of the new dissipator designs is required to fully understand their behaviour and investigate factors such as low cycle fatigue in more detail. This is important for the grooved bar dissipator in particular S which may be particularly susceptible to low cycle fatigue failure due to the sharp cross sectional profile of the dissipator.

Chapter 4

Development and Testing of High Damage Pier Systems

4.1 Introduction

This chapter presents the development and testing of two precast connection types for bridge substructures which emulate the behaviour of cast-in-place connections through the formation of plastic hinges in the column elements. Since the formation of plastic hinges results in damage to both concrete and reinforcing steel in the connection, along with residual drift of the structure, these types of connections are defined as High Damage (HD) connection types.

Two types of ABC HD connections are presented. The first is named the HD Grouted Duct Connection (GDC) (Figure 4.1b) and the second is named the HD Member Socket Connection (MSC) (Figure 4.1d). Four columns were tested in the first phase of column testing as summarised in Table 4.1. These tests formed the benchmark for evaluation of Controlled Damage (CD) connection types in Chapter 5.

This chapter presents the prototype structure and testing arrangement used for both the HD and CD connection types. Design, detailing, construction and testing of the HD columns is then presented.

Test Name	Primary Connection	Section Shape	Testing Protocol
HDS1	Grouted Duct Connection	Square	Uniaxial
HDS2	Grouted Duct Connection	Square	Biaxial
HDC1	Member Socket Connection	Circular	Uniaxial
HDC2	Member Socket Connection	Circular	Biaxial

Table 4.1: Summary of High Damage tests

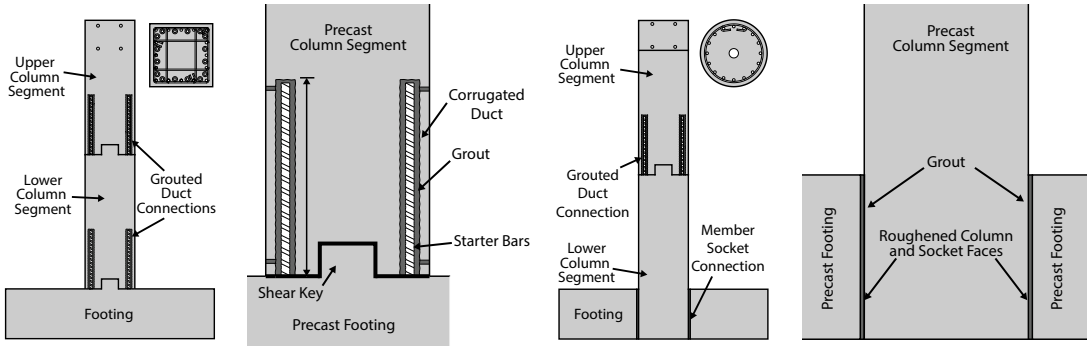

(a) HDS column type (b) Grouted Duct Connection (c) HDC column type (d) Member Socket Connection

Figure 4.1: High Damage test columns and connections

4.2 Prototype Structure Design

A prototype structure that is representative of a typical New Zealand highway bridge will be used as the basis for the development of the experimental test specimens. The prototype is illustrated in Figure 4.2 The longitudinal configuration of the prototype structure is based on Port Hills Overbridge 1 in Christchurch (-43.571096, 172.693392). This bridge was chosen as it presents a good example of typical 1970's bridge construction and is representative of the highway bridge stock in New Zealand. The bridge has six spans of an average length of 12 metres each giving an overall bridge length of 72 metres. For the prototype structure (Figure 4.2a), a height to the centre of mass of the superstructure of 5 metres was adopted with an overall width of 10.4 metres. Both circular and rectangular pier cross section shapes are considered for the prototype structure.

The deck configuration of the prototype structure is based on a standard deck system as specified in the NZTA Research Report 364 [NZ Transport Agency, 2008]. Prototype

A has a Double Hollowcore deck with a beam depth of 587 mm. Figure 4.2b shows the transverse configuration of the prototype structure.

The bridge is assumed to be situated on non-liquefiable soil. Specific footing details are not considered in the design of the prototype bridge however it is assumed that the footings are fully fixed. The axial load considered in the design and testing of the test columns is based on the dead load of the bridge deck without accounting for service loads acting in conjunction with earthquake loads.

Force based design was used to determine the design lateral loads for the prototype structure. The design was based on the method outlined in the New Zealand Bridge Manual Second Edition [NZ Transport Agency, 2003] and NZS1170.5 [New Zealand Standards, 2004]. Since design of the prototype structure, the New Zealand Bridge Manual Third Edition has been released which contains amendments to the seismic design of bridges, in particular the alignment of the forced based design methodology with that presented in NZS1170.5. Force based design was used as it offers a code compliant method of design and is the typical approach used in bride design in New Zealand. Displacement based design is an alternative to force based design in which displacement limits for the structure form the basis of design which is particularly useful for rocking type structures [Priestley et al., 2007]. Displacement based approaches for bridge design are to be included in future revisions of the Bridge Manual.

The parameters used for force based design are summarised in Table 4.2.

Hazard factor, Z	0.3
Soil class	C
Return period, T_R	1000 years
Return period factor, R	1.3
Near fault factor, N	1
Ductility, μ	3
Structural performance factor, S_p	0.7
Fundamental natural period, T	0.4 sec
Design lateral load, V	680 kN
Scaled lateral load V_{scaled}	170 kN
Design gravity load, W	1800 kN
Scaled gravity load, W_{scaled}	450 kN

Table 4.2: Force based design parameters

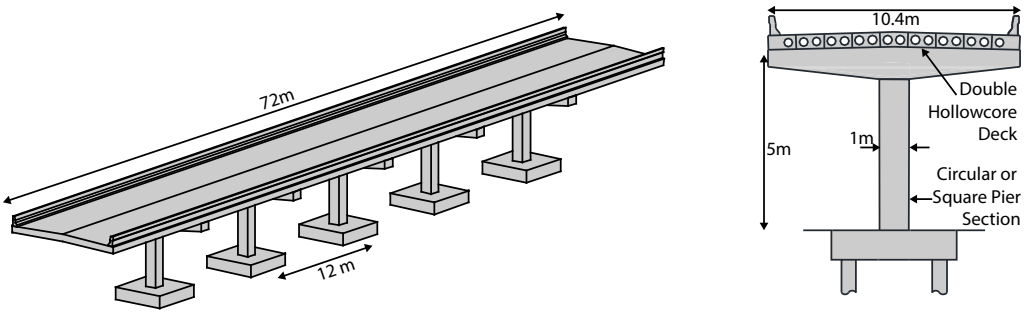

(a) Prototype bridge system (b) Prototype bridge pier

Figure 4.2: Prototype bridge system

4.3 Testing Arrangement

Half scale test columns were used to test the behaviour of each connection type under uniaxial and biaxial loading. Figure 4.3 shows how the loads acting in the bridge structure are represented in the half scale testing arrangement.

The uniaxial test case represents a structure where the bridge piers carry only the transverse seismic loads, with the bridge acting as a locked-in structure in the longitudinal direction where seismic loads are transferred to the abutments. The biaxial test case represents a structure in which both the longitudinal and transverse loads are carried by

the bridge piers. In the test arrangement, 400kN rams acting in the North-South (NS) and East-West (EW) directions are used to represent the longitudinal and transverse seismic loads in the structure, respectively.

A post-tensioned bar is used in the testing arrangement to represent the dead load of the superstructure applying axial load to the bridge pier. In later CD testing, the post-tensioned bar also represents post-tensioning in the brige structure. The post-tensioning in the test column consists of a post-tensioned bar running down the centre of the column. The bar is stressed using a hydraulic cylinder mounted on the top of the column, with a load cell used to monitor the post-tensioning load.

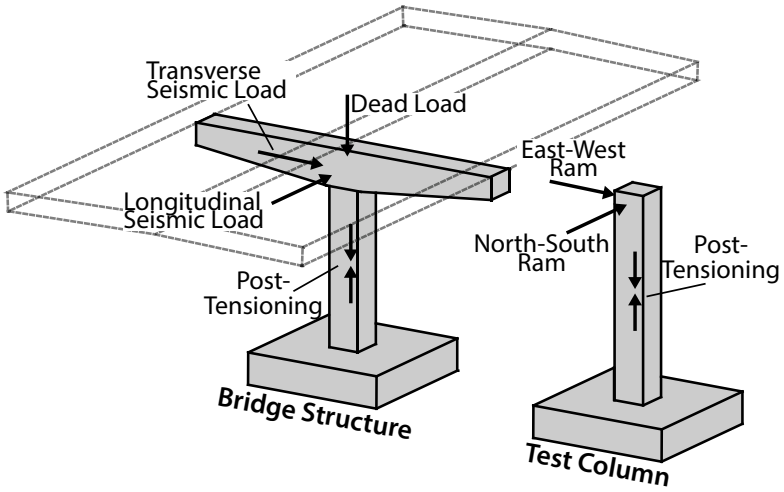

Figure 4.3: Representation of bridge loads in test arrangement

4.3.1 Uniaxial Loading Protocol

The uniaxial quasi-static loading protocol is illustrated in Figure 4.4b. The loading input consists of three cycles at each drift limit followed by a smaller cycle, with consecutive drift limits increasing by a factor of 1.2 to 1.5. The loading protocol was adopted from ACI reccommendations [ACI Innovation Task Group 1, 2001].

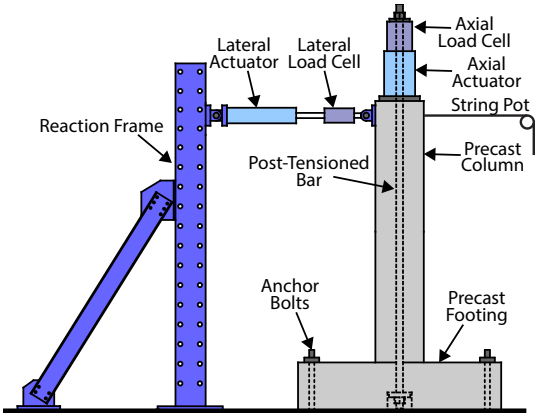

(a) Testing arrangement

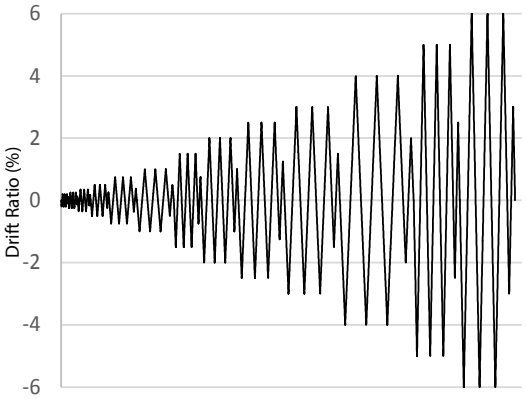

(b) Drift Input

(c) Uniaxial testing of HDC1

Figure 4.4: Uniaxial testing arrangement

4.3.2 Biaxial Loading Protocol

The biaxial quasi-static loading protocol is illustrated in Figure 4.5b. The same drift amplitude limits as used in uniaxial testing were applied to the biaxial loading protocol. Each drift cycle consisted of a uni-directional push and pull in the EW direction followed by the NS direction before simultaneously loading both directions resulting in a clover shaped drift path as illustrated in Figure 4.5e. The use of a clover shaped displacement path is a conservative approach as bridge piers are rarely subjected to equal loading in the longitudinal and transverse directions. Generally, the transverse direction demand will exceed that of the longitudinal direction as some or all of the longitudinal load is transferred through the superstructure to the bridge abutments as outlined in Section 4.3.

The radius **r** at any point during the clover loading path is equal to $r(\theta) = R.sin(2\theta)$. The **x** and **y** coordinates are given by $x(\theta) = r(\theta).cos(\theta)$ and $y(\theta) = r(\theta).sin(\theta)$, respectively. The maximum x and y displacements occur at $\theta = 35°$ and $\theta = 55°$, respectively, with the maximum resultant displacement of the column defined by **R** occurring at $\theta = 45°$. One complete biaxial cycle was applied to the test specimen at each drift limit. This resulted in three positive and negative excursions of both the NS and EW actuators during each drift cycle, similar to the uniaxial loading protocol. The loading regime is based on that used by Marriott [2009].

It should be noted that the drift limits stated for the biaxial input are for each actuator in the NS and EW direction. During the clover stage of the drift input, the maximum resultant drift of the column is larger than the stated drift limit for each actuator at 1.3 times the stated drift limit for the cycle. So during the 5% loading cycle for example, the column is subjected to a peak resultant drift of $1.3 \times 5\% = 6.5\%$.

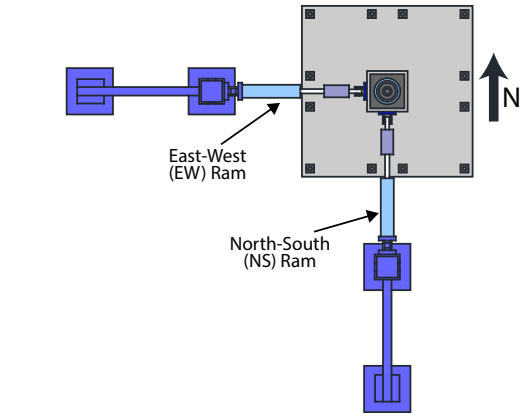

(a) Testing arrangement

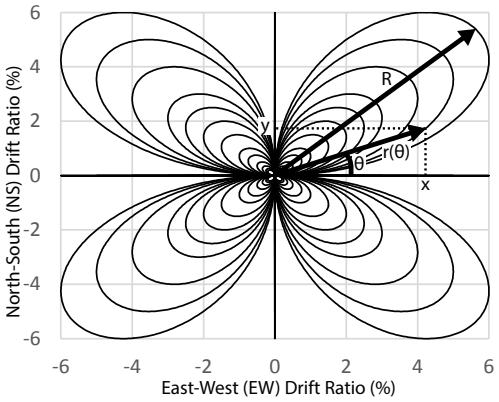

(b) Biaxial Drift Input

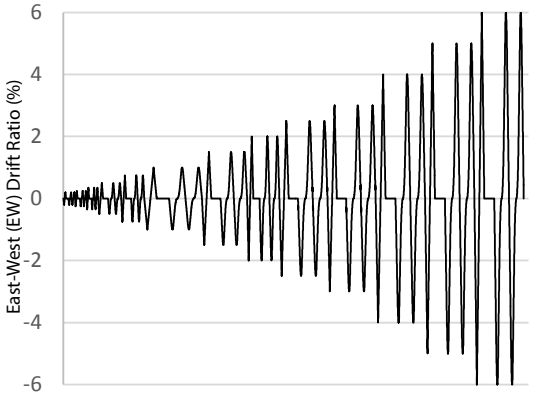

(c) East-West Drift Input

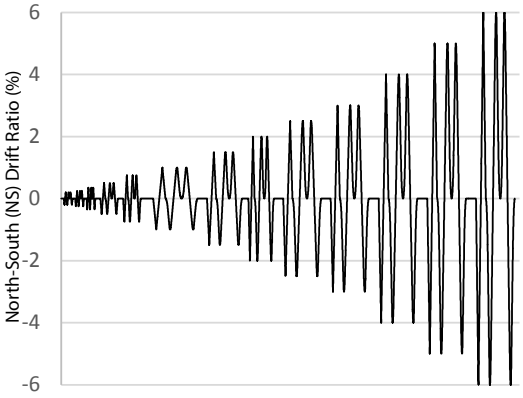

(d) North-South Drift Input

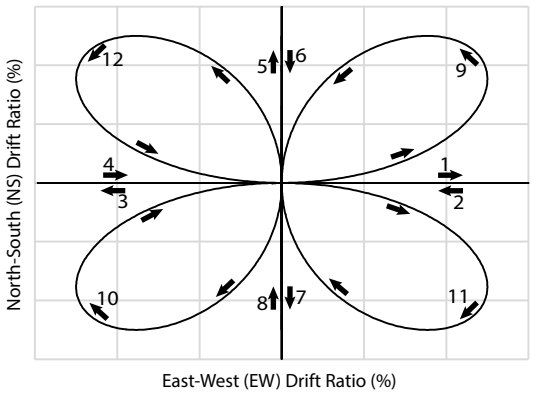

(e) Loading Sequence

Figure 4.5: Biaxial testing

4.3.3 Data Acquisition

a) Measuring Lateral Displacements

Lateral displacements in each direction were measured using string potentiometers fixed to a wall or steel frame which was independent of the reaction frame used for loading.

This eliminates any effect of reaction frame deformation on the results.

b) Measuring Lateral and Axial Loads

Lateral loads were measured using load cells that were mounted inline with the lateral loading rams. Axial loads were measured using a load cell located on the top of the column between the hollow hydraulic actuator and the top washer and nut of the post-tensioned bar.

c) Measuring Structure Deformation

Deformation of the column was measured using an array of rod end potentiometers located on the faces of the test column. These potentiometers measured the deformation of the column between two points, with the resolution of the data dependent on the spacing of these points. This deformation data was used to calculate curvature and neutral axis depth up the height of the structure. The array of potentiometers can be seen on the face of the column in Figure 4.4c with an additional array located on the adjacent face for biaxial loading.

4.3.4 Material Properties

Concrete of $f'_c = 40MPa$ at 28 days compressive strength was specified for all components of the HD columns. Grade 500 steel was specified for both the transverse and longitudinal reinforcement in all columns. Grout of $f'_c = 55MPa$ at 28 days was specified for grouting of GDCs and grout of $f'_c = 60MPa$ at 28 days was specified for grouting of MSCs.

The actual material properties at the time of testing are summarised in Table 4.3.

Material	**HDS1**	**HDS2**	**HDC1**	**HDC2**
Concrete - Footing	59	51	43	44
Concrete - Column	60	51	54	45
Steel - Longitudinal	516	516	516	516
Steel - Transverse	556	556	556	556
Grout	65	38	58	44

Table 4.3: Summary of High Damage material strengths (MPa)

4.4 High Damage Grouted Duct Connection

4.4.1 Connection Overview

The GDC is one in which the reinforcing starter bars extending from one precast element are inserted into ducts which are cast into a second element. Grout is pumped into the ducts through external tubes after assembly and alignment of the segments on top of each other, which bonds the two elements together. This type of connection accelerates the construction process as it eliminates the need for on-site concrete pouring, with the only wet work required being the formation of a grout bed between the segments and the pumping of grout which remains contained inside the ducts of the precast element.

This type of connection can be used for pile to pile cap, spread footing or pile cap to column, column to cap beam and for splices between the column segments or cap beam segments [Marsh et al., 2011]. Examples of the application of GDC between different precast members can be found in NCHRP Report 681 [Restrepo et al., 2011]. The grouted duct connection has had widespread use worldwide for these purposes, however it is typically used in capacity protected or low demand regions of the structure where the precast elements are likely to remain elastic during seismic loading. Although this type of connection isn't new, there has been limited research into application of the connection types in regions of moderate to high seismicity. Marriott [2009] demonstrated the use of GDCs in post-tensioned rocking connections with good results. This research project considers the GDC for use in non-post-tensioned connections of footing to column where plastic hinging is expected to occur and at the connection of column segments.

4.4.2 Design

Two half scale segmental columns which feature the GDC as the primary connection, HDS1 and HDS2, were tested. HDS1 was tested uniaxially while HDS2 was tested biaxially. GDCs were located at the interface between column and footing and between the two column segments.

The columns were designed in accordance with NZS3101 [New Zealand Standards, 2006b] and the New Zealand Bridge Manual [NZ Transport Agency, 2003] with the design loads obtained in Section 4.2. Based on the structural demand for the prototype structure, the pier was required to resist a lateral load of 170kN giving a moment demand of 425kNm at the base connection interface.The column was designed assuming a gravity load of 450kN, based on the tributary weight of the scaled prototype deck.

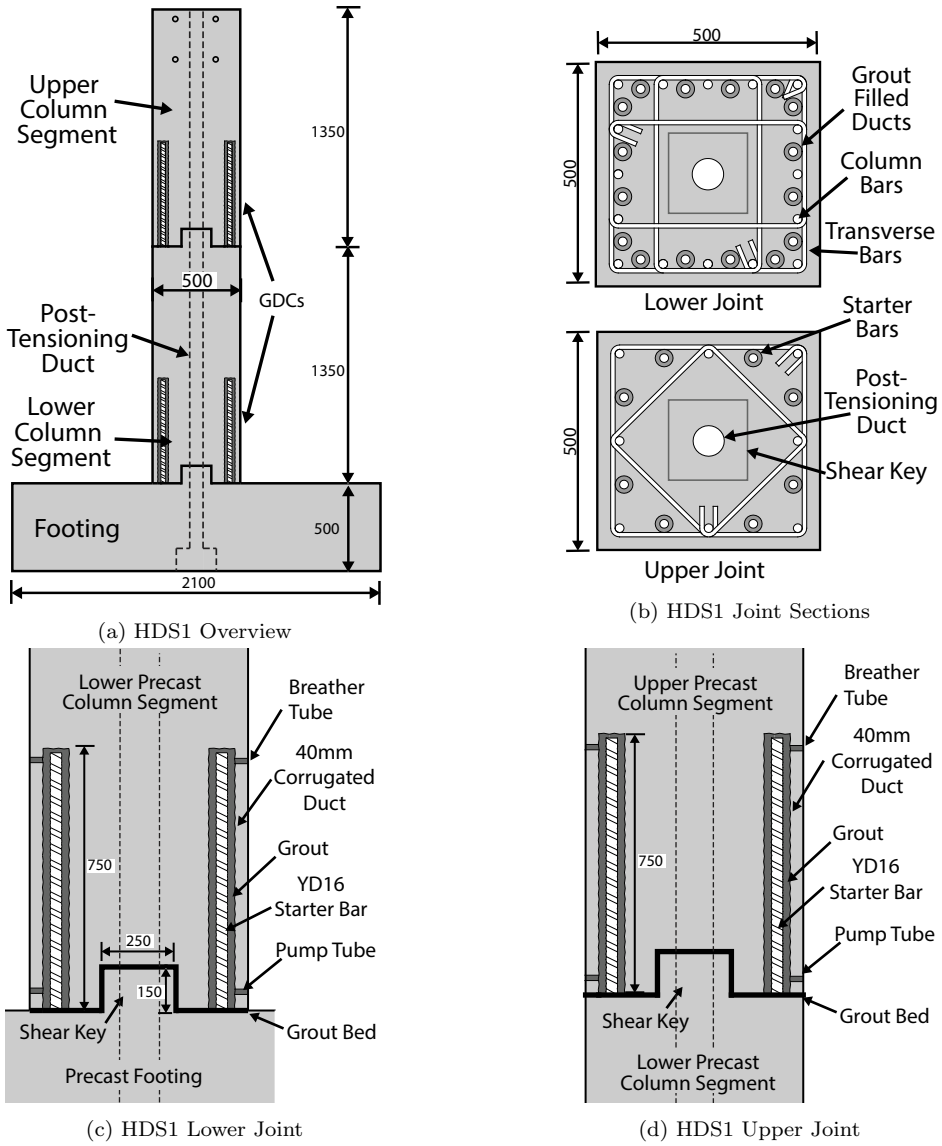

(a) HDS1 Overview

(b) HDS1 Joint Sections

(c) HDS1 Lower Joint

(d) HDS1 Upper Joint

Figure 4.6: HDS1 design

A total of 16-YD16 longitudinal bars were located at the lower connection (Figure4.6d while 8-YD16 bars were used at the upper connection (Figure 4.6d) due to reduced flexural demand. The longitudinal bars were grouted into corrugated steel ducts of 40mm diameter which were cast into the base of each column segment. YD10 stirrups at 50mm spacing were used to provide shear, confinement and anti-buckling capacity in the plastic hinge regions of the columns as specified in NZCS3101 [New Zealand Standards, 2006b]. A stirrup spacing of 100mm was used above the plastic hinge regions.

A 70mm diameter duct was located at the center of the column and footing to house the post-tensioned bar which was used to apply axial load to the specimen to simulate gravity loads in the structure. The post-tensioned bar remained unbonded over the full

length, with mechanical anchorages used at each end. It should be restated that in an actual bridge featuring HD connections, the duct and post-tensioned bar are included in the structure, with axial load being applied by the weight of the superstructure.

Column HDS2 featured some improved details over connection one. Firstly, armouring was added at the base of the column to protect against spalling damage of the precast concrete at the connection interface. The armouring consisted of 100x100x5 Equal Angle located around the bottom edges of the lower column segment. Secondly, the longitudinal starter bars were debonded over a length of 120mm, with the aim of reducing strain concentration effects at the connection interface which in turn increases the ultimate drift capacity of the structure. The design of these details is discussed further in Section 4.4.3.

Shear keys were located at both connections to transfer shear loads across the connection interface. In this instance, the contribution of dowel action of the longitudinal starter bars to shear capacity was neglected, with all shear load assumed to be carried by the shear key. The shear key was designed using shear friction principals as outlined in NZS3101 [New Zealand Standards, 2006b].

A 2.1 metre square footing with depth of 500mm was used at the base of the columns and was anchored to the floor using hold-down bolts. Footing reinforcement consisted of a top and bottom grid of YD16 bars at an average spacing of 150mm.

Technical drawings of the HDS columns are presented in Appendix A.

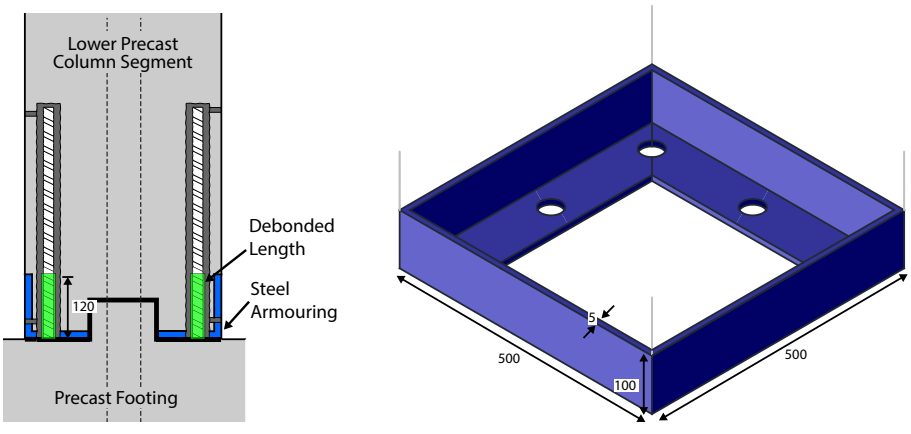

(a) HDS2 Lower Joint (b) HDS2 Armouring

Figure 4.7: HDS2 detailing

4.4.3 Detailing

Figure 4.8a shows the internal actions in the grouted duct connection under vertical loading, while Figure 4.8b shows the internal actions under lateral loading. Shear is transferred across the grouted duct connections through a combination of friction and bond in the grouted interface and bearing of the column against the shear keys. For design purposes, it was assumed that the shear load is transferred only through the shear key. The shear key was designed in a similar manner to a corbel using the principal of shear friction [New Zealand Standards, 2006b, Priestley et al., 1996].

Figure 4.9a shows the primary bond mechanism in the corrugated ducts, where tension loads in the column are transferred to the longitudinal starter bars extending from the footing. The primary transfer mechanism in the duct is through bearing of the deformations of the corrugated duct and reinforcing bar against the surrounding grout and concrete. Only a small amount of stress is transferred through chemical adhesion and friction between the steel and surrounding concrete or grout [Brenes et al., 2006, Raynor et al., 2002]. It is for this reason that a corrugated duct must be used in this application. The use of a straight pipe with no corrugations would mean no interlock of the grout and concrete keys leading to greatly reduced ultimate bond strength. The effects of duct size and material on connection performance is further explored by Brenes et al. [2006].

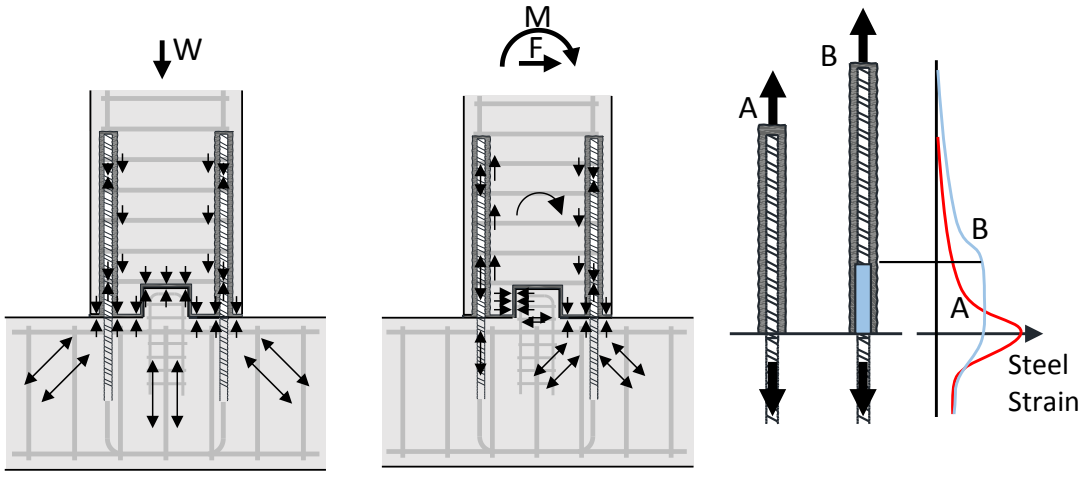

(a) Vertical internal actions (b) Lateral internal actions (c) Effect of debonding

Figure 4.8: Grouted Duct Connection internal actions and effect of debonding

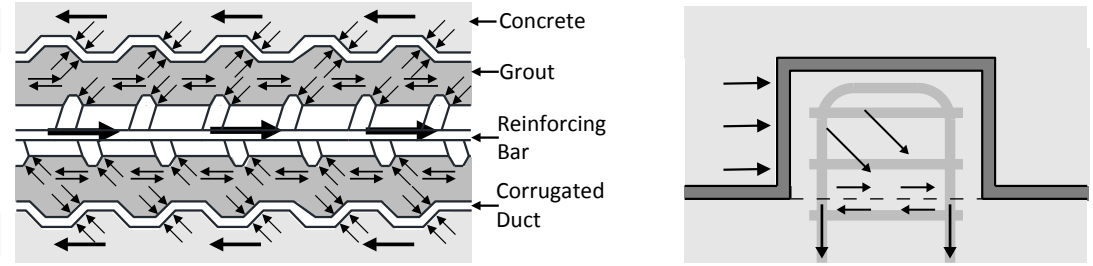

(a) GDC bond mechanism in duct

(b) Shear key internal actions

Figure 4.9: Grouted Duct Connection bond mechanism and shear key detail

The corrugated duct provides confinement to the grout surrounding the bar, enhancing the strength of the grout and increasing the ultimate bond strength of the bar Raynor et al. [2002]. This means that full transfer of stress from the surrounding concrete to the reinforcing bar can occur over a shorter length that is achieved in a conventionally reinforced column. However, in this research, the full development length for the bars as specified in NZS3101 [New Zealand Standards, 2006b] was allowed for. The increased bond strength leads to a lower length of strain penetration at the connection interface.

As the column displaces during lateral loading, the largest cracks occur at the interface of the column and footing. Since no tension load is carried across these cracks by the concrete, the steel must carry the load. A shortened length of strain penetration caused by duct confinement means a shorter length of bar is accommodating the total deformation of the bar. This leads to strain concentrations in the bar at the connection interface [Raynor et al., 2002]. This is illustrated by Line A in Figure 4.8c. Strain concentrations lead to a reduction in ultimate drift capacity and larger peak strains reduce the ductility capacity of the bar, reducing the number of cycles until failure [Coffin, 1954, Mander et al., 1994, Manson, 1953, Stanton et al., 2005].

Kawashima et al. [2001] studied the effects of unbonded length on reinforced concrete columns. The study concludes that the failure of concrete in the column with unbonded length was significantly less than the column in which the full length of the rebars was bonded and that the unbonded length can enhance the ductility of the concrete bridge columns. The use of an unbonded length at the connection interface helps to mitigate the effect of strain penetration by spreading the total longitudinal deformation of the bar over a larger length, reducing the peak strain in the bar. This is illustrated by Line B in Figure 4.8c.

It should be noted that providing unbonded length also increases the yield drift of the column. However, it has been observed that the increase in yield drift is generally less than the increase in ultimate drift capacity, which means a higher level of displacement ductility at the failure point of the column is achieved overall. The required unbonded length for the bars in specimen SQ-2 was estimated from the results of the testing of specimen SQ-1.

The plastic hinge length, L_p for a conventional monolithic column can be estimated using:

$$L_p = 0.08L_{cant} + l_{sp} \tag{4.1}$$

Where L_{cant} is the distance from the footing face to the point of contraflexure in the column and l_{sp} is the strain penetration length. In a conventional column where the bars are not enclosed in ducts, the strain penetration length is defined by Priestley and Park (1984) as follows:

$$l_{sp} = 0.022d_b f_y \tag{4.2}$$

where d_b is the bar diameter and f_y is the yield strength of the bar. For a 2.5 metre tall column with 16mm diameter, grade 500 bars, we would expect a strain penetration length of 176mm and a plastic hinge length of 376mm. Re-arranging equation 1 gives:

$$l_{sp} = L_p - 0.08L_{cant} \tag{4.3}$$

This allows the strain penetration length to be estimated from a plastic hinge length observed during testing.

Testing of the first grouted duct connection with no unbonded length left at the connection interface showed the plastic hinge length to be approximately 250mm. This gives a length of strain penetration of just 50mm which is considerably less than the 176mm that would be expected of the same longitudinal bar without the confinement provided by the duct. Using these values, it was estimated that an unbonded length of 120mm would give an effective length of strain penetration of approximately 170mm,

leading to similar behavior from the grouted duct connection as would be expected in a conventional monolithic connection.

A more accurate method for determining the required unbonded length is to consider the connection as a rocking interface as outlined in the NZCS PRESSS Design Handbook [Pampanin et al., 2010], where sufficient unbonded length is provided to limit the strain in the reinforcing bars to less than 5%.

Armouring was included in the construction of the HDS2 column at the interface between the column and footing. Its purpose was to limit damage to the concrete at the base of the column and provide buckling restraint to the longitudinal bars at the base of the column. Protecting the concrete enhances column performance especially at higher levels of drift as the full section can act in compression with limited spalling.

The armouring was designed using a concrete confinement model [Mander et al., 1988] targeting a confinement ratio of:

$$\frac{f'_{cc}}{f'_c} = 1.25 \tag{4.4}$$

where f'_{cc} is the confined concrete compressive strength and f'_c is the unconfined concrete compressive strength. The confined compressive strength is found using:

$$f'_{cc} = f'_c(-1.254 + 2.254\sqrt{1 + \frac{7.94f'_l}{f'_c}} - 2\frac{f'_l}{f'_c} \tag{4.5}$$

where f'_l is the effective lateral pressure from the armouring. For a confinement ratio of 1.25, f'_l is equal to 1.58MPa. f'_l is found using:

$$f'_l = k_e f_l \tag{4.6}$$

where f_l is the lateral pressure from the armouring and k_e is the confinement effectiveness coefficient. For a square column, k_e is equal to 0.33 giving $f_l = 4.74MPa$ in this case. f_l is defined as:

$$f_l = \frac{A_s f_y}{hb} \tag{4.7}$$

where $A_s = 2ht$ meaning equation 4.7 can be rearranged to find required armouring wall thickness, t:

$$t \geq \frac{2.37b}{f_y} \tag{4.8}$$

Hence, for a column with a square cross section of 1000mm assuming $f_y = 300MPa$, the required wall thickness is equal to:

$$t \geq \frac{2.37 \times 1000}{300} = 7.9mm \tag{4.9}$$

Note that this equation is independent of armouring height, h, therefore an appropriate height should be selected. For the HDS2 column, an armouring height of 100mm was used, however a larger height may have been more effective at preventing corner spalling during biaxial loading.

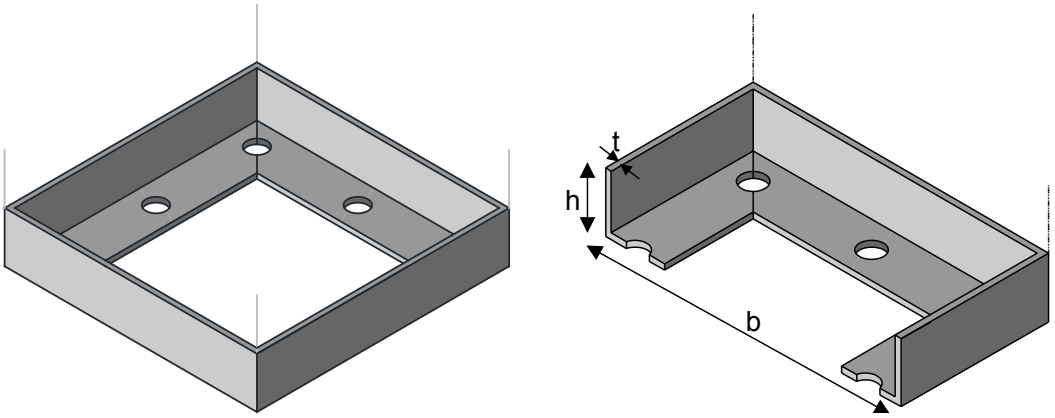

(a) (b)

Figure 4.10: HDS2 armouring detail

4.4.4 Construction

Figure 4.11a shows the corrugated duct that was cast into the column segments. The footing and two column segments of the HDS columns were all cast as separate elements using 40 MPa concrete with 100mm slump. A plywood template was used to ensure good alignment of the starter bars and drossbachs between all elements at both connection interfaces. The column elements were poured horizontally in plywood formwork (Figure 4.11b). Figure 4.11c shows pouring of the footing concrete with the starter bars supported by the plywood template. Figure 4.11d shows the column segments after pouring with starter bars extending from the top of the column segment. Figures 4.13a and 4.13c show the precast components after casting.

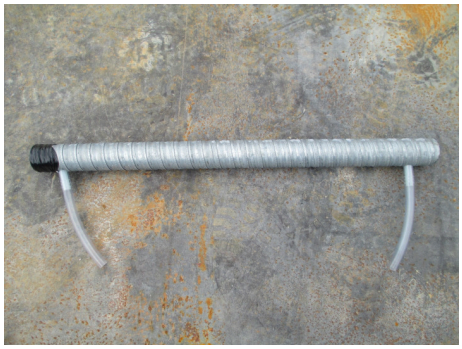

(a) Corrugated duct

(b) Column reinforcement in formwork

(c) Pouring of footing

(d) Column segments after pouring

Figure 4.11: Casting of HDS1 column

The lower column segment was placed on top of the footing, aligning the starter bars from the lower column with the drossbach ducts in the upper column (Figure 4.13d). Shims were positioned to ensure the segment was properly aligned. The upper segment was then lifted allowing a grout bed to be formed between the two elements (Figure 4.12a). A foam torus with a bead of silicon caulk was used to seal the centre duct to avoid leakage of grout (Figure 4.13b). If match casting were used during precasting of componenets, shims and a grout bed would not be required and instead a thin layer of epoxy would be applied between the elements. The segment was then lowered onto the shims, displacing any excess grout from the grout bed (Figure 4.12b). The same procedure was followed for the connection between upper and lower segments.

Some alignment issues were met while trying to align the starter bars and corrugated ducts. This misalignment is a risk that must be considered with the GDC [Marsh et al., 2011]. Mitigation methods include thorough checking of alignment during casting of components, and provision of sufficient duct diameter to allow tolerance with the alignment of starter bars and ducts.

After both column segments were placed, the connections were ready for grouting. The corrugated ducts of both connections were filled with water (Figures 4.12c and 4.12d) and then flushed prior to grouting to remove any debris and help the grout to flow (Figure 4.12e). This also allowed any leaks to be plugged prior to grouting and gave an idea of the volume of grout required to fill the connection. A water plugging mortar was used to stop any leaks. Grout was then pumped into the lower fill tube (Figure 4.12f) and allowed to flow upwards and out of the upper breather tubes at each joint. Pumping of grout continued until good grout could be seen flowing out of all breather tubes (Figure 4.12g). At this point, all tubes were closed off and the grout was allowed to cure (Figure 4.12h). The fully constructed column is shown in Figure 4.13e.

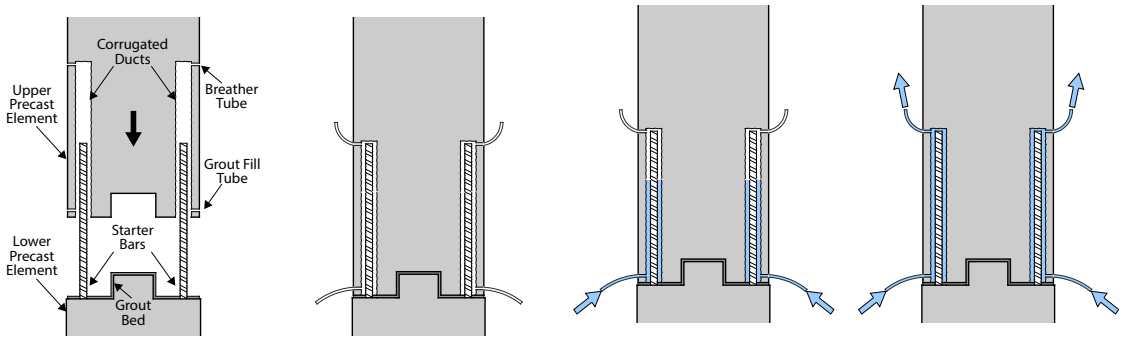

(a) Grout bed formed (b) Upper segment placed (c) Water pumped into ducts (d) Water pumped until flowing out of top tubes

(e) Water drained (f) Grout pumped into ducts (g) Grout pumped until grout flows out top tubes (h) Pump tubes blocked off

Figure 4.12: Grouted Duct Connection assembly process

(a) Column footing

(b) Foam Torus

(c) Column segments after casting

(d) Column segment being placed

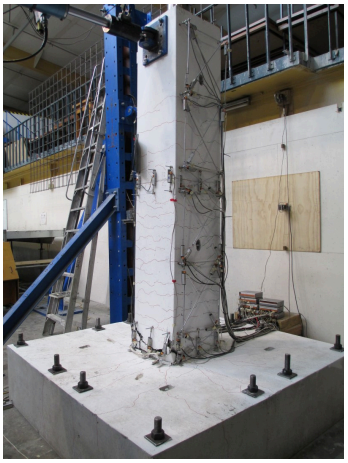

(e) Assembled column

Figure 4.13: Assembly of HDS1 column

4.4.5 Testing

a) HDS1

Column HDS1 was tested uniaxially. Minor flexural cracking of the grouted joint at the base of the columns initiated at a drift of 0.35%. Further cracks appeared throughout the segments during the 0.5% drift cycle and increased in density throughout larger cycles with no significant increase in width. The width of the majority of cracks remained less than 0.4mm during testing with most of the deformation in the column constrained to the grouted regions of the column. 7mm of gap opening occurred between column and footing at 3% drift (Figure 4.14c). Some gap opening also occurred at the upper joint during larger levels of drift, however the gap closed following loading with no sign of spalling. All cracks were marked during testing, with the distribution shown in Figure 4.14a.

Spalling of concrete occurred during the 3% drift cycle (Figure 4.14b) corresponding to the ULS performance level. The extent of spalling increased during the 4% drift cycle reaching a height of approximately 200mm above the top face of the footing. At the end of testing, spalling had occurred up to a height of 250mm from the base of the column located mainly on the northern and southern corners and faces (Figure 4.14d).

Longitudinal bar failure occurred during the first cycle of the 5% drift limit as the column reached its maximum drift corresponding to the MCE performance level. Buckling of the longitudinal bars occurred during the 5% drift cycle between the footing and lowest column stirrup as shown in Figure 4.14e. This may have contributed to bar failure through low cycle fatigue.

(a) Column at point of failure

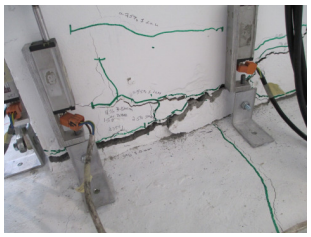

(b) Initial spalling of column at 3%

(c) Gap Opening at 3%

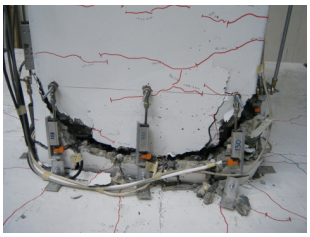

(d) Spalling of column at 5% drift

(e) Buckled longitudinal bars

Figure 4.14: Performance of HDS1 column during testing

b) HDS2

Column HDS2 was tested biaxially. Although the column was put through a more demanding loading cycle, the performance was similar to that of the HDS1 column. Cracking initiated during the 0.25% drift cycle and was of a similar distribution as HDS1. Figure 4.15a shows the column following testing.

The armouring was effective at limiting spalling in the column with spalling of the corners of the column occuring during the 2.5% loading cycle (3.25% resultant drift, ULS performance level) as shown in Figure 4.15b. This performance is essentially the same as the HDS1 column despite being subjected to biaxial loading. At the end of

testing, spalling had occurred up to a height of 250mm from the base of the column located mainly at the corners of the section (Figure 4.15d).

Bar failure occurred during the 5% drift cycle (6.5% resultant drift, MCE performance level) which is larger than the failure point of the HDS1 column indicating that debonding was effective in limiting longitudinal steel strains and increasing the ultimate drift capacity of the column. It appeared that bar buckling had been prevented through the use of armouring however upon disassembly it was found that some buckling had occured in the parallel direction to the column faces.

(a) Column at point of failure

(b) Spalling of column at 2.5%

(c) Gap opening at 5%

(d) Spalling at 5%

Figure 4.15: Performance of HDS2 column during testing

4.4.6 Results and Discussion

a) HDS1 - Uniaxial Testing

From the load-drift plot (Figure 4.16) it can be seen that the column yielded at a drift of 0.75% corresponding to a displacement ductility of 4 at the ultimate limit state when spalling initiated. At the point of failure, the displacement ductility was over 6. Large residual displacements were observed for drift cycles larger than the yield drift with the residual displacement equaling greater than half the peak displacement for the 4% and 5% drift cycles.

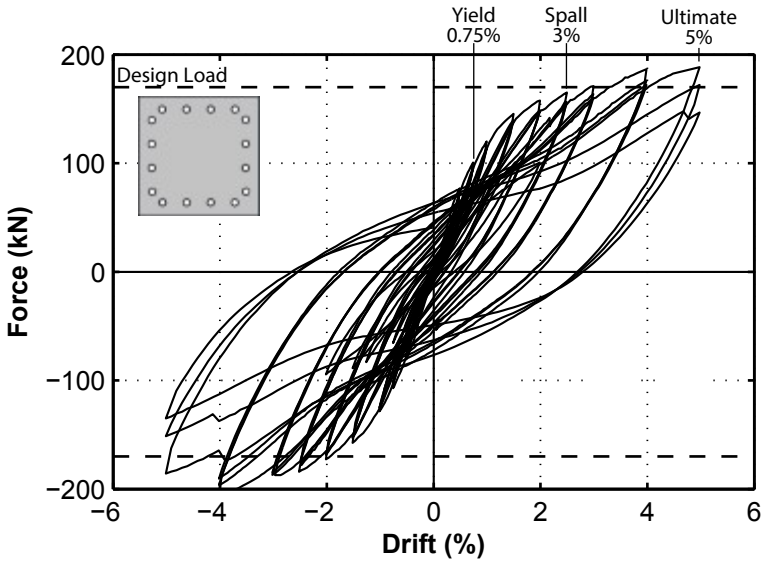

Figure 4.16: HDS1 force-drift response

The column achieved a peak lateral load of 205kN corresponding to a moment capacity of 510kNm. This is larger than the design lateral load of 170kN. Figure 4.17 shows the moment curvature behavior of the column.

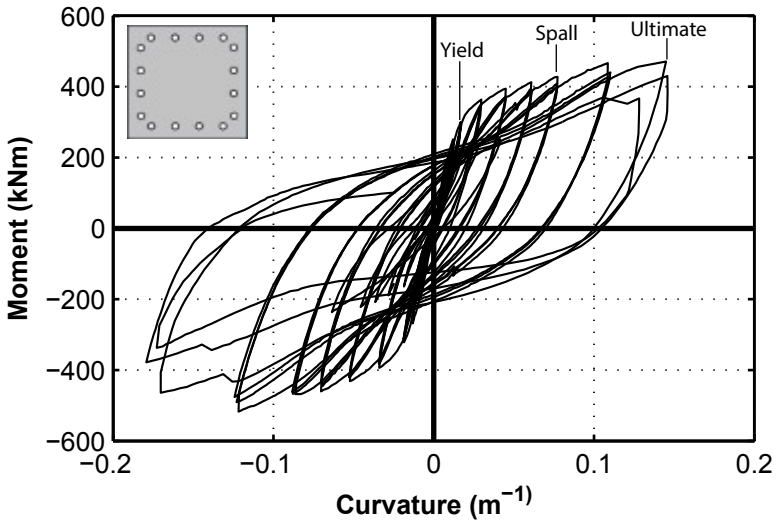

Figure 4.17: HDS1 moment-curvature response

Upon inspection following disassembly, it was found that grout had flowed into the central duct causing the post-tensioned bar to become bonded across the interface between the footing and column. As the column was displaced, there was no load increase in

the post-tensioned bar indicating that the bar was fully bonded across the interface where most of the deformation was observed. This meant that the axial load provided by the post-tensioned bar was only acting in the column above the interface between footing and column with no axial load being transferred to the footing. Bonding of the post-tensioned bar leads to it behaving as a bonded reinforcing bar which leads to an increased post-yield stiffness as the bar load increases with increasing drift.

Figure 4.18 shows the distribution of curvature up the height of the column at the peak of each drift cycle. Increased levels of curvature can be seen at both the base of the column along and at the joint between the two column segments. This indicates that inelastic deformation occurred at both connection interfaces, although the majority of deformation occurred at the base joint. Inelastic deformation of the upper joint was not intended, but could be used to increase the energy dissipation capacity of the structure as well as allowing for a higher level of ultimate drift to be achieved through distribution of inelastic deformation.

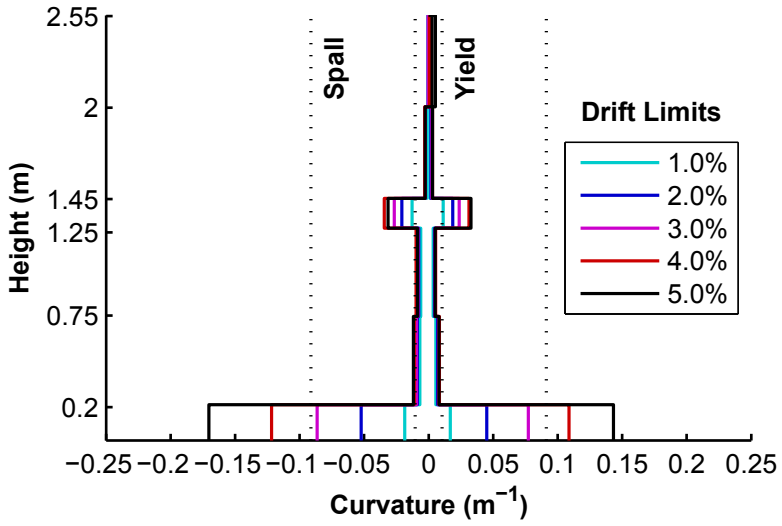

Figure 4.18: HDS1 curvature distribution

The curvature distribution shows the majority of deformation occurred in the lower 200mm of the column height with curvatures above this region indicating elastic behaviour until the upper joint. This observation correlates with the observed plastic hinge length of 250mm which is the height to which spalling extended.

Figure 4.19 shows the area based hysteretic damping of the column at increasing levels of displacement ductility. This was calculated from the loop areas of the force-drift hysteresis plot using Equation 4.10.

$$\xi_{hyst} = \frac{A_h}{2\pi F_m \delta_m} \tag{4.10}$$

Where A_h is the area of the hysteresis loop found through integration, F_m is the peak force of the loop and δ_m is the peak displacement of the loop.

A correction factor was applied to the area based damping values to obtain time-history-calibrated, equivalent viscous damping [Priestley et al., 2007].

$$\frac{\xi_{THA}}{\xi_{hyst}} = -0.018\xi_{hyst} + 0.0875\mu + 0.723 \tag{4.11}$$

The corrected experimental damping curve was plotted alongside theoretical hysteretic damping curves for Takeda Fat and Takeda Thin hysteresis rules based on the Dwairi-Kowalsky damping rule [Dwairi et al., 2007]. The general form of the theoretical curves is:

$$\xi_{hyst} = C\left(\frac{\mu - 1}{\mu\pi}\right) \tag{4.12}$$

It was assumed that $C = 50$ for the Takeda Thin curve and $C = 60$ for the Takeda Fat curve.

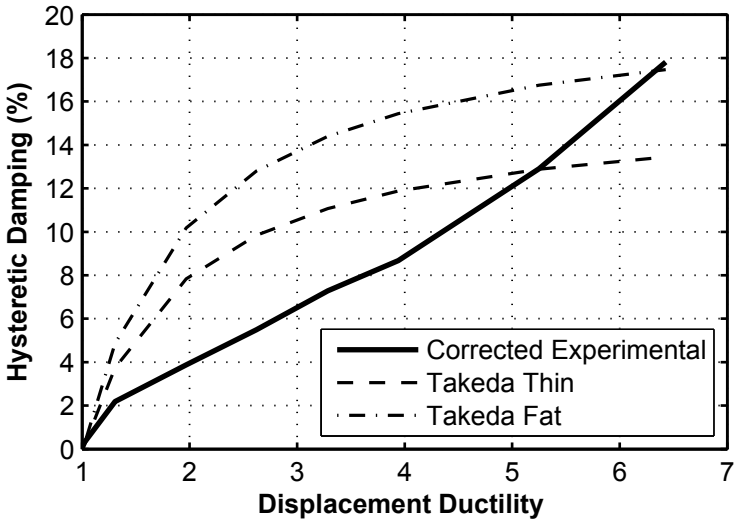

Figure 4.19: HDS1 area based hysteretic damping

A relatively linear trend between hysteretic damping and ductility was observed. The hysteretic damping observed from the experiment is lower than that of the Takeda Thin curve, up until a ductility of 5.2. For ductilities higher than 5.2, the experimental curve lies between the Takeda Fat and Thin curves, reaching a value of 18% at the failure point of the column.

This damping relationship was used to evaluate the performance of the column using an Acceleration Displacement Response Spectrum (ADRS) [Marriott, 2009]. The experimental data was normalised to units compatible for comparison with ADRS by dividing applied lateral force by the design axial load for each pier.

The elastic ADRS curves were generated using Standard NZS1170.5 [New Zealand Standards, 2004] for return periods of 25 years, 1000 years and 2500 years corresponding to the Servicability Limit State (SLS), Ultimate Limit State (ULS) and Maximum Credible Earthquake (MCE) limit states, respectively. The displacement values for each curve were divided by two to account for the scale factor of 0.5 used for experimental testing.

The damped ADRS curves were obtained through application of a reduction factor (η) that is a function of equivalent viscous damping [Priestley et al., 2007]:

$$\eta = \sqrt{\frac{0.07}{0.02 + \xi_{eq}}} \tag{4.13}$$

$$\xi_{eq} = \xi_{hyst} + \kappa\xi_{el} \tag{4.14}$$

where $\kappa\xi_{el}$ is the elastic component of equivalent viscous damping given by:

$$\kappa = \mu^{\lambda} \tag{4.15}$$

$$\xi_{el} = 5\% \tag{4.16}$$

λ is the ductility at the drift being considered. λ represents the tangent stiffness of the system and is assumed to be $\lambda = -0.378$ for a Takeda Thin system. For flag-shaped systems, a value of $\lambda = -0.544$ is assumed.

Figure 4.20 shows the ADRS performance evaluation for HDS1. The intercept points between the backbone curve and ADRS curves represented by crosses on the plot indicate the performance of the system that is expected for each hazard level. It can be seen that at SLS, the column will reach a peak drift of 0.2% which is well within the elastic range of the structures response. An ULS limit earthquake will generate a drift of 2.4% drift while a MCE limit earthquake will generate a 3.8% drift. The ULS drift response is less than the value of 3% adopted for design of the structure. It should be noted that a higher than expected post-yield stiffness was observed in the response of the structure due to the grouting of the post-tensioned bar during construction. If it wasnt for this error, it is expected that a lower post-yield stiffness would be observed and the drift at the ULS state would be close to the design value of 3% as observed in the MSC test HDC1.

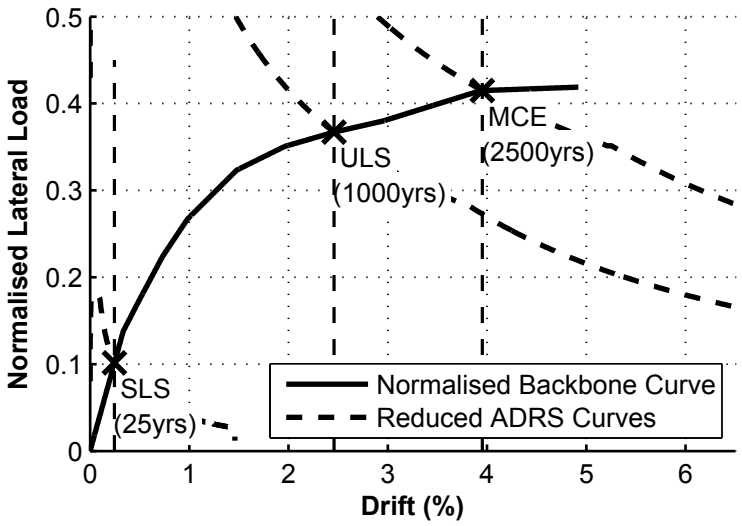

Figure 4.20: HDS1 ADRS performance evaluation

Figure 4.21 shows the energy dissipated for every loop of each drift cycle along with the cumulative amount of energy dissipated throughout the test. The energy dissipated per loop was calculated by numerical integration of the area enclosed within the hysteresis loops for each loading loop. The sum of energy dissipated per loop gives the cumulative energy dissipated at each drift limit.

Looking at the energy dissipated per loop, it can be seen that the amount of energy decreases with each loop of the drift cycle. This is due to deterioration of the structure as damage occurs under cyclic loading. The reduction in energy dissipated is most prominent at the 5% drift cycle where failure of the longitudinal bars initiated.

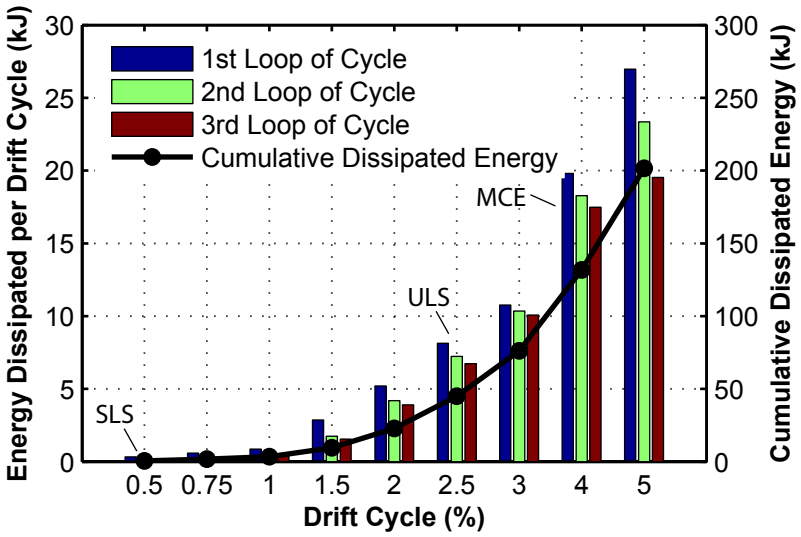

Figure 4.21: HDS1 dissipated energy

b) HDS2 - Biaxial Testing

Figures 4.41a and 4.41b show the lateral behaviour of the HDC2 column. Figure 4.41a shows the behaviour of the column under uniaxial loading in both the NS and EW directions at the start of each drift cycle. Figure 4.41b gives the biaxial behaviour during the clover stage of each drift cycle. The resultant force F_{rslt} and displacement $\triangle_{rslt}$ during clover loading are found using:

$$\triangle_{rslt} = \sqrt{\triangle_{EW}{}^2 + \triangle_{NS}{}^2} \tag{4.17}$$

and

$$F_{rslt} = \sqrt{F_{EW}{}^2 + F_{NS}{}^2} \tag{4.18}$$

The biaxial forces and displacements have been plotted in their respective quadrants of the figure based on the clover quadrant they represent.

It can be seen that HDS2 achieved a peak lateral load of 240kN with the only degradation in strength occurring during the final drift cycle even though the column was subjected to a more demanding biaxial loading cycle. This indicates that the armouring worked as intended in limiting column damage. The column showed 20% higher strength when

loaded in the South-West (SW) clover than the other clovers. This may be due to asymmetry in the construction of the column.

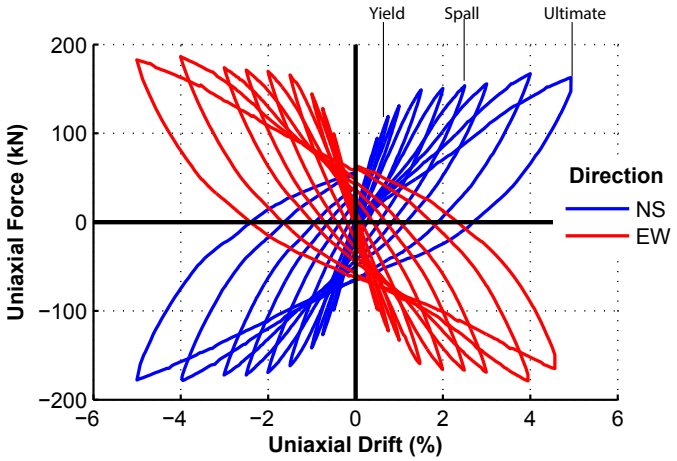

(a) Uniaxial force-drift response

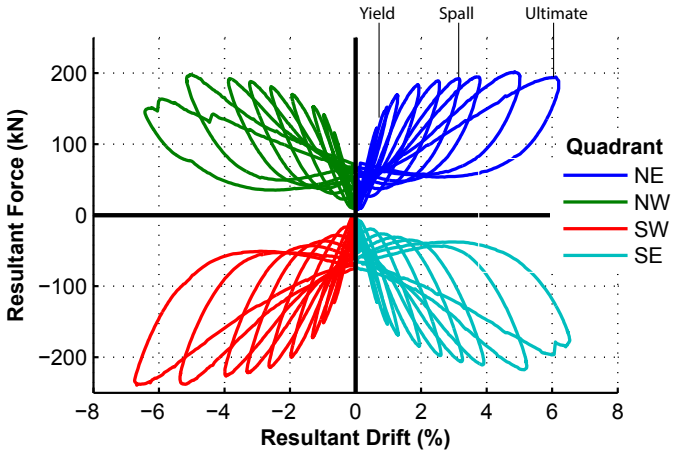

(b) Biaxial force-drift response

Figure 4.22: HDS2 force-drift response

Biaxial hysteretic damping was calculated by averaging the NS and EW damping values from the uniaxial stage of each drift cycle. HDS2 showed a lower level of damping than HDS1 reaching a hysteretic damping value of 13% at the failure ductility. This is partially due to the increased yield displacement causing a decrease in displacement ductility for a given drift level which results in a reduction of hysteretic and elastic damping.

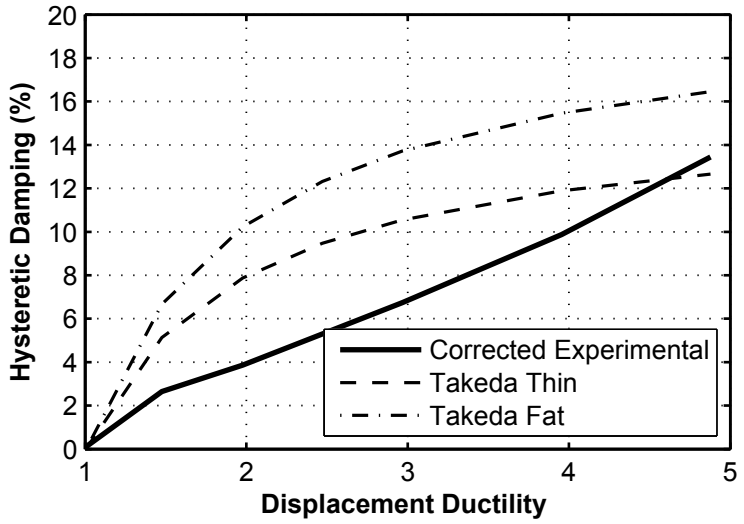

Figure 4.23: HDS2 area based hysteretic damping

The ADRS performance evaluation shows that a SLS earthquake will generate a drift of 0.3%, a ULS earthquake will generate a drift of 2.2% and a MCE earthquake will generate a a drift of 3.8%. These values are very close to what was observed in the uniaxial HDS1 test.

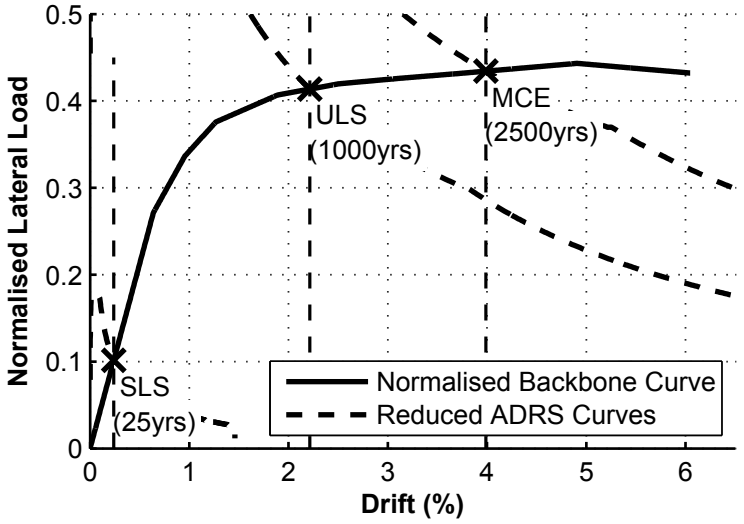

Figure 4.24: HDS2 ADRS performance evaluation

Figure 4.25 gives the energy plotted in each drift loop along with the cumulative energy dissipation throughout the test. The drift loops are separated into the unidirectional

stages of loading in the EW and NS directions followed by the biaxial loading loops separated into clover quadrants.

In the smaller drift cycles, there is a small variation in the amount of energy dissipation during each drift loop. In larger cycles, this variation becomes much more pronounced with the SE and NW clovers showing a significant reduction in dissipated energy when compared with the earlier drift loops. This indicates degradation occurring in the structure during the larger drift cycles.

In all drift cycles, the SW clover shows a slightly larger level of dissipated energy. It would be expected that this loop shows less energy dissipation than the North-East (NE) loop as it is later in the loading cycle. This reflects the higher strength of the column when loaded in the SW clover as shown in Figure 4.22b.

The cumulative dissipated energy is almost exactly double that of the HDS1 column which is expected, as the equivalent drift input of the uniaxial test was applied through both lateral rams during the biaxial test.

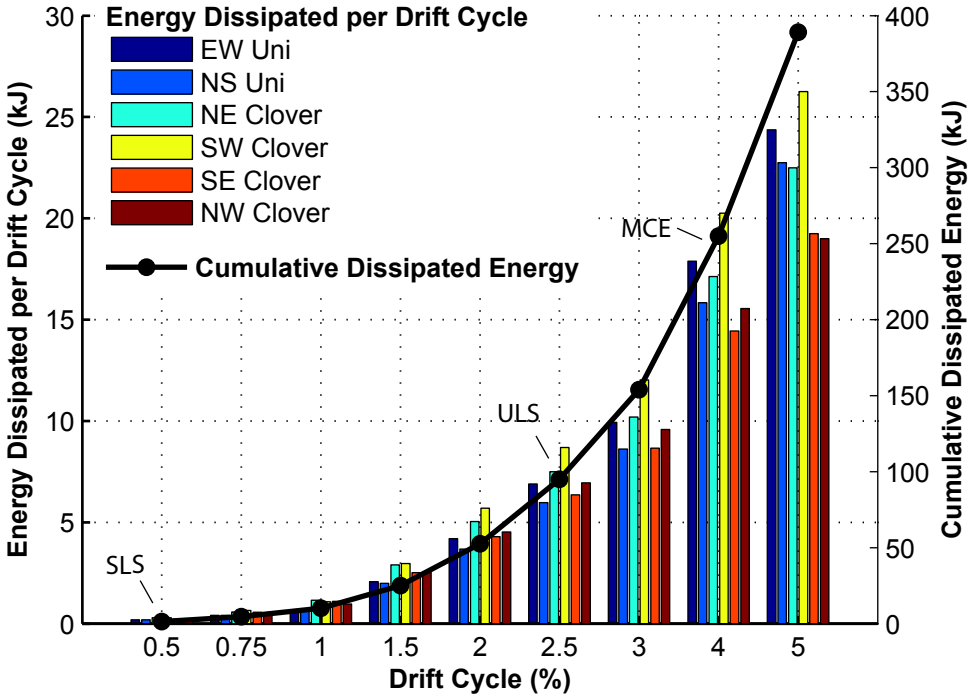

Figure 4.25: HDS2 dissipated energy

4.5 High Damage Member Socket Connection

4.5.1 Connection Overview

The MSC is formed by embedding a precast element inside another element which can be either precast or cast-in-place. If both elements are precast, grout or concrete is poured into the gap between the elements, bonding them together. The other option is to have the second element cast around the first one [Marsh et al., 2011]. The former case where both elements are precast was considered in this case as it allows for the minimum amount of on-site labour required for construction. The cast-in-place solution, however, offers the advantage of increased tolerance in the placement of the column element.

MSCs can be used for footing to column, column to cap beam, and pile to pile cap locations. This research project considers the member socket connection for use in the connection of column and footing . These connections have been used in the building industry, but there are few records of their use in bridge structure ([Marsh et al., 2011]).

4.5.2 Design

Two half scale segmental columns which feature the MSC as the primary connection, HDC1 and HDC2, were tested. HDC1 was tested uniaxially while HDC2 was tested biaxially. A MSC was used for connection of footing and column with a GDC used to connect the two column segments.

The columns were designed in accordance with NZS3101 [New Zealand Standards, 2006b] and the New Zealand Bridge Manual [NZ Transport Agency, 2003] with the design loads obtained in Section 4.2. Based on the structural demand for the prototype structure, the pier was required to resist a lateral load of 170kN giving a moment demand of 425kNm at the base connection interface. The column was designed assuming a gravity load of 450kN, based on the tributary weight of the scaled prototype deck.

The lower segment contains 16-YD16 bars while the upper segment contains 8-YD16 bars. Transverse reinforcement consists of YD10 bars at a spacing of 50mm in the socket and plastic hinge region of the column, with the spacing increasing to 100mm above the plastic hinge region.

Like the HDS columns, a 70mm diameter duct was located at the center of the column and footing to accommodate the post-tensioned bar which was used to apply axial load to the specimen to simulate gravity loads in the structure. In an actual bridge featuring HD connections, the duct and post-tensioned bar are not required.

2.1 metre square footings with a depth of 500mm were used for HDC1 and HDC2. The footing was reinforced using a top and bottom grid of YD16 bars at an average spacing of 150mm. A socket of 500mm depth and 520mm diameter was used to support the columns. Both the socket walls, and base of the column were left roughened during casting through the use of a retarding agent. This leaves aggregate exposed after casting, which provides a better bond between the layer of grout and the precast surfaces.

Technical drawings of the HDC columns are presented in Appendix B.

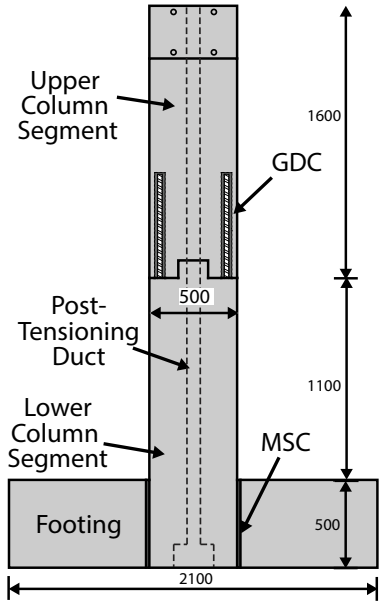

(a) HDC1 Overview

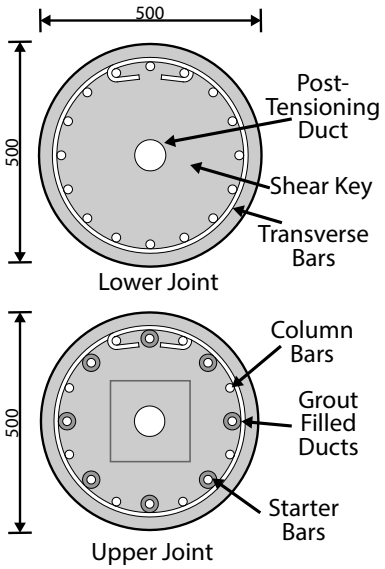

(b) HDC1 Joint Sections

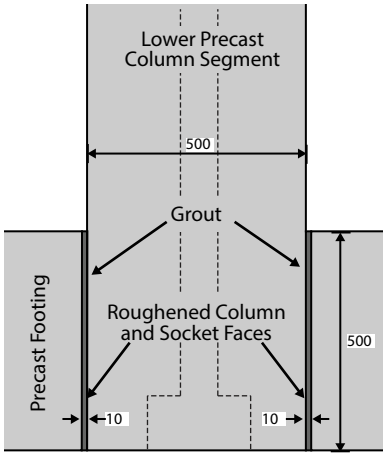

(c) HDC1 Lower Joint

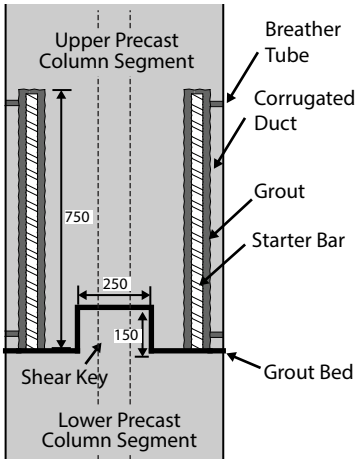

(d) HDC1 Upper Joint

Figure 4.26: HDC1 design

4.5.3 Detailing

The main considerations that are required for this type of connection are the socket depth, column diameter, and the socket diameter relative to the column diameter. Sufficient socket depth is required for the loads from the column to be transferred to the footing. The loads that must be transferred are axial loads from the weight of the piers and superstructure, and vertical acceleration loads during seismic excitation.

Shear and bearing loads must be transferred through the grouted interface between column and footing. Shear forces are induced by vertical loads in the structure including

dead loads from the weight of the structure, live loads from vehicle loading, and vertical acceleration loads during seismic loading. Lateral loads also contribute to shear in the grouted interface as shown in Figure 4.27b [Osanai et al., 1996]. Inadequate socket depth means there is an insufficient area over which the shear loads can be carried and shear failure of the grouted interface may occur. This leads to the potential for punching shear failure of the structure where the column slips through the footing [Marsh et al., 2011]. The effect of socket depth on the transfer of vertical loads through the MSC is illustrated in Figure 4.28b.

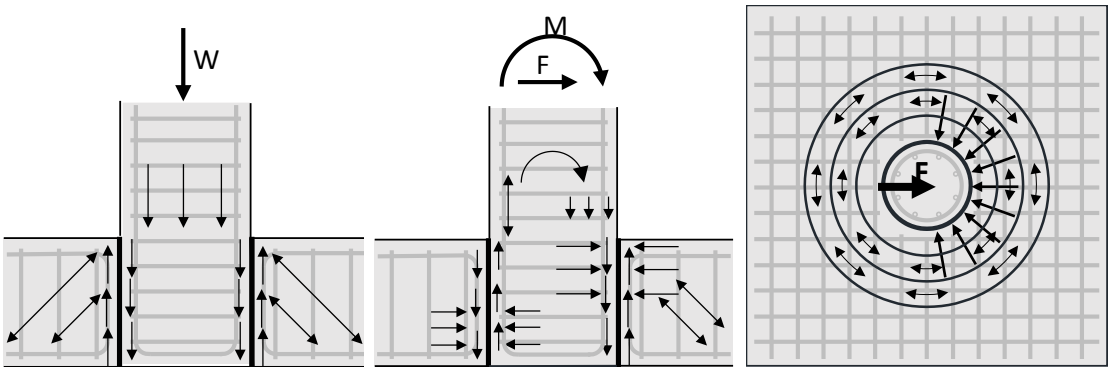

(a) Vertical load transfer (b) Lateral load transfer (c) Footing internal actions

Figure 4.27: Member Socket Connection internal actions

Lateral loads induce bearing stress in the grouted interface forming a load couple in the socket as shown in Figure 4.28a. Increasing the socket depth, h, increases the distance between the coupled loads, meaning less bearing stress is required to overcome the moment caused by the lateral loading. Insufficient socket depth leads to bearing loads in the interface that exceed the grouts compressive capacity, causing failure of the grout. This is illustrated by Figure 4.28a where a reduction in socket depth of 25% leads to an increase in bearing stresses of 60%, assuming bearing stresses are distributed over a depth of 0.2h at the top and bottom of the socket.

If insufficient socket depth is available, a partial socket where the socket does not extend all the way through the footing could be used. Alternatively, a shear key in the socket could be used to provide interlock between the footing and column. Figure 4.29. Increasing column and socket diameter also reduces internal actions in the connection as more area is provided to transfer loads. This is generally less convenient than increasing socket depth as it alters the performance of the entire structure requiring a re-design.

The bearing stresses induced in the footing by lateral loads are shown in Figure 4.27c. It can be seen that accompanying the compressive stresses in the radial direction are hoop tensile stresses that lie at a perpendicular direction to the compressive bearing stresses. This tensile stress field causes radial cracks to form which originate at the socket and propagate to the perimeter of the footing. This cracking can be mitigated by providing reinforcement orientated in the direction of these tensile hoop stresses. This can be achieved by providing circular hoops or straight bars in the footing orientated tangentially to the hoop stresses.

Sufficient gap must be left between the column and footing to allow for tolerance when assembling the precast elements, and to allow for flow of grout when pouring into the joint. The gap should not be too large however, as this will reduce the effectiveness of the grout interface to transfer shear between the precast elements [Osanai et al., 1996]. The experimental testing presented in this research found that a 10mm gap was sufficient for adequate grout flow and shear transfer, however a larger gap may be required on-site to accommodate for construction tolerances. Further research is required to determine the maximum gap width that is permitted to ensure effective load transfer through the grout layer.

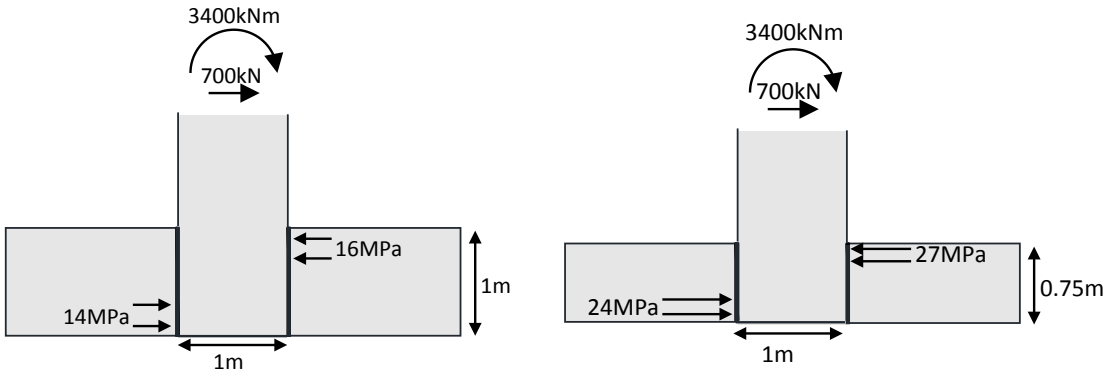

(a) Lateral load transfer

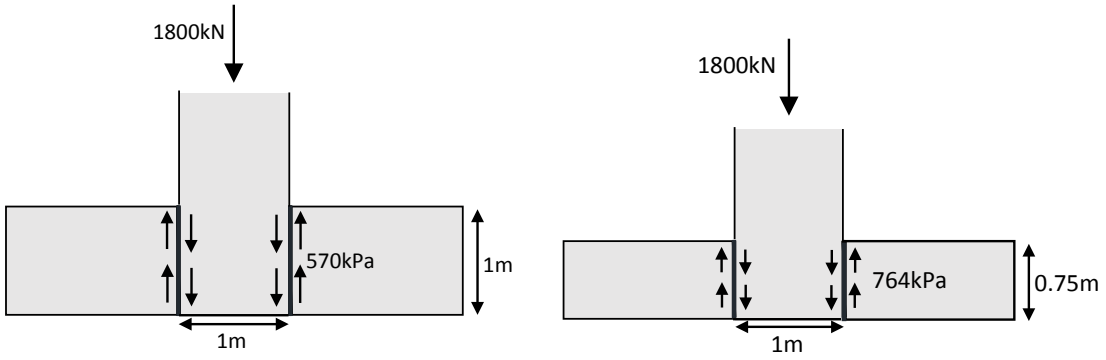

(b) Vertical load transfer

Figure 4.28: Effect of socket depth on load transfer

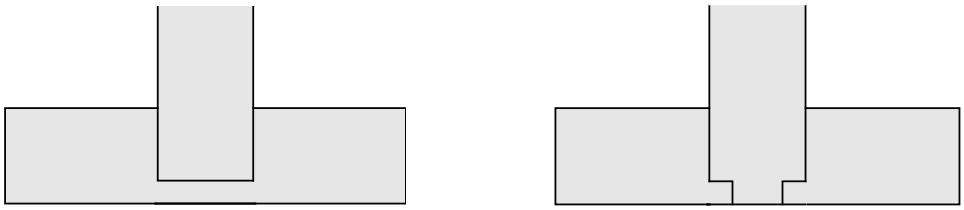

(a) (b)

Figure 4.29: Alternative socket details

4.5.4 Construction

Circular steel casing was used for casting of the HDC columns (Figure 4.30b). The footing socket was formed using a plastic cylinder with retarding agent applied to the outside (Figure 4.30a). The column segments were each cast as separate elements. A plywood template was used to ensure good alignment of the starter bars and corrugated ducts between the two column elements.

After tying of the reinforcing steel cage and placement into the formwork, the casing was lifted into a vertical position for pouring of the concrete. 40 MPa concrete with 100mm slump was then poured and allowed to cure before being removed from the formwork.

(a) Pouring of footing (b) Column Formwork

Figure 4.30: Casting of HDC1

Assembly of the HDC column first involved placement of the precast footing. The base of the socket was sealed using a bead of silicon caulk. A foam torus and bead of silicon caulk was placed in the centre of the socket to prevent the flow of grout into the anchorage area of the post-tensioned bar.

After sealing, the precast column was placed into the socket (Figure 4.31a). Wooden blocks were used to centre the column and ensure it sat vertically. The upper column was then placed on top of the lower, aligning the starter bars from the lower column with the drossbach ducts in the upper column. Shims were positioned to ensure the top segment was properly aligned. The upper segment was then lifted allowing a grout bed to be formed between the two segments (Figure 4.31c). The upper segment was then lowered onto the shims, displacing any excess grout from the grout bed.

Once the column components were positioned and aligned, the pier was ready to be grouted. Grouting of the lower joint involved spraying water into the joint to achieve a saturated surface dry condition. Grout was then poured into the gap between column and footing, using a thin strip of metal to agitate the grout to avoid air voids, until the entire annulus was filled (Figure 4.31b). The wooden blocks were left in place during pouring and removed once the grout had started to cure. In some cases, not all of the wooden block could be removed however the volume of wooden block was very small

when compared with the volume of grout and so it is expected to have no effect on the performance of the connection.

The drossbach tubes of the upper joint were filled with water and then flushed prior to grouting to remove any debris and help the grout to flow. This also allowed any leaks to be plugged prior to grouting. A water plugging mortar was used to stop any leaks. Grout was then pumped into the lower fill tube and allowed to flow upwards and out of the upper breather tubes (Figure 4.31d). Pumping of grout continued until grout could be seen flowing out of all breather tubes. At this point, all tubes were closed off and the grout was allowed to cure. The column following construction is shown in Figure 4.31e.

(a) Placing of column segments

(b) Pouring grout into socket

(c) Forming grout bed

(d) Pumping grout into ducts

(e) Assembled Column

Figure 4.31: Assembly of HDC1

4.5.5 Testing

a) HDC1

Column HDC1 was tested uniaxially. Cracking of the column was first observed during the 0.25% drift cycle and continued throughout testing up the height of the column. The majority of these cracks were of hairline thickness and closed once the lateral load had been released from the column. The distribution of cracks was similar to that of the HDS1 column however there was a larger distribution of thick cracks at the base of the column indicating a larger plastic hinge region (Figure 4.32a). This plastic hinge length is approximately equal to the depth of the section, which is what would be expected of a ductile monolithic column as given in equation 4.1 [Pampanin et al., 2010].

Spalling initiated during the 3% drift cycle as shown in Figure 4.32b corresponding to the ULS performance level. During the 6% drift cycle, the lateral actuator hit the stroke limit during the pulling stage of the cycle meaning a displacement in the South direction of only 130mm (5.2% drift ratio) could be achieved. At the end of testing, spalling had occurred up to a height of 500mm from the base of the column mainly on the northern and southern sides of the column (Figure 4.32c).

Longitudinal bar rupture occurred during the second cycle of the 6% cycle as the column reached its maximum drift (Figure 4.32d) corresponding to the MCE performance level. The fact that rupture occurred on the second cycle indicates that low cycle fatigue was a factor in failure. Buckling of longitudinal bars was observed near the connection interface during the larger drift cycles and may have contributed to low cycle fatigue of the bars.

(a) Column at point of failure

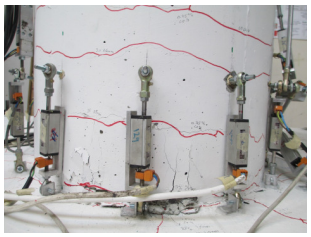

(b) Initial spalling of column at 3%

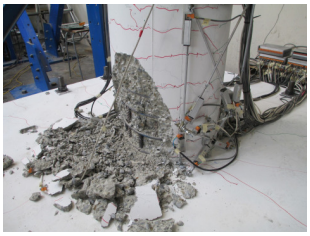

(c) Spalling of column at 6%

(d) Bar fracture at 6%

Figure 4.32: Performance of HDC1 column during testing

b) HDC2

Column HDC2 was tested biaxially. Cracking initiated during the 0.2% drift cycle with a similar distribution to HDC1 (Figure 4.33a). Further cracking occurred up the full height of the column with larger drift cycles however the majority of these cracks closed when the lateral load was released.

Minor spalling initiated during the 2.5% cycle (3.25% resultant drift, ULS performance level) as shown in Figure 4.33b with more significant spalling occuring during the 3% drift cycle. At the end of testing, spalling had occurred up to a height of 500mm from the base of the column. Due to biaxial loading, the spalling was much more significant than observed in the HDC1 test, extending all around the base of the column (Figure 4.33c).

The actuator in the East West direction hit the stroke limit at a drift of 5% meaning the full 6% actuator excursion could not be applied however bar failure occurred during the 6% drift cycle as the column entered the clover region cycle (MCE performance level). Again, some bar buckling was observed as shown in Figure 4.33d.

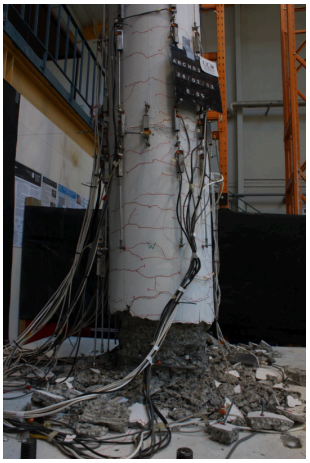

(a) Column at point of failure

(b) Initial spalling of column at 2.5%

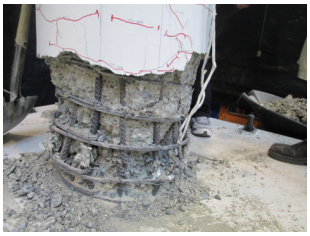

(c) Spalling of column at 6%

(d) Bar buckling at 6%

Figure 4.33: Performance of HDC2 column during testing

c) Punching Shear Test

To ensure sufficient capacity remained in the grouted interface of the member socket connection, a punching shear test was undertaken as illustrated in Figure 4.34. A hydraulic cylinder was placed under the center of the column stub remaining after deconstruction of the column and the load was increased to 1350kN with no visible slipping of the column stub occurring. Radial cracking occurred in the footing, propagating from the socket and extending to the perimeter of the footing. The axial load applied during punching shear testing corresponds to 1.5 times the ultimate limit state axial load of the half-scale prototype bridge structure. This indicates that sufficient gravity capacity of the connection remains after cyclic loading with no substantial grout degradation.

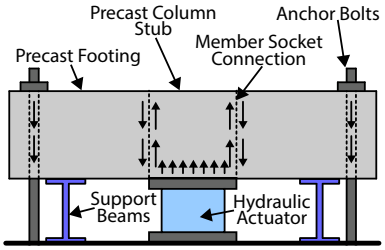

(a)

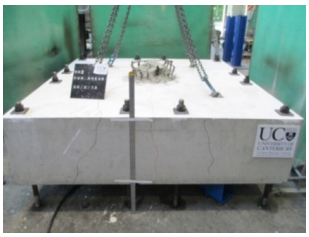

(b)

(c)

Figure 4.34: Punching shear testing arrangement

4.5.6 Results and Discussion

a) HDC1 - Uniaxial Loading

Figure 4.35 shows the force-drift behaviour of the HDC1 column. The column shows an ultimate lateral force of 150kN. The post yield stiffness of this column is much lower than that seen in the HDS1 indicating the post-tensioned bar performed as desired in simulating the axial load in the structure.

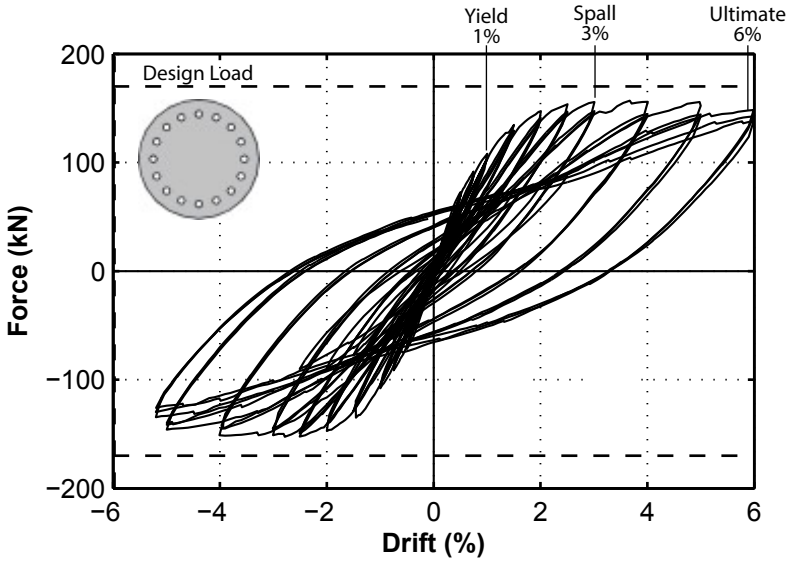

Figure 4.35: HDC1 force-drift response

Figure 4.35 shows that the column yielded at a drift of 1% corresponding to a displacement ductility of 3 at the ultimate limit state when spalling initiated. The ductility at failure point was equal to 6. The residual displacements observed in the second column were slightly smaller than those of the first column but still significant. The column achieved a peak base shear of 160kN.

Figure 4.36 gives the moment curvature behaviour at the base of the column.

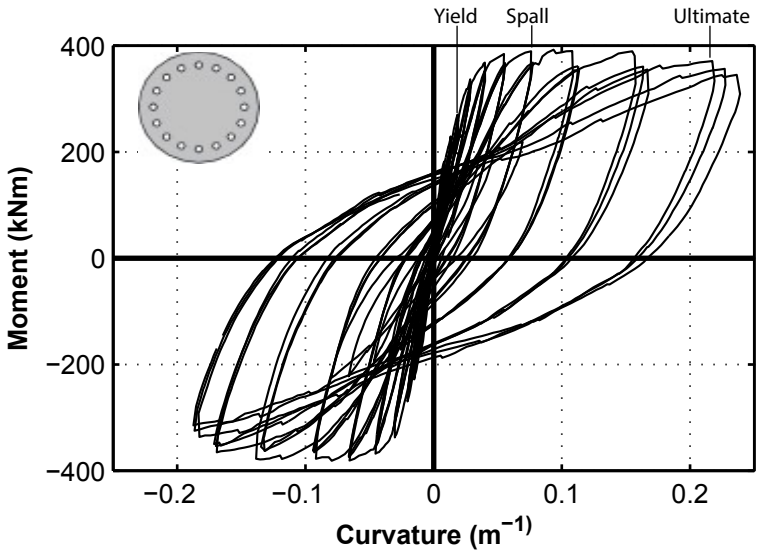

Figure 4.36: HDC1 moment-curvature response

Figure 4.37 gives the curvature distribution for the HDC1 column. Similar to the HDS1 column, the largest curvature values occurred at the base of the column with a second hinge forming half way up the column. The second pot array from the base of the column from a height of 0.2m to 0.65m shows higher levels of curvature than observed in the HDS1 column indicating that the plastic hinge region extended further up the column in this case. This was confirmed by visual inspection where the plastic hinge length appeared to be 500mm.

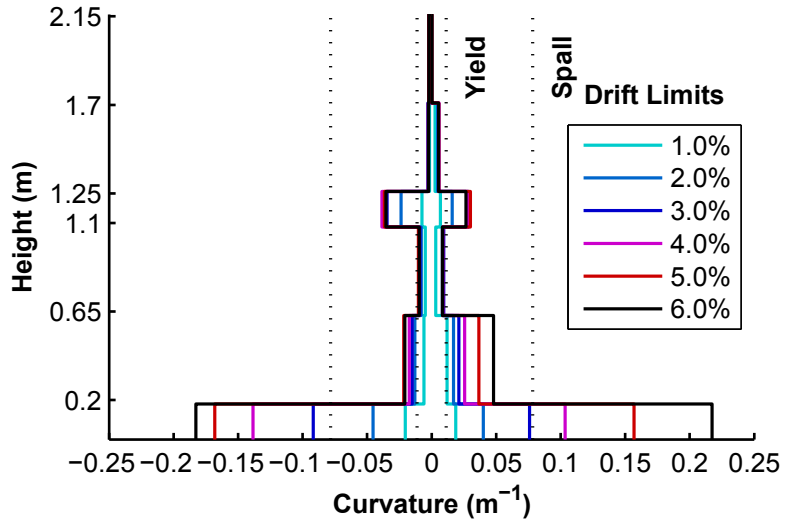

Figure 4.37: HDC1 curvature distribution

Figure 4.38 gives the area based damping for the HDC1 column at increasing levels of displacement ductility. Again, a relatively linear relationship between damping and ductility was observed. Like the HDS1 column, an hysteretic damping value of 17% was achieved in the column at the failure point of the column similar to that of the HDS1 column. The experimental curve lies below the Takeda Thin curve up until a ductility of just under 5 where it then crosses and sites between the Takeda Thin and Fat curves.

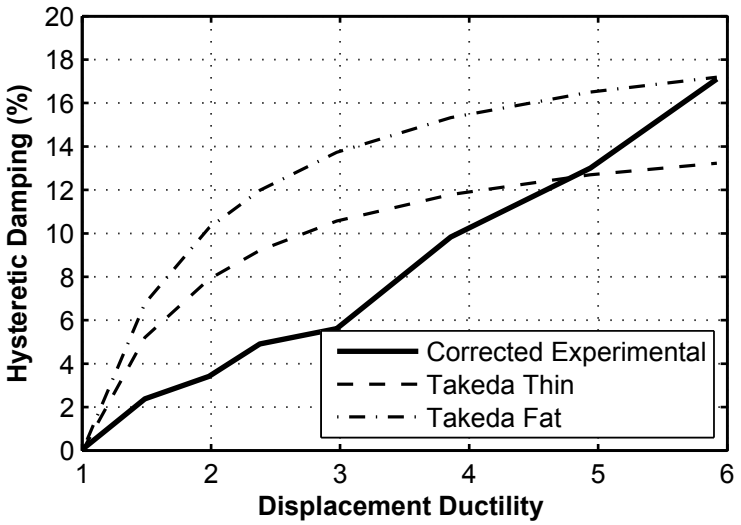

Figure 4.38: HDC1 area based hysteretic damping

Figure 4.39 gives the ADRS performance evaluation for the HDC1 column. The lower post yield stiffness gives higher levels of drift for the ULS and MCE limit states. The ULS limit state generates just under 3% of drift which was the value adopted for the force based design of the prototype structure indicated good assumptions were made during the design process. The MCS limit state generates 4.8% drift in the structure.

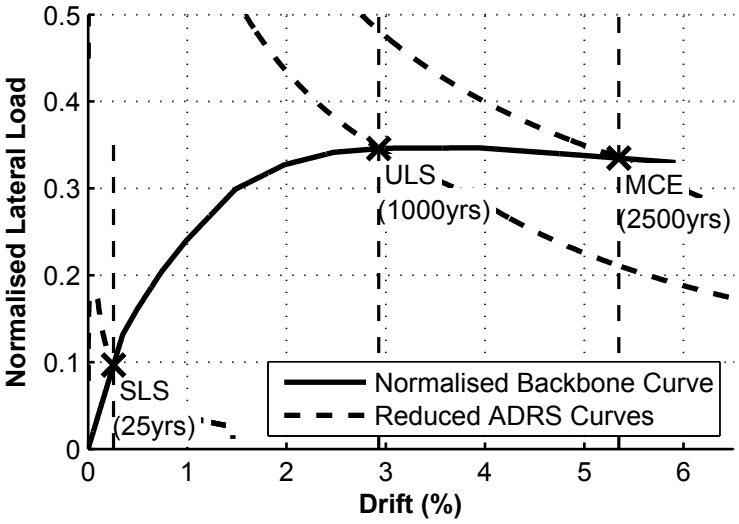

Figure 4.39: HDC1 ADRS performance evaluation

Figure 4.40 shows the energy dissipated by the structure during each loop at increasing drift limits. The HDC1 column shows significantly less cumulative dissipated energy at the 5% drift cycle. The ability for the HDC1 column to reach an ultimate drift of 6% however means that it was able to dissipate slightly more energy than the HDS1 column overall.

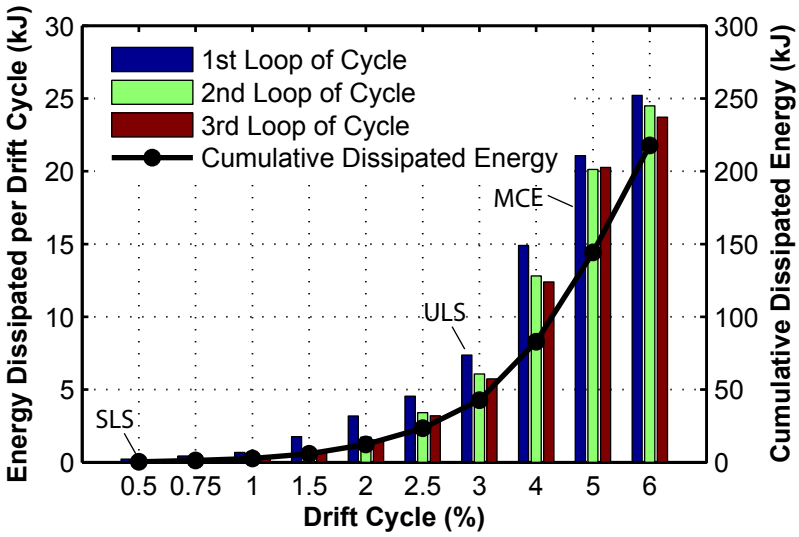

Figure 4.40: HDC1 dissipated energy

b) HDC2 - Biaxial Loading

Figure 4.41 gives the force-drift behaviour of the HDS2 column. This column achieved a peak lateral load of 155kN. Degradation in the strength of the column initiated during the 3% loading cycle while degradation in the HDC1 column initiated during the 5% loading. The HDS2 column showed significantly greater spalling damage due to the demanding biaxial loading regime contributing to the strength degradation.

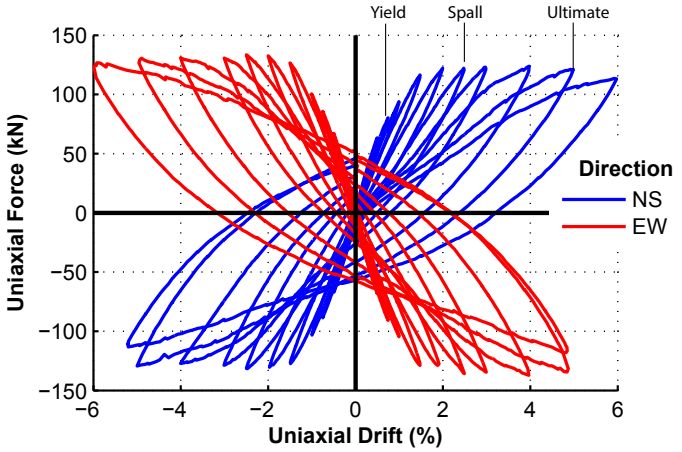

(a) Uniaxial force-drift response

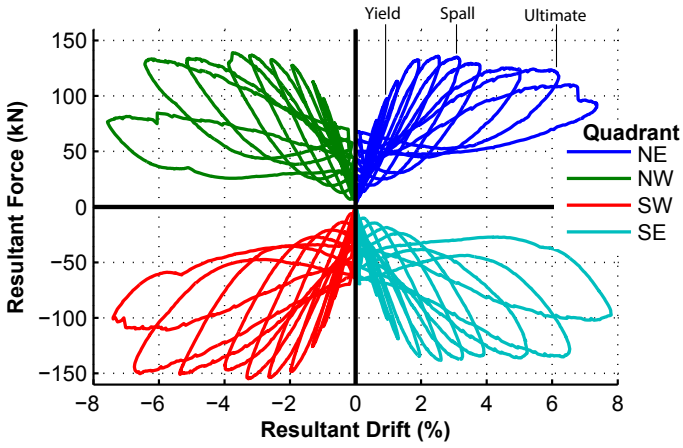

(b) Biaxial force-drift response

Figure 4.41: HDC2 force-drift response

Although the column showed a higher level of strength degradation than previous tests, it showed good energy dissipation properties, achieving an ultimate hysteretic damping value of 17% which is equal to that of the uniaxial test. It should be noted that the

damping values are calculated from the uniaxial hysteresis loops which show less strength degradation than the biaxial loops, giving larger damping values.

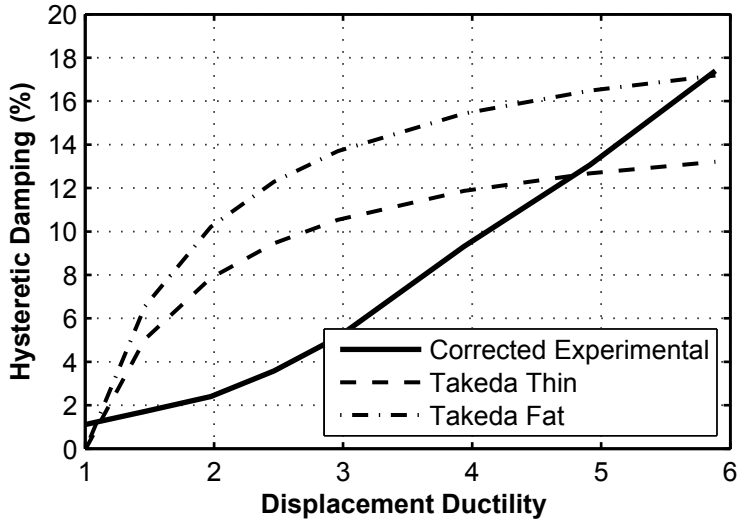

Figure 4.42: HDC2 area based hysteretic damping

The ADRS performance evaluation also shows similar performance to the HDC1 column up to the ULS earthquake. The strength degradation however means a MCE earthquake generates a drift of 5.7% which is significantly higher than the HDC1 column at 4.8%.

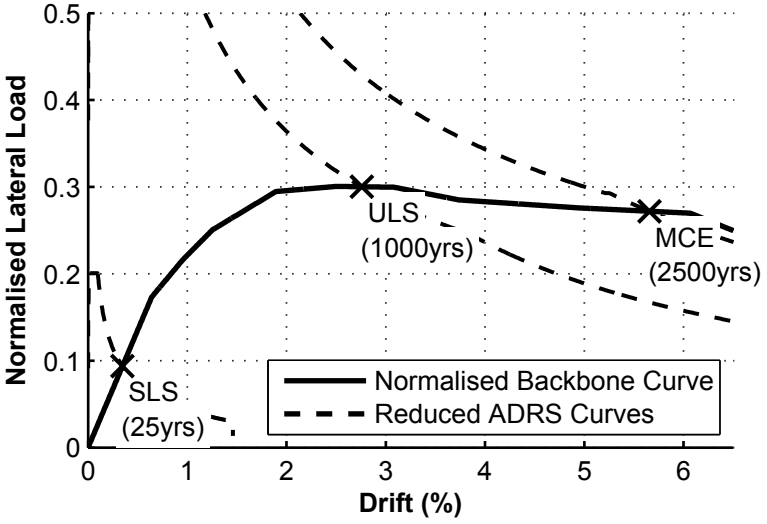

Figure 4.43: HDC2 ADRS performance evaluation

Figure 4.44 shows the dissipated energy during testing of HDC2. This figure reflects the strength degradation shown in Figure 4.41b with a significant reduction in dissipated energy in the later drift cycles.

The cumulative dissipated energy was 375kJ which is less than double the uniaxial cumulative dissipated energy of 225kJ. This is lower than expected and can be attributed to the higher level of damage sustained by the column.

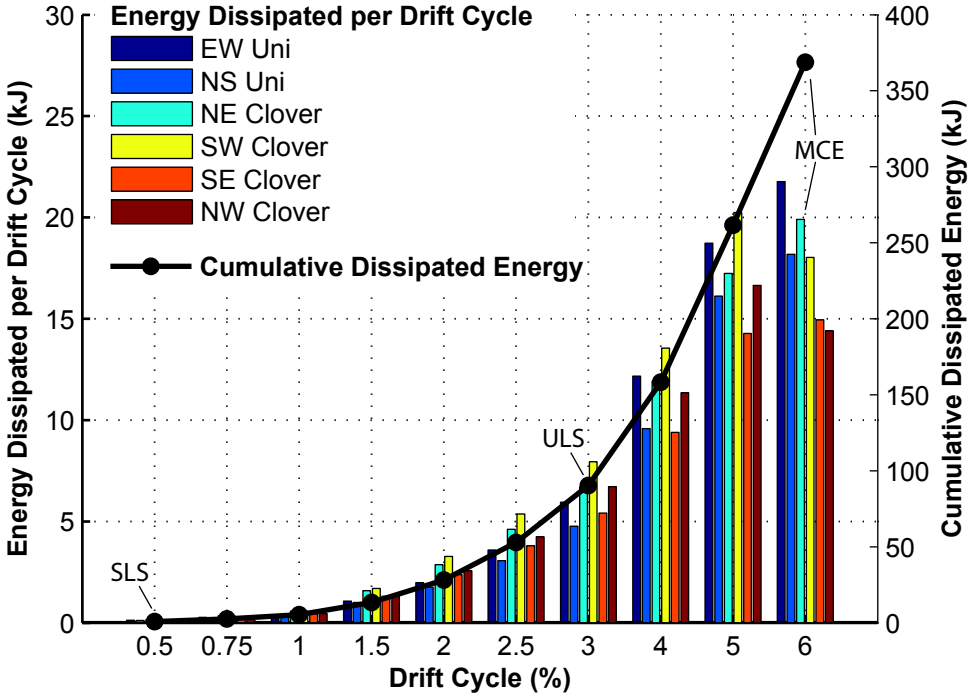

Figure 4.44: HDC2 dissipated energy

4.6 Connection Comparison and Conclusions

ABC High Damage connection types offer a precast construction system for bridge substructures with advantages over the conventional monolithic approach to bridge construction while achieving similar seismic performance. Advantages include increased construction speed and quality with reduced maintenance requirements. Less labour and equipment is required for assembly on-site, leading to a safer work environment with minimal disruption to the surrounding community and traffic networks. ABC substructure types have been widely implemented in regions of low seismicity, but their use

in regions of moderate to high seismicity has been limited due to concerns in the seismic performance of precast connections.

The experimental testing of four High Damage precast columns was presented in this chapter to demonstrate the construction procedure and performance of precast substructure systems. Two columns featuring the Grouted Duct Connection as the primary connection type and two columns featuring the Member Socket Connection as the primary connection type were tested under uniaxial and biaxial loading. Two variations of the Grouted Duct Connection were tested, with one featuring steel armouring and debonding of longitudinal starter bars to improve performance. The ease and speed of construction of all columns illustrates the benefits of precast construction over cast-in-place construction. Minimal wet work was required during assembly, greatly simplifying the construction process.

Column HDS1

- Column HDS1 featured the Grouted Duct Connection for connection of footing and column, and column segments with no armouring or debonding.
- An ultimate drift of 5% under uniaxial loading was achieved before bar failure occurred.
- Fine cracking initiated during the 0.35% drift cycle, with cracks distributed up the height of the column.
- Spalling initiated during the 3% drift cycle and extended to a height of 250mm by the end of testing.
- A major gap opened at the base of the column, reaching a width of 7mm at the design drift of 3%.
- Buckling of longitudinal bars occurred in the larger drift cycles, which may have contributed to low cycle fatigue failure.
- Some inelastic gap opening occurred at the interface between column segments. This wasn't intended but could be used to distribute inelastic deformation and enhance energy dissipation capacities in the column.

Column HDS2

- Column HDS2 featured the Grouted Duct Connection with armouring and debonding of longitudinal starter bars. A biaxial loading regime was used in this case.

- Amouring was very effective at controlling spalling, with only minor spalling occurring at the corners of the section above the armouring.
- Armouring also prevented outward buckling of the longitudinal bars. Upon disassembly, it was found that buckling of the bars had occurred parallel to the column faces.
- Debonding of the longitudinal starter bars over a length of 120mm resulted in an increase in ultimate drift of the column of 30%, giving an ultimate drift capacity of 6.25% which is equal to that of the HDC columns.

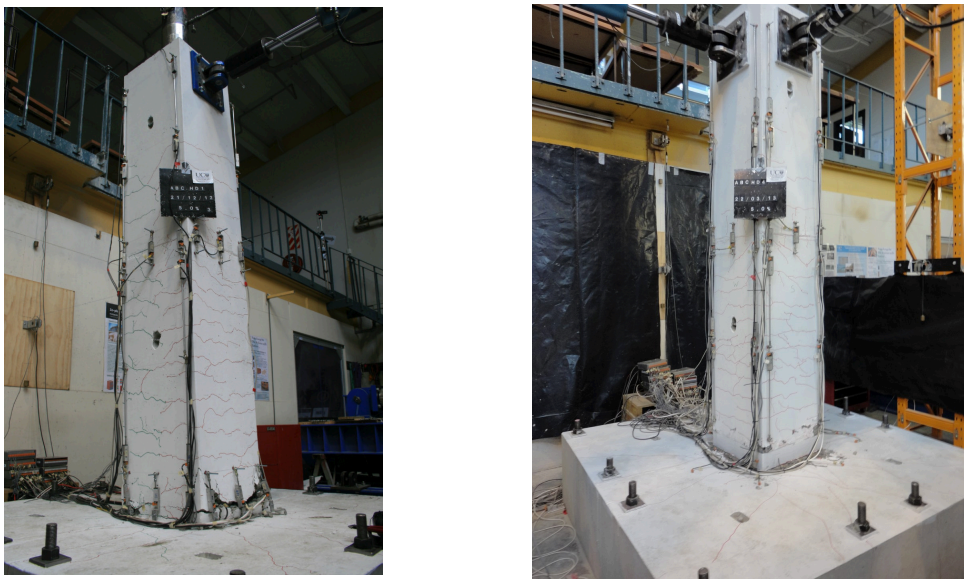

(a) Column HDS1

(b) Column HDS2

Figure 4.45: Comparision of HDS column damage

Column HDC1

- Column HDC1 featuring the Member Socket Connection with a Grouted Duct Connection used to connect the two column segments.
- An ultimate drift of 6% was achieved.
- Cracking of the column was first observed during the 0.25% drift cycle. Like the HDS columns, cracking was distrbuted up the height of the column. In the HDC coumns, however, there was a distribution of cracks of relatively large width at the base of the column, rather than the single wide gap opening observed in the HDS columns.
- Spalling initiated during the 3% drift cycle, reaching a height of 500mm by the end of testing. This is significantly higher than observed in the HDS columns and is similar to what would be expected from a ductile monolithic conneciton.
- Bar buckling was also observed in this case, with bar fracture occurring during the 6% drift cycle.

- Like the HDS columns, there was inelastic gap opening at the connection between the column segments.

Column HDC2

- Column HDC2 featured the same construction as HDC2 featuring the Grouted Duct Connection, but was subjected to a biaxial loading regime.
- Similar results to HDC1 were observed, with the column acheiving the same drift limits for initiation of cracking, spalling and bar failure.
- A considerably higher level of spalling occurred as a result of the biaxial loading regime, however the same overall height of spalling was observed.

Punching Shear Test

- Punching shear testing of both Member Socket Connections showed that sufficient axial load capacity remained in the connections following testing.
- Both punching shear tests achieved axial loads of 1.5 times the ultimate limit state axial load of the half-scale prototype bridge structure with no sign of failure of the grouted interface.

(a) Column HDC1 (b) Column HDC2

Figure 4.46: Comparision of HDC column damage

The length of drossbach ducts in the test columns was equal to the required development length as stated in NZS3101 [New Zealand Standards, 2006b]. The corrugated duct provides additional passive confinement to the starter bars meaning in reality, less development length is needed to develop full bar strength. The increased confinement

provided by the ducts also leads to less strain penetration, increasing strain concentration in the bars at the connection interface. This causes a shorter plastic hinge length but also decreases the ultimate drift capacity of the column. Debonding starter bars at the connection interface helps to reduce the strain concentration effects, increasing the ultimate drift capacity of the column.

Sufficient socket diameter must be provided when using Member Socket Connections to allow tolerance in placing of the column, however further investigation of maximum gap widths to allow for adequate stress transfer in the connection is required. Sufficient socket depth must also be provided to limit stress demands in the joint. In monolithic bridge pier construction, the column is generally cast after the footing, resulting in a cold joint between the two elements with reinforcement crossing the joint. The member socket connection offers the advantage of no construction joint between the column and footing, leading to better durability and the possibility for improved performance [Marsh et al., 2011].

The member socket connection offers simpler assembly than the Grouted Duct Connection with less risk of delay as only the column and socket need to be aligned for each connection. Particular care must be taken with the casting of Grouted Duct Connections as there is a risk of misalignment of starter bars and corrugated ducts between each segment which could lead to significant delays during construction [Marsh et al., 2011]. Sufficient tolerance must be allowed for in the sizing of drossbach ducts relative to the starter bars.

Both connection types showed promising results with slightly lower energy dissipation capabilities when compared with models for monolithic systems. Good strength and ductility characteristics indicate suitability for use in regions of moderate to high seismicity. The speed and relative ease of construction of the test columns demonstrates the benefits of precast construction. Considerably less equipment, labour and time was required for assembly of the columns than would be required for monolithic construction.

Further research into durability of these precast connections - in particular the Grouted Duct Connection - is being carried out at the University of Canterbury at the time of writing [Andisheh, 2013].

Chapter 5

Development and Testing of Controlled Damage Pier Systems

5.1 Introduction

This chapter presents the design and testing of two half scale bridge piers featuring ABC CD connections. With ABC HD and conventional monolithic connections, the connection is intended to sustain damage during severe seismic loading through the formation of ductile plastic hinges. This approach is economical, as it allows for significantly reduced seismic demands when compared to structures designed to remain elastic during seismic loading. The problem with this approach is that the structure is left with significant damage including residual drift, spalled concrete and yielded, buckled or fractured bars. This repair is difficult and costly to investigate repair with the chance of significant downtime in bridge serviceability. In the case of buckled or fractured longitudinal bars, replacement of the bridge structure will generally be required [Priestley et al., 1996].

ABC LD rocking connections on the other hand, target very little to no damage. This is achieved through the use of unbonded post-tensioning to limit residual drifts, steel armouring to prevent damage to precast concrete components, and replaceable external dissipators allowing for simple, fast and cost effective post-earthquake replacement. This approach is more costly in terms of initial construction, but offers significantly faster and more cost effective repair options than monolithic or HD systems.

In many cases, it is unlikely that repair of a bridge structure will be required during its life, making it hard for infrastructure owners to justify the increased construction costs associated with low damage technologies. They understand however, that the consequences of a significant earthquake event can be severe, including significant down-time in the serviceability of bridge structures along with the need for costly repair or replacement of the bridge.

ABC CD connections limit and control damage in the connection during seismic loading. The damage that does occur is easily repairable, with pre-planned repair strategies that are developed and detailed for at the design stage of the structures life. Controlled damage is achieved through the use of post-tensioning to limit residual drifts and armouring to protect precast components from excessive spalling. Conventional mild steel reinforcement is generally used as the method of energy dissipation for initial construction, with provision of anchorages or coupled connections for replacement of damaged bars as part of the specific repair strategies. This removes the need for external dissipation devices and connections during initial construction, and moves the cost of these components to the repair stage. The result is a connection that offer a compromise between ABC HD and LD options with relatively low construction costs, along with minimal residual drifts and straightforward methods of repair.

The repair strategies are cost effective, meaning they can be implemented in situations of uncertainty into the residual strength or ductility of the system, removing the need for costly investigative processes. The repair strategies presented involve replacement of all energy dissipating components of the system, giving greater confidence in the performance of the structure following repair.

Two columns featuring Controlled Damage Connection types are presented in this chapter as summarised in Table 5.1. The first is Column CDC (Figure 5.1a) featuring the CD MSC which is similar to the HD MSC presented in Chapter 4. In the CD connection, however, post-tensioning and cover confinement is provided at the connection interface. Threaded inserts are cast into the connection during construction to facilitate installation of external dissipators as part of the repair strategy. During a seismic event, the column forms a natural rocking interface through opening the of a major crack at the base of the column between the armouring and footing. Energy is dissipated through yielding of the longituinal reinforcement in the column, which is debonded over a length

at the connection interface to localise yielding, and further encourage formation of a rocking interface. Limited damage to precast components is expected. Following a severe seismic event, the internal bars are cut, removing their contribution to strength of the connection, and external dissipators are installed which offer connection performance that is equivalent to the pre-repair connection.

The second is Column CDS (Figure 5.1b) featuring the Controlled Damage CBC. This connection uses replaceable segments of longitudinal bar connected to threaded studs formed in the ends of permanent reinforcement using threaded bar couplers. The bar segments, couplers and threaded studs are located in a recess in the base of the column. Conventional mild steel stirrups are placed around the bar segments and the recess is filled with cast-in-place concrete or grout, enclosing the components of the energy dissipation system. During a seismic event, spalling of the fill material is expected, along with yielding of the replaceable segments of bar. No damage to threads, couplers or precast components will occur. To repair the connection, the cast-in-place material and stirrups are removed, allowing access to the bar segments for replacement. Following replacement, new stirrups are installed and fill material is cast.

The same test arrangement as presented in Section 4.3 was used for testing of the CD columns. Rather than regulating the axial load, however, the axial load was allowed to increase due to bar elongation as the structure was displaced, as would occur in an actual post-tensioned pier. Since higher axial loads were required for the post-tensioned pier, the axial ram capacity was increased to 1500kN and the diameter of post-tensioned bar was increased from 40mm to 50mm. Following benchmark testing of each connection, repair and retesting was carried out to demonstrate application and effectiveness of the repair strategy in each case.

This chapter gives an overview of the design and detailing of each connection type. The construction, testing and repair of each test column is outlined followed by a discussion and comparison of the test results.

Test Name	**Connection**	**Section Shape**	**Testing Protocol**
CDC	Member Socket Connection	Circular	Biaxial
CDS	Coupled Bar Connection	Square	Biaxial

Table 5.1: Summary of Controlled Damage test columns

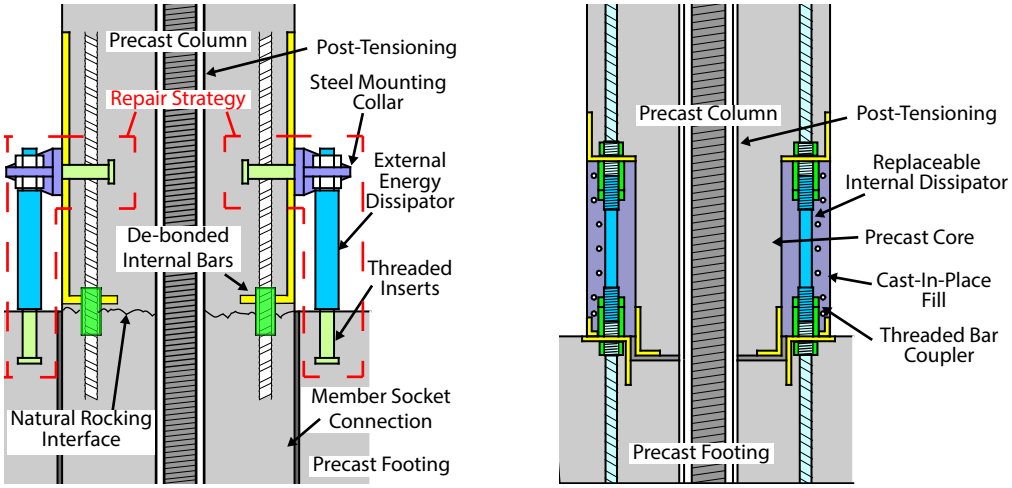

(a) Column CDC with Controlled Damage Member Socket Connection

(b) Column CDS with Controlled Damage Coupled Bar Connection

Figure 5.1: Controlled Damage connection types

5.2 Controlled Damage Member Socket Pier System

5.2.1 Connection Overview

The Controlled Damage Member Socket Connection is similar to the MSCs tested in the previous chapter. In this case however, pre-tensioned or post-tensioned bars or tendons are included to limit residual drifts in the structure [Marsh et al., 2011, Stanton, 2010]. Cover confinement is used to limit spalling damage which is otherwise induced at lower levels of drift in this type of connection due to the increased levels of axial load in the connection.

Following the benchmark testing, the connection was repaired and retested to demonstrate the application and effectiveness of the repair strategy. In this case, the repair strategy involves cutting of the damaged internal longitudinal reinforcing bars which are then replaced with external mild steel dissipators. The dissipators used in the repair of the column are Grooved Bar Dissipator as presented in Chapter 3, which are effective in both tension and compression with almost no buckling effects apparent.

This section outlines the design, detailing, testing and results of the CD MSC. The proposed repair strategy for this type of connection will be presented along with results of the testing following repair.

5.2.2 Design and Repair Strategy

a) Design

A half scale column featuring the CD MSC, named Column CDC, was tested in the lab. An overview of the column design is given in Figure 5.2 with detailed drawings given in Appendix C. The column features a circular cross section of 500mm depth with a square column cap. The full column length is 3.2m. The footing has dimensions of 2.1m by 2.1m with a depth of 500mm. A socket of 520mm diameter was formed in the centre of the footing. The test column was based on the bridge prototype presented in Section 4.2 with the CD connections having the same moment capacity as the HD columns.

The design of the column was based on the PRESSS design handbook targeting a recentering ratio, λ, of 1.3 to 1.5. [New Zealand Standards, 2006a, Palermo, 2004, Pampanin

et al., 2010]. The target recentering ratio is higher than the suggested minimum of 1.15 which corresponds to the overstrength factor for non-prestressed steel reinforcement or the energy dissipating devices [New Zealand Standards, 2006a]. Higher values result in less energy dissipation capacity of the system, but help to ensure good recentering behaviour of the connection. It was assumed that a rocking interface would form naturally in the form of a single large crack at the interface between the column and footing. To encourage a single crack to form, the longitudinal bars were debonded over a length of 50mm at the connection interface. Reducing the bar area by necking of the reinforcement would offer the best connection performance with a higher level of control over yielding of the bar and the amount of strain penetration, however this would add some construction costs. An initial level of post-tensioning of 900kN was used for both the benchmark and repaired test cases, representing both the axial loads and post-tensioning loads in an actual structure. A design was required for both the pre and post-repair cases. The design parameters are summarised in Table 5.2.

	CDC-Initial	**CDC-Repaired**
Design Drift, θ_d	3%	3%
Nominal Moment Capacity, M_n (kNm)	390	420
Mild Steel Contribution, M_s (kNm)	152	177
Post-Tensioning Contribution, M_{pt} (kNm)	1.56	1.35
Recentering Ratio, λ	1.56	1.35
Initial PT Force, $T_{pt,initial}$ (kN)	900	900
Design PT Force, $T_{pt,design}$ (kN)	1200	1200

Table 5.2: CDC design summary

The column was initally specified to be constructed with no confinement provided for the cover concrete located outside the stirrups. However, after commencement of preliminary testing it was found that the large axial loads caused premature spalling damage to the column during testing. The damage to the cover concrete was repaired and cover confinement was provided using Fibre Reinforced Polymer (FRP) wrap based on Mander et al. [1988]. The FRP wrapped column was then adopted as the benchmark for the system for comparison with the subsequent repair strategy. It was assumed that sufficient strength and ductility remained in the longitudinal bars after the initial test since the

column was subjected to drifts of up to 2.5% which corresponds to the Ultimate Limit State (ULS) [NZ Transport Agency, 2003].

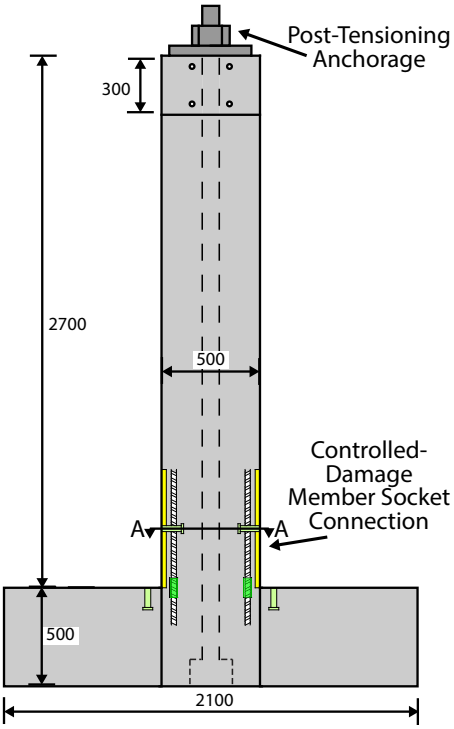

(a) Column overview

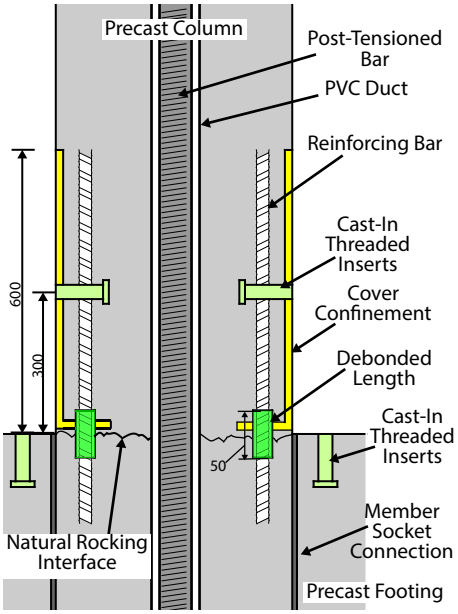

(b) Connection detail

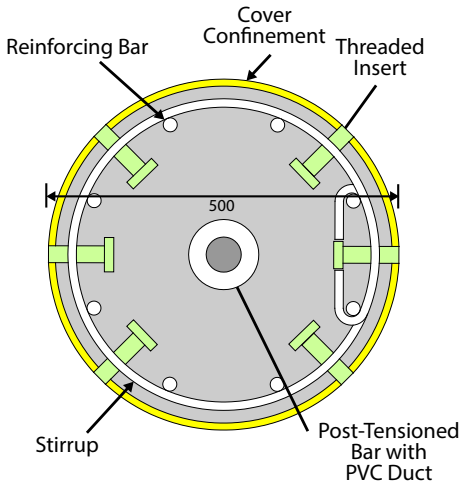

(c) Section A

Figure 5.2: CDC design

Specimen Design Limitations

A 50mm diameter post-tensioned bar was used to simulate both the gravity and post-tensioning loads in the structure. This load was not regulated throughout testing meaning it increased with increasing levels of column drift. In an actual structure, the post-tensioned component of axial load in the column would increase with increasing drift,

however the gravity component from the weight of the superstructure would not. Since the required axial load was specified at 3% drift, the axial load in the structure is lower than it would be in an actual structure at drifts lower than 3%, and higher at drifts higher than 3%. It was assumed that this effect would have minimal impact on the results, while greatly simplifying the testing process.

The connection features threaded inserts for connection of external dissipators during application of the repair strategy. In the test column, threaded inserts were not included in the initial construction due to space constraints in the half scale column, and the reuse of the precast footing from a previous test. It is intended that the threaded inserts are cast into the column during the initial precasting process.

Material Properties

Concrete of $f'_c = 40MPa$ was used for the design of the test column, however $f'_c = 50MPa$ compressive strength was specified since testing of the column was intended to occur earlier than 28 days after casting. Grade 500 steel was specified for all reinforcing in the footing and the transverse reinforcement in the column. The longitudinal bars in the column and external dissipators were specified as Grade 300 steel. Grout of $f'_c = 55MPa$ was specified for grouting of the MSCs in Column CDC with structural mortar of $f'_c = 55MPa$ specified for the preliminary repair. All compressive strength values are the 28 day nominal strengths. The actual material properties at the time of testing are summarised in Table 5.3.

Material	**Specified**	**Actual**
Concrete		
Column	50	55
Footing	50	55
Steel		
Column Longitudinal	300	350
External Dissipators	300	360
Column Transverse	500	580
Footing	500	520
Grout		
Construction	55	41

Table 5.3: Summary of CDC material strengths (MPa)

b) Repair Strategy

During the design stage, the proposed repair strategy was defined and is illustrated in Figure 5.3 with the cross section and mounting hoop shown in Figure 5.4. For the Controlled Damage Member Socket pier system, the proposed repair strategy is as follows:

- Existing longitudinal bars are cut using a concrete saw at the base of the column (Figure 5.3b). The saw cut should be deep enough to clear the longitudinal bars but should not interfere with the post-tensioning located at the center of the column.
- Grout or epoxy is pumped into the saw cut to seal the joint and provide an interface for transfer of axial loads and rocking behaviour (Figure 5.3c).
- The steel collar is mounted to the face of the column and bolted into threaded inserts that are cast into the column during construction (Figure 5.3d).
- External dissipators are screwed into threaded inserts that are cast into the footing during construction (Figure 5.3d). The external dissipators are also bolted to the steel collar.
- Steel angles are mounted to to the footing to assist with carrying shear as shear friction. Located at four positions around the column, staggered with the position of dissipators (Figure 5.3e and 5.4a).

The use of steel angles may not be required if it can be shown that sufficient shear transfer capacity exists through shear friction alone. New Zealand codes do not permit reliance on shear friction alone in this case, so steel angles were provided to assist in the shear transfer mechanism of the connection [New Zealand Standards, 2006b].

During application of the repair strategy in the lab, the post-tensioning load was removed. In an actual structure, this would not be required, provided that the cut depth is shallow enough to preserve sufficient core concrete to carry the axial load in the connection.

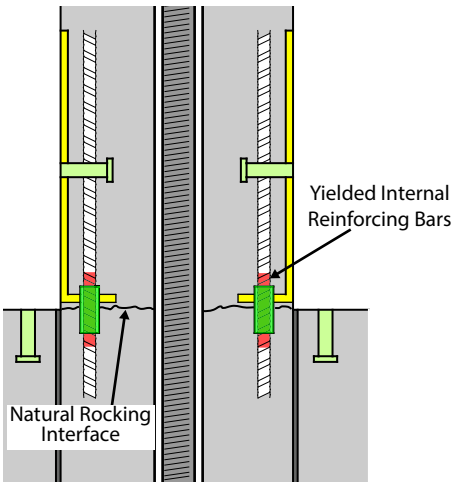

(a) Damaged connection

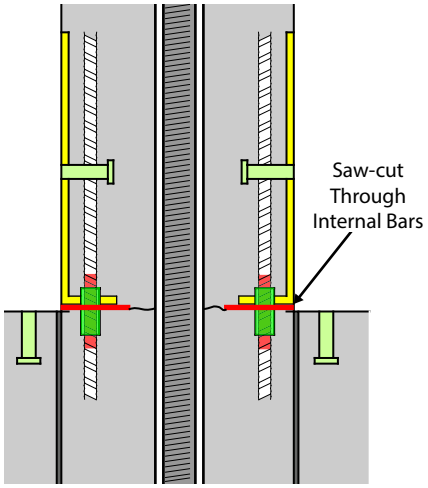

(b) Damaged internal bars cut with concrete saw

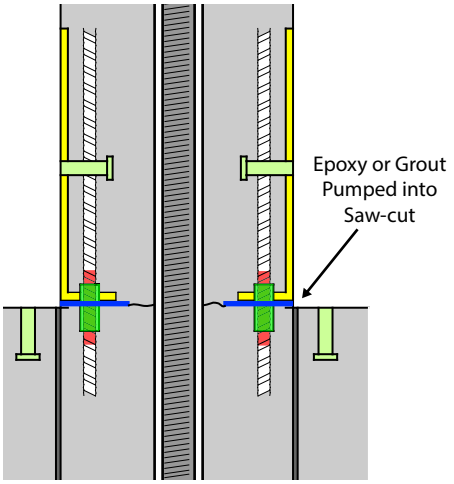

(c) Epoxy or grout pumped into saw cut

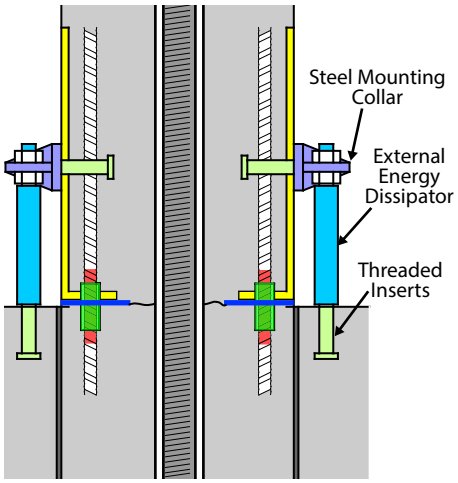

(d) External dissipation system installed

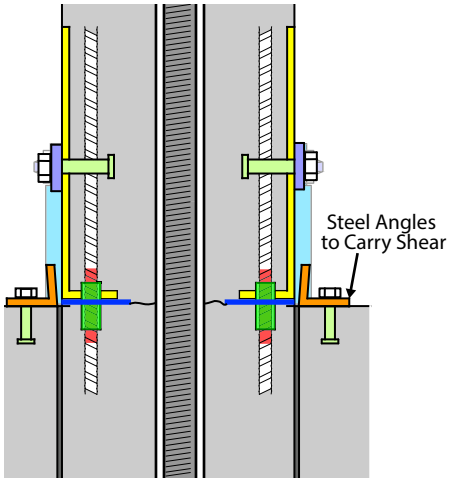

(e) Steel angles installed to carry shear

Figure 5.3: CDC repair procedure

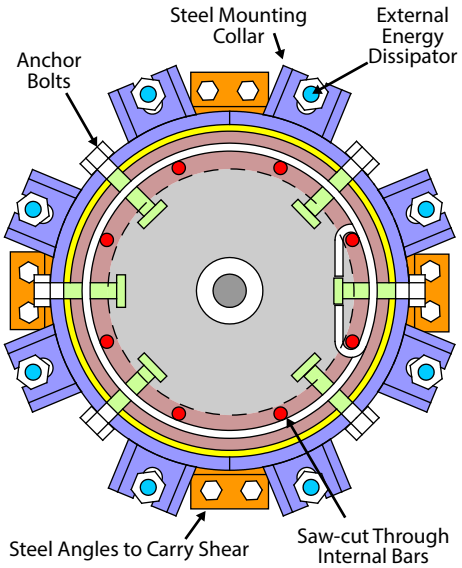

(a) Section A

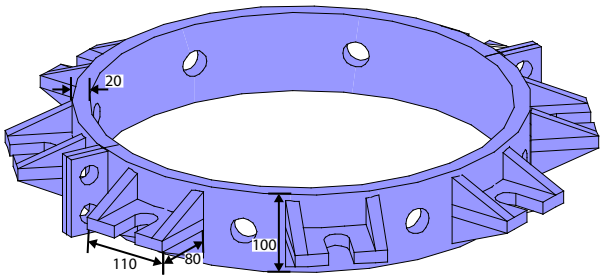

(b) Steel Collar

Figure 5.4: Repaired section and mounting collar

The dissipators used for repair were buckling-restrained grooved bar type dissipators as presented in Chapter 3. Figure 5.5 shows the details of the dissipators used for repair. Since cast-in-place threaded inserts were not installed during initial construction due to space constraints and the re-use of the precast footing, chemical anchorages were instead used for installation of the dissipators with an anchorage depth of 290mm.

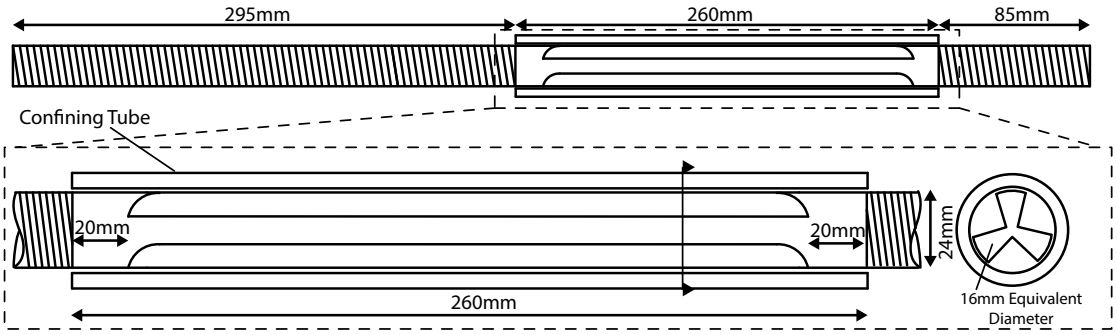

Figure 5.5: Grooved bar type dissipator used for repair of Column CDC

In a seismic event, the longitudinal reinforcing steel in reinforced structural concrete members may be expected to undergo large tension and compression strain reversals of typically one to five fully reversed equiamplitudes (Mander et al. 1992).

A low cycle fatigue model is presented by Coffin [1954] and Manson [1953] which relates plastic strain amplitude, $\Delta\epsilon_p$ to the number of reversals to failure, $2N$.

$$\frac{\Delta\epsilon_p}{2} = \epsilon'_f(2N)^c \tag{5.1}$$

Where, ϵ_f is an empirical constant known as the fatigue ductility coefficient, the failure strain for a single reversal and c is an empirical constant known as the fatigue ductility exponent. An example of the relationship compared to results of experimental testing is presented in Figure 5.6 [Mander et al., 1994].

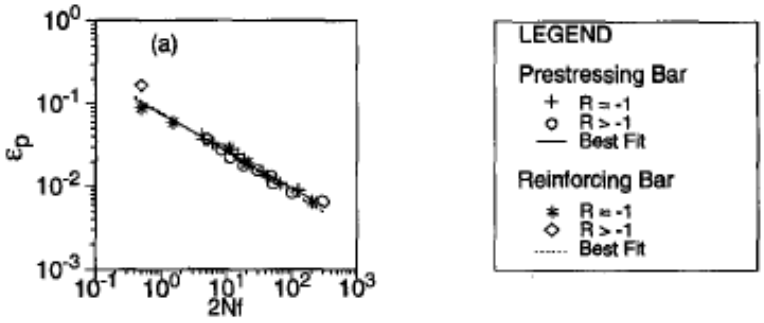

Figure 5.6: Coffin-Mason relationship of strain-amplitude to number of reversals to failure [Mander et al., 1994]

The residual strain capacity of the longitudinal reinforcement reduces with each loading cycle due to these low cycle fatigue effects. In an actual structure that has sustained seismic damage, it is difficult to accurately predict the number of cycles and level of strain that the longitudinal bars have been subjected to, and therefore it is difficult to determine the residual deformation capacity of the structure [Mander et al., 1994, Momtahan et al., 2009].

This repair strategy completely removes any contribution of the existing internal reinforcing bars to the capacity of the structure, thus also reducing uncertainty into the residual strength and ductility of the structure. This allows the post-repair performance of the column to be more simply and accurately predicted and gives confidence that the column will continue to behave as intended in potential future earthquake events. Since the post-tensioning bars or tendons are designed to remain elastic at the design level of drift, no low cycle fatigue degradation occurs, meaning replacement of post-tensioning components in the structure not required following an earthquake event.

5.2.3 Detailing

Much of the detailing considerations for this type of connection are outlined in Section 4.6.2. This section will outline detailing considerations specific to post-tensioning, confinement and application of repair strategy for the Controlled Damage Member Socket Connection which aim to limit and control damage to the structure.

a) Confinement

The addition of post-tensioning in CD connections means the concrete in the connection is subjected to higher levels of compressive strain at all stages of loading. This leads to a reduction in drift capacity of the structure if the cover concrete is left unconfined, with spalling initiating at lower levels of drift.

To accomodate the increased strain demands in the concrete, cover confinement should be provided in the design. This may be in the form of steel casing, fibre wrap or through similar means. Design for the cover concrete is based on Mander's model for confined concrete [Mander et al., 1988]. The process for design of cover confinement and armouring is outlined in Section 4.6.1.

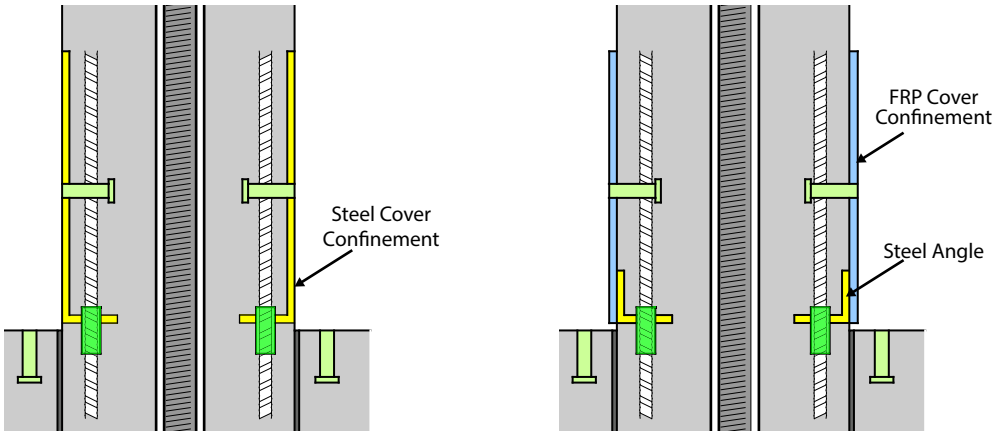

(a) Steel cover confinement (b) FRP cover confinement with steel angle

Figure 5.7: Options for cover confinement of the CD MSC

b) Post-tensioning

Post-tensioning may be provided through the use of either post-tensioned bars or tendons. This should be detailed appropriately to ensure sufficient anchorage at each end of

the column elements. The post-tensioned is unbonded for the full length of the column, remaining elastic during loading of the column.

In the testing outlined in the previous sections, post-tensioning occurred after placement and grouting of the precast column segment. Alternatively, it may be possible to utilise pre-tensioning rather than post-tensioning [Marsh et al., 2011, Stanton, 2010] where tensioning of the bar or strand occurs before placement of the column segment into the socket.

Two options for pre-tensioning are available [Stanton, 2010]. The first is to tension the strands or bar prior to casting of the column, with the ends of the strands or bar cast into the concrete to provide anchorage (along with additional mechanical anchorage if required). This option requires a more involved precasting process, however, and larger pre-stressing losses due to creep and shrinkage will need to be accommodated for, since younger concrete is being pre-stressed.

The second is to use fully unbonded strands or bars as used in the testing outlined previously, but to stress the strands or bars before placing the column in the socket. The advantage of this option is that de-tensioning and re-tensioning of the bar or strands may still be carried out after assembly, if required.

Both options offer further on-site time savings as stressing can be carried out outside of the immediate assembly area and in parallel with other assembly tasks. Tensioning of the columns is simplified as it can be carried out at ground level.

c) Dissipator Connection

Adequate dissipator connections must be used when applying the repair strategy. The connections must have both sufficient strength and stiffness to ensure effective dissipator activation. Elastic deformation in the dissipator and mounting arrangement reduces the amount of plastic deformation in the dissipator, reducing the energy dissipation capabilities and increasing the yield displacement of the column.

During testing, some sliding of the steel mounting collar, and pull-out of dissipators occurred. This highlights the need for adequate detailing of the connection of dissipators. The use of threaded inserts rather than post-drilled and epoxied anchorages

would have reduced the chance of pull-out failure and slippage of the mounting collar, and is recommended for application of this connection in an actual bridge structure (Figure 5.8a).

A form of shear key to provide interlock between the mounting collar and column would have greatly reduced or eliminated any relative movement between mounting collar and column (Figure 5.8b). Tolerance for placing of the dissipators is provided by using oversized slots in the mounting collar, and through adjustment of the nuts used to connect the dissipators and mounting hoops. If steel armouring were used to provide cover confinement to the column, welding of the collar to the armouring would also have been an effective method of fixing the collar and preventing slip as shown in Figure 5.8a.

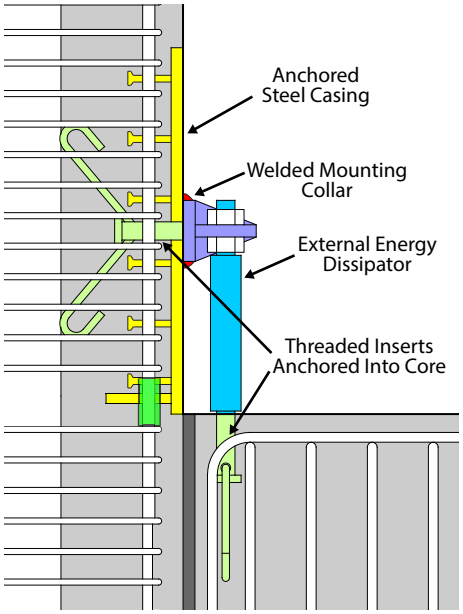

(a) Anchorage of threaded inserts

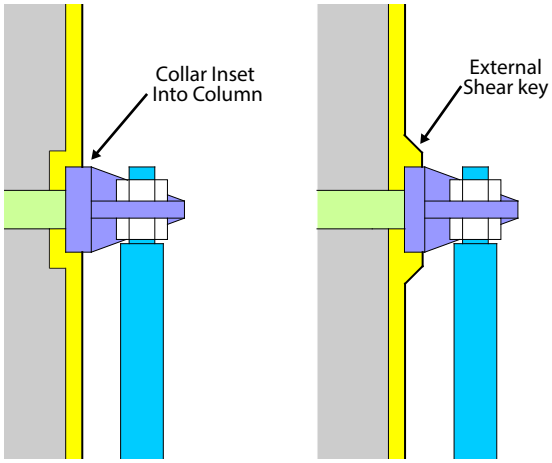

(b) Options for interlock of mounting hoop

Figure 5.8: Dissipator anchorage

5.2.4 Construction

The casting process of the CDC column was very similar to that of the HDC columns in Chapter 4 (Figure 5.9). The only difference between the CD and HD variant is the inclusion of armouring and threaded inserts in the CDC column. In the column that was used for testing, armouring and threaded inserts were not included in the initial construction with FRP being added after the initial testing. Anchorages for the attachment of dissipators were post-drilled rather than bolted into threaded anchors. 50 MPa concrete with 100mm slump was used for the column and footing.

The mounting collar (Figure 5.9d) was fabricated from 20mm flat steel with 15mm flat steel used for the anchorage points of the dissipators. The collar was fabricated at the same time as construction of the column ready for application of the repair strategy.

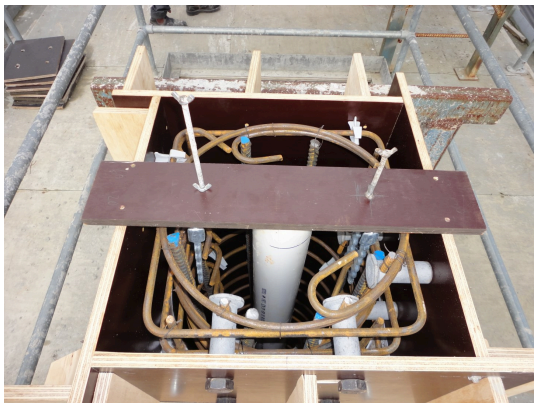

(a) Column Reinforcement

(b) Footing Reinforcement

(c) Pouring Column

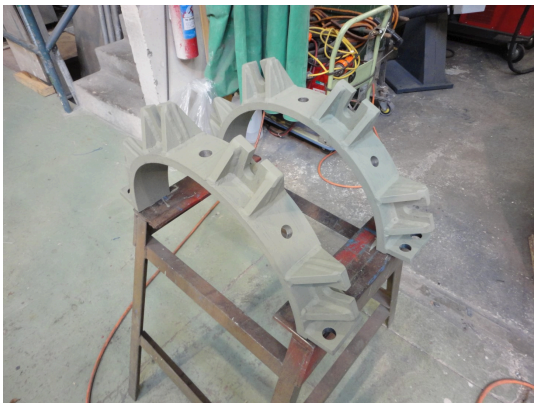

(d) Collar before painting

Figure 5.9: CDC construction

Assembly of Column CDC is illustrated in Figure 5.10.

- Firstly, the precast footing was placed (Figure 5.10b). The footing was reused from a previous HD test and so had some cracks from previous loading.
- The base of the socket of the footing was sealed using a bead of silicon caulk.
- A foam torus and bead of silicon caulk was placed in the centre of the socket to prevent the flow of grout into the anchorage area of the post-tensioning bar.
- The post-tensioning bar was placed into the column and secured by the anchorage at the top of the column, preventing the bar from sliding out of the column during lifting.
- The precast column was then placed into the socket (Figure 5.10d). In the test column, the socket diameter was 20mm larger than the column diameter to allow for placement tolerances and adequate flow of grout in the connection. Wooden blocks were

used to centre the column and ensure it sat vertically.

Once the column was positioned and aligned, the connection was ready to be grouted:

- Grouting of the member socket connection involved spraying water into the joint to achieve a 'saturated surface dry' condition.
- Grout was then poured into the gap between column and footing, using a thin strip of metal to agitate the grout to avoid air voids, until the entire annulus was filled.
- The wooden blocks were left in place during pouring and removed once the grout had started to cure. In some cases, not all of the wooden block could be removed however the volume of wooden block was very small when compared with the volume of grout and so it is expected to have no effect on the performance of the connection.
- The grout was allowed to cure for at least one week before testing, at which point it had obtained 70-80% of its 28 day compressive strength.
- The post-tensioning load was applied at the point of testing (Figure 5.10f).

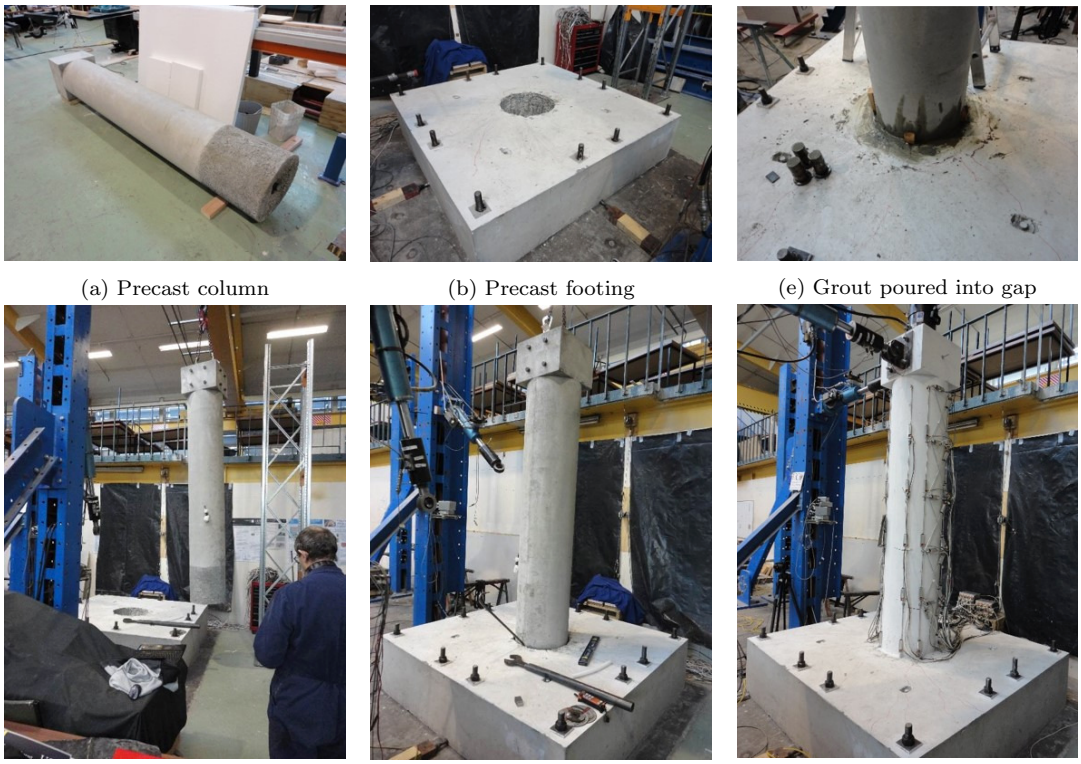

(a) Precast column (b) Precast footing (e) Grout poured into gap

(c) Lifting column into place (d) Column in place (f) Assembled column

Figure 5.10: Assembly of CDC

5.2.5 Testing and Repair

The column was subjected to bi-directional testing using the same testing arrangement and input history as used in the bi-directional testing of the HD connections as discussed in Chapter 4.

a) CDC1 - Preliminary Test

The as-built column was subjected to drifts of up to 2.5% in each direction (Figure 5.11a).

During testing, it was found that there was some loss of axial load in the post-tensioned bar during each drift cycle. This loss was relatively small at around 2% per cycle so it is assumed that the effects on the results are negligible. The axial load was increased at the end of each cycle to the design initial load.

Fine cracking of the column initiated during the 0.35% drift cycle and with further cracks forming up the height of the column in subsequent drift cycles. Spalling initiated in the column during the 2% drift cycle corresponding to the ULS performance level (Figure 5.11c). This is earlier than observed in previous tests where spalling generally occurred in the 2.5% or 3% drift cycles. This premature spalling is caused by a significantly higher level of post-tensioning of the column when compared to the HD tests. This test illustrates the need for cover confinement in a post-tensioned pier system.

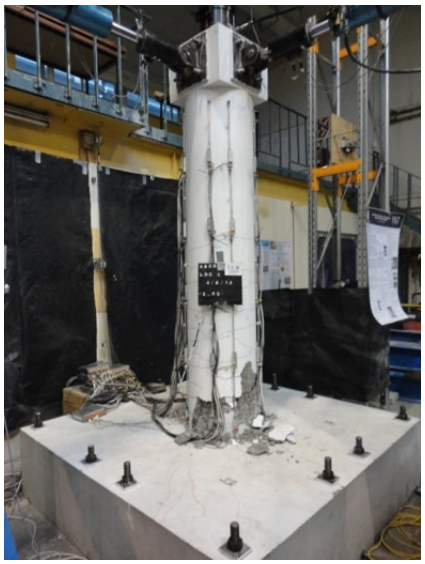

(a) Damage overview

(b) CD MSC following testing

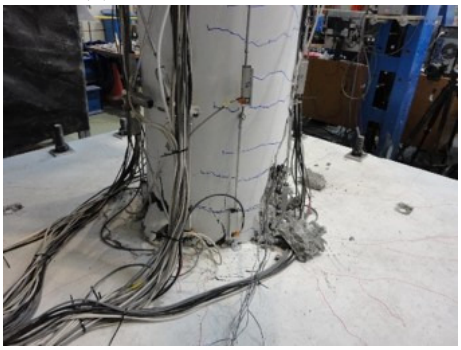

(c) Spalling damage

Figure 5.11: Initial testing of CDC

b) Preliminary Repair

Spalling damage to the column was first repaired after the preliminary test of the column with no cover confinement was undertaken. This repair process is similar to the repair of a High Damage Connection type after moderate seismic loading where it is assumed that sufficient residual strength and ductility remains in the longitudinal reinforcing bars. Fibre Reinforced Polymer (FRP) wrap was applied after repair of the concrete to provide cover confinement to the base of the column.

It should be noted that the initial repair was due to premature spalling of the cover concrete in the first test and is not part of the proposed repair strategy for the Controlled Damage Member Socket pier system. In an actual structure using this connection type, it is recommended that sufficient cover confinement is provided at the initial construction stage of the structure as part of the damage control aspect of the connection.

Initial Repair Process (Figures 5.12 and 5.13):

- Loose concrete material was removed from the damaged plastic hinge region.
- A clean line was cut at the top of the area to be repaired and the cover concrete was broken back to meet the line (Figure 5.13b).
- The damaged area was patched by building up layers of structural repair mortar (Figure 5.13c).
- After patching the concrete and leaving it to cure for a couple of days (Figure 5.13d), Glass FRP wrap was applied to the concrete to provide confinement to the repaired cover concrete (Figure 5.13e).

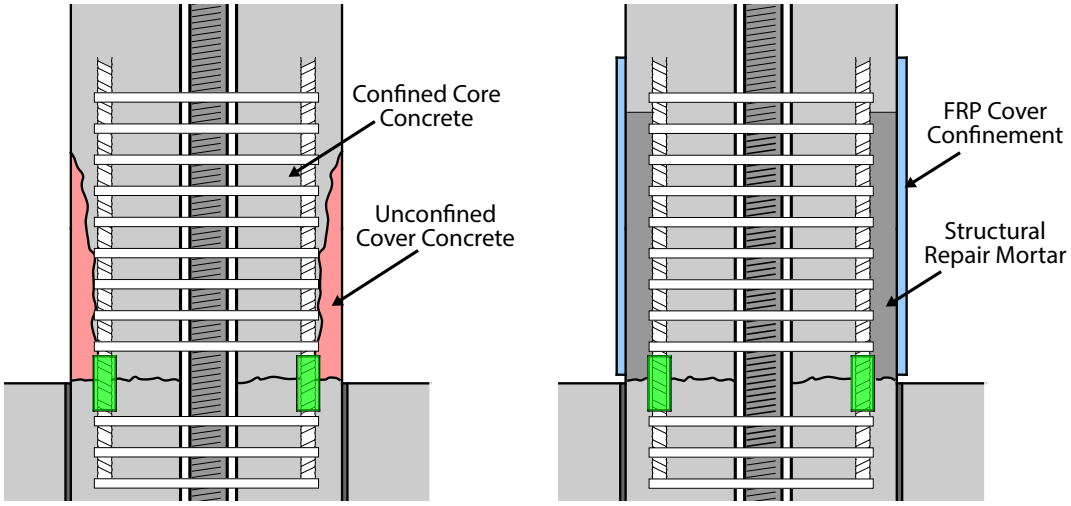

(a) Connection before preliminary repair (b) Connection following preliminary repair

Figure 5.12: Preliminary repair of Column CDC

(a) Column before repair (b) Damaged concrete removed (c) Mortar applied

(d) Mortar cured (e) Glass FRP wrap applied (f) Repair completed

Figure 5.13: Initial repair of CDC

c) CDC2 - Benchmark Test

After repair and application of FRP wrap, the column was tested to drifts of up to 2.5% in each direction (3.25% resultant drift). A considerably lower level of damage was observed with no apparent concrete spalling. The only observed damage was horizontal cracking of the FRP wrap (Figure 5.14b). Since the cracks ran parallel to the FRP thread direction, no reduction in confinement capacity of the FRP wrap was expected to have occurred.

(a) CDC during testing (b) Cracking of FRP

Figure 5.14: Benchmark testing of CDC

d) Application of Repair Strategy

Following the benchamrk testing, the repair strategy was applied to the damaged column (Figure 5.16).

A concrete saw was used to cut the internal bars at the base of the column (Figure 5.16b). The saw-cut was filled with epoxy to seal the gap and form an interface for transfer of gravity loads.

The external dissipators were connected to the precast footing through post-drilling and chemical anchoring (Figure 5.15 , 5.16a and 5.16c). This method was used since the footing was being reused from a previous test and there were space constraints in the half scale column. In an actual structure, threaded inserts would be installed into the footing during the initial construction, allowing for a much simpler repair process and more reliable force transfer between the dissipators and footing. Similarly, chemically anchored threaded rod was used to connect the steel collar to the column. In an actual structure, threaded inserts would be installed during the initial casting of the column.

The repair was completed by fastening the dissipators to the collar using nuts (Figure 5.16d) and mounting steel angles to the footing to assist in shear transfer in the connection. The steel angles were 100x50x10UA of 100mm length and were anchored using chemical anchorage, in an actual structure, cast-in-place threaded inserts would be used for anchorage.

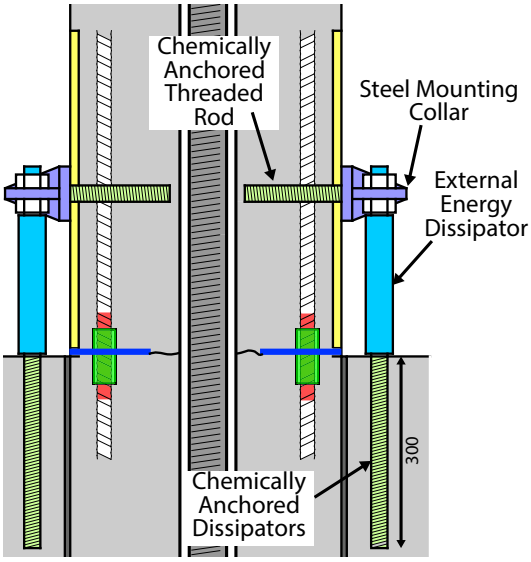

Figure 5.15: Chemical anchoring of dissipators and threaded rod

(a) Post drilling holes for dissipators

(b) Cutting existing longitudinal bars

(c) External dissipators installed

(d) Steel collar attached

Figure 5.16: Application of repair strategy

e) CDC3 - Testing of Repair Strategy

After the repair strategy was applied to the column, a further test was undertaken subjecting the column to drifts of up to 6% in each direction (7.8% resultant drift) as shown in Figure 5.17a. As occurred in previous tests, ram stroke limitation meant that the full 6% could not be applied in the pull direction of each ram.

Some unintended slipping of the steel mounting collar and pull-out of dissipators was observed (Figure 5.17c). Dissipator pull-out was partly due to existing damage of the precast footing from the HD testing. The chance of dissipator pull-out would be greatly reduced with the use of adequately detailed threaded inserts tied into the footing reinforcement. Although dissipator pull-out occurred, there was no failure of dissipators themselves. The external tubes providing buckling restraint were very effective with no visible buckling of the dissipators visible upon disassembly.

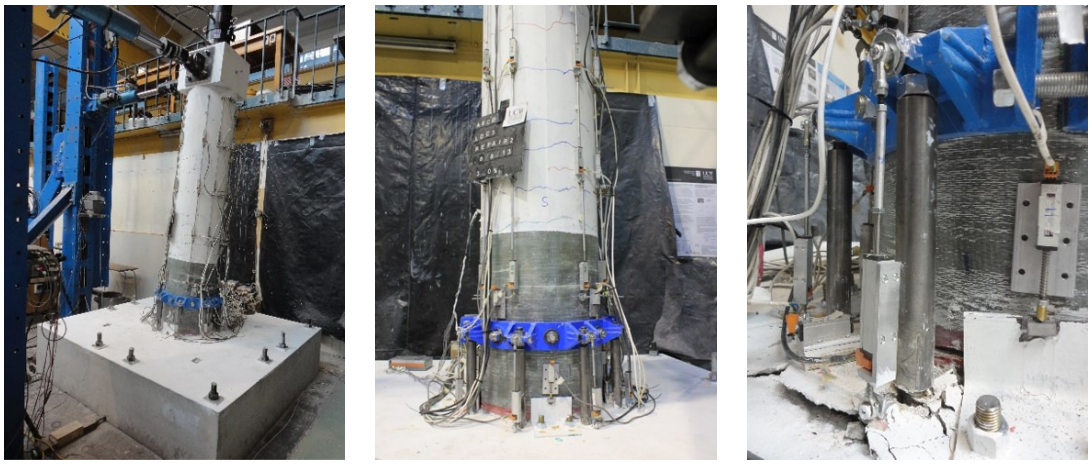

(a) Column at peak drift (b) Column following test (c) Dissipator pull-out

Figure 5.17: Post-repair testing of CDC

f) Dissipator Pull-Out Testing

Pull-out tests were carried out on each of the dissipators following testing (Figure 5.18a). Half of the dissipators failed due to pull-out rather than bar failure as illustrated by Figure 5.18b with the failure mechanism shown in Figure 5.19. This may partly be due to previous damage to the footing during previous column and punching shear testing as part of the HD tests leading to a reduction in effective embedment length of the dissipator anchorage. Pull-out of the dissipators leads to a reduction of strength and stiffness of the column, as reflected in the results. This illustrates the importance of

adequate anchorage of all components of the dissipation system. The use of pre-installed threaded inserts, tied back into the footing reinforcement reduces the risk of pull-out failure of the dissipators while offering increased stiffness of the system.

(a) Pull-out test setup

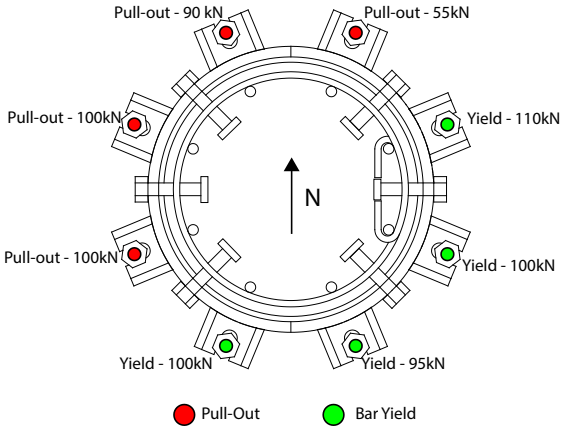

(b) Pull-out test results

Figure 5.18: Pull-out testing

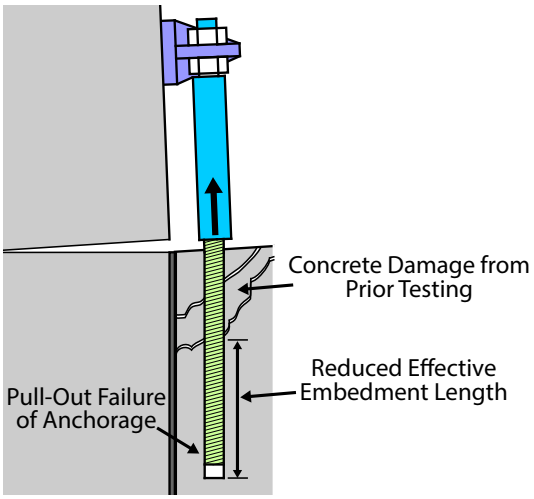

Figure 5.19: Pull-out failure mechanism

5.2.6 Results and Discussion

a) CDC1 - Preliminary Test

In the preliminary test, the column showed a lower than expected strength with degradation occurring in the 2% drift cycle as shown in Figure 5.20. The spalling of concrete corresponds to the Ultimate Limit State (ULS) of the structure and does not satisfy the damage control requirements of the connection. The connection was designed to achieve

a drift of 3%. This early degradation can be attributed to the omission of cover confinement in the plastic hinge region. Since the subsequent test with cover confinement added to the column is being considered as the benchamark case, no further discussion of results will be presented for the preliminary test.

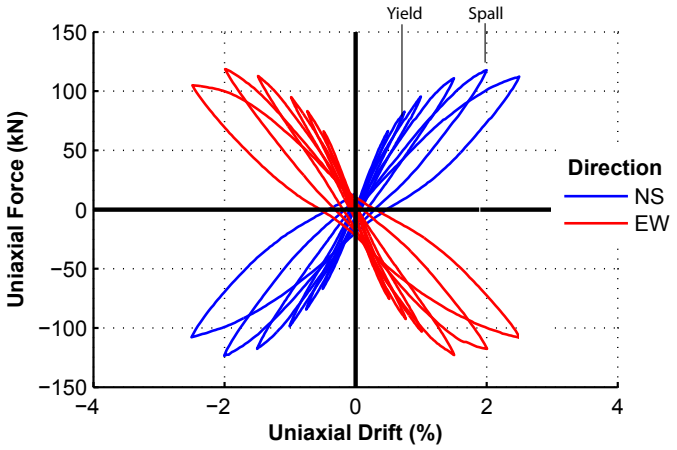

(a) Uniaxial force-drift response

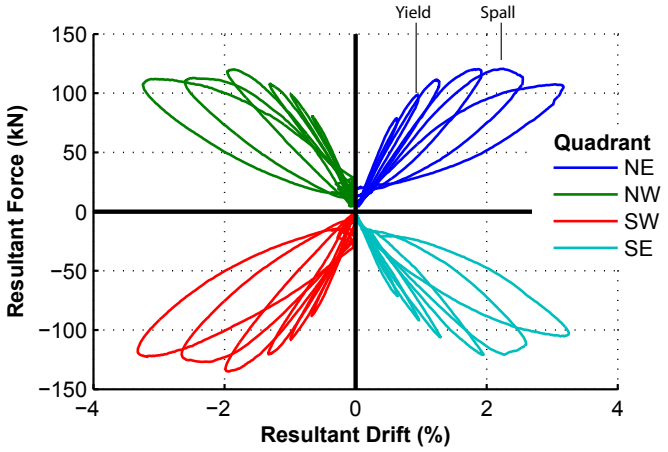

(b) Biaxial force-drift response

Figure 5.20: CDC1 force-drift response

b) CDC2 - Benchmark Test

A higher column strength was seen in the Benchmark Test following the addition of cover confinement (Figure 5.21). No strength degradation was observed in this case up to a drift of 2.5% in the uni-axial stage of loading and 3.25% in the bi-axial stage of loading. Thinner hysteretic loops were observed in the force-drift plot due to the column undergoing significantly less inelastic deformation of the concrete.

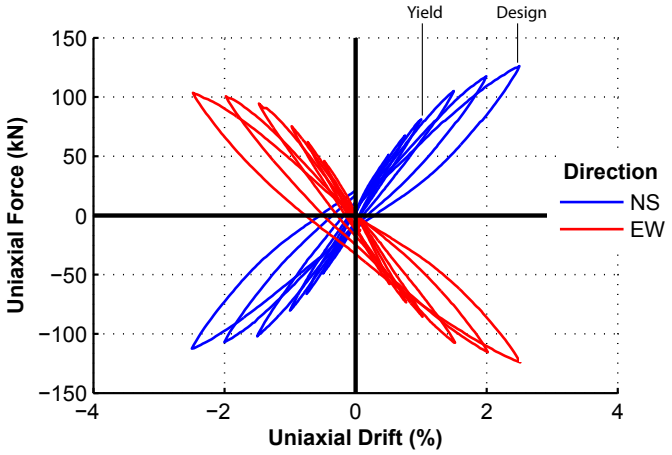

(a) Uniaxial force-drift response

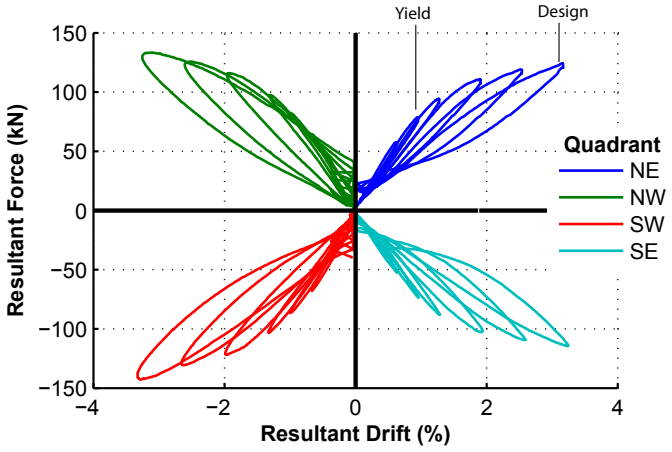

(b) Biaxial force-drift response

Figure 5.21: CDC2 force-drift response

Figure 5.22 gives the hysteretic damping observed in the CDC2 test with increasing levels of drift. The theoretical curve is again based on the Dwairi-Kowalsky damping rule [Dwairi et al., 2007], but in this case a value of C=20 was assumed, representing a hybrid system with a recentering ratio, λ, of 1.5. A good match between theoretical and observed levels of damping was observed with the experimental values slightly higher than the theoretical values.

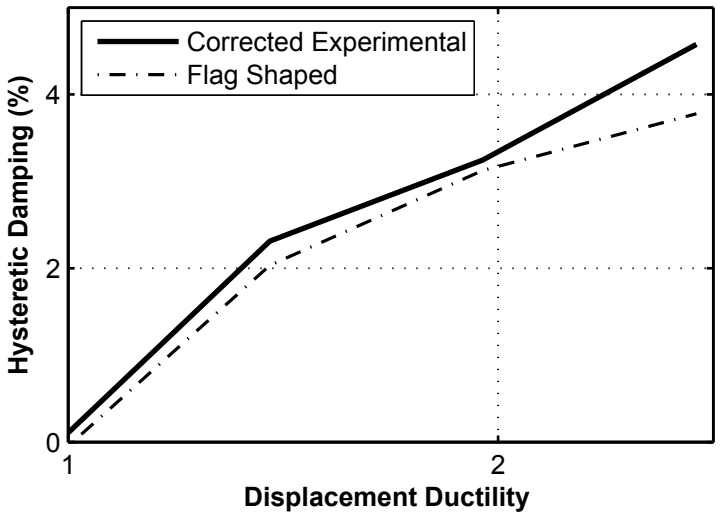

Figure 5.22: CDC2 area based hysteretic damping

Figure 5.23 gives the Acceleration-Displacement Response Spectrum (ADRS) performance evaluation for test CDC2. Like in previous tests, the Servicability Limit State (SLS) is well within the elastic region of the backbone curve meaning no damage is expected in this case. No intercept was reached for the ULS indicating a drift of larger than 3.25% would be expected for this limit state.

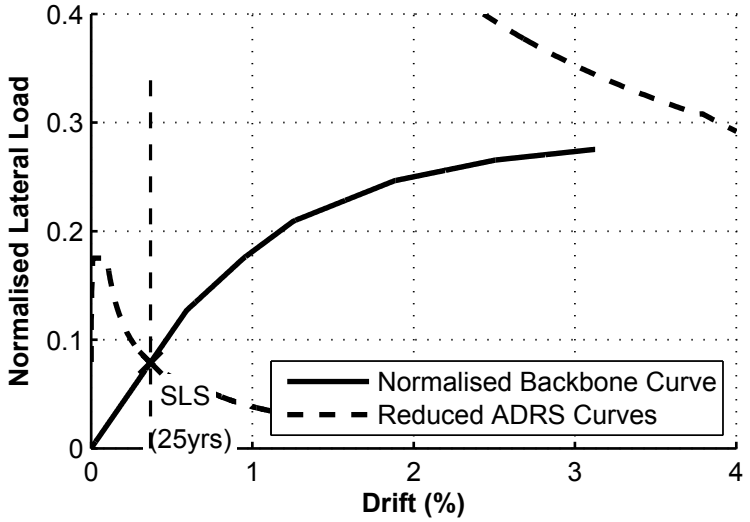

Figure 5.23: CDC2 ADRS performance evaluation

Figure 5.24 gives the amount of energy dissipated per loop for test CDC2. The total cumulative energy dissipated in this test was about half that of the HD tests for the same level of drift reflecting the lower damping levels shown in Figure 5.24.

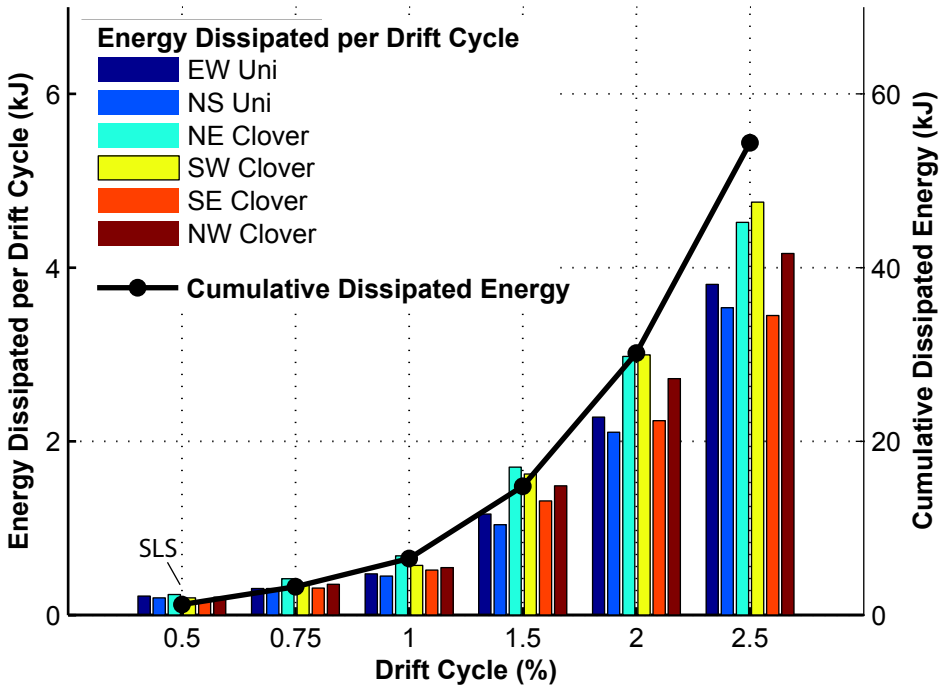

Figure 5.24: CDC2 dissipated energy

Figure 5.25 gives shows the change in post-tensioning (PT) load with drift of the column. This change in post-tensioning force is due to gap opening at the connection interface causing elongation of the post-tensioned bar. In the CDS2 test, the initial post-tensioning force was 900kN, increasing to 1070kN at the design drift of 3%. This is 10% lower than the design post-tensioning force of 1200kN. The reduced post-tensioning force indicates that the neutral axis depth was greater than expected, which may be caused by a reduction in strength of the concrete at the connection due to cyclic loading [Pampanin et al., 2010].

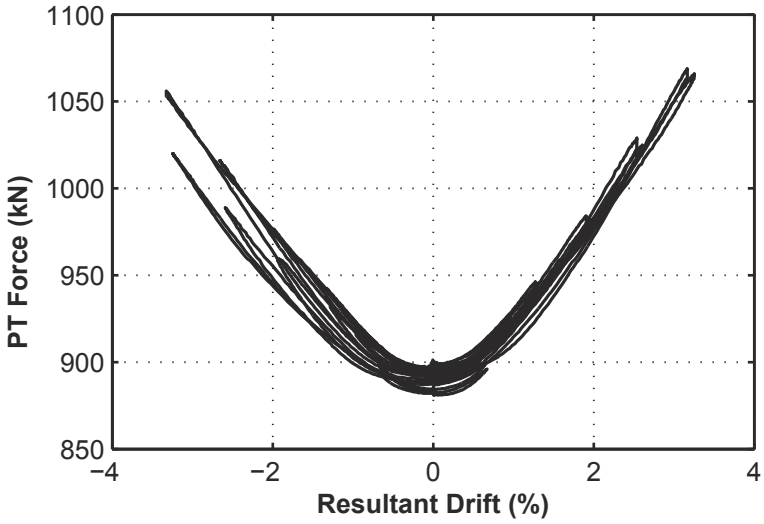

Figure 5.25: CDC2 post-tensioning (PT) force

c) CDC3 - Testing of Repair Strategy

Figure 5.26 gives the force-drift response of the column during test CDC3. During this test, the column was subjected to drifts of up to 6% in each direction (7.8% resultant drift). The Force-Drift loops show no strength degradation until drifts of about 5%. A clear flag-shaped response can be seen in the uniaxial force-drift plot with residual drifts much lower than those observed in the HD tests. The maximum residual drift observed during testing was 1% while in the HD tests, maximum residual drifts of 2-4% occurred. The hysteretic loops of the CDC3 test were much thinner than those of the HD tests as is expected with post-tensioned connections.

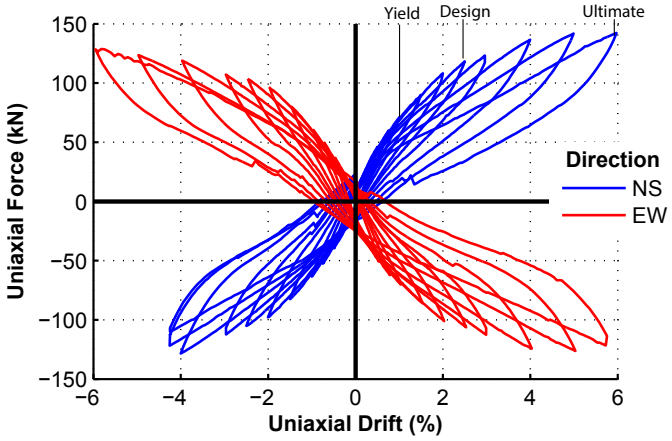

(a) Uniaxial force-drift response

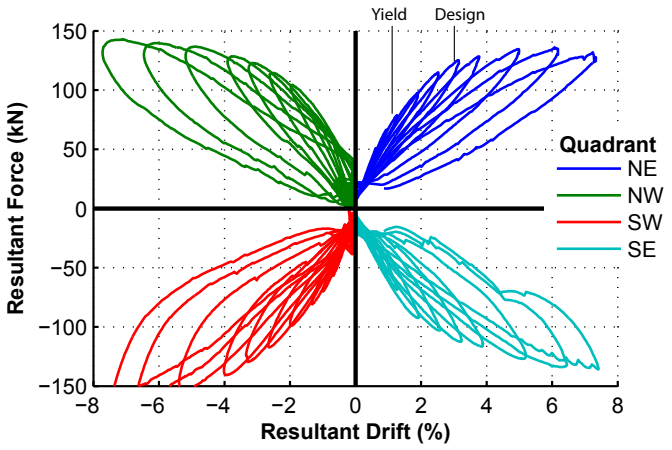

(b) Biaxial force-drift response

Figure 5.26: CDC3 force-drift response

A fairly good match between experimental and theoretical values of damping was found (Figure 5.27) for ductilities up to 3. Again, the experimental values were larger than the theoretical values, with the difference becoming more pronounced at ductilities greater than 3.

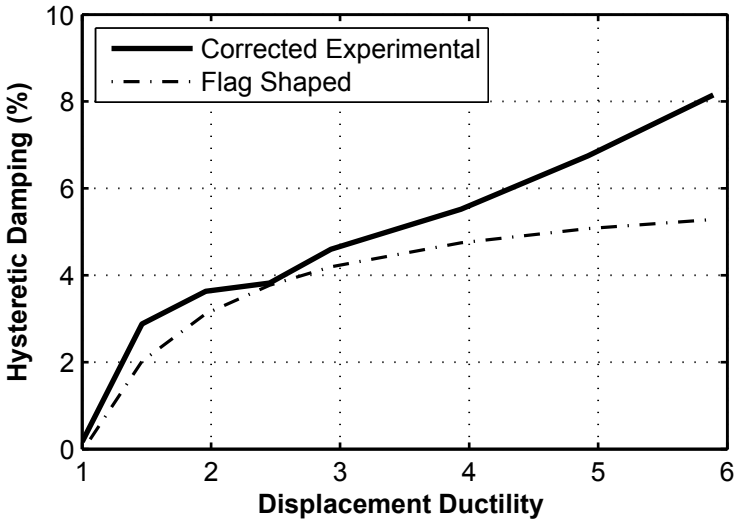

Figure 5.27: CDC3 area based hysteretic damping

Figure 5.28 gives the ADRS performance evaluation for CDC3. It can be seen that a ULS earthquake is expected to generate a drift of 4% in the structure while a Maximum Considered Earthquake (MCE) earthquake is expected to generate a drift of greater than 7%. The ULS drift of 4% is greater than the value considered for design of 3%. This can be attributed to the lower level of hysteretic damping achieved by the post-tensioned system. Lower levels of energy dissipation mean higher peak displacements are to be expected than with HD or conventional monolithic systems. Adequate detailing to accomodate these increased displacements is therefore required.

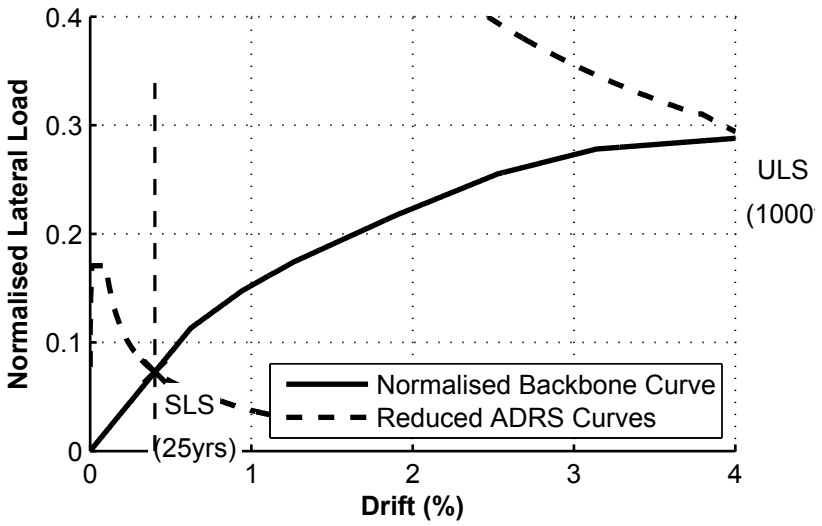

Figure 5.28: CDC3 ADRS performance evaluation

In Figure 5.29 it can be seen that a similar level of cumulative dissipated energy was achieved by the repaired system during CDC3 as in the benchmark test CDC2 indicating the repair strategy was effective at reinstating the capacity of the system with little difference in response under lateral loading. A large variation in energy dissipated per loop occurred in the largest three drift cycles. This is due to degradation of the joint, in particular pull-out failure of the dissipators and damage to the footing. Overall, the energy dissipated in CDC3 was about 60% that of the HD test HDC2.

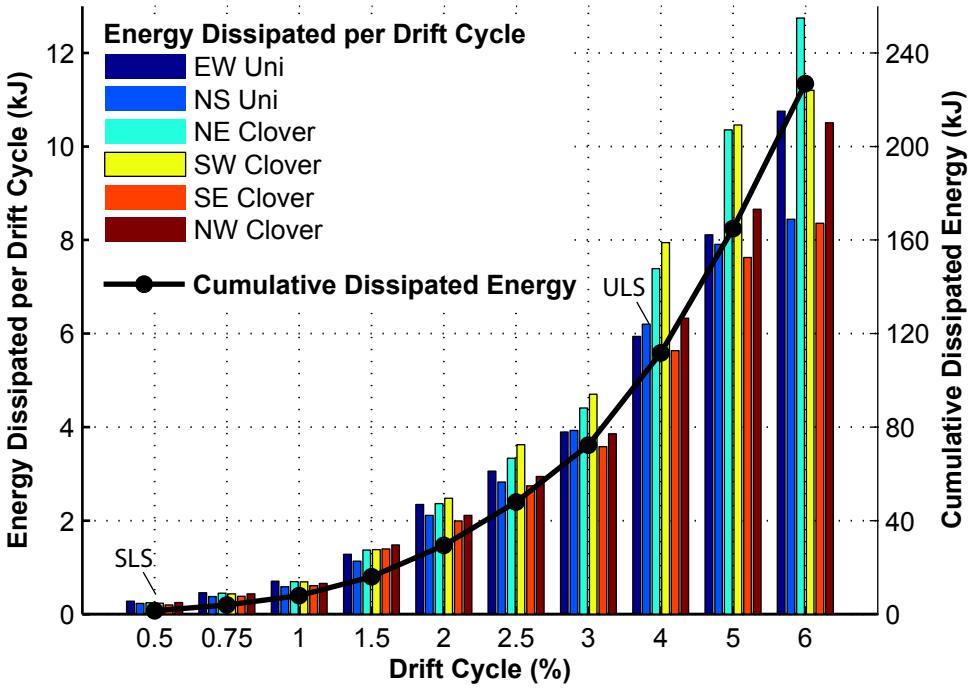

Figure 5.29: CDC3 dissipated energy

In the CDC3 test, the peak post-tensioning load was 1380kN at the ultimate drift of 7.8%. The variation in post-tensioning load at higher drift may be attributable to the asymmetric column behaviour, due partly to slipping of the steel mounting hoop and pull-out of dissipators.

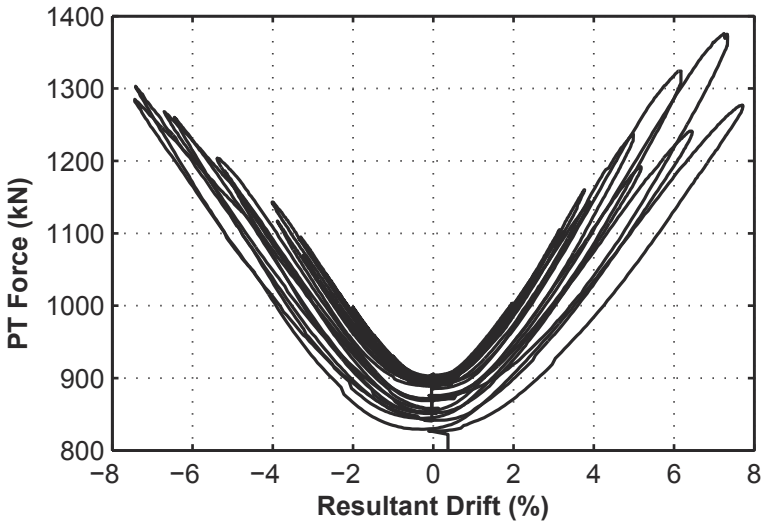

Figure 5.30: CDC3 post-tensioning (PT) force

5.3 Controlled Damage Coupled Bar Pier System

5.3.1 Connection Overview

The second Controlled Damage (CD) connection type presented is named the CD Coupled Bar Connection (CBC) (Figure 5.31). This connection uses replaceable segments of longitudinal bar connected to permanent reinforcement using parallel thread bar couplers. The replaceable segments of bar are located in a recess in the precast column element which is filled with cast-in-place concrete or grout during construction. Steel armouring is used to protect the precast concrete core, meaning all damage is constrained to the cast-in-place material and replaceable dissipators. The armouring also provides a rocking interface between the column and footing.

Following seismic loading, the cast-in-place material is removed allowing for access and replacement of the damaged segments of bar. Conventional necked steel dissipators were used for the initial construction of the Controlled Damage Coupled Bar pier. For the repair of the structure, Grooved Bar Dissipators were used as presented in Chapter 3.

This section outlines the design, detailing, testing and results of the CD CBC. The proposed repair strategy for this type of connection will be presented along with results of the testing following repair.

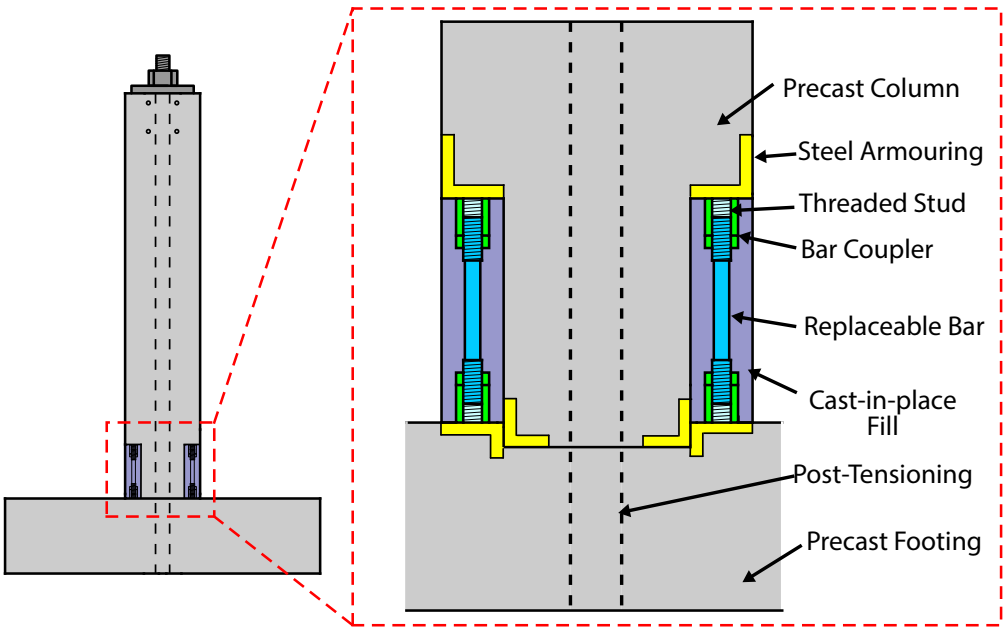

Figure 5.31: Controlled Damage Coupled Bar Connection

5.3.2 Design and Repair Strategy

a) Design

A half scale column featuring the CD CBC, named Column CDS, was tested. An overview of the column is given in Figure 5.32 with detailed drawings given in Appendix D. The test column was based on the bridge prototype presented in Section 4.2 with the CD connections having the same moment capacity as the HD columns.

The column features a square cross section of 500mm depth with a length of 2.7m. The footing has dimensions of 2.1m by 2.1m with a depth of 500mm. The design of the column was based on the PRESSS design handbook targeting a recentering ratio, λ, of 1.3 to 1.5. [New Zealand Standards, 2006a, Palermo, 2004, Pampanin et al., 2010]. The target recentering ratio is higher than the suggested minimum of 1.15 which corresponds to the overstrength factor for non-prestressed steel reinforcement or the energy dissipating devices [New Zealand Standards, 2006a]. Higher values result in less energy dissipation capacity of the system, but help to ensure good recentering behaviour of the connection. An initial level of post-tensioning of 1100kN was used for both the benchmark and repaired test cases, representing both the axial loads and post-tensioning loads in an actual structure. Two design cases were analysed as summarised in Table 5.4. The first assumes 2mm slip of the coupled bar connection under the yield force of the dissipator, which is the approximate value observed in preliminary testing of the connection. The second case assumes no slip between bar and coupler. It is expected that the performance of the column will lie between these extremes. The parameters used for design are summarised in Table 5.4.

	CDS-2mm Slip	**CDS-No Slip**
Design Drift, θ_d	3%	3%
Nominal Moment Capacity, M_n (kNm)	414	468
Mild Steel Contribution, M_s (kNm)	178	218
Post-Tensioning Contribution, M_{pt} (kNm)	233	247
Recentering Ratio, λ	1.33	1.14
Initial PT Force, $T_{pt,initial}$ (kN)	1100	1100
Design PT Force, $T_{pt,design}$ (kN)	1340	1360

Table 5.4: CDS design summary

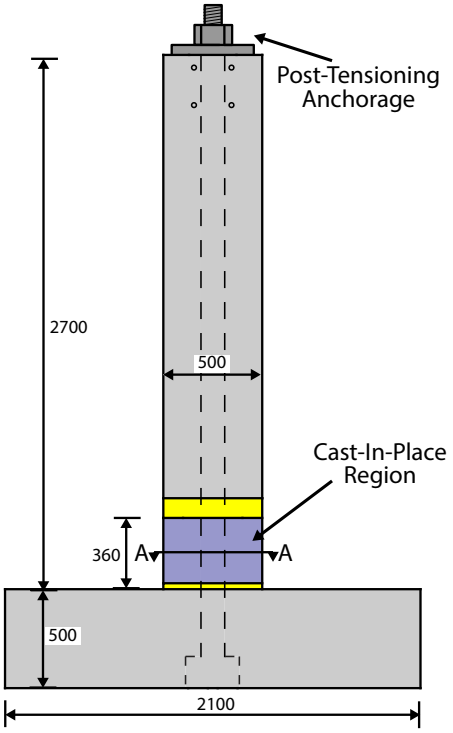

(a) Column Overview

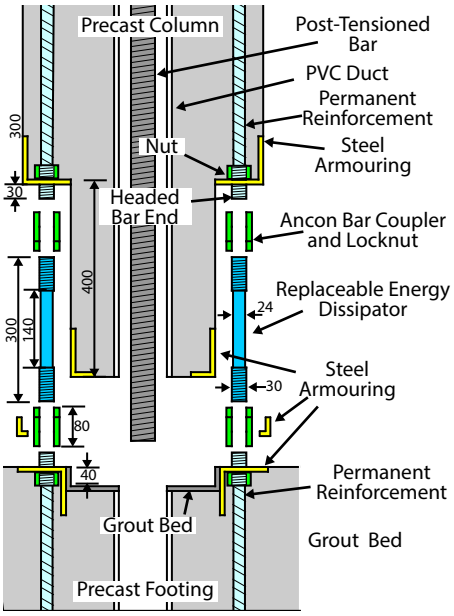

(b) Connection Components

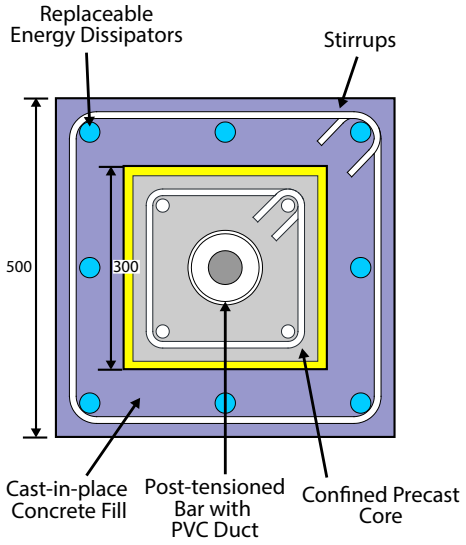

(c) Section A

Figure 5.32: CDS design

The CD CBC features replaceable mild steel energy dissipators located internally in the column. To acheive this, a confined precast concrete core is used in the connection, with the dissipators located outside of this core. Cast-in-place micro-concrete fill encloses the dissipators. The core is designed to carry the full axial and shear loads acting in the structure, while the dissipators and concrete fill carry the tensile and compressive

loads induced by bending moments at the connection interface. The proposed assembly sequence is given in Figure 5.34.

The dissipators are connected to permanent reinforcement using parallel thread bar couplers. The permanent reinforcement used in the test specimens is Grade 500, 24mm diameter reinforcement. The end of the permanent reinforcement is enlarged to 30mm diameter by cold forging and a thread is cut to form a threaded stud for connection of the replaceable dissipators.

The dissipators have a total length of 300mm with a reduced cross section over a length of 140mm at the centre of the dissipator which accommodates all inelastic deformation during loading. The outside diameter of the dissipator in the threaded regions is 30mm while the effective diameter is 24mm in the reduced length of the dissipator. The dissipators were constructed using Grade 300 steel bar, with the reduced section formed by turning down the bar to a smaller diameter (Figure 5.33a). The replacement dissipators used in the application of the repair strategy were grooved dissipators as presented in Chapter 3 and used in Column CDC (Figure 5.33b).

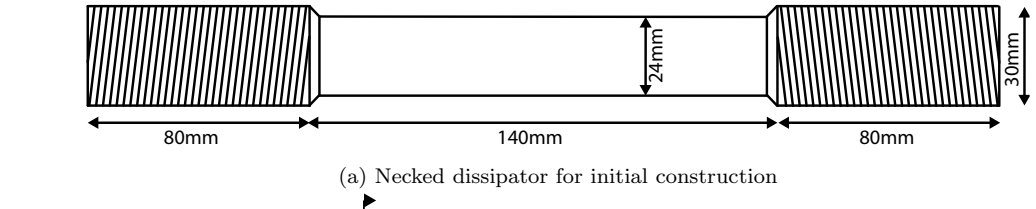

(a) Necked dissipator for initial construction

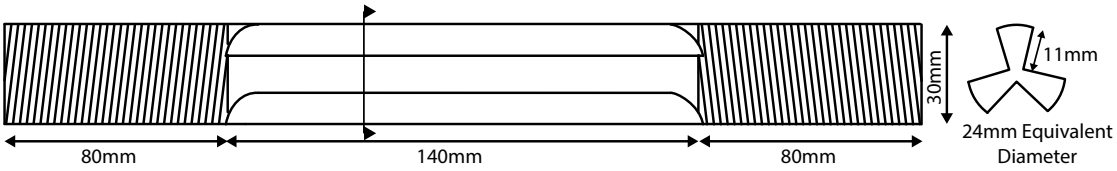

(b) Necked dissipator for repair

Figure 5.33: Dissipators for Column CDS

The dissipators and couplers are debonded from the surrounding cast-in-place fill over their full length. This was achieved through application of grease tape to the dissipators. A smooth profile was achieved to avoid any interlock between the dissipators and couplers, and the surrounding fill. Failure to prevent interlock can mean the dissipators exhibit a significant increase in stiffness when deformed in compression, as the surrounding concrete carries some of the compressive load that would normally be carried by the dissipator [Sarti et al., 2013].

Stirrups are placed around the dissipators during construction and cast-in-place concrete fill is used to enclose the dissipators and complete the connection. During an earthquake, damage to the fill material is expected and allowed for. The inclusion of stirrups provides confinement to the core meaning that although damage occurs, the concrete fill behaves in a ductile manner. The stirrups also provide buckling resistance to the dissipators. Additional armouring was included at the base of the cast-in-place fill to help prevent premature failure of the bottom edge of the fill material. This armouring was also used to fix the formwork while casting of the fill material.

Additional buckling-restraint in the form of confining tubes (as presented in Chapter 3) may be used to further prevent buckling of the replaceable longitudinal bars or dissipators. Stirrups or external cover confinement would be used to confine the fill material, allowing ductile behaviour. This would improve the performance of the connection but would add to fabrication costs.

No damage is intended to occur in the permanent reinforcement, couplers or threaded ends of the dissipators during an earthquake event. Similarly, no damage to any precast concrete is intended. This is partly achieved through inclusion of steel armouring in both the footing and column. The additional purpose of this armouring is to accurately position the reinforcing bars during casting.

The footing features a shallow socket within which the base of the precast core sits, acting as a shear key to transfer shear loads acting in the column. A thin grout bed was formed in the socket between the column and footing to ensure a good interface for transfer of vertical loads exists. It is assumed that lift-up of the precast core inside the socket will occur as the column rocks, without full lift-out of the core occuring meaning shear interlock between the column and footing is always maintained.

Headed anchorages were used to anchor the vertical bars in the precase footing, reducing congestion in the footing. In the column, transition couplers were used to reduce the longitudinal bar diameter from 25mm to 16mm (Appendix D).

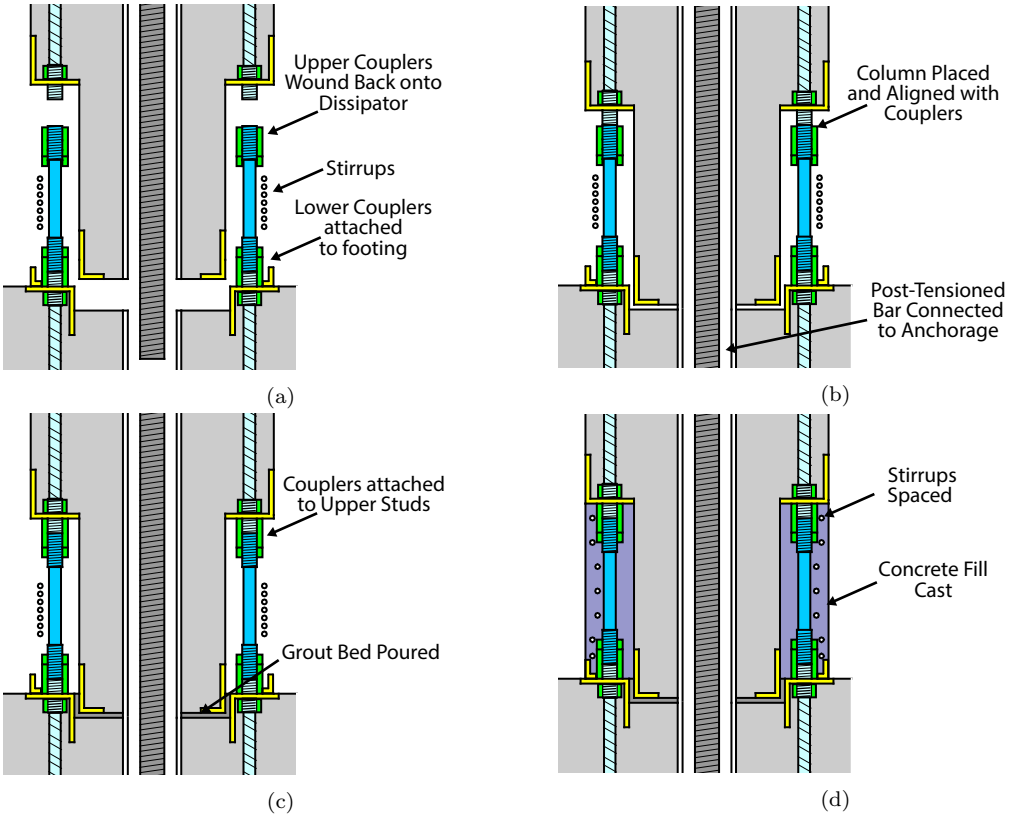

Figure 5.34: CDS assembly process

Specimen Design Limitations

Like the CD MSC, this connection features post-tensioning to provide recentering capabilities to the structure during an earthquake event. During testing, a 50mm diameter post-tensioned bar was used to represent both the post-tensioning and gravity loads in the column. As discussed previously, this load was not regulated throughout testing meaning it increased with increasing levels of drift. In an actual structure, the post-tensioned component of axial load in the column would increase with increasing drift, however the weight of the superstructure would not. Since the required axial load was specified at 3% drift, the axial load in the structure is lower than it would be in an actual structure at drifts lower than 3%, and higher at drifts higher than 3%. It was assumed that this effect would have minimal impact on the results, while greatly simplifying the testing process.

For a full scale construction, regular Grade 300 reinforcing bars with cold-upset, threaded ends may be used as dissipators instead of manufacturing dissipators from steel bar. The use of reinforcing bars as dissipators would reduce the amount of steel fabrication work

for the joint. Regular reinforcing bar could not be used in this case as the total length of dissipator was too short for the cold-upsetting process to be applied.

Material Properties

Concrete of $f'_c = 40MPa$ was used for the design of the test column, however $f'_c = 50MPa$ compressive strength after 28 days was specified since testing of the column was intended to occur earlier than 28 days after casting. Grade 500 steel was specified for all reinforcing in the footing and the column. The replaceable longitudinal bars in the column were specified as Grade 300 steel. Micro-concrete of $f'_c = 50MPa$ after 7 days was specified for initial casting of the fill with grout of $f'_c = 55MPa$ after 28 days specified for repair of the cast-in-place fill. The grout showed to be understrength after 7 days of curing, but this had no adverse effects as sufficient confinement of the fill was provided.

The actual material properties at the time of testing are summarised in Table 5.5.

Material	**Specified**	**Actual**
Concrete		
Column	50	50
Footing	50	60
Steel		
Column Longitudinal	500	520
Column Transverse	500	580
Footing	500	520
Replaceable Dissipators	300	380
Grout		
Construction	50	23
Repair	55	39

Table 5.5: Summary of CDS material strengths (MPa)

b) Repair Strategy

During an earthquake event, the connection is detailed such that all damage is constrained to the cast-in-place concrete fill and necked regions of the replaceable dissipators. No damage is expected to occur to the threads or couplers used to connect the

dissipators, any precast component, or the post-tensioning components. The provision of steel armouring and rocking nature of the joint helps to protect the precast core from damage during lateral loading.

The repair strategy is illustrated in Figure 5.35 consisting of:

- Removal of cast-in-place fill and stirrups.
- Removal of damaged dissipators through cutting of dissipator or winding back of couplers onto dissipator. Removal by winding back couplers is a simpler option, but may not be possible if buckling of the dissipator has occurred.
- Replacement of dissipators, stirrups and cast-in-place fill following the construction procedure outlined previously.

Since the precast core of the connection is detailed to carry the full axial load in the structure, release of post-tensioning force before repair is not necessary.

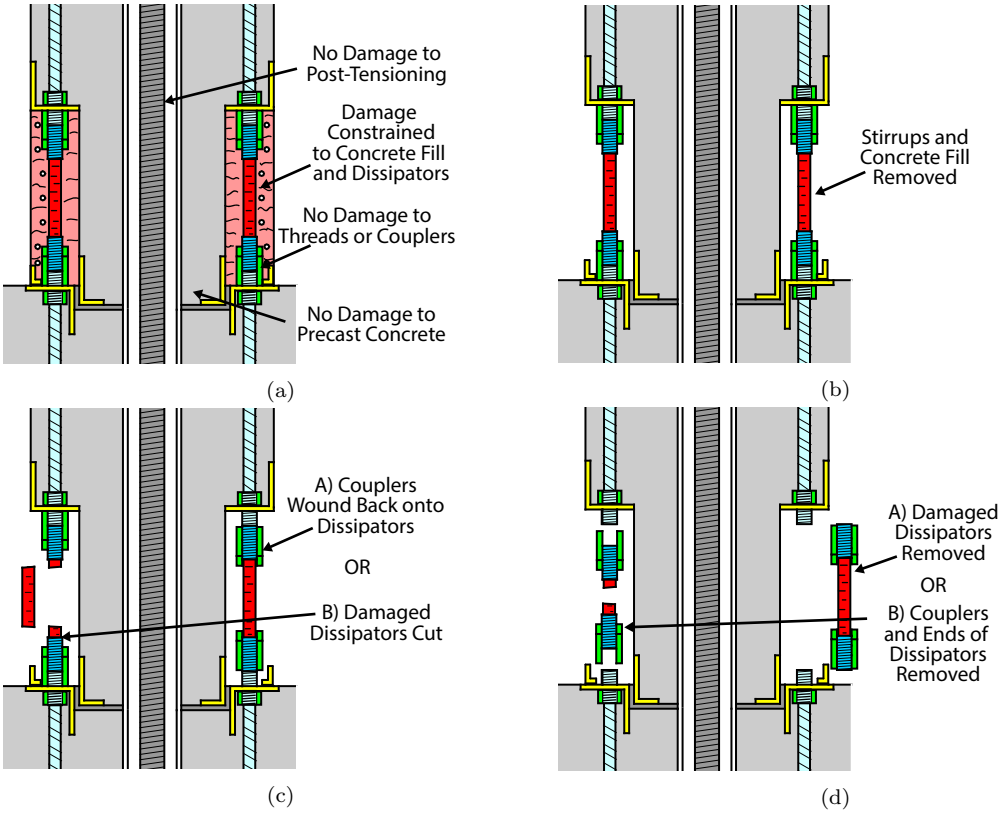

Figure 5.35: CDS repair procedure

5.3.3 Detailing

a) Tolerance

In any construction, there must be sufficient tolerance for placement and alignment of components to avoid any costs and delays associated with misalignment of components during construction. The use of couplers offers some challenges in terms of tolerance which must be considered during design. The alignment directions considered in the discussion of tolerance are shown in Figure 5.36.

In the CD CBC, accurate horizontal positioning of the threaded studs which are part of the permanent reinforcement is required for both the construction and repair of the column. Positioning of these studs is helped by the armouring that is located in both the footing and column. Holes were drilled in the armouring during fabrication and the threaded studs passed through these holes during casting to ensure good alignment between the top and bottom studs.

Testing of the couplers used in the construction of the CBC shows that only 60% of the thread length is required to achieve full bar strength in Grade 500 bar. This means a small gap between dissipators and studs is permitted giving vertical tolerance in placement of the dissipators. This is particularly useful during application of the repair strategy where the replacement dissipator is placed between the two studs. It also gives some tolerance in stud length, simplifying the casting process.

In the testing, Grade 300 bars with reduced cross sections were used, meaning even less thread length is required to exceed the tension capacity of the dissipator. This further ensures that no coupler or thread damage will occur as the dissipators are yielded.

There is the potential for rotational misalignment in the dissipators where the end of the thread at the end of the dissipator does not align with the start of the thread on the threaded stud. This prevents the coupler from being able to be wound from the dissipator onto the threaded stud. This alignment issue did not cause any major problems during application of the repair strategy however it did require some trial to find the most suitable loacation for each dissipator and should be considered during design. Alternative coupler designs as outlined in Section c) may help to alleviate or eliminate this potential issue.

In testing, there was a slight slackness between the threads of the coupler and threaded studs. Tensile tests carried out in the lab showed that the full bar strength was still achieved despite the slackness. The slackness actually helped with installation of the dissipators as it gave some tolerance when winding the couplers onto the studs. The use of locknuts with the couplers helps to take up this slackness, removing its influence on the deformation of the dissipators under lateral displacement of the column.

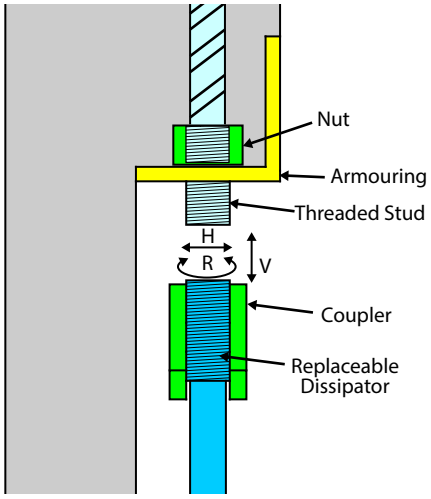

Figure 5.36: Alignment directions

b) Shear Key

Interlock between the precast core of the column and a shallow socket in the footing provided the shear transfer mechanism for the connection. Sufficient socket depth must be provided to ensure that failure of the precast core or edges of the shear key does not occur. A deep socket, however, can lead to binding of the connection, preventing rocking behaviour. Bevelling the socket could help to prevent binding of the column in deeper sockets. The provision of armouring and active confinement provided by the post-tensioning increases the capacity of the concrete in the shear key region, helping to prevent failure.

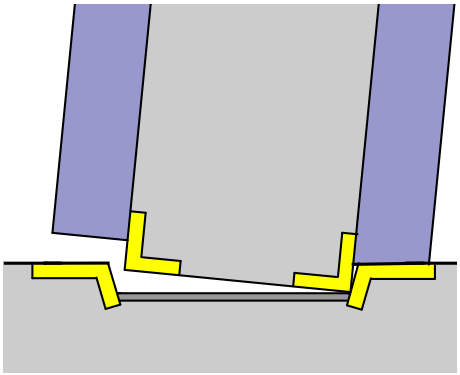

Figure 5.37: Rocking mechanism with bevelled socket

During deconstruction, it was found that the precast core had become bonded to the footing during pouring of the grout bed between the two elements. This is undesirable as it prevents rocking and lift-out of the precast core in the socket, meaning the core is subjected to additional bending moment forces. This increases the capacity of the connection but leads to an undesirable reduction of recentering ratio and damage to the precast core. To avoid bonding of the column and footing, a debonding agent could be applied to the base of the column segment before assembly. Alternatively, the grout bed may be cast before placement of the column.

Match casting is a technique used in the precasting industry where one precast concrete element is used as formwork for casting of an adjacent element [Podolny and Muller, 1982]. This forms a perfect interface between the two elements, removing the need for a grout bed. Match casting in this case would mean no grout bed is required and would simplify and increase the speed of assembly.

c) Coupler Type

Parallel threaded couplers were used in the testing of the CBC and were found to be effective with good performance and straightforward construction and replacement. However, a number of alternative couplers exist which may offer other advantages in terms of construction tolerance and ease of assembly. Position couplers and sleeve type couplers will be briefly outlined.

Position couplers (Figure 5.38) can be extended and retracted, meaning they can be used to close gaps between two bars [Ancon Building Products, 2013]. The use of position

couplers in the CBC gives more vertical tolerance in the assembly and replacement of dissipators. The use of tapered threads also helps to locate the dissipator connections horizontally. Position couplers could not be used in the test column as the amount of length adjustment of the coupler was insufficient to close the gap between dissipator and threaded stud. This may not be a limitation for full scale construction.

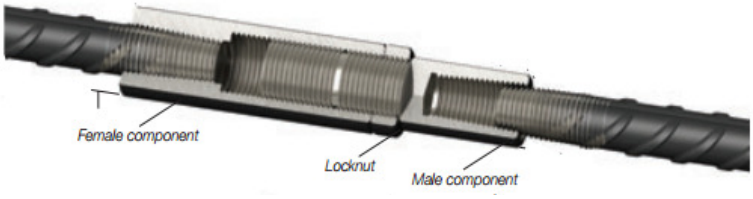

Figure 5.38: Ancon position coupler

Caltrans have developed a coupled connection which uses a replaceable fuse bar similar to that investigated in the CD CBC (Figure 5.39) [Marsh et al., 2011]. The coupler type has been developed for use in precast bridge structures, allowing replacement of damaged reinforcing bars following seismic events. A head is formed on the end of each bar and two threaded coupling pieces draw the bars together. This differs from the couplers used in the CDS column, which provided connection by threading the couplers onto the bars themselves. To ensure contact for transferring compression, a shim may be placed between the bar ends. This type of coupled connection offers better vertical alignment of the replaceable dissipator as the shim thickness can be varied to close the gap between the dissipators and mounting studs. Rotational alignment issues are also avoided as there is no thread to be aligned between dissipator and studs. This type of coupler may offer slightly more horizontal tolerance in the connection also.

Figure 5.39: Caltrans sleeve type coupler [Marsh et al., 2011]

One factor that must be considered in all cases is the safety and code compliance of coupler use in the plastic hinge region of columns. In particular, as part of the energy dissipation system of the structure where coupler failure could have serious consequences. New Zealand codes do not permit the use of bar couplers in the plastic hinge region of

columns [Kirkcaldie and Lloyd, 2013, NZ Transport Agency, 2013] meaning re-evaluation of the codes is required before a structure utilising the CBC can be compliant.

The main concern raised in the NZTA Bridge Manual Third Edition [NZ Transport Agency, 2013] relates to the use of cast iron couplers, which may fail in a brittle manner. However, Kirkcaldie and Lloyd [2013] also express concern in the use of coupling systems featuring enlarged bar ends by cold upsetting presented in this research. In particular, it is expected that cold forging will alter the mechanical properties of the bar, reducing its impact resistance. The NZTA Bridge Manual Third Edition [NZ Transport Agency, 2013] specifies that the coupler strength must exceed the maximum upper bound ultimate tensile strength of the reinforcing bar size and grade to be joined or anchored. Testing requirements are specified, which must be fulfilled before use of couplers in the bridge structure is permitted.

In this case, the coupled connections used had capacity that exceeded the full bar strength in Grade 500 reinforcing bar of full dimension as proven by experimental testing. The forces that the coupled connections are actually subjected to during an earthquake event are those to yield Grade 300 steel bar of a reduced cross section which is significantly less than the capacity of the coupled connection as illustrated in Figure 5.40, even when considering a strain hardening factor of 1.25 [New Zealand Standards, 2006b]. This offers a significant factor of safety of the coupled connection which significantly reduces the probability of unexpected failure and should be considered when evaluating the safety and suitability of the use of couplers in this type of connection.

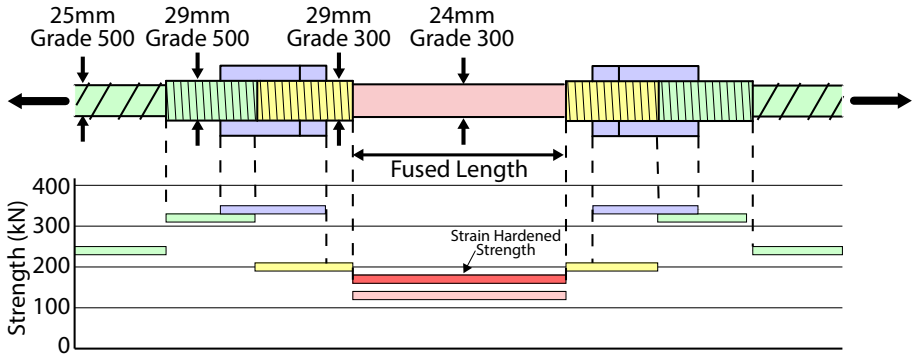

Figure 5.40: Strength distribution along coupled connection

d) Buckling Restraint of Replaceable Dissipators

In the test column, conventional stirrups were used to provide confinement to the cast-in-place fill and prevent buckling of the replaceable dissipators.

As an alternative, steel tubes may be placed around the dissipators as used in the CD MSC. This solution is particularly applicable to the grooved dissipators, where contact between the tube and dissipator is maintained for the full length of the tube as discussed further in Chapter 3. When using necked dissipators, a fill material such as grout or epoxy is required in the tube to close the gap between the dissipator and tube [Amaris Mesa, 2010, Christopoulos et al., 2002, Marriott, 2009, Sarti et al., 2013]. In this case, additional confinement to the cast-in-place material is required if the fill material is to contribute to the moment capacity of the connection. In some cases, it may be acceptable for the fill material to remain unconfined, removing its contribution to the moment capacity of the connection and allowing spalling damage to occur throughout the full depth of the fill.

An alternative mechanism for providing confinement and anti-buckling capacity is to provide external armouring to the cast-in-place region of the column in the form of steel casing or FRP wrap. Ideally, replaceable steel casing would be used, meaning it could be reused for application of the repair strategy and could act as formwork when pouring the cast-in-place fill (Figure 5.41b). This would require further steel fabrication, but would save time during assembly and remove the need for timber formwork.

Threaded, headed anchors are also an option for preventing buckling of the dissipators (Figure 5.41a). These products are available from manufacturers of bar couplers as used in the CD CBC. They may also offer confinement to the cast-in-place fill of the connection. The headed ends of the bars are removable allowing access and removal of the dissipators. The bars and heads are then re-used during the repair stage, reducing material costs of the repair.

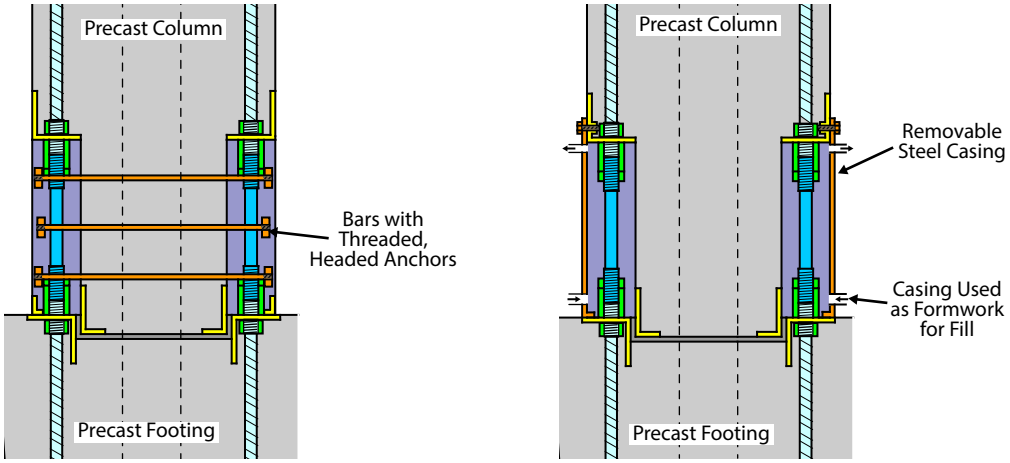

(a) Headed bar solution (b) Steel casing solution

Figure 5.41: Alternative buckling restraint options

5.3.4 Construction

Steel armouring was fabricated from steel angle and holes were drilled into the armouring corresponding to the threaded stud locations. Cold forging and threading of the reinforcement to form the headed, threaded studs on the ends of the bars for connection of removable dissipators was done offsite. Fabrication of the replaceable dissipators was carried out in the lab workshop using steel bar. For full scale projects, the dissipators could be manufactured from reinforcing bars, using the cold forging method used for the permanent reinforcement. The smaller length of the dissipators used in the half scale testing meant the cold forging process could not be applied and so steel bar was turned down on the lathe and threaded to produce the necked dissipators used for the initial construction. The grooved dissipators used in the repair of the column were also fabricated at this point, ready for application of the repair strategy.

The reinforcing cages, armouring, permanent reinforcing, dissipators and couplers were test fitted before casting of the column and footing (Figure5.43a). Once the correct stud length and position was determined, nuts were attached to both the inside and outside of the armouring to secure the bars for casting(Figure 5.42). The outer nuts were removed once casting was complete allowing the couplers to be attached. During casting, the nuts and exposed thread were covered in tape for protection.

Transition couplers were used to reduce the bar diamater from 25mm to 16mm midway up the column (Figure 5.43g). Headed anchors were used in the footing to anchor the

longitudinal bars without the need for hooks, reducing congestion. 50 MPa concrete with 100mm slump was poured for the column and footing.

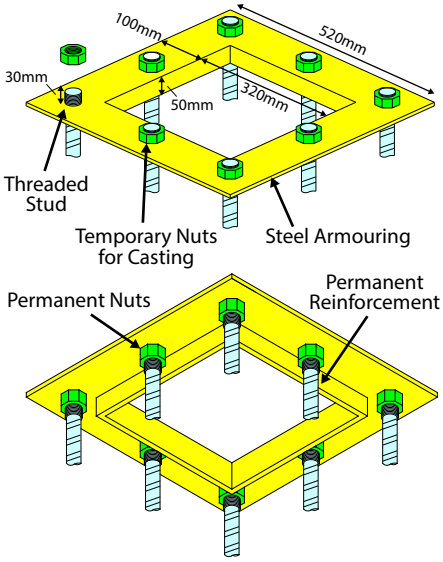

(a) Footing armouring

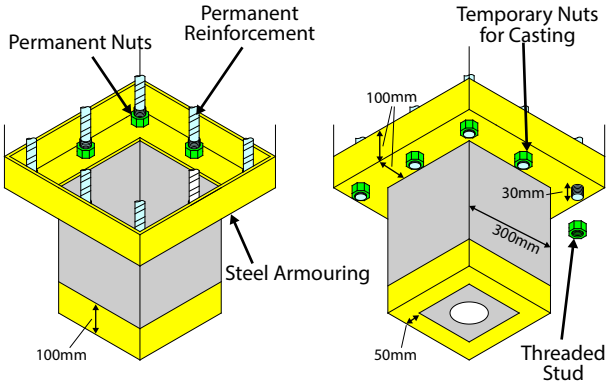

(b) Column armouring

Figure 5.42: Armouring and nuts used to position reinforcement while precasting

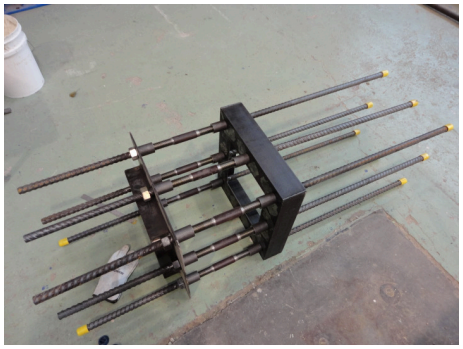

(a) Test fit of dissipators and couplers

(b) Temporary nuts fitted

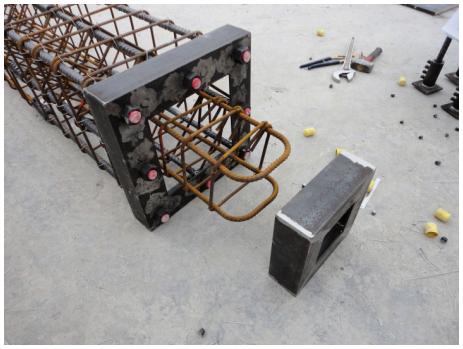

(c) Armouring and threaded studs

(d) Footing reinforcement in formwork

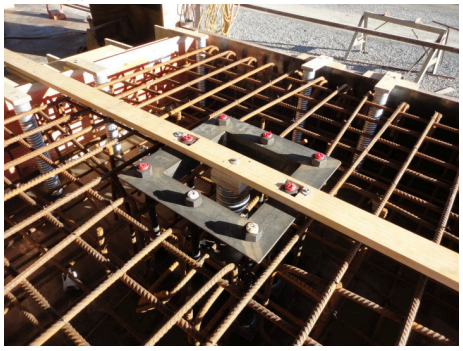

(e) Footing armouring and threaded studs

(f) Footing after pouring

(g) Column reinforcement

(h) Column formwork

(i) Column after pouring

Figure 5.43: CDS Construction

The assembly process is illustrated in Figure 5.44 and is described as follows:

- The footing was placed with the steel anchor plate located in the socket on the underside of the footing.
- A foam torus was placed around the central duct on the top of the footing. Silicon caulk was applied around the foam torus.
- The external dissipators were attached to the threaded studs on the footing using the bottom bar couplers.
- A layer of grease tape was applied to the central necked region of the dissipators.
- Stirrup hoops were placed around the dissipators with the hook location of each stirrup staggered to avoid congestion.
- The upper bar coupler was attached to each dissipator ready for column placement.
- The post-tensioning bar was positioned inside the column member before lifting with a washer and nut at the top of the bar preventing it from sliding through the column during lifting.
- The column was placed aligning each dissipator with the threaded studs on the underside of the column.
- Each upper bar coupler was wound up onto the threaded stud connecting the column and footing. On a number of connections, there was a small gap between the end of the dissipator and stud. This gap was within tolerance for achieving full bar strength in the coupled connection (Appendix E). This is futher discussed in Section 5.3.3.
- After placement and attachement of dissipators, the post-tensioning bar was turned by hand to attach it to the plate on the underside of the footing.
- The upper plate, load cell and axial ram were placed on top of the column before the top washer and nut were attached to the post-tensioning bar.
- At this point the post-tensioning load can be applied to the pier however we applied the post-tensioning load just before testing commenced.
- An additonal layer of grease tape was applied over the full length of dissipators and couplers. A smooth profile was formed to avoid interlock of concrete and steel bars and couplers as the dissipators deform in compression (Figure 5.44f).
- The stirrups were then spaced to provide restraint over the full length of dissipator and coupled regions (Figure 5.44g).
- Formwork was assembled around the precast core and bar couplers (Figure 5.44h). Grout was then gravity fed into the lower fill tube and filling the void from the base until grout flowed out of the top breather tubes (Figure 5.44k).

- After leaving the grout to cure for a day, the formwork was removed, completing construction of the joint (Figure 5.44i).

(a) Footing studs with couplers

(b) Necked dissipators attached

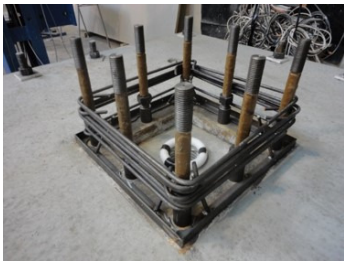

(c) Necked dissipators attached

(d) Column placed

(e) Dissipators attached to column

(f) Denso tape applied

(g) Stirrups spaced

(h) Formwork applied

(k) Micro-concrete gravity fed into formwork

(i) Formwork removed

(j) Construction complete

Figure 5.44: Construction of CDS

5.3.5 Testing and Repair

The column was subjected to bi-directional testing using the same testing arrangement and input history as used in the bi-directional testing of the High Damage Connections as discussed in Chapter 4.

a) CDS1 - Benchmark Test

The column was subjected to drifts of up to 2.5% in each direction (3.25% resultant drift) as shown in Figure 5.45. As observed in previous tests, fine horizontal cracking initiated at the base of the column during the 0.35% drift cycle. Further cracking occurred up the height of the column during larger drift cycles. These cracks all closed to hairline cracks upon unloading of the structure.

As intended, all damage was constrained to the cast-in-place region of the connection with spalling initiating during the 2% drift cycle (2.6% resultant drift, ULS performance level). By the end of testing, spalling had extended to a height of 100mm (Figure 5.45c).

(a) Column during testing

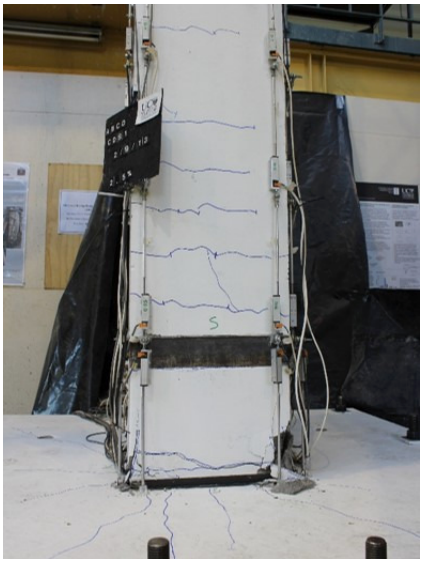

(b) Column following testing

(c) Spalling damage following test

Figure 5.45: Benchmark test of CDS

b) Application of Repair Strategy

Following the benchmark test, the repair strategy was applied as illustrated in Figures 5.46 and 5.47 and outlined in Section 5.3.2b. Upon disassembly, it was found that some buckling of the dissipators had occurred indicating that further buckling restraint is required if buckling of dissipators is to be avoided at the design level of loading.

As intended, it appears that no coupler or thread damage occurred. There was some fine cracking of the precast core however it is not expected to have a detrimental effect on the performance of the column. Upon dissassembly of the column following testing, it was found that the precast core had become bonded to the footing while pouring of the grout bed meaning the core was restrained from lifting out which may have contributed to cracking of the core. It is recommended bonding of the precast core is prevented either by greasing the base of the column before construction or by casting the grout bed before placement of the column.

There was some difficulty with rotational alignment of threads when installing the replacement dissipators as the threads on the threaded studs did not line up with threads of the dissipators. The difficulty was overcome by swapping the location of dissipators and did not prevent the repair strategy from being applied but should be considered during design. The replacement of dissipators was straightforward otherwise.

For the repair of the column, grout was used for the cast-in-place fill rather than micro-concrete as used in the initial construction. This is due to difficulties with gravity feeding of the micro-concrete where aggregate blockage occurred. The grout was of similar strength to the micro-concrete and there was no change in construction methodology.

(a) Cast in-situ concrete removed

(b) Dissipators cut and removed with couplers

(c) New grooved dissipators installed

(d) Denso tape applied to debond bars

Figure 5.46: Application of CDS repair strategy


(a) U-shaped stirrups placed


(b) Stirrup halves welded together and formwork placed


(c) Grout is gravity fed into formwork to fill recess


(d) Formwork is removed after a day of curing

Figure 5.47: Application of CDS repair strategy (continued)

c) CDS2 - Testing of Repair Strategy

The repaired column was then tested up to drifts of 3% in each direction (3.9% resultant drift) as shown in Figure 5.49.

In this test, spalling initiated during the 2.5% drift cycle (3.25% resultant drift) which corresponds to the ULS performance level and extended the full height of the cast-in-place region of the connection (Figure 5.49c). As intended, no damage occurred in the precast column above the cast-in-place region or in the footing. As discussed previously, some cracking of the precast core occurred but this damage was minor when compared to the damage sustained to the cast-in-place fill around the outside of the core.

Premature dissipator failure occurred during uniaxial stage of the 4% drift cycle (MCE performance level). This was due to a detailing error in the dissipators where there was an overlap of the threaded and grooved lengths of the dissipator. Fracture of the dissipator occurred in this overlapped region (Figures 5.49d and 5.48).

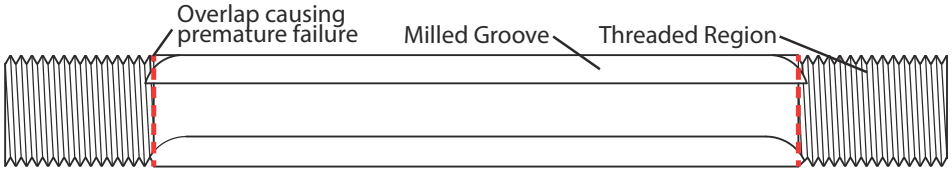

Figure 5.48: Overlap of grooved and threaded lengths of dissipator leading to premature failure

(a) Column during testing

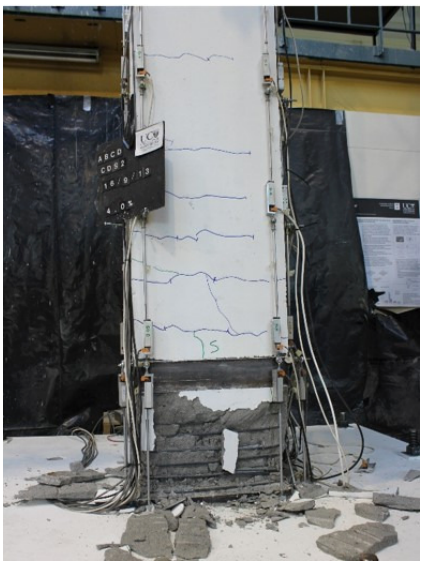

(b) Column damage following test

(c) Spalling damage to column

(d) Damaged region after removal of grout

Figure 5.49: Post-repair testing of CDS

5.3.6 Results and Discussion

a) CDS1 - Benchmark Test

Figure 5.50 gives the force-drift response of the CDS column during the benchmark test. A higher than expected column capacity was observed. Upon disassembly it was found that the precast core of the connection which was supposed to be able to lift and rock in the socket was actually bonded to the socket meaning it enhanced the strength of the connection. This reduced the recentering ratio of the connection leading to a less emphasised flag-shaped hsyteresis loop and larger residual drifts. No connection slackness is visible in the results indicating good activation of the internal dissipators with no slackness in the coupled connection.

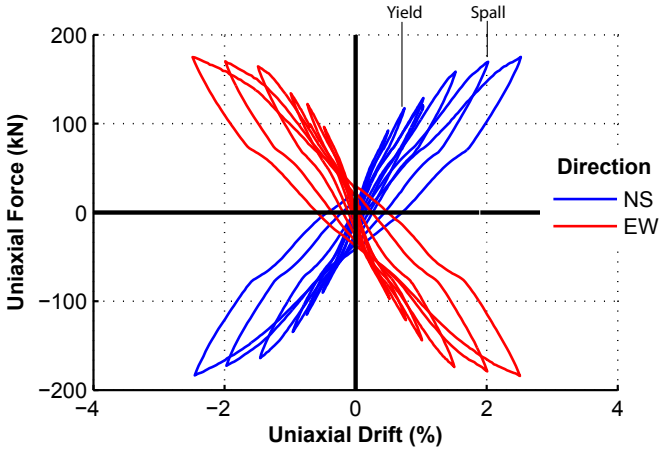

(a) Uniaxial Force-Drift response

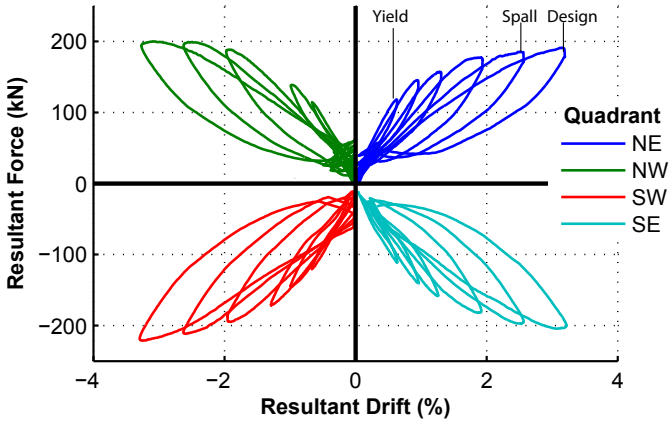

(b) Biaxial Force-Drift response

Figure 5.50: CDS1 Force-Drift response

The values of damping observed in the CDS column were higher than those of the CDC column and what would be expected of a theoretical hybrid connection with a recentering ration, λ, of 1.5 (Figure 5.51). This is partly due to bonding of the precast core as discussed previously.

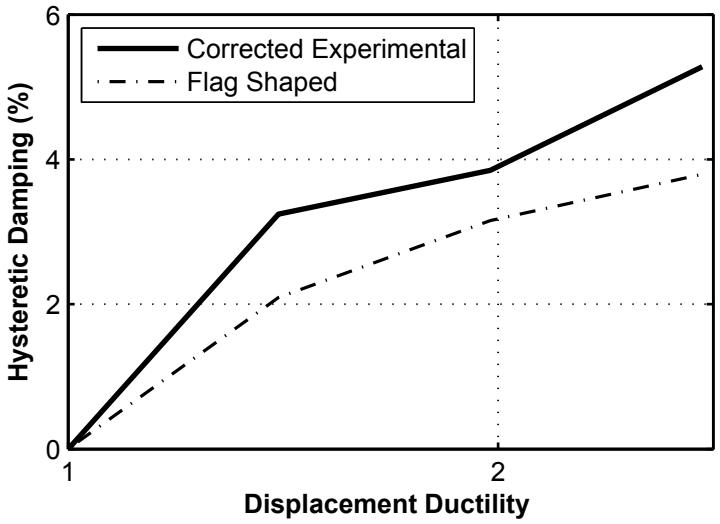

Figure 5.51: CDS1 area based hysteretic damping

Figure 5.52 shows that an SLS earthquake is expected to generate a drift of 0.3% while an ULS earthquake is expected to generate a drift of 2.3%. These values are lower than those of the CDC column due to an increase in both strength and energy dissipation of the CDS column. The ULS value is lower than the design level drift of 3% however larger levels of drift would be expected if bonding of the core had not occurred.

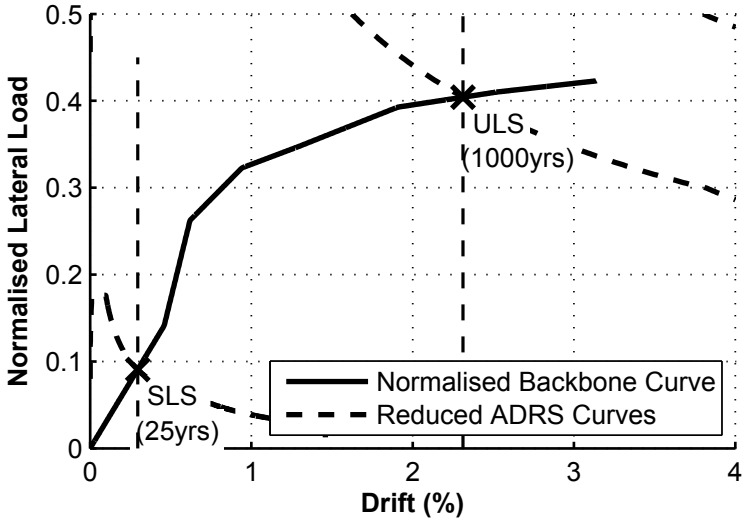

Figure 5.52: CDS1 ADRS performance evaluation

Figure 5.53 shows the energy dissipated during each cycle of loading during test CDS1 along with the cumulative dissipated energy. At the 2.5% drift level, the CDS column showed a cumulative dissipated energy of 100kJ which is about double that of the CDC column for the same drift level and similar to that of the HDS2 column.

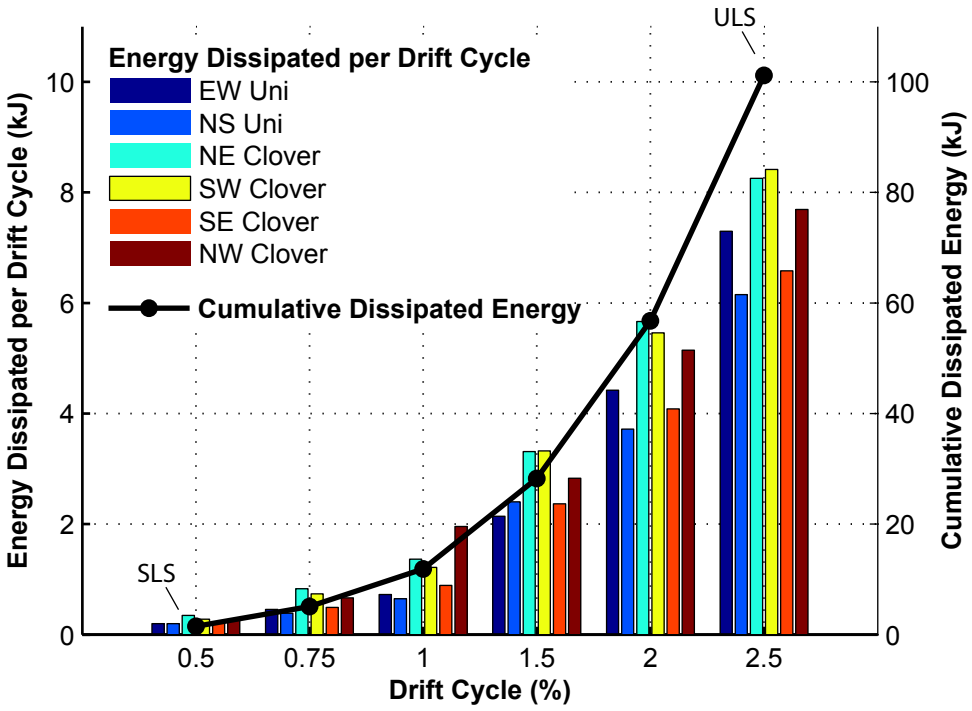

Figure 5.53: CDS1 dissipated energy

Figure 5.54 gives shows the change in post-tensioning (PT) force with drift of the column. In the CDS1 test, the initial PT force was 1100kN, increasing to 1300kN at the design level of drift. The observed post-tensioning force at the design level of drift is almost equal to the design force of 1340kN.

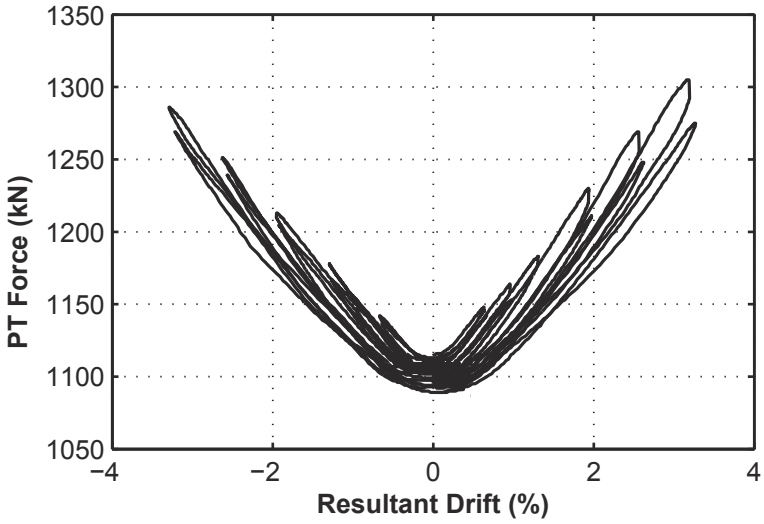

Figure 5.54: CDS1 post-tensioning (PT) force

b) CDS2 - Testing of Repair Strategy

Following repair, the column was subjected to drifts of up to 3% in each direction (3.9% residual drift). During the maximum drift cycle, premature failure of the dissipators occurred due to an error in the design of the dissipators (Section 3.5.3c). Dissipator testing carried out prior to this test suggests that a greater level of drift could have been achieved, had the dissipators been correctly detailed.

A similar force-drift behaviour was observed in CDS2 when compared with the benchmark test with no sign of degradation until the 3% drift cycle (Figure 5.55). A flag shape can be seen in the unaxial force-drift plot, however it is not as well defined as in the CDC tests. As discussed previously, this is due to bonding of the precast core at the centre of the connection causing an increase in recentering ratio of the connection.

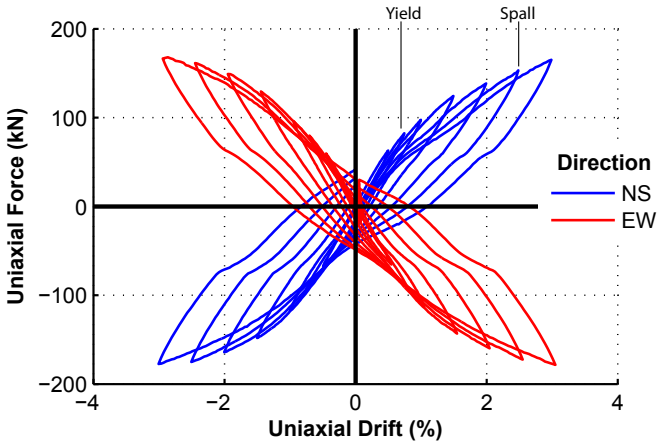

(a) Uniaxial Force-Drift response

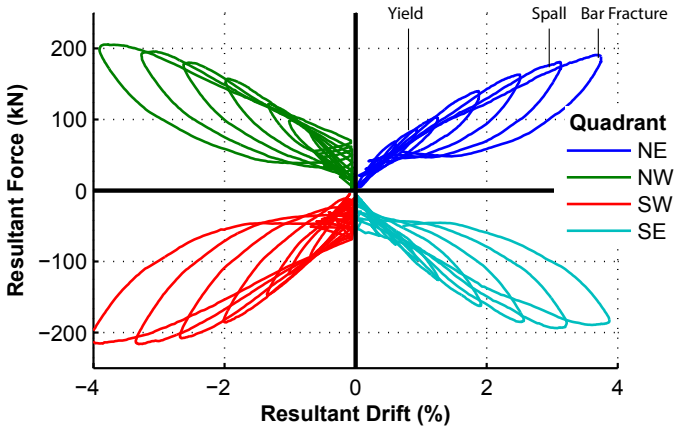

(b) Biaxial Force-Drift response

Figure 5.55: CDS2 Force-Drift response

Again, higher amounts of damping than would be expected of a hybrid system with recentering ratio, λ, or 1.5 were observed (Figure 5.56). A similar level of damping was observed in test CDS2 as CDS1 indicating that the repair process was successful reinstating the capacity and energy dissipation capacities of the connection.

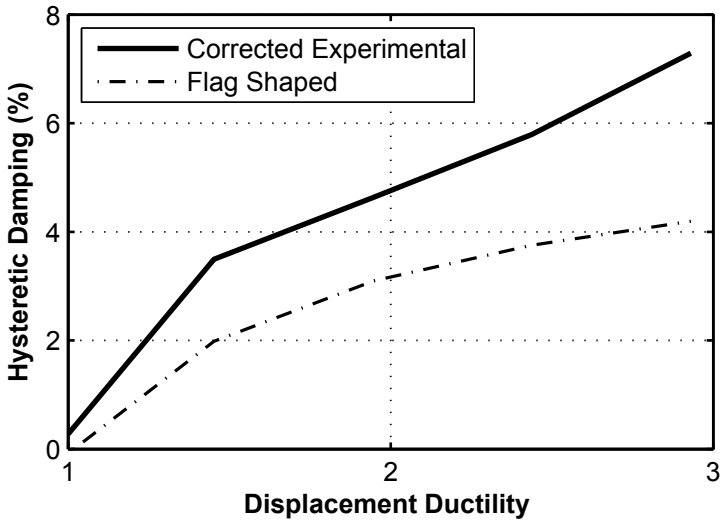

Figure 5.56: CDS2 area based hysteretic damping

The ADRS performance evaluation (Figure 5.57) shows similar results as CDS1, however there appears to be a reduction in initial stiffness of the system. This may be due to degradation of the precast core during the benchmark test. This doesn't appear to have had a significant effect on the expected drift for the ULS earthquake with an expected drift of 2.3% which is equal to that of the CDS1 test. The test ended before reaching the expected MCE level of drift.

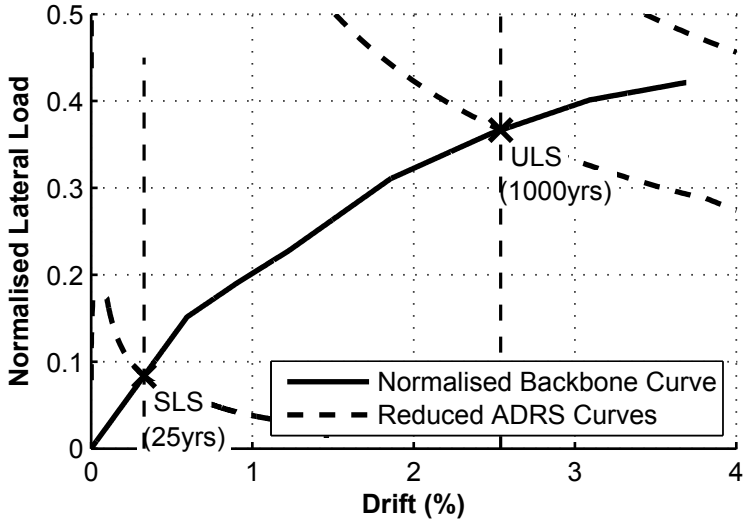

Figure 5.57: CDS2 ADRS performance evaluation

The cumulative dissipated energy plot (Figure 5.58) shows almost exactly the same level of dissipated energy in the CDS1 and CDS2 tests indicating the repair strategy is effective at reinstating both the strength and energy dissipation capacities of the system. The cumulative dissipated energy is similar to that observed in the HD test, HDS2.

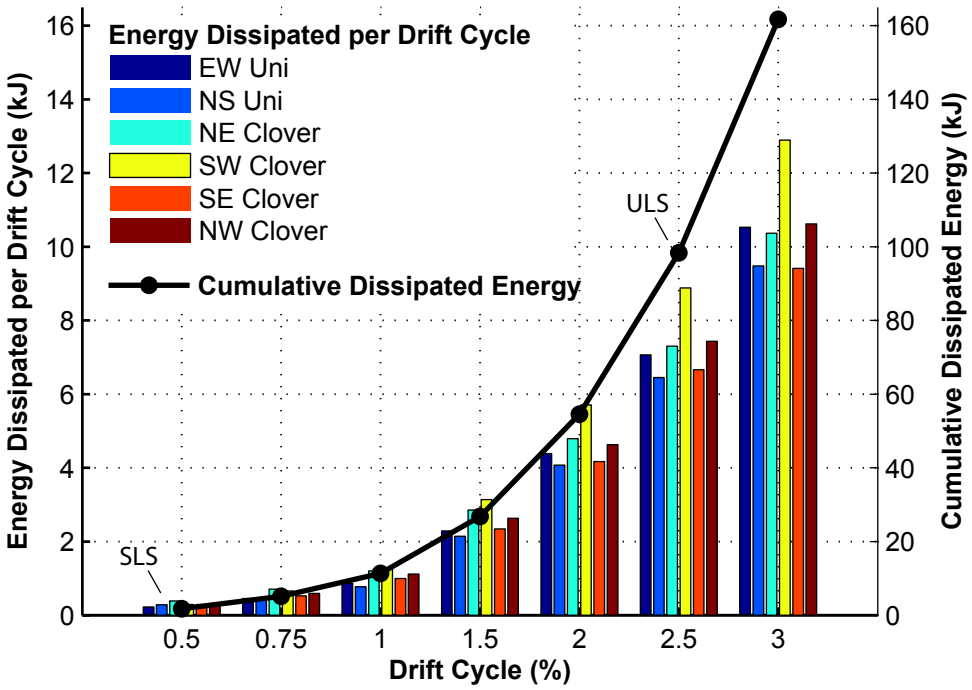

Figure 5.58: CDS2 dissipated energy

Figure 5.59 shows an increase in post-tensioning load from 1100kN at the initial state to 1320kN at 4% drift which corresponds to the ultimate drift of the structure. There appears to be some degradation in post-tensioning load, with the peak at 4% drift almost equal to that at 3% drift. This may be due to deterioration of the precast core which did not rock as intended.

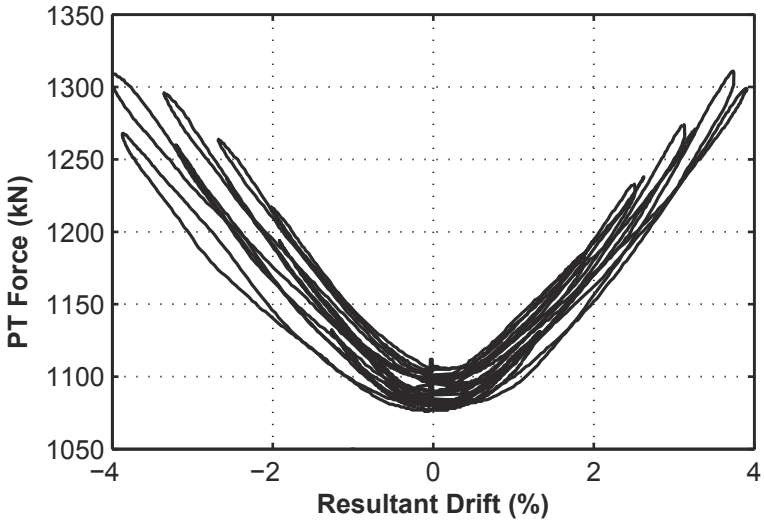

Figure 5.59: CDS2 post-tensioning (PT) force

5.4 Connection Comparison and Conclusions

Like High Damage connections, Controlled Damage connections use precast concrete components to increase construction speed and quality, while reducing life cycle costs of the structure. While HD connections aim to emulate the behaviour of monolithic structures, Controlled Damage connections use Dissipative Controlled Rocking to minimise residual drifts in the structure while also minimising or avoiding damage to precast components of the structure. Repair strategies specific to the connection being used are developed and detailed for at the design stage of the structure, greatly increasing the repair speed while decreasing repair costs and downtime.

Controlled Damage Connections will generally have a higher initial construction cost than High Damage Connections due to the inclusion of post-tensioning, armouring and replaceable energy dissipation components. This additional cost, however, is balanced by the reduced repair cost should a significant earthquake event occur. Consideration of the full life cycle costs of the structure is required when comparing Controlled Damage Connections in order to account for all benefits associated with the system, rather than focusing only on initial construction cost. This includes using a reasonable discount factor when undertaking a benefit cost analysis to appropriately account for future benefits of a system.

Application of the repair strategy reduces uncertainty of the residual strength and ductility capacity of the connection, as all energy dissipation components of the connection are replaced. The relatively low cost of the repair strategies mean they can be implemented in situations where there is uncertainty in the level of damage of components and residual capacity of the substructure as a whole, avoiding the need for costly investigative procedures to be implemented.

The experimental testing of the Controlled Damage Member Socket Connection and Coupled Bar Connection was presented in this chapter. The two test columns featuring these connections were subjected to biaxial loading. Following testing of each connection, a repair strategy was applied to each connection type and the columns were re-tested to demonstrate the repair process and effectiveness. Assembly of both connections was straightforward and demonstrates the advantages of precast substructures in terms of speed and ease of assembly.

The Controlled Damage Member Socket Connection is similar to the High Damage Member Socket Connection that was presented in Chapter 4, however it includes post-tensioning and cover confinement to minimise residual drift and damage to the connection. The repair strategy involves cutting of the damaged internal reinforcement that has been yielded during the earthquake event and installation of external dissipators which restore the capacity and ductility of the connection. Anchorage points for the external dissipators are included during the initial construction meaning no post-drilling for anchorages is required during application of the repair strategy, speeding up the repair process.

- Preliminary testing of CDC showed premature spalling of cover concrete due to the omission of cover confinement at the base of the column
- After repair of cover concrete and addition of Glass Fibre Reinforced Polymer for cover confinement, a significant increase in column performance was observed with no spalling damage up to drifts of 3.25% during the benchmark test.
- Following benchmark testing, application of the repair strategy was carried out. In the test column, threaded inserts were not pre-installed during the casting process due to re-use of the footing and space constraints in the half-scale column. Instead, post-drilled anchorages were used for connection of dissipators which complicated the repair process.

- Testing of the effectiveness of the repair strategy showed some slipping of the mounting collar and pull-out of dissipators which was partly due to prior damage to the footing and the use of post-drilled anchorages.
- The column was subjected to drifts of up to 7.8% with no failure of the dissipators themselves.
- Despite the shortcomings in anchorage of the dissipators, good performance was seen in both the pre and post-repair connection with a clear flag shape visible in the hysteresis loops.

The Controlled Damage Coupled Bar Connection uses replaceable segments of longitudinal bar connected to permanent reinforcement using parallel thread bar couplers. The replaceable segments of bar are located in a recess in the precast column element which is filled with cast-in-place concrete or grout during construction. Following the benchmark test, the cast-in-place fill and stirrups were removed giving access to the dissipators. The damaged dissipators and stirrups were replaced before re-pouring the cast-in-place fill. A re-test of the column showed that the repair strategy was effective at restoring capacity to the structure with very similar pre and post-repair behaviour of the connection.

- Benchmark testing of Column CDS showed good results although the flag shape was not as pronounced as in the previous CD tests. This is partly due to unintended bonding of the precast core to the footing which restrained the rocking behaviour of the joint and increased capacity and energy dissipation. This led to increased residual drifts in the structure however they were still considerably smaller than those of the HD tests.
- No slackness in the results was observed indicating good connection between replaceable dissipator, coupler and threaded stud with little slippage of the connection.
- After removal of cast-in-place fill and stirrups as part of the repair process, it was noticed that some buckling of the dissipators had occurred. The amount of buckling was limited but could be further reduced with an increase in the amount of buckling restraint in the form of stirrups, steel tubes over the dissipators or external cover confinement in the cast-in-place region.
- The damaged dissipators were removed and replacement Grooved Bar dissipators were installed. Some thread alignment challenges were faced during replacement but these were overcome by swapping the location of replacement dissipators which did not cause significant delays to the repair process.

- Replacement stirrups were installed and fill material was cast, completing the repair of the connection. During casting, aggregate blockage of the fill tube was encountered and so grout was used in place of micro-concrete with no apparent effect on the performance of the column.
- During testing of the repair process, premature failure of the replacement dissipators occurred due to an identified detailing error. Previous tests have shown that with appropriate detailing, the dissipators could achieve larger strains without failure and so it is expected that the connection could have reached a higher level of ultimate drift.
- Otherwise, good performance with very similar results to the pre-repair testing indicating that the repair process was effective at reinstating both the strength and ductility capacity of the column.

The two connection types demonstrate different approaches in the development and application of repair strategies. For the Controlled Damage Member Socket Connection, damaged energy dissipation components were severed and new components were installed on the exterior of the pier, offering an alternative energy dissipation system. This approach requires design for both internal and external dissipation systems but offers a much simpler repair process with no repair or replacement of concrete or grout required.

For the Coupled Bar Connection, the repair approach involved replacement of the components of the energy dissipation system rather than installation of an alternative system. This approach offers a simpler design process where only one dissipation system needs to be considered and offers aesthetic advantages but requires a more involved repair process with removal and replacement of cast-in-place fill and stirrups. The repair process however is still significantly simpler than that of the High Damage or conventional monolithic systems where repair or replacement of reinforcing bars and cast-in-place concrete may be required along with difficulties associated with residual drifts of the structure.

Both connection types show good potential for use in bridge substructures offering the advantages of precast construction, notably increased speed and quality of construction, along with considerably simpler and more cost effective repair options when compared with High Damage or conventional monolithic construction. Further investigation into the durability and dynamic behaviour of bridge structures is required and at the time of

writing is being carried out at the University of Canterbury [Andisheh, 2013]. Although Controlled Damage connections have higher intial construction costs, with appropriate consideration of life cycle costs it is expected that Controlled Damage can be a competitive alternative to conventional construction approaches while improving post-earthquake serviceability and repair options for bridge structures.

Chapter 6

Conclusion and Further Research

6.1 Conclusion

ABC uses precast concrete in place of conventional reinforced concrete members to offer advantages including improved construction speed and quality, reduced maintenance requirements and in turn reduced life cycle costs of the structure. While ABC has been widely implemented in regions of low seismicity, further development of precast connections suitable for use in regions of moderate to high seismicity is required.

This thesis explores HD and CD connections for precast bridge piers utilising ABC concepts to address the drawbacks of conventional construction. HD connection types emulate the seismic behaviour of conventional construction while offering advantages including increased construction speed and quality. Controlled Damage connection types use unbonded post-tensioned precast connection types to offer additional advantages including reduced residual drifts, limited and controlled damage and simple repair options. CD connections are intended for use in precast bridge substructures in regions of moderate to high seismicity and offer a compromise between the relatively low initial costs of ABC High Damage or monolithic solutions and the ease of repair of LD rocking systems. This is illustrated in Table 6.1 where a qualitative comparison of the systems is made. Red colour indicates a high value, orange indicates a moderate value and green indicates a low value. This conclusion provides a summary of the outcomes of this research, with a discussion of the benefits and drawbacks of each system investigated, along with an

outline of further research and development that is required for implementation of these technologies.

		Low	Moderate	High
Monolithic	Material / Fabrication Cost			
	Construction Time			
	Repair Cost and Time			
ABC High Damage	Material / Fabrication Cost			
	Construction Time			
	Repair Cost and Time			
ABC Controlled Damage	Material / Fabrication Cost			
	Construction Time			
	Repair Cost and Time			
ABC Low Damage	Material / Fabrication Cost			
	Construction Time			
	Repair Cost and Time			

Table 6.1: Comparison of connection types

The specific objectives of the research are split into three sections, as summarised:

1. **Development of Buckling-Restrained, Fused Mild Steel Energy Dissipators**

    - Explore current options for energy dissipation in structures utilising Dissipative Controlled Rocking (DCR).
    - Develop and test new types of 'dry' buckling-restrained mild steel dissiptors.
    - Compare the performance of these new dissipators with existing dissipator options.

2. **Development and Testing of High Damage (HD) Pier Systems**

    - Explore existing precast connection types that are designed to emulate the behaviour of conventional methods of construction.
    - Demonstrate the design, detailing and construction processes for precast bridge substructures using a selection of HD connection types in a half scale bridge pier.
    - Test the performance of the HD connections under both uniaxial and biaxial loading regimes.

3. **Development and Testing of Controlled Damage (CD) Pier Systems**

   - Develop CD connection types and repair strategies that provide a compromise between High Damage and Low Damage connection types in terms of initial construction cost and ease of repair.
   - Demonstrate the design, detailing and construction processes for precast bridge substructures using a selection of CD connection types in a half scale bridge pier.
   - Demonstrate application of repair strategies for each connection type.
   - Test the performance of the connections both before and after repair, including the performance of novel buckling-restrained, fused mild steel energy dissipators
   - Compare the performance of the CD solutions with that of the HD solutions.

In Chapter 3, four novel 'dry' buckling-restrained dissipator designs were presented which offer good performance in tension and compression with little or no buckling. These dissipators feature a dissipating mild steel bar which yields in both tension and compression. Buckling restraint is provided through the use of a confining tube, which provides lateral support to the bar preventing buckling under compressive loading. The novel options presented were split tube, deformed tube, supported bar and grooved bar type dissipators. All four offered the advantage of 'dry' fabrication, meaning no grout or epoxy filling material was required between the dissipating bar and confining tube. An additional advantage is the ability of the dissipator to undergo net negative displacements with significant increases in stiffness as occurs in BRF type dissipators [Sarti et al., 2013].

The dissipators were subjected to cyclic tension-compression loading until failure, with three cycles completed at each strain limit. The exception to this testing regime was the split tube type dissipator, which was cyclicly loaded up to a strain of 7.5% before being subjected to monotonic loading until failure. The deformed tube, supported bar and grooved bar type dissipators all successfully completed drift cycles of 9% before failure. It is expected that the split tube type dissipator would have successfully completed the 9% drift cycle, had it been applied.

Strain ductilities of between 5.3 and 6.9 were achieved by the dissipators. Design strain limits of 70% and 90% of the maximum achieved strain cycle were assumed corresponding the the ULS and MCE design cases, respectively. Using these values, ULS and MCE strain limit of 5.3% and 6.8% are assumed for the split tube type dissipator, with strain limits of 6.3% and 8.1% assumed for the deformed tube, supported bar and grooved bar type dissipators.

Out of the new dissipator designs presented, the grooved bar dissipator stood out as a strong alternative to conventional dissipator designs. This dissipator is simple to construct and requires a regular steel confining tube without the need for reduction in diameter of the tube or welding. Contact is maintained between bar and tube for the full length of the dissipator giving very good buckling restraint. More research is necessary into fracture mechanics and low cycle fatigue of the dissipator but preliminary testing has shown very good results. This dissipator was therefore selected for use in the repair of the CD test columns as presented in Chapter 5.

In Chapter 4, the development and testing of four half scale segmental columns featuring ABC High Damage (HD) connections was presented. The connection types considered were two variations of Grouted Duct Connection (GDC), and the Member Socket Connection (GDC). The aim of HD connection types is to emulate the seismic behaviour of conventional monolithic construction while offering the advantages associated with precast construction. Allowing damage to occur in these connection types through the formation of plastic hinges leads to low initial construction costs with no need for armouring and post-tensioning, but can lead to increased repair costs and downtime.

The testing regime was based on a prototype structure which is representative of a typical New Zealand highway bridge structure with a span length of 12 metres, a height of 5 metres to the centre of mass of the superstructure and a column section depth of 1 metre. Two of the HD columns were subjected to a uniaxial loading regime, representing a structure where only transverse loads are resisted by the bridge piers with the longitudinal loads being transferred through the superstructure to the abutments. The remaining two columns were subjected to biaxial loading, representing a structure where both longitudinal and transverse loads are resisted by the bridge piers.

- Both connection types showed promising results with good strength and ductility.

- As expected, significant damage to the columns was sustained in each case including spalling of concrete and yielding, buckling and fracture of longitudinal reinforcing bars.
- Large residual drifts of up to 50% of the peak drift were observed.
- Strain concentration effects in the GDC caused a reduction in plastic hinge length and ultimate drift capacity of the Column HDS1.
- The inclusion of armouring and debonding of longitudinal reinforcement at the connection interface of the Grouted Duct Connection (Column HDS2) significantly improved the connection performance with reduced spalling and an increase in ultimate drift capacity of 30%.

- Columns HDC1 and HDC2 featured the Member Socket Connection as the primary connection between column and footing with a GDC used to connect the two column segments.
- The MSCs showed similar performance to what would be expected from a monolithic connection, with a plastic hinge length equal to the depth of the section.
- Spalling damage was much more significant in the HDC2 column due to the biaxial loading regime.
- Lower levels of energy dissipation were observed the GDC and MSC types than what would be expected of a monolithic column type was observed.

In Chapter 5, the development and testing of two half scale columns featuring ABC Controlled Damage (CD) connections was presented. The connection types developed were the CD Member Socket Connection (MSC) and the CD Coupled Bar Connection (CBC). CD connection types are based on the concept of DCR and allow some damage in the connection during seismic loading, however this damage is limited and constrained making it easily repairable. Unbonded post-tensioning reduces residual drifts in the structure, improving the post-earthquake serviceability and greatly simplifying the repair process. The use of armouring helps to protect the precast concrete from spalling damage. Repair strategies are developed and detailed for at the design stage of the structure, reducing the downtime and costs associated with repair of the structure.

- Preliminary testing of CDC showed premature spalling of cover concrete due to the omission of cover confinement at the base of the column
- After repair of cover concrete and addition of Glass Fibre Reinforced Polymer for

cover confinement, a significant increase in column performance was observed with no spalling damage up to drifts of 3.25% during the benchmark test.

- Following benchmark testing, application of the repair strategy was carried out. This involved cutting of existing internal reinforcement, and installing of externally mounted grooved bar dissipators.
- Testing of the effectiveness of the repair strategy showed some slipping of the mounting collar and pull-out of dissipators which was partly due to prior damage to the footing and the use of post-drilled anchorages.
- The column was subjected to drifts of up to 7.8% with no failure of the dissipators themselves.
- Despite the shortcomings in anchorage of the dissipators, good performance was seen in both the pre and post-repair connection with a clear flag shape visible in the hysteresis loops.

- Benchmark testing of Column CDS showed good results although the flag shape was not as pronounced as in the previous CD tests. This is partly due to unintended bonding of the precast core to the footing which restrained the rocking behaviour of the joint and increased capacity and energy dissipation. This led to increased residual drifts in the structure however they were still considerably smaller than those of the HD tests.
- No slackness in the results was observed indicating good connection between replaceable dissipator, coupler and threaded stud with little slippage of the connection.
- After removal of cast-in-place fill and stirrups as part of the repair process, it was noticed that some buckling of the dissipators had occurred. The amount of buckling was limited but could be further reduced with an increase in the amount of buckling restraint in the form of stirrups, steel tubes over the dissipators or external cover confinement in the cast-in-place region.
- The damaged dissipators were removed and replacement Grooved Bar dissipators were installed. Some thread alignment challenges were faced during replacement but were overcome by swapping the location of replacement dissipators which did not offer significant delays to the repair process.
- Replacement stirrups were installed and fill material was cast, completing the repair of the connection. During casting, aggregate blockage of the fill tube was encountered and so grout was used in place of micro-concrete with no apparent effect on the performance of the column.

- During testing of the repair process, premature failure of the replacement dissipators occurred due to an identified detailing error. Previous tests have shown that with appropriate detailing, the dissipators could achieve larger strains without failure and so it is expected that the connection could have reached a higher level of ultimate drift.
- Otherwise, good performance with very similar results to the pre-repair testing indicating that the repair process was effective at reinstating both the strength and ductility capacity of the column.

In many cases, it is unlikely that repair of a bridge structure will be required during its life, making it hard for infrastructure owners to justify the increased construction costs associated with low damage technologies. They understand however, that the consequences of a significant earthquake event can be severe, including significant downtime in the serviceability of bridge structures along with the need for costly repair or replacement of the bridge.

CD connection types offer a compromise between ABC HD and LD options with relatively low construction costs, along with minimal residual drifts and straightforward methods of repair that are determined and detailed for at the design stage of the structure. The repair strategies presented are cost effective, meaning they can be implemented in situations of uncertainty into the residual strength or ductility of the system, removing the need for costly investigative processes. The repair strategies presented involve replacement of all energy dissipating components of the system, giving greater confidence into the performance of the structure following repair.

In order to fully account for the benefits of ABC construction, in particular CD and LD systems, appropriate consideration and acknowledgement of future benefits needs to be carried out. This includes proper consideration of not only initial construction cost, but maintenance costs, the probability of damage to the structure in its lifetime, consequences of bridge damage or loss of serviceability, and cost and downtime associated with repair or replacement of bridge structures.

It is important to acknowledge that, like all engineering problems, not one solution will fit all applications. A number of considerations must be made when selecting an appropriate solution including importance of the structure, implications of disruptions associated with construction and repair, level of seismicity, soil conditions, structure type and span length.

A normal importance structure in a region of low seismicity may benefit highly from the advantages offered by precast construction, but with low probability for need of repair, and low consequences of damage, an ABC HD solution may be most suitable. Conversely, a high importance structure located in a region of high seismicity may benefit most from an ABC LD structure type.

A high importance stucture in a region of moderate seismicity, however, may face more serious consequences of structural damage including disruption to traffic networks leading to severe economic impacts and need for costly repair or replacement. With a CD system, infrastructure owners can be confident that the structure will sustain limited damage, with little or no residual drift leading to little or no downtime in the serviceability of the bridge and simple repair options to reinstate full strength and ductility to the structure. The moderate increase in initial construction cost is justified against the level of certainty that the system provides.

Overall, this thesis has found promising results from both ABC High Damage and Controlled Damage connection types. The novel buckling-restrained fused dissipators presented, in particular the grooved bar dissipator, offer a strong alternative to conventional dissipator design, with cost effective and simple fabrication requirements with good cyclic performance. These connection and dissipator types offer a competitive alternative to conventional methods of bridge pier construction with the potential for improved construction speed and quality, minimised disruption during construction, improved on-site safety, low life cycle costs and minimal cost and downtime associated with repair.

6.2 Further Research and Development

Chapter 3 presented preliminary testing of 'dry' types of buckling-restrained mild steel dissipators. The testing involved cyclic deformation of each dissipator in tension and compression to determine the hysteretic behvaiour of the dissipator and evaluate the effectiveness of the buckling restraint.

Further research into these dissipators is required to fully understand their behaviour. The testing carried out in this research subjected the dissipators to net positive deformation where the deformed length of the dissipator remained greater than its initial length. Net negative deformation of dissipators occurs in rocking structure, although

the peak negative net deformations are generally significantly smaller than the net positive deformations. Cyclic testing involving net negative displacements will offer further understanding of the behaviour of the dissipators, in particular to investigate whether significant increases in stiffness occur as observed in the behaviour of BRF type dissipators [Sarti et al., 2013].

Investigation of low cycle fatigue of the dissipators and fracture mechanics is required to determine optimum dissipator longitudinal profile and cross section. This is particularly important in the Grooved Bar type dissipator which features a number of sharp edges that could cause premature initiation of low cycle fatigue. Developments in detailing and fabrication methods could help to limit low cycle fatigue effects.

Further research into the required tube thickness to effectively prevent buckling of the dissipator is also required. Similarly, allowable clearance between tube and bar needs to be determined. There should be enough tolerance to allow for reliable assembly of dissipators and accommodation of lateral expansion due to the Poisson effect, but not so much as to allow for significant out of place deformation of the bar before contact with the tube is made, which could accelerate low cycle fatigue failure of the dissipator.

Precast structures generally offer better material quality due to more controlled casting conditions. This leads to a higher level of durability of the concrete components of the structure. However, further research into jointed precast connections to determine appropriate detailing to achieve the required 100 years of serviceability is required. CD and LD connections feature unbonded post-tensioning which is the main contributor to the strength of the system. Corrosion of this tendon could cause loss of post-tensioning force, or failure of the tendon during rocking leading to failure of the rocking connection. Protection of the tendon through pumping the duct with grease during construction could help to prevent corrosion issues. Grouted Duct Connections feature a joint between precast elements which could allow for accelerated ingress of corroding agents, particularly if cracking of the jointed interface occurs. MSCs offer an advantage in this regard, as no construction joint with crossing reinforcement exists. CD and LD also feature exposed steelwork which will required protection. Severe corrosion of this armouring could lead to a degradation of connection performance, however a number of options already exist to protect against this including the use of stainless steel or coating of exposed mild steel. Research is currently underway at the University of Canterbury in the

performance of corroded precast bridge pier systems, along with methods of preventing corrosion [Andisheh, 2013].

ABC and DCR systems offer benefits that span the life of the structure. Thus, life cycle costs must be considered when comparing these systems to conventional construction options. Detailed loss modelling analysis is a useful tool to fully understand the benefits of LD and CD systems and to provide quantitative comparisons of different systems, whether they be monolithic, HD, CD or LD, for a variety of seismic hazards. Performance-based earthquake engineering (PBEE) assessment allows for quantitative comparison of the relative performance of systems in terms of parameters such as peak drift ratio, along with expected repair costs and downtime. There has been extensive research into loss modelling including contributions from Bradley et al. [2010], Christopoulos et al. [2003], Dhakal and Mander [2006], Lee and Billington [2011], Mander et al. [2007], Marriott et al. [2009], Pampanin et al. [2003], Solberg et al. [2008], Uma et al. [2006, 2010]. Analysis of the structural systems presented in this research using the PBEE framework would allow designers and infrastructure asset owners to clearly identify the probability of damage to a structure in a region for each structural option, the expected cost of repair, and the associated damage.

PBEE assessment involves four stages of analysis [Lee and Billington, 2011]:

Hazard Analysis Given a site location and structural design, perform a Probabilistic Seismic Hazard Analysis to calculate the annual frequency with which a given seismic Intensity Measure (IM), e.g. spectral acceleration, will exceed certain levels (expressed with a hazard curve).

Structural Analysis Given the IM and the structural design, perform simulations on models of the structure to determine resulting Engineering Demand Parameters (EDPs), which are measures of the structural response to the given IM.

Damage Analysis Given the EDP, determine the probability that a structural component or system will experience a certain level of damage. The levels of damage are defined by damage states or damage measures (DMs) particular to the system under consideration. Examples of DMs include concrete cover spalling and reinforcing bar buckling.

Loss Analysis Given the levels of damage sustained, calculate measures of performance termed Decision Variables (DVs), which can be used by owners of a structure for decision making. DVs are typically given in terms of monetary losses, structure or facility downtime, or casualties.

The outcomes of this analysis are fragility curves which relate peak deformations, repair costs and downtime to mean annual probability of exceedance specific to the structural system being considered. For this type of system to be implemented, detailing costing information for the construction, maintenance and repair of different bridge systems is required. This information is readily available for conventional monolithic construction, especially in New Zealand following the Canterbury earthquakes. Information for ABC type bridge substructures however will be harder to come by, particularly for CD and LD systems which have had limited application in bridge structures.

Appendix A

Appendix A. HDS Technical Drawings

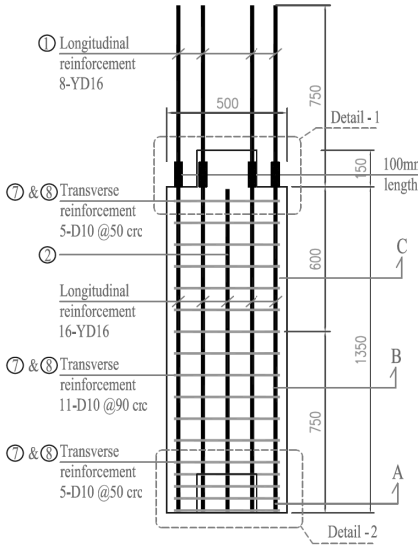

REINFORCMENT DETAILS OF THE BASE SEGMENT

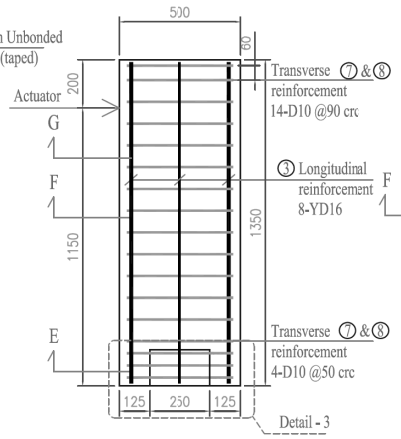

REINFORCMENT DETAILS OF THE TOP SEGMENT

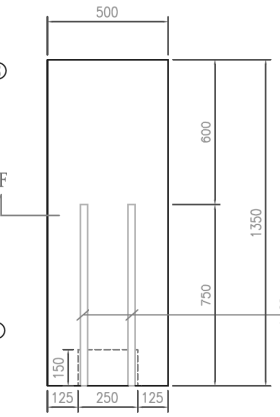

DROSSBACHS DETAIL OF THE TOP SEGMENT

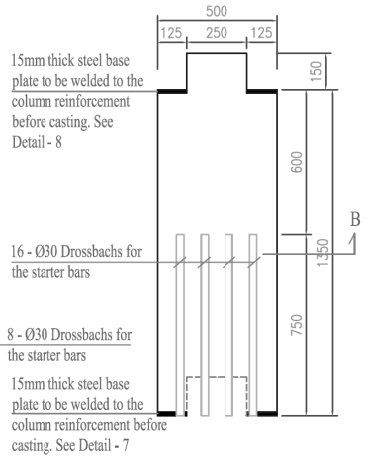

DROSSBACHS DETAIL OF THE BASE SEGMENT

NOTES:

1- All dimensions are in mm.
2- Concrete strength (f'c) is 40 MPa.
3- Steel grade is 500E seismic (fy = 500 MPa).
4- All starter bars are to be grouted inside the drossbachs with high strength mortar and hand pumped. Please refer to unbonded length in drawings while assembling the segments for the specimen.
5- Swift lift anchors should be provided at appropriate locations for lifting purpose of each segment and the whole specimen by the crane.
6- The actuator will be connected at the cap part of the top column segment later in lab. In order to connect the steel plate on the face of the cap, appropriate anchor bolt should be placed during casting the segment so the steel plate can be attached later in lab.

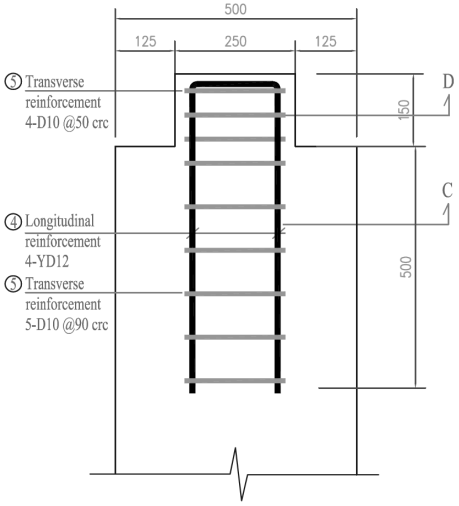

DETAIL - 1

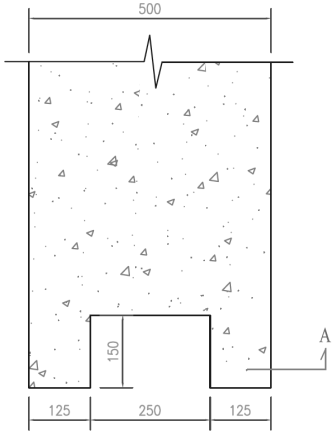

DETAIL - 2

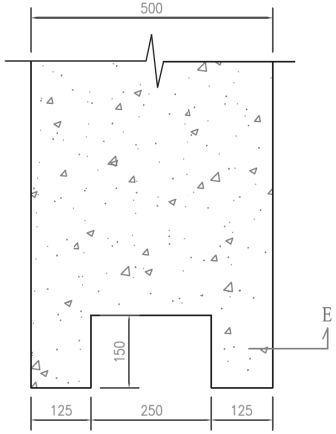

DETAIL - 3

Issue	Date	Description
1	03/09/2012	SPECIMEN NO - 1

UNIVERSITY OF CANTERBURY
Te Whare Wānanga o Waitaha
CHRISTCHURCH NEW ZEALAND

Project Title

Advanced Bridge Construction and Design
(Natural Hazard Research Platform)

Drawing Name
PRECAST SQUARE COLUMN

Engineered by : **M.Mashal / S.White** Date : **09/2012**
Drawn by : **Mustafa Mashal** Date : **09/2012**

Drawing Scale 1:20 AT A3

CONTRACTOR MUST VERIFY ALL DIMENSIONS ON SITE

Sheet No:
S-01

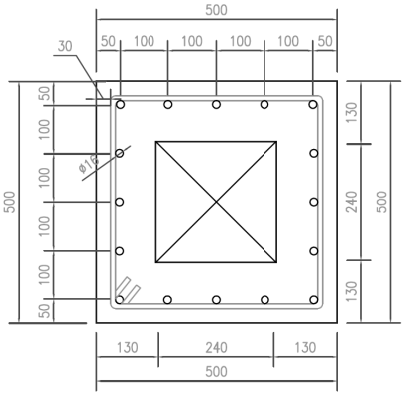

SECTION - A

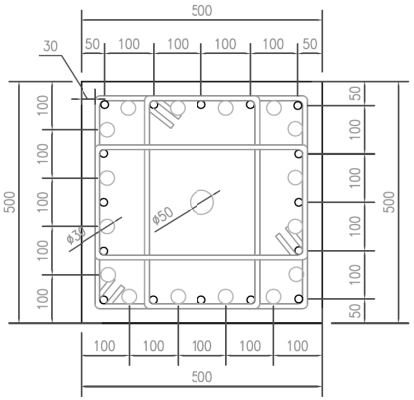

SECTION - B

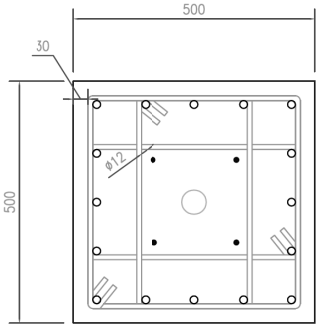

SECTION - C

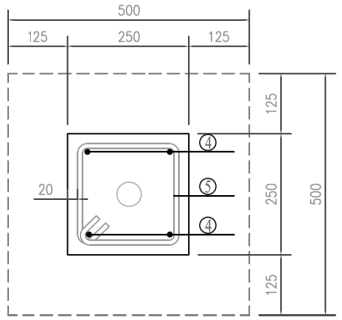

SECTION - D

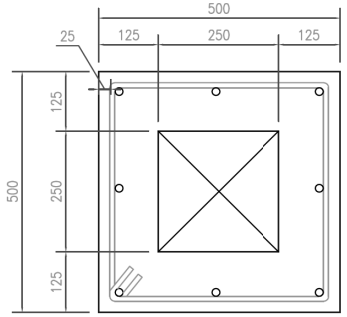

SECTION - E

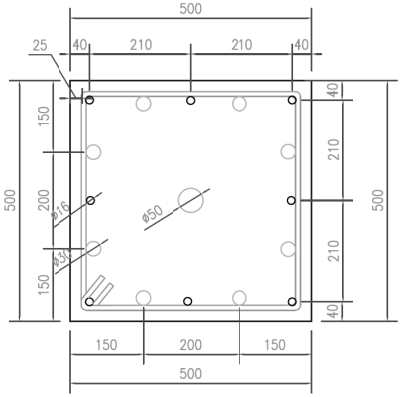

SECTION - F

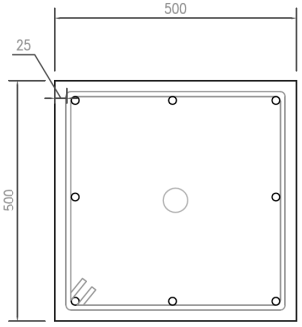

SECTION -G

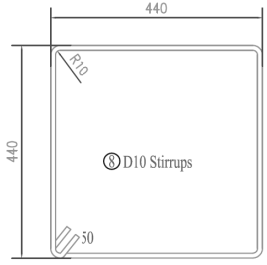

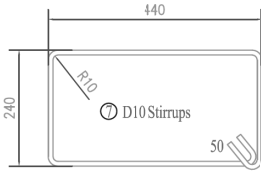

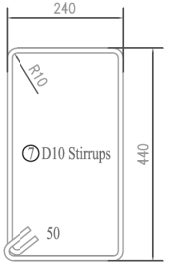

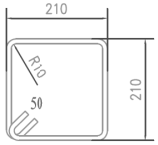

⑤ D10 Stirrups

STIRRUPS DETAILS

LEGENDS

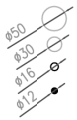

Ø50 drossbach
Ø30 Drossbachs
D16 Longitudinal rebars
D12 Longitudinal rebars

NOTES:

1- All dimensions are in mm.
2- Concrete strength (f'c) is 40 MPa.
3- Steel grade is 500E seismic (fy = 500 MPa).

Issue	Date	Description
1	03/09/2012	SPECIMEN NO - 1

UNIVERSITY OF CANTERBURY
Te Whare Wānanga o Waitaha
CHRISTCHURCH NEW ZEALAND

Project Title

Advanced Bridge Construction and Design
(Natural Hazard Research Platform)

Drawing Name
SQUARE COLUMN SECTIONS

Engineered by : **M.Mashal / S.White** Date : **09/2012**
Drawn by : **Mustafa Mashal** Date : **09/2012**

Drawing Scale 1:10 AT A3

Sheet No:
S-02

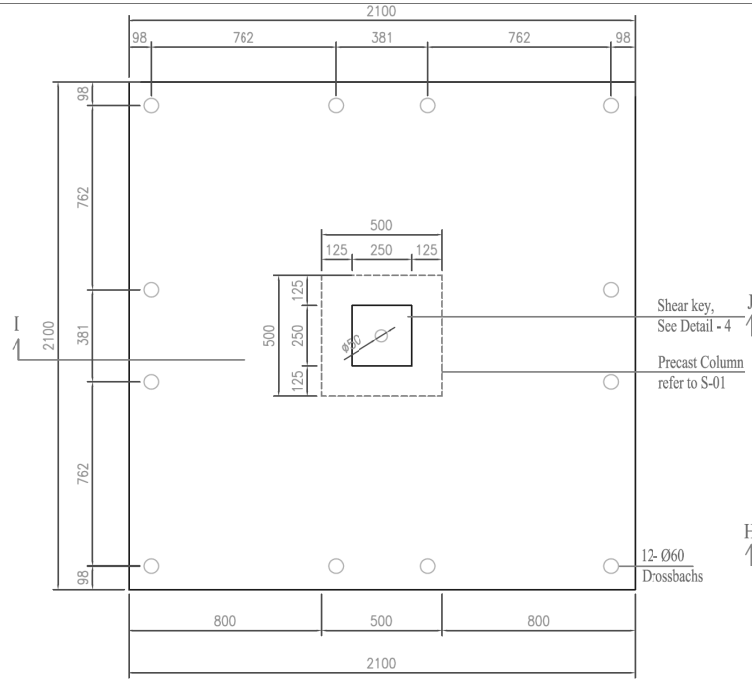

PRECAST FOUNDATION PLAN

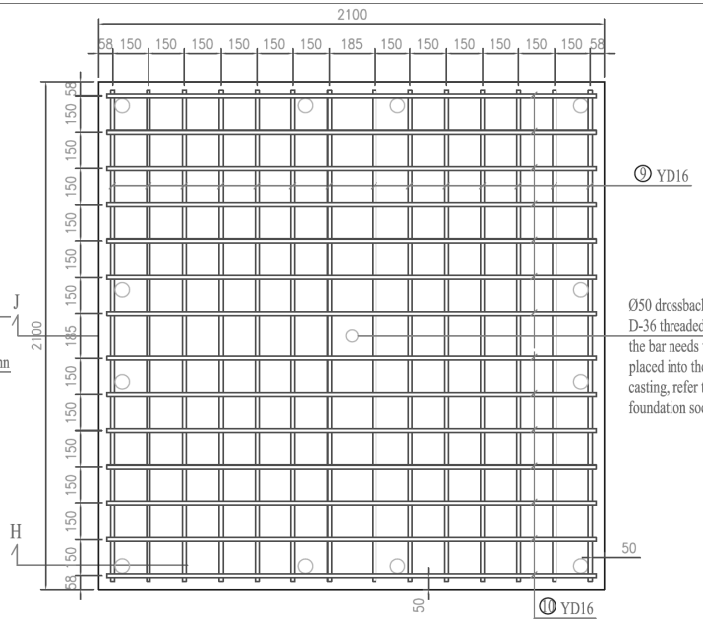

FOUNDATION REINFORCEMENT DETAILS

NOTES:

1- All dimensions are in mm.
2- Concrete strength (f'c) is 40 MPa.
3- Steel grade is 500E seismic (fy = 500 MPa).
4- All starter bars are to be grouted inside the drossbachs with high strength mortar and hand pumped. Please refer to unbonded length in drawings while assembling the segments for the specimen.
5- All reinforcement for the foundation are YD16, please refer to the reinforcement table for the dimensions.

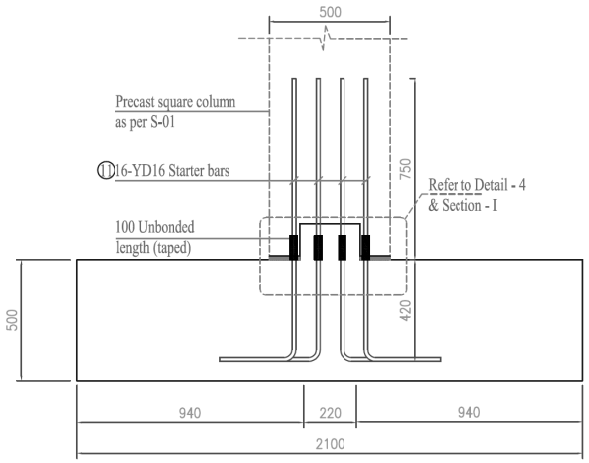

SECTION - I

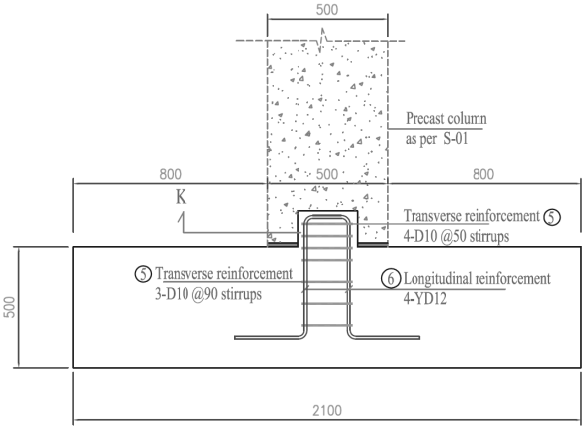

SECTION - J

Issue	Date	Description
1	03/09/2012	SPECIMEN NO - 1

UNIVERSITY OF CANTERBURY
Te Whare Wānanga o Waitaha
CHRISTCHURCH NEW ZEALAND

Project Title

Advanced Bridge Construction and Design
(Natural Hazard Research Platform)

Drawing Name
PRECAST FOUNDATION PLANS

Engineered by : **M.Mashal / S.White** Date : **09/2012**
Drawn by : **Mustafa Mashal** Date : **09/2012**

Drawing Scale 1:20 AT A3

Sheet No:
S-03

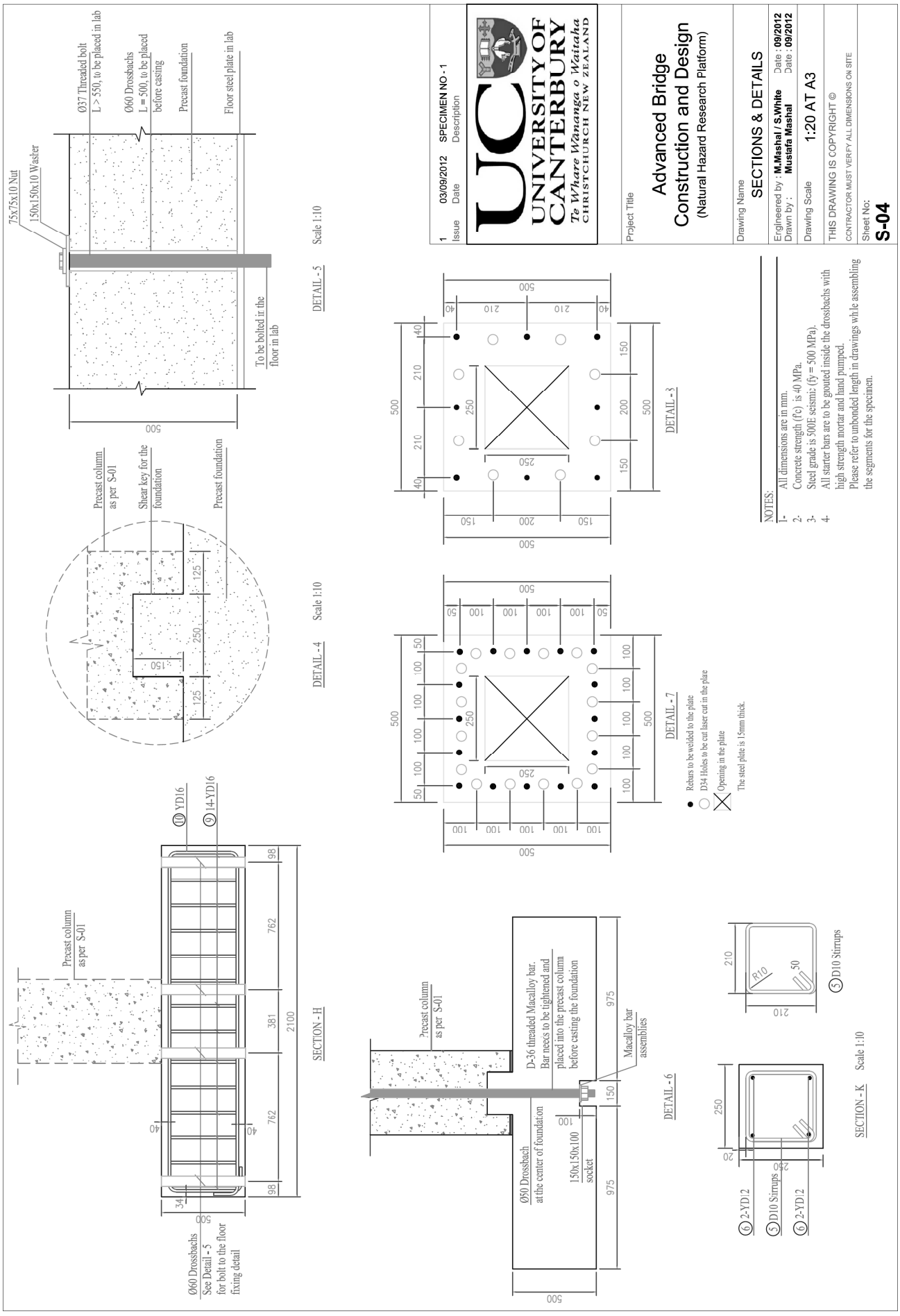
75x75x10 Nut
150x150x10 Washer
Ø37 Threaded bolt
L > 550, to be placed in lab
Ø60 Drossbachs
L = 500, to be placed
before casting
Precast foundation
Floor steel plate in lab
To be bolted in the
floor in lab
500
DETAIL - 5 Scale 1:10
Precast column
as per S-01
Shear key for the
foundation
Precast foundation
150
250
125
125
DETAIL - 4 Scale 1:10
⑩ YD16
⑨ 14-YD16
Precast column
as per S-01
98
762
381
762
98
2100
40
40
34
500
Ø60 Drossbachs
See Detail - 5
for bolt to the floor
fixing detail
SECTION - H
500
210
210
40
40
150
200
150
250
250
DETAIL - 3
DETAIL - 7
Rebars to be welded to the plate
D34 Holes to be cut laser cut in the plate
Opening in the plate
The steel plate is 15mm thick.
Precast column
as per S-01
D-36 threaded Macalloy bar.
Bar needs to be tightened and
placed into the precast column
before casting the foundation
Macalloy bar
assemblies
975
150
100
Ø50 Drossbach
at the center of foundation
150x150x100
socket
975
500
DETAIL - 6
210
R10
50
210
⑤ D10 Stirrups
250
20
250
⑥ 2-YD12
⑤ D10 Stirrups
⑥ 2-YD12
SECTION - K Scale 1:10
NOTES:
1- All dimensions are in mm.
2- Concrete strength (f'c) is 40 MPa.
3- Steel grade is 500E seismic: (fy = 500 MPa).
4- All starter bars are to be grouted inside the drosbachs with high strength mortar and hand pumped. Please refer to unbonded length in drawings while assembling the segments for the specimen.
1 Issue
03/09/2012 Date
SPECIMEN NO - 1 Description
UNIVERSITY OF CANTERBURY
Te Whare Wananga o Waitaha
CHRISTCHURCH NEW ZEALAND
Project Title
Advanced Bridge Construction and Design
(Natural Hazard Research Platform)
Drawing Name
SECTIONS & DETAILS
Engineered by : M.Mashal / S.White Date : 09/2012
Drawn by : Muslafa Mashal Date : 09/2012
Drawing Scale 1:20 AT A3
THIS DRAWING IS COPYRIGHT ©
CONTRACTOR MUST VERFY ALL DIMENSIONS ON SITE
Sheet No:
S-04

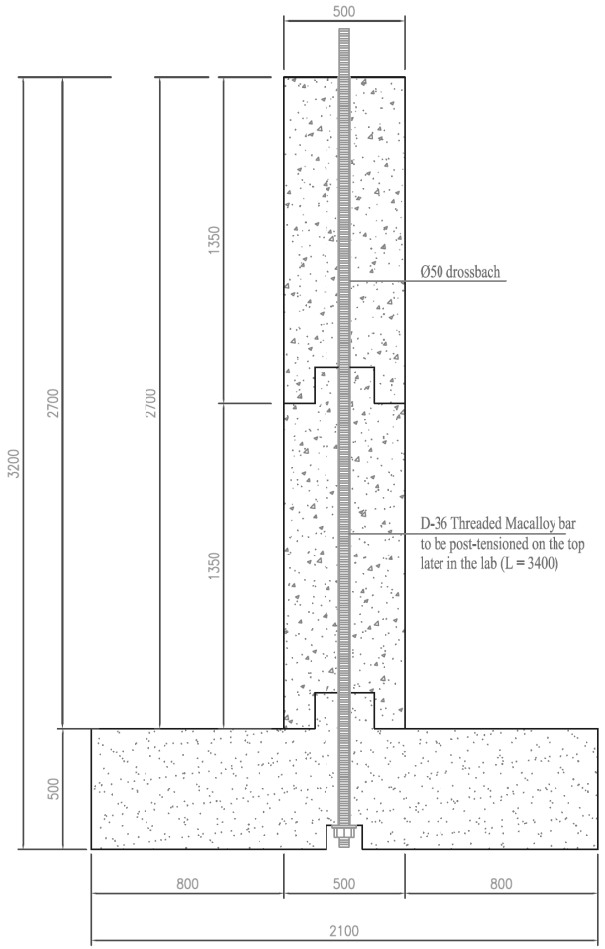

ASSEMBLED SPECIMEN TO BE DELIVERED
(SPECIMEN NO - 1)
QUANTITY NEEDED = 2

GENERAL NOTES:

1- All dimensions are in mm.
2- Concrete strength (f'c) is 40 MPa.
3- Steel grade is 500E seismic (fy = 500 MPa).
4- All starter bars are to be grouted inside the drossbachs with high strength mortar and hand pumped.
Please refer to unbonded length in drawings while assembling the segments for the specimen.
5- In order to have precise measurement of the formwork for the segments and shear keys, match casting procedure is proposed.
6- The total weight of the specimen with the dimensions shown in these drawings is expected to be 6.91 Tons.
7- For quality control purposes, a minimum of five standard concrete cylinders per specimen are to be taken while casting the elements.
8- Swift lift anchors should be provided at appropriate locations for lifting purpose of each segment and the whole specimen by the crane.

Issue	Date	Description
1	03/09/2012	SPECIMEN NO - 1

UNIVERSITY OF CANTERBURY
Te Whare Wānanga o Waitaha
CHRISTCHURCH NEW ZEALAND

Project Title

Advanced Bridge Construction and Design
(Natural Hazard Research Platform)

Drawing Name
ASSEMBLED SPECIMEN

Engineered by : **M.Mashal / S.White** Date : **09/2012**
Drawn by : **Mustafa Mashal** Date : **09/2012**

Drawing Scale 1:20 AT A3

Sheet No:
S-05

NO OF REBAR	DIAMETER	QUANTITY	DIMENSIONS	LENGTH	TOTAL LENGTH	TYPE
①	Ø16	8	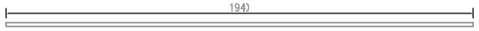	1940	15520	DEFORMED
②	Ø16	8	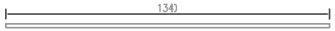	1340	10720	DEFORMED
③	Ø16	8	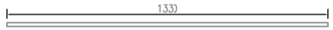	1330	10640	DEFORMED
④	Ø12	2	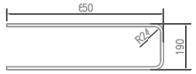	1460	2920	DEFORMED
⑤	Ø10	18		925	16650	PLAIN
⑪	Ø12	2	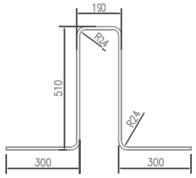	1640	3280	DEFORMED
⑦	Ø10	70	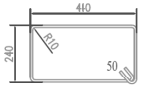	1470	102900	PLAIN
⑧	Ø10	36	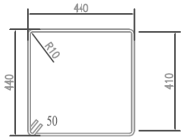	1900	68400	PLAIN
⑨	Ø16	14		5120	71680	DEFORMED
⑩	Ø16	14		5060	70840	DEFORMED
⑪	Ø16	16	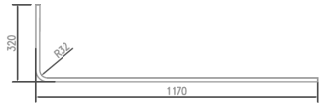	1470	23520	DEFORMED

SUMMARY CHART OF REINFORCEMENT FOR TWO SPECIMENS

DIAMETER	TOTAL LENGTH	TYPE
Ø10	375900	PLAIN
Ø12	12400	DEFORMED
Ø16	405840	DEFORMED

SUMMARY CHART OF CONCRETE FOR TWO SPECIMENS

ELEMENT	VOLUME (m³)
FOUNDATION	4.43
COLUMN	1.33
TOTAL	5.76

SUMMARY CHART OF CROSSBACHS FOR TWO SPECIMENS

DIAMETER	TOTAL LENGTH
Ø30	36000
Ø50	5400
Ø60	12000

SUMMARY CHART OF STEEL PLATES FOR TWO SPECIMENS

NO	TICKNESS (mm)	DIMENSIONS (mm)
4	30	500x500

SPECIFIC NOTES:

1- All dimensions are in mm.
2- Concrete strength (f'c) is 40 MPa.
3- Steel grade is 500E seismic (fy = 500 MPa). All bars shown are deformed unless specified in the tables.
4- The summary charts show the amount of materials needed for both specimens with circular section.
5- Formwork, tying wire, spacer and amount of high strength mortar are not included in this bill of quantity.
6- For quality control purposes, a minimum of five standard concrete cylinders per specimen are to be taken while casting the elements.
7- A minimum length of 2000mm of reinforcement for the all three diameters shown in the table shall be added with the total amount. This will be used for testing of the bars in the lab to verify the strength.

Issue	Date	Description
1	03/09/2012	SPECIMEN NO - 1

UNIVERSITY OF CANTERBURY
Te Whare Wānanga o Waitaha
CHRISTCHURCH NEW ZEALAND

Project Title

Advanced Bridge Construction and Design
(Natural Hazard Research Platform)

Drawing Name
BILL OF QUANTITY

Engineered by : **M.Mashal / S.White** Date : **09/2012**
Drawn by : **Mustafa Mashal** Date : **09/2012**

Drawing Scale 1:20 AT A3

Sheet No:
S-06

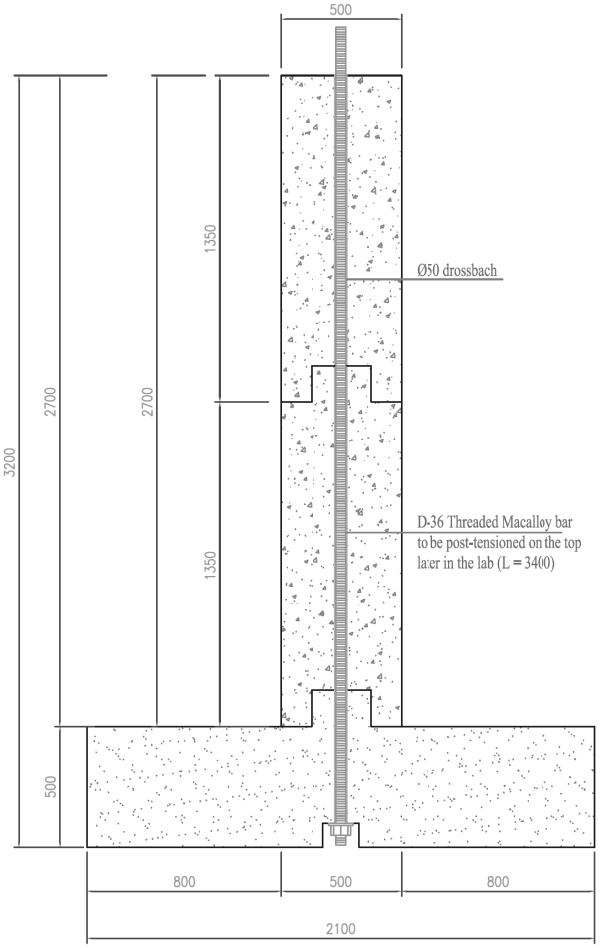

ASSEMBLED SPECIMEN TO BE DELIVERED
(SPECIMEN NO - 1)
QUANTITY NEEDED = 2

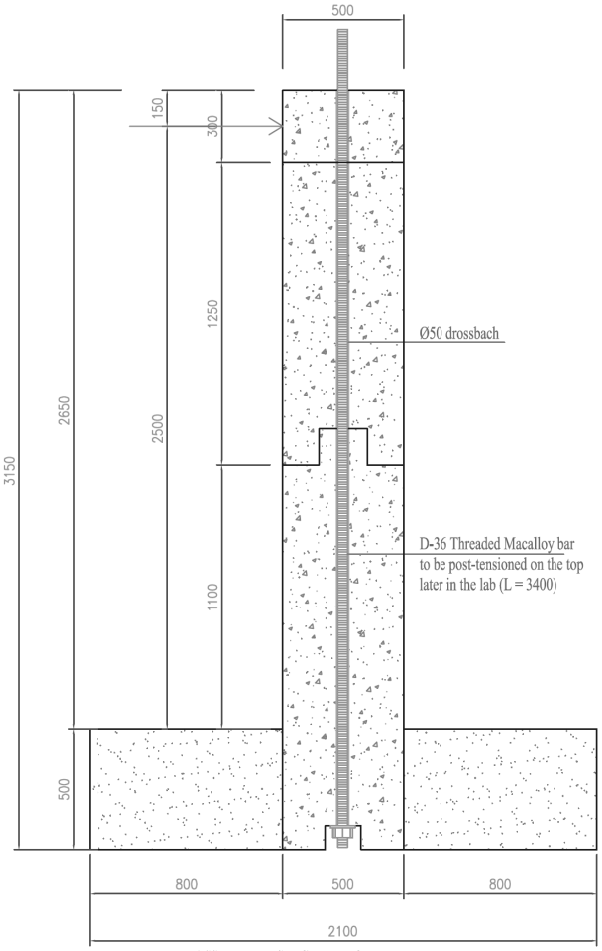

ASSEMBLED SPECIMEN TO BE DELIVERED
(SPECIMEN NO - 2)
QUANTITY NEEDED = 2

SUMMARY CHART OF REINFORCEMENT
FOR ALL FOUR SPECIMENS

DIAMETER	TOTAL LENGTH	TYPE
Ø10	524840	PLAIN
Ø12	18160	DEFORMED
Ø16	759680	DEFORMED

SUMMARY CHART OF CONCRETE
FOR ALL FOUR SPECIMENS

ELEMENT	VOLUME (m^3)
FOUNDATION	8.64
COLUMN	2.54
TOTAL	11.18

SUMMARY CHART OF DROSSBACHS
FOR ALL FOUR SPECIMENS

DIAMETER	TOTAL LENGTH
Ø30	48000
Ø50	12740
Ø60	24000

SUMMARY CHART OF STEEL PLATES
FOR ALL FOUR SPECIMENS

NO	TICKNESS (mm)	DIMENSIONS (mm)
4	30	500x500

SPECIFIC NOTES:

1- All dimensions are in mm.
2- Concrete strength (f'c) is 40 MPa.
3- Steel grade is 500E seismic (fy = 500 MPa). All bars showr are deformed unless specified in the tables.
4- Macalloy bar is to be threaded 1030 bar.
5- The summary charts show the amount of materials needed for both specimens with circular section.
6- Formwork, tying wire, spacer and amount of high strength mortar are not included in this bill of quantity.

Issue	Date	Description
1	03/09/2012	SPECIMEN 1 & 2

UNIVERSITY OF CANTERBURY
Te Whare Wānanga o Waitaha
CHRISTCHURCH NEW ZEALAND

Project Title

Advanced Bridge Construction and Design
(Natural Hazard Research Platform)

Drawing Name
BQ. FOR ALL 4 SPECIMENS

Engineered by : **M.Mashal / S.White** Date : **09/2012**
Drawn by : **Mustafa Mashal** Date : **09/2012**

Drawing Scale 1:20 AT A3

Sheet No:
S-00

Appendix B

Appendix B. HDC Technical Drawings

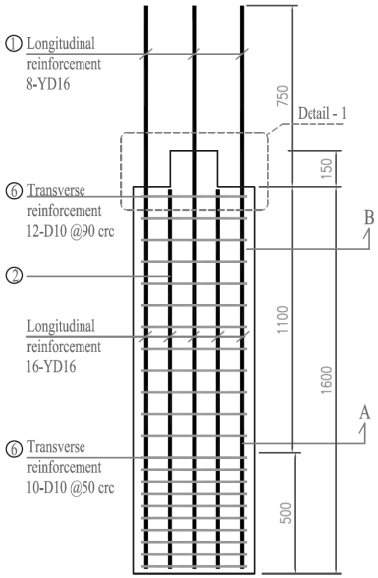

REINFORCMENT DETAILS OF THE BASE SEGMENT

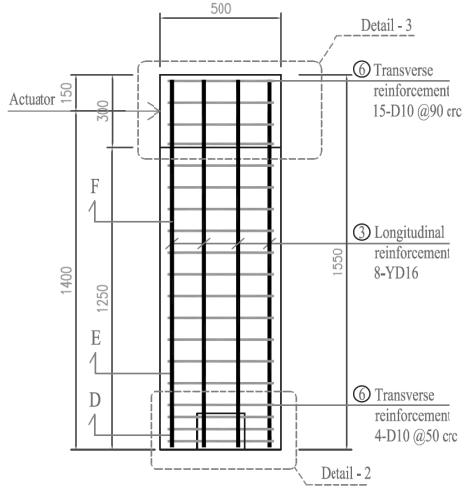

REINFORCMENT DETAILS OF THE TOP SEGMENT

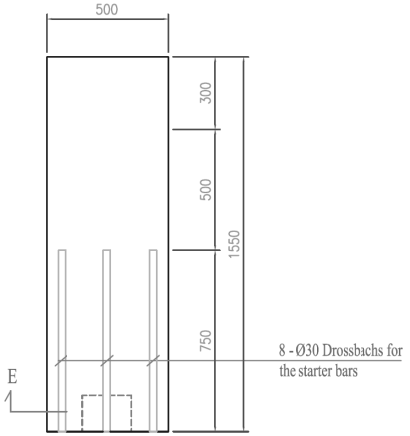

DROSSEACHS DETAIL OF THE TOP SEGMENT

NOTES:

1- All cimensions are in mm.
2- Concrete strength (f'c) is 40 MPa.
3- Steel grade is 500E seismic (fy = 500 MPa).
4- All starter bars are to be grouted inside the drossbachs with high strength mortar and hand pumped.
5- Swift lift anchors should be provided at appropriate locations for lifting purpose of each segment and the whole specimen by the crane.
6- The actuator will be connected at the cap part of the top column segment later in lab. In order to connect the steel plate on the face of the cap, appropriate anchor bolt should be placed during casting the segment so the steel plate can be attached later in lab.

Issue	Date	Description
1	03/09/2012	SPECIMEN NO - 2

UNIVERSITY OF CANTERBURY
Te Whare Wānanga o Waitaha
CHRISTCHURCH NEW ZEALAND

Project Title

Advanced Bridge Construction and Design
(Natural Hazard Research Platform)

Drawing Name
PRECAST CIRCULAR COLUMN

Engineered by : **M.Mashal / S.White** Date : **09/2012**
Drawn by : **Mustafa Mashal** Date : **09/2012**

Drawing Scale 1:20 AT A3

CONTRACTOR MUST VERIFY ALL DIMENSIONS ON SITE

Sheet No:
S-01

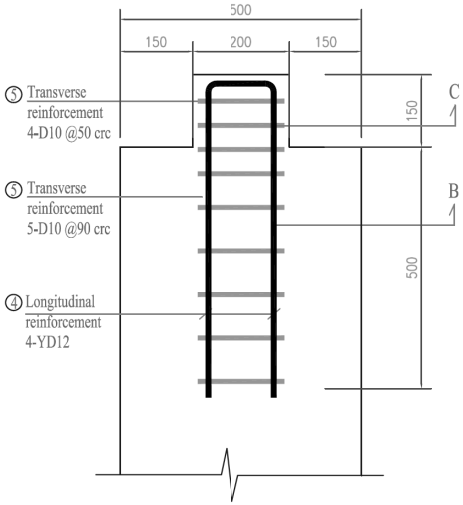

DETAIL - 1

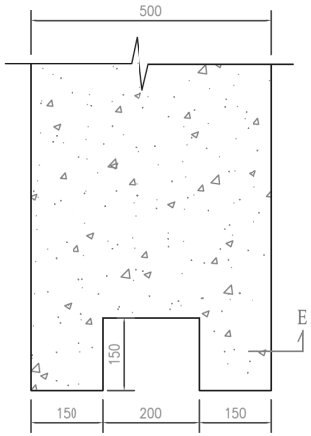

DETAIL - 2

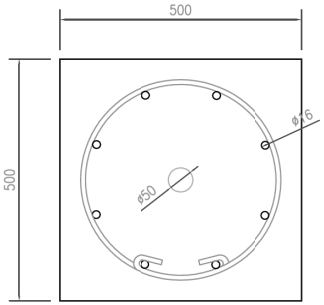

SECTION -Z

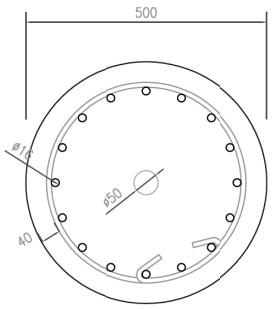

SECTION - A

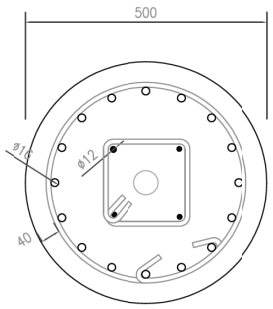

SECTION - B

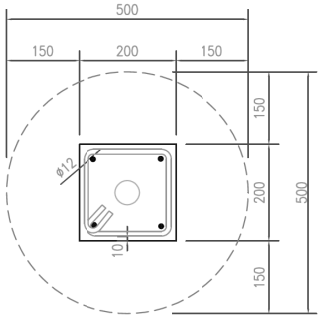

SECTION -C

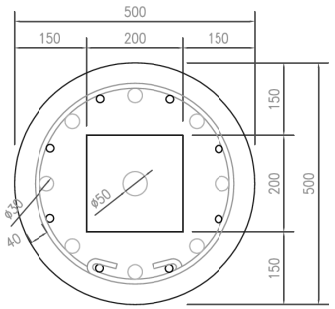

SECTION -D

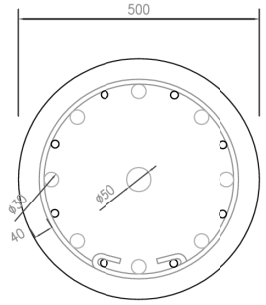

SECTION -E

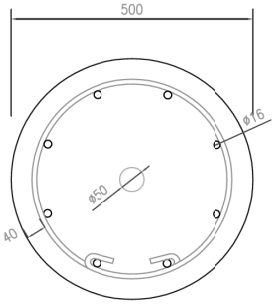

SECTION -F

⑥ D10 Stirrups

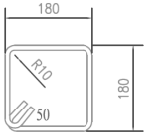

⑤ D10 Stirrups

STIRRUPS DETAILS

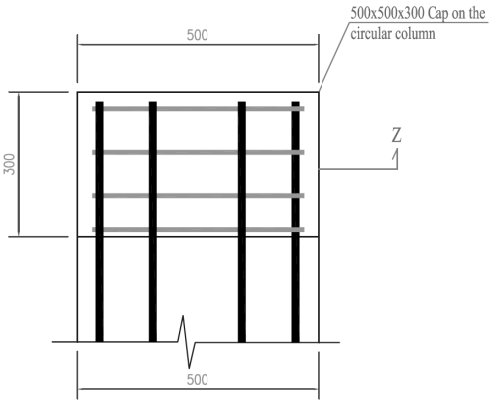

DETAIL - 3

NOTES:

1- All dimensions are in mm.
2- Concrete strength (f'c) is 40 MPa.
3- Steel grade is 500E seismic (f_y = 500 MPa).

Issue	Date	Description
1	03/09/2012	SPECIMEN NO - 2

UNIVERSITY OF CANTERBURY
Te Whare Wānanga o Waitaha
CHRISTCHURCH NEW ZEALAND

Project Title

Advanced Bridge Construction and Design
(Natural Hazard Research Platform)

Drawing Name
CIRCULAR COLUMN SECTIONS

Engineered by : **M.Mashal / S.White** Date : **09/2012**
Drawn by : **Mustafa Mashal** Date : **09/2012**

Drawing Scale 1:10 AT A3

Sheet No:
S-02

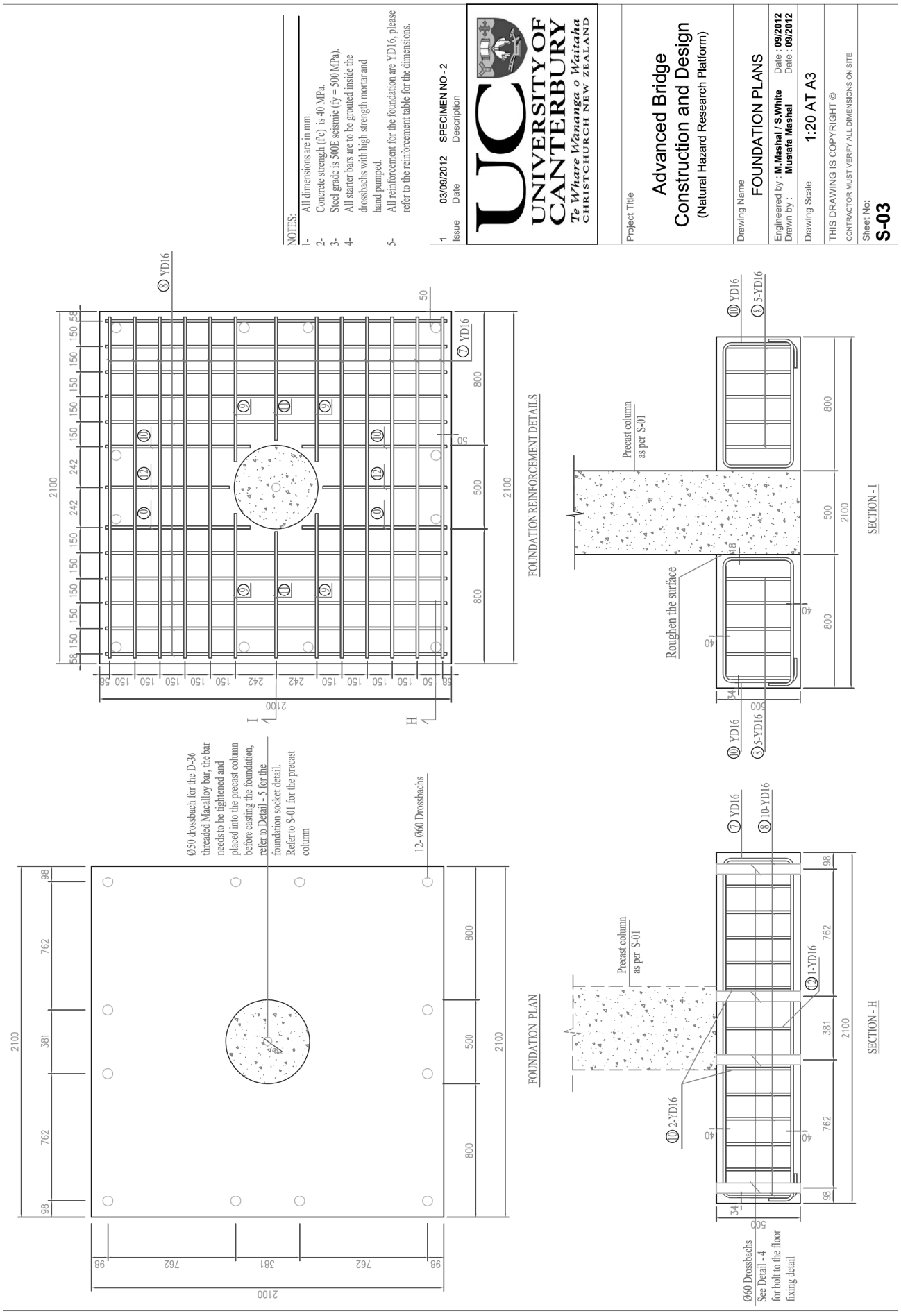
NOTES:
1- All dimensions are in mm.
2- Concrete strength (f'c) is 40 MPa.
3- Steel grade is 500E seismic (fy = 500 MPa).
4- All starter bars are to be grouted inside the drossbachs with high strength mortar and hand pumped.
5- All reinforcement for the foundation are YD16, please refer to the reinforcement table for the dimensions.
1 03/09/2012 SPECIMEN NO - 2
Issue Date Description
UNIVERSITY OF CANTERBURY
Te Whare Wananga o Waitaha
CHRISTCHURCH NEW ZEALAND
Project Title
Advanced Bridge Construction and Design
(Natural Hazard Research Platform)
Drawing Name
FOUNDATION PLANS
Engineered by : M.Mashal / S.White Date : 09/2012
Drawn by : Mustafa Mashal Date : 09/2012
Drawing Scale 1:20 AT A3
THIS DRAWING IS COPYRIGHT ©
CONTRACTOR MUST VERFY ALL DIMENSIONS ON SITE
Sheet No:
S-03
FOUNDATION REINFORCEMENT DETAILS
FOUNDATION PLAN
SECTION - I
SECTION - H
Precast column as per S-01
Roughen the surface
Ø50 drossbach for the D-36 threaded Macalloy bar, the bar needs to be tightened and placed into the precast column before casting the foundation, refer to Detail - 5 for the foundation socket detail. Refer to S-01 for the precast column
12- Ø60 Drossbachs
Ø60 Drossbachs See Detail - 4 for bolt to the floor fixing detail
8 YD16
7 YD16
10 YD16
5-YD16
10-YD16
2-YD16
1-YD16

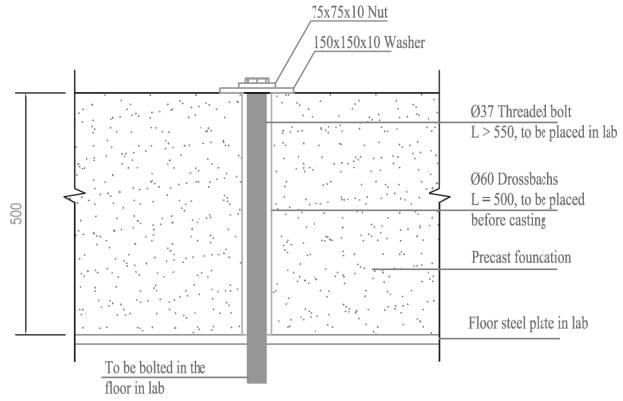

DETAIL - 4 Scale 1:10

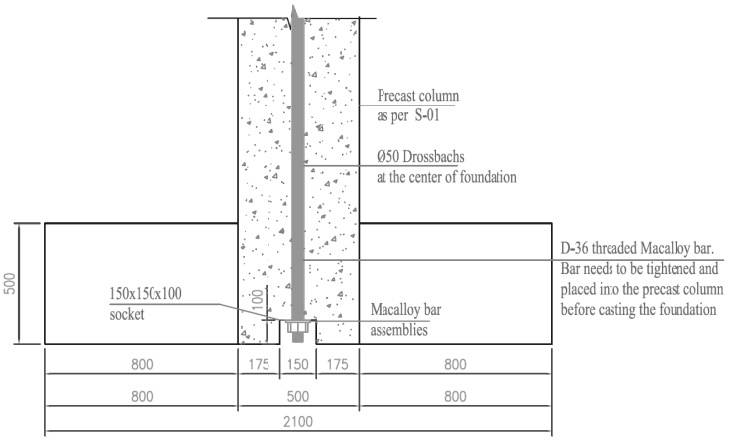

DETAIL - 5

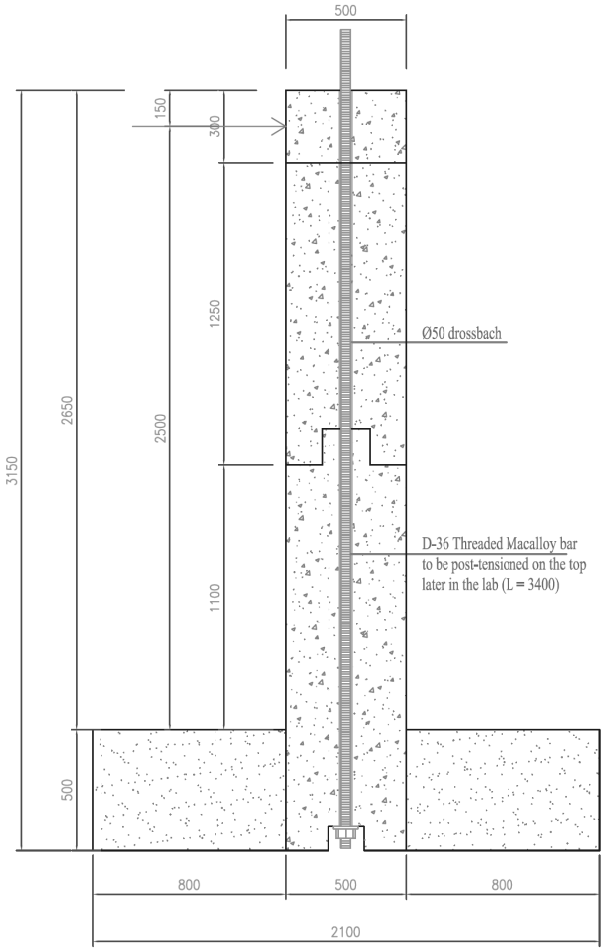

ASSEMBLED SPECIMEN TO BE DELIVERED
(SPECIMEN NO - 2)
QUANTITY NEEDED = 2

GENERAL NOTES:

1- All dimensions are in mm.
2- Concrete strength (f'c) is 40 MPa.
3- Steel grade is 500E seismic (fy = 500 MPa).
4- All starter bars are to be grouted inside the drossbachs with high strength mortar and hand pumped.
5- In order to have precise measurement of the fomwork for the segments and shear keys, match casting procedure is proposed.
6- The total weight of the specimen with the dimensions shown in these drawings is expected to be 6.5 Tons.
7- For quality control purposes, a minimum of five standard concrete cylinders per specimen are to be taken while casting the elements.
8- Swift lift anchors should be provided at appropriate locations for lifting purpose of each segment and the whole specimen by the crane.

Issue	Date	Description
1	03/09/2012	SPECIMEN NO - 2

UNIVERSITY OF CANTERBURY
Te Whare Wānanga o Waitaha
CHRISTCHURCH NEW ZEALAND

Project Title

Advanced Bridge Construction and Design
(Natural Hazard Research Platform)

Drawing Name
DETAILS & ASSEMBLED SPECIMEN

Engineered by : **M.Mashal / S.White** Date : **09/2012**
Drawn by : **Mustafa Mashal** Date : **09/2012**

Drawing Scale 1:20 AT A3

CONTRACTOR MUST VERIFY ALL DIMENSIONS ON SITE

Sheet No:
S-04

NO OF REBAR	DIAMETER	QUANTITY	DIMENSIONS	LENGTH	TOTAL LENGTH	TYPE
①	Ø16	8	2330	2330	18640	DEFORMED
②	Ø16	8	1570	1570	12560	DEFORMED
③	Ø16	8	1520	1520	12160	DEFORMED
④	Ø12	2	660, R24, 150	1440	2880	DEFORMED
⑤	Ø10	10	180, R10, 50, 100	715	7150	PLAIN
⑥	Ø10	44	R200, 50	1530	67320	PLAIN
⑦	Ø16	10	2030, R32, 420, 150, 150	5120	51200	DEFORMED
⑧	Ø16	10	2030, R32, 390, 150, 150	5060	50600	DEFORMED
⑨	Ø16	4	860, R32, 420, 150, 150	2750	11000	DEFORMED
⑩	Ø16	4	860, R32, 390, 150, 150	2690	10760	DEFORMED
⑪	Ø16	2	750, R32, 420, 150, 150	2530	5060	DEFORMED
⑫	Ø16	2	750, R32, 390, 150, 150	2470	4940	DEFORMED

SUMMARY CHART OF REINFORCEMENT FOR TWO SPECIMENS

DIAMETER	TOTAL LENGTH	TYPE
Ø10	148940	PLAIN
Ø12	5760	DEFORMED
Ø16	353840	DEFORMED

SUMMARY CHART OF CONCRETE FOR TWO SPECIMENS

ELEMENT	VOLUME (m³)
FOUNDATION	4.21
COLUMN	1.21
TOTAL	5.42

SUMMARY CHART OF DROSSBACHS FOR TWO SPECIMENS

DIAMETER	TOTAL LENGTH
Ø30	12000
Ø50	6340
Ø60	12000

SPECIFIC NOTES:

1- All dimensions are in mm.
2- Concrete strength (f'c) is 40 MPa.
3- Steel grade is 500E seismic (fy = 500 MPa). All bars shown are deformed unless specified in the tables.
4- The summary charts show the amount of materials needed for both specimens with circular section.
5- Formwork, tying wire, spacer and amount of high strength mortar are not included in this bill of quantity.
6- For quality control purposes, a minimum of five standard concrete cylinders per specimen are to be taken while casting the elements.
7- A minimum length of 2000mm of reinforcement for the all three diameters shown in the table shall be added with the total amount. This will be used for testing of the bars in the lab to verify the strength.

Issue	Date	Description
1	03/09/2012	SPECIMEN NO - 2

UNIVERSITY OF CANTERBURY
Te Whare Wānanga o Waitaha
CHRISTCHURCH NEW ZEALAND

Project Title

Advanced Bridge Construction and Design
(Natural Hazard Research Platform)

Drawing Name
BILL OF QUANTITY

Engineered by : **M.Mashal / S.White** Date : **09/2012**
Drawn by : **Mustafa Mashal** Date : **09/2012**

Drawing Scale 1:20 AT A3

CONTRACTOR MUST VERIFY ALL DIMENSIONS ON SITE

Sheet No:
S-05

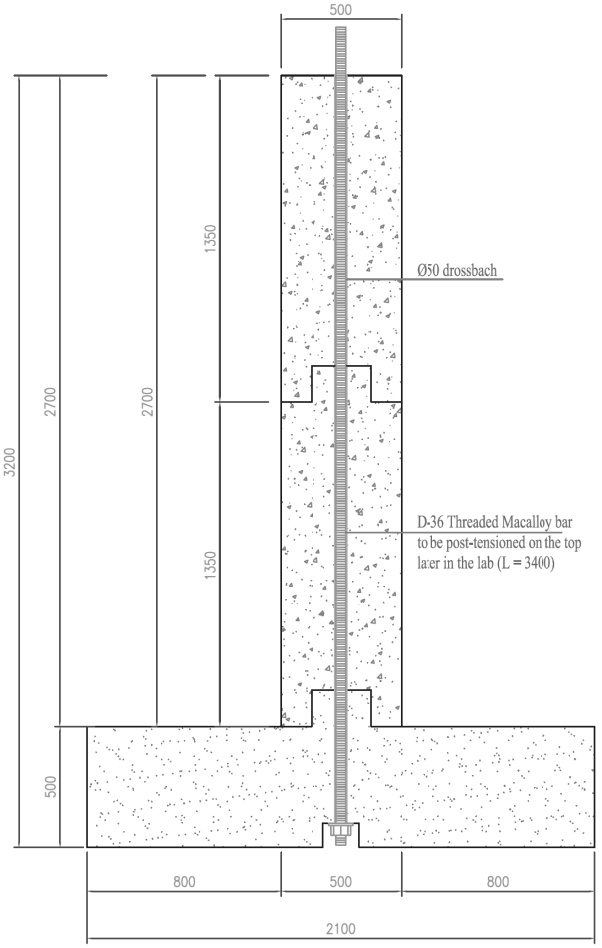

ASSEMBLED SPECIMEN TO BE DELIVERED
(SPECIMEN NO - 1)
QUANTITY NEEDED = 2

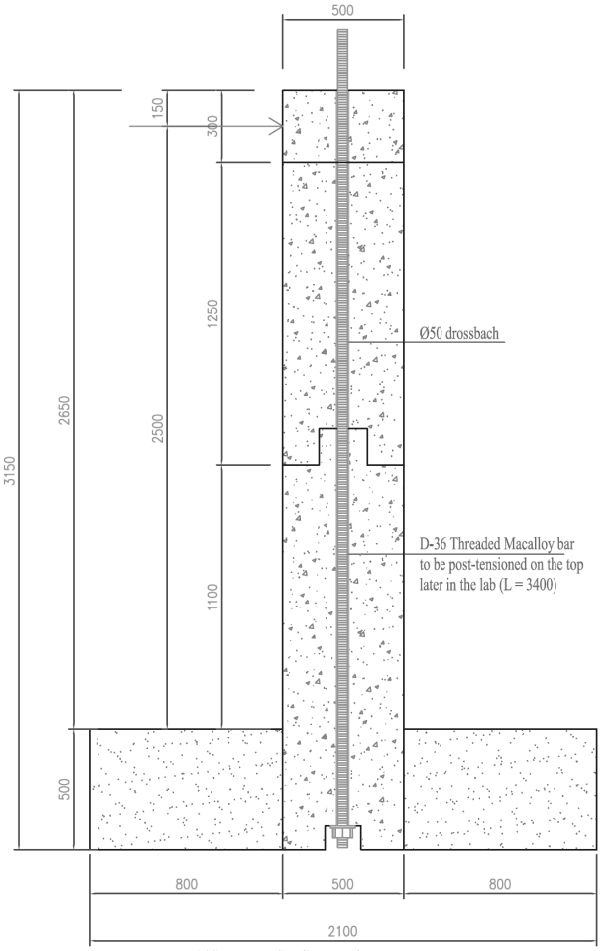

ASSEMBLED SPECIMEN TO BE DELIVERED
(SPECIMEN NO - 2)
QUANTITY NEEDED = 2

SUMMARY CHART OF REINFORCEMENT
FOR ALL FOUR SPECIMENS

DIAMETER	TOTAL LENGTH	TYPE
Ø10	524840	PLAIN
Ø12	18160	DEFORMED
Ø16	759680	DEFORMED

SUMMARY CHART OF CONCRETE
FOR ALL FOUR SPECIMENS

ELEMENT	VOLUME (m^3)
FOUNDATION	8.64
COLUMN	2.54
TOTAL	11.18

SUMMARY CHART OF DROSSBACHS
FOR ALL FOUR SPECIMENS

DIAMETER	TOTAL LENGTH
Ø30	48000
Ø50	12740
Ø60	24000

SUMMARY CHART OF STEEL PLATES
FOR ALL FOUR SPECIMENS

NO	TICKNESS (mm)	DIMENSIONS (mm)
4	30	500x500

SPECIFIC NOTES:

1- All dimensions are in mm.
2- Concrete strength (f'c) is 40 MPa.
3- Steel grade is 500E seismic (fy = 500 MPa). All bars showr are deformed unless specified in the tables.
4- Macalloy bar is to be threaded 1030 bar.
5- The summary charts show the amount of materials needed for both specimens with circular section.
6- Formwork, tying wire, spacer and amount of high strength mortar are not included in this bill of quantity.

Issue	Date	Description
1	03/09/2012	SPECIMEN 1 & 2

UNIVERSITY OF CANTERBURY
Te Whare Wānanga o Waitaha
CHRISTCHURCH NEW ZEALAND

Project Title

Advanced Bridge Construction and Design
(Natural Hazard Research Platform)

Drawing Name
BQ. FOR ALL 4 SPECIMENS

Engineered by : **M.Mashal / S.White** Date : **09/2012**
Drawn by : **Mustafa Mashal** Date : **09/2012**

Drawing Scale 1:20 AT A3

Sheet No:
S-00

Appendix C

Appendix C. CDC Technical Drawings

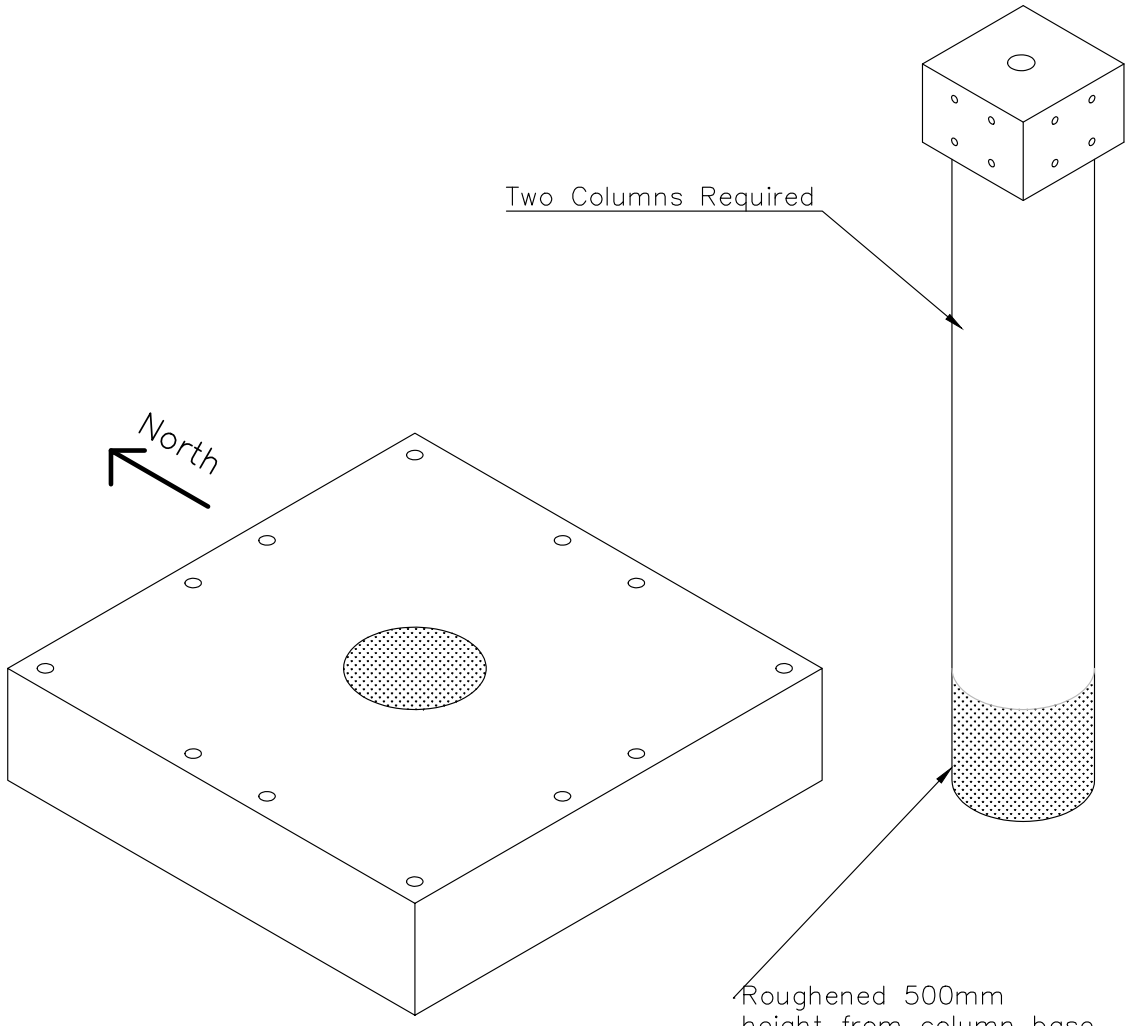

NOTES:

1- Two LDC-1 columns are required with no footing
2- All dimensions are in mm.
3- Concrete strength (f'c) is 40 MPa.
4- Steel grade and type is specified in Sheet C-05
5- For quality control purposes, six standard concrete cylinders per specimen are to be taken while casting the elements.
6- A minimum length of 2000mm of reinforcement for all diameters shown in the table shall be added with the total amount. This will be used for testing of the bars in the lab to verify the strength.

Issue	Date	Description
1	28/02/2013	COLUMN LDC-1

Project Title

Advanced Bridge Construction and Design
(Natural Hazard Research Platform)

Drawing Name
Isometric Components

Engineered by : **S. White** Date : **01/2013**
Drawn by : **S. White** Date : **01/2013**

Drawing Scale 1:20 AT A3

Sheet No:
C-01

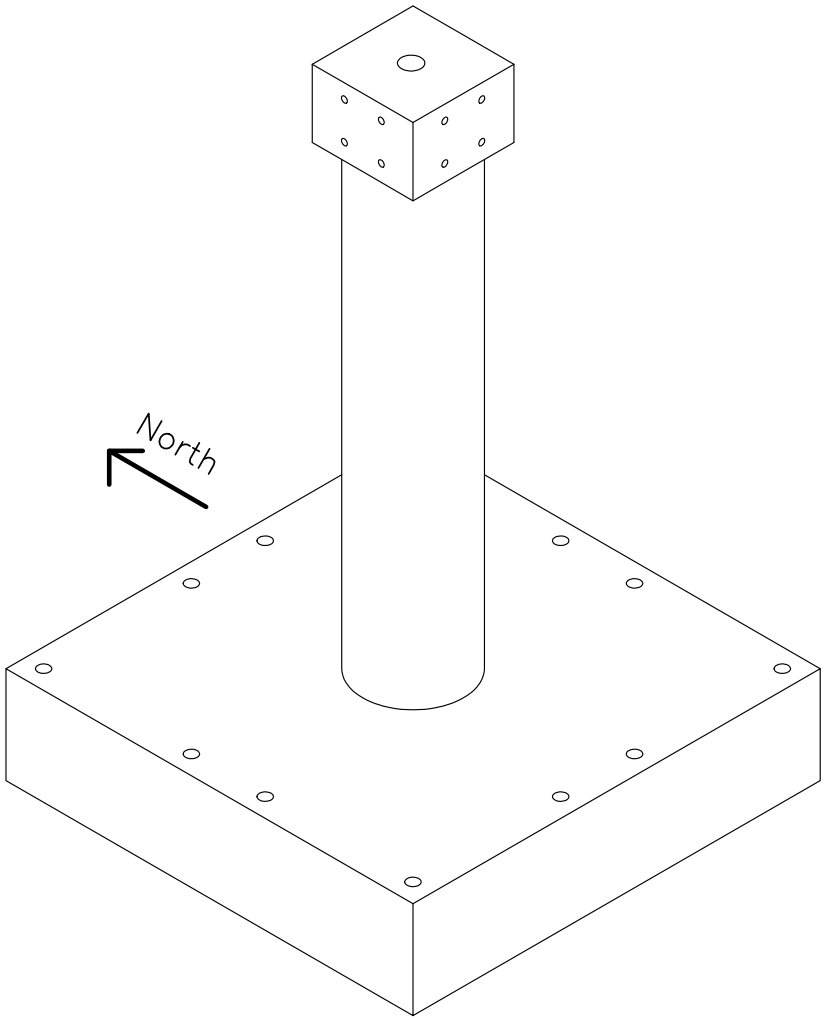

Note: Footing not required

NOTES:

1- Two LDC-1 columns are required with no footing
2- All dimensions are in mm.
3- Concrete strength (f'c) is 40 MPa.
4- Steel grade and type is specified in Sheet C-05
5- For quality control purposes, six standard concrete cylinders per specimen are to be taken while casting the elements.
6- A minimum length of 2000mm of reinforcement for all diameters shown in the table shall be added with the total amount. This will be used for testing of the bars in the lab to verify the strength.

Issue	Date	Description
1	28/02/2013	COLUMN LDC-1

Project Title

Advanced Bridge Construction and Design
(Natural Hazard Research Platform)

Drawing Name

Isometric Assembled

Engineered by : **S. White** Date : **01/2013**
Drawn by : **S. White** Date : **01/2013**

Drawing Scale 1:20 AT A3

Sheet No:
C-02

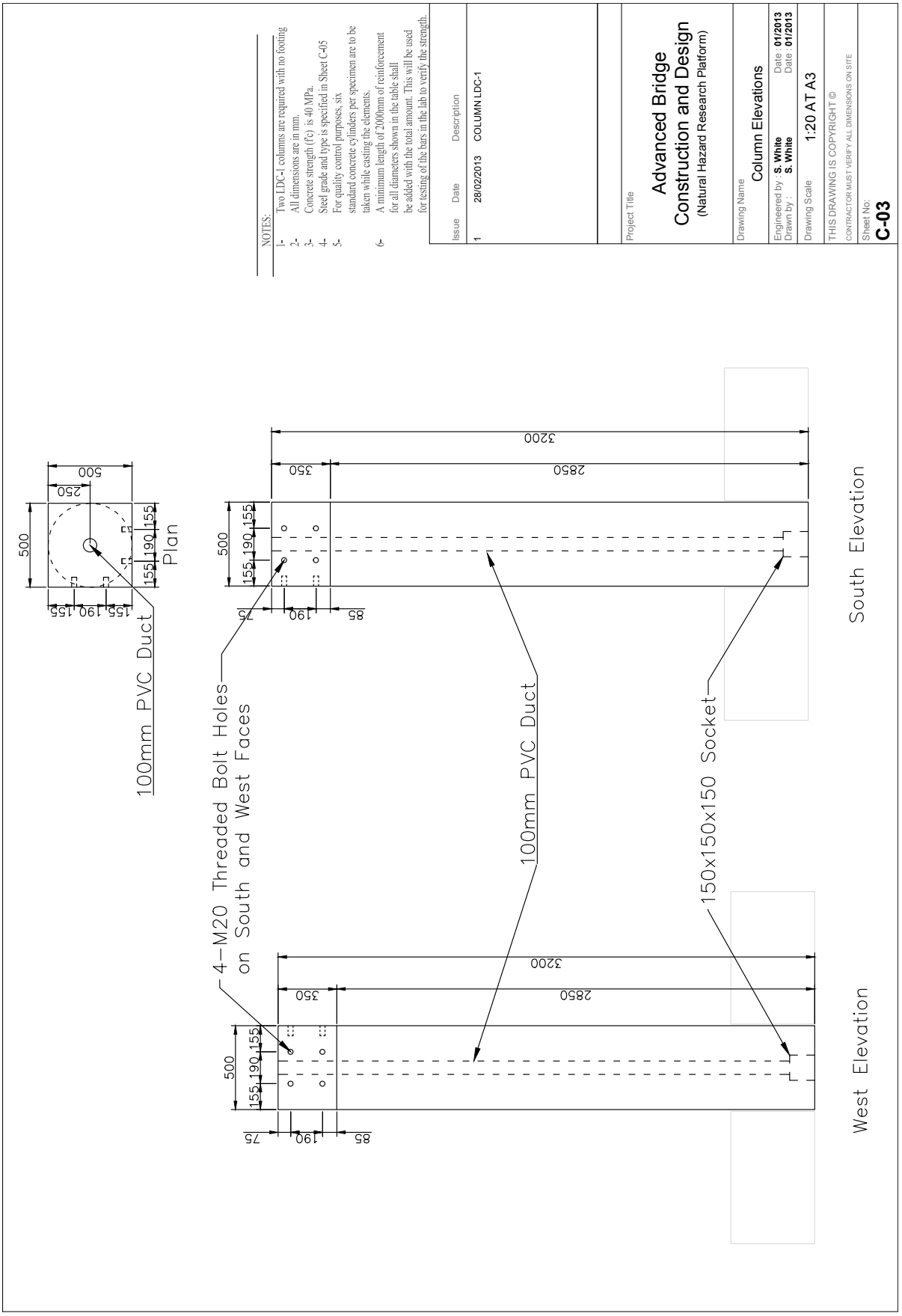
NOTES:
1- Two LDC-1 columns are required with no footing
2- All dimensions are in mm.
3- Concrete strength (f'c) is 40 MPa.
4- Steel grade and type is specified in Sheet C-05
5- For quality control purposes, six standard concrete cylinders per specimen are to be taken while casting the elements.
6- A minimum length of 2000mm of reinforcement for all diameters shown in the table shall be added with the total amount. This will be used for testing of the bars in the lab to verify the strength.
Issue Date Description
1 28/02/2013 COLUMN LDC-1
Project Title
Advanced Bridge Construction and Design
(Natural Hazard Research Platform)
Drawing Name
Column Elevations
Engineered by : S. White Date : 01/2013
Drawn by : S. White Date : 01/2013
Drawing Scale 1:20 AT A3
THIS DRAWING IS COPYRIGHT ©
CONTRACTOR MUST VERIFY ALL DIMENSIONS ON SITE
Sheet No:
C-03
Plan
100mm PVC Duct
4-M20 Threaded Bolt Holes on South and West Faces
100mm PVC Duct
150x150x150 Socket
South Elevation
West Elevation
500
250
155
190
3200
2850
350
85
75

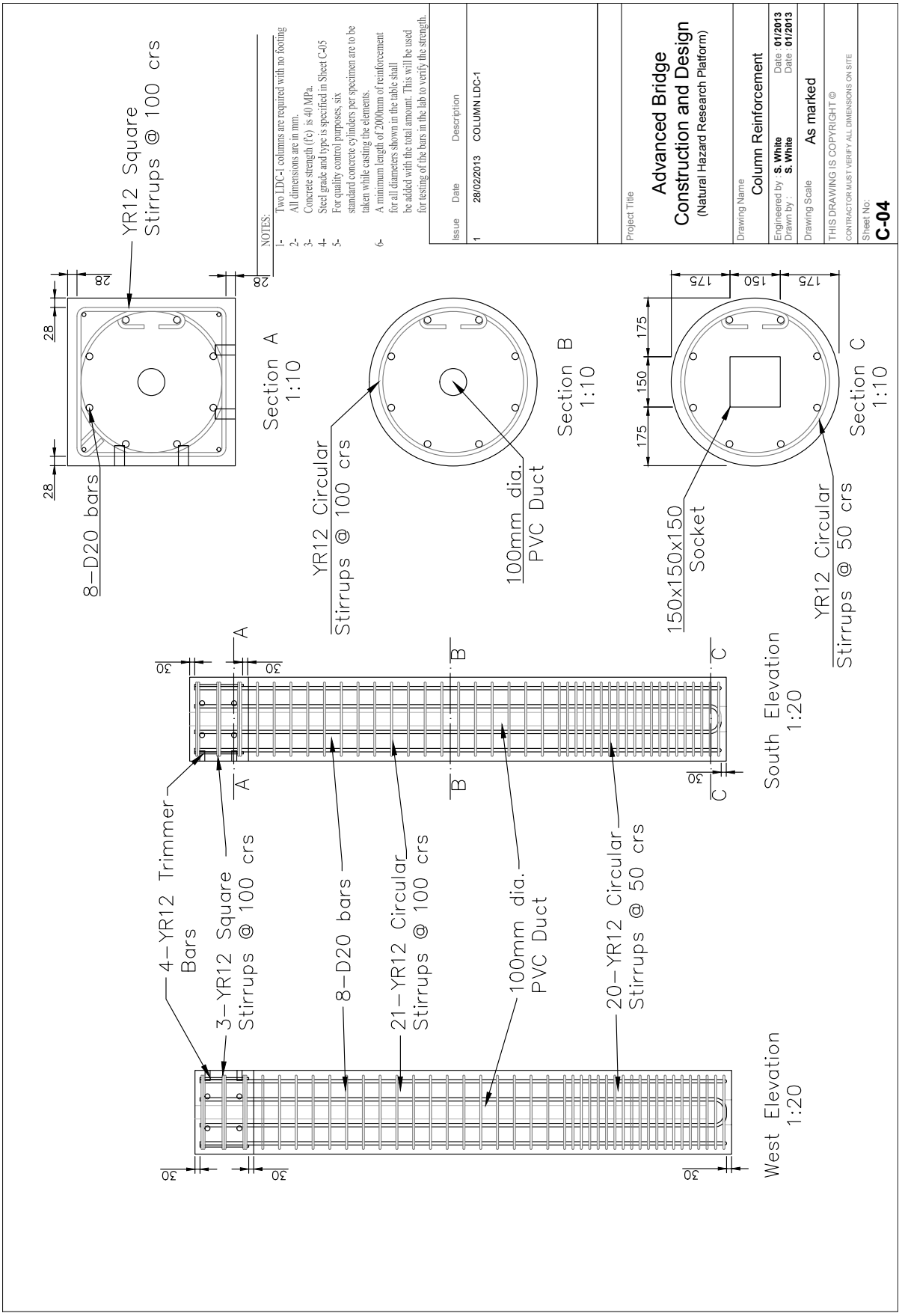
NOTES:
1- Two LDC-1 columns are required with no footing
2- All dimensions are in mm.
3- Concrete strength (f'c) is 40 MPa.
4- Steel grade and type is specified in Sheet C-05
5- For quality control purposes, six standard concrete cylinders per specimen are to be taken while casting the elements.
6- A minimum length of 2000mm of reinforcement for all diameters shown in the table shall be added with the total amount. This will be used for testing of the bars in the lab to verify the strength.
Issue Date Description
1 28/02/2013 COLUMN LDC-1
Project Title
Advanced Bridge Construction and Design
(Natural Hazard Research Platform)
Drawing Name
Column Reinforcement
Engineered by S. White Date 01/2013
Drawn by : S. White Date 01/2013
Drawing Scale As marked
THIS DRAWING IS COPYRIGHT ©
CONTRACTOR MUST VERIFY ALL DIMENSIONS ON SITE
Sheet No:
C-04
YR12 Square Stirrups @ 100 crs
8-D20 bars
Section A 1:10
YR12 Circular Stirrups @ 100 crs
100mm dia. PVC Duct
Section B 1:10
150x150x150 Socket
YR12 Circular Stirrups @ 50 crs
Section C 1:10
4-YR12 Trimmer Bars
3-YR12 Square Stirrups @ 100 crs
8-D20 bars
21-YR12 Circular Stirrups @ 100 crs
100mm dia. PVC Duct
20-YR12 Circular Stirrups @ 50 crs
West Elevation 1:20
South Elevation 1:20

Reinforcement Summary				
Bar ID	No. Required	Diameter	Grade	Type
A	8	12 mm	500 MPa	Plain
B	6	12 mm	500 MPa	Plain
C	82	12 mm	500 MPa	Plain
D	8	20 mm	300 MPa	Deformed

Note: Reinforcement quantities are for two columns

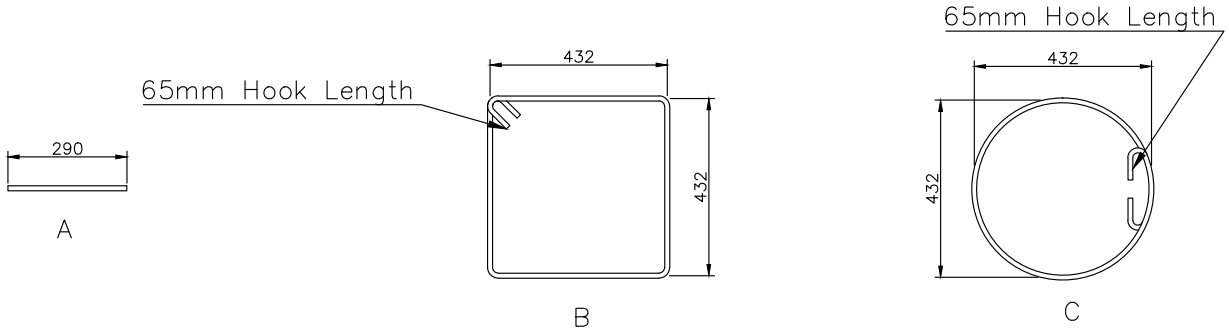

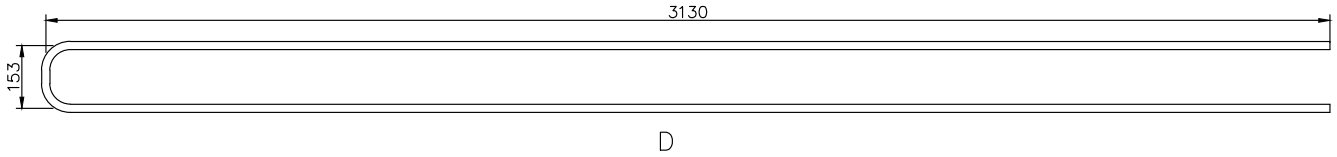

Note: Centreline dimensions shown

NOTES:

1- Two LDC-1 columns are required with no footing
2- All dimensions are in mm.
3- Concrete strength (f'c) is 40 MPa.
4- Steel grade and type is specified in Sheet C-05
5- For quality control purposes, six standard concrete cylinders per specimen are to be taken while casting the elements.
6- A minimum length of 2000mm of reinforcement for all diameters shown in the table shall be added with the total amount. This will be used for testing of the bars in the lab to verify the strength.

Issue	Date	Description
1	28/02/2013	COLUMN LDC-1

Project Title

Advanced Bridge Construction and Design
(Natural Hazard Research Platform)

Drawing Name
Reinforcement Summary

Engineered by : **S. White** Date : **01/2013**
Drawn by : **S. White** Date : **01/2013**

Drawing Scale 1:20 AT A3

Sheet No:
C-05

Appendix D

Appendix D. CDS Technical Drawings

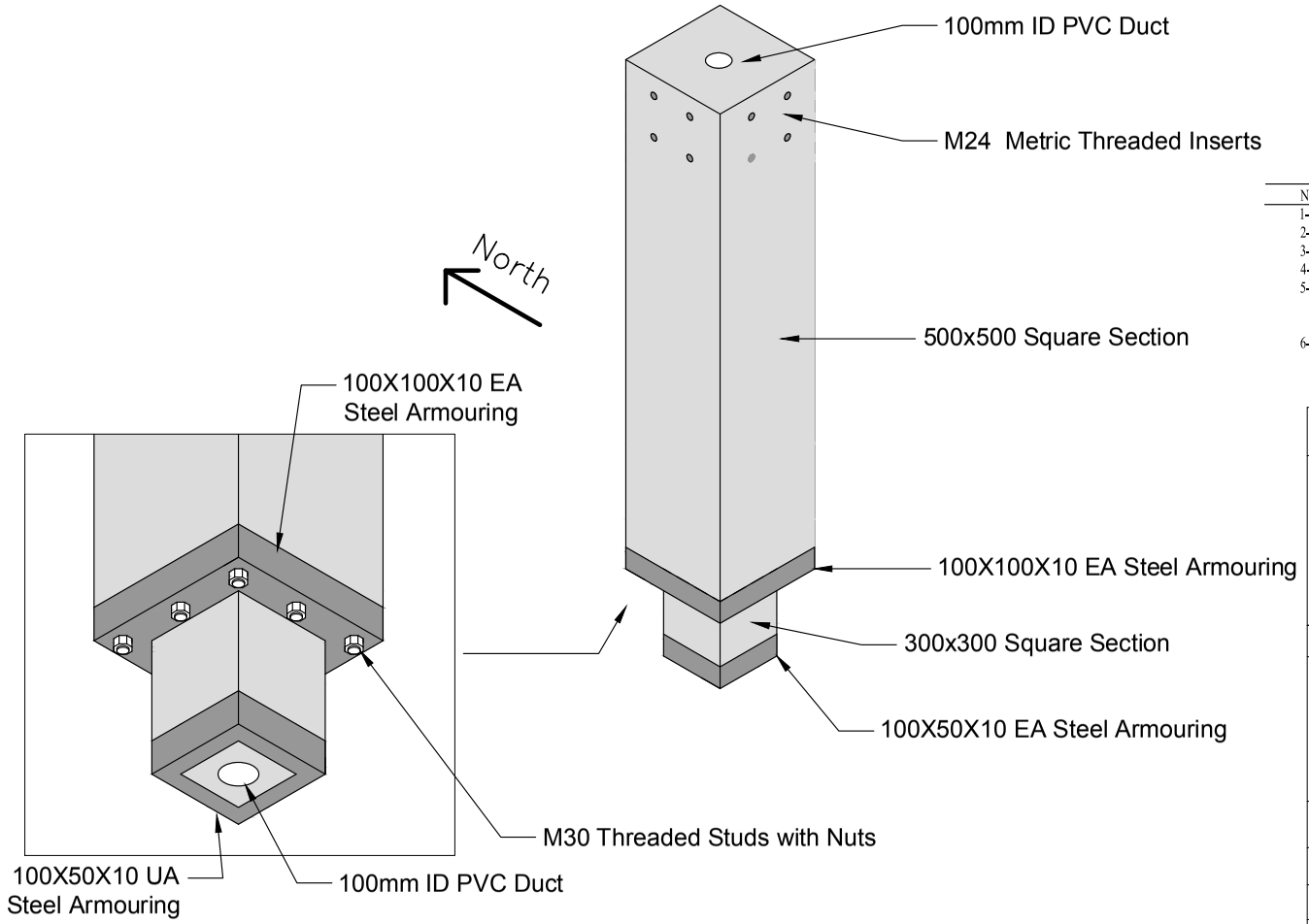

NOTES:

1- One LDS-1 column with footing is required
2- All dimensions are in mm.
3- Concrete strength (f'c) is 50 MPa.
4- Steel grade and type is specified in Sheet S-04
5- For quality control purposes, six standard concrete cylinders per specimen are to be taken while casting the elements.
6- A minimum length of 2000mm of reinforcement for all diameters shown in the table shall be added with the total amount. This will be used for testing of the bars in the lab to verify the strength.

Issue	Date	Description
1	07/05/2013	SPECIMEN LDS-1
2	10/06/2013	SPECIMEN LDS-1

Project Title

Advanced Bridge Construction and Design

(Natural Hazard Research Platform)

Drawing Name

Column Isometric View

Engineered by : **S. White** Date : **05/2013**
Drawn by : **S. White** Date : **05/2013**

Drawing Scale 1:20 AT A3

Sheet No:

S-01

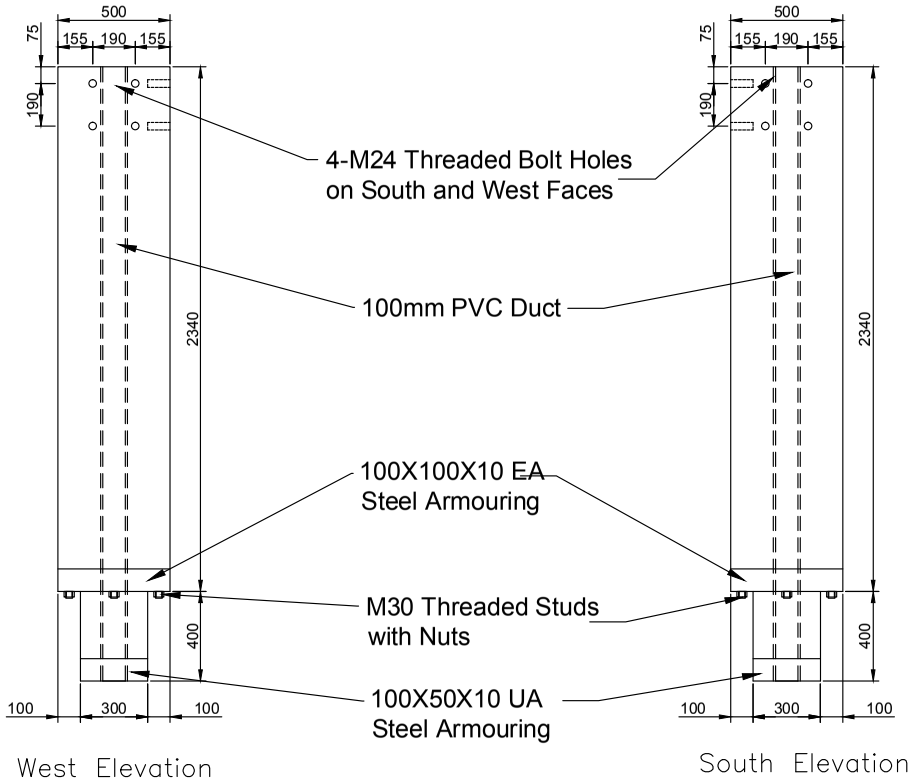

Note: All armouring, headed bars, couplers and nuts will be provided by UC

NOTES:

1- One LDS-1 column with footing is required
2- All dimensions are in mm.
3- Concrete strength (f'c) is 50 MPa.
4- Steel grade and type is specified in Sheet S-04
5- For quality control purposes, six standard concrete cylinders per specimen are to be taken while casting the elements.
6- A minimum length of 2000mm of reinforcement for all diameters shown in the table shall be added with the total amount. This will be used for testing of the bars in the lab to verify the strength.

Issue	Date	Description
1	07/05/2013	SPECIMEN LDS-1
2	10/06/2013	SPECIMEN LDS-1

Project Title

Advanced Bridge Construction and Design
(Natural Hazard Research Platform)

Drawing Name
Column Elevations

Engineered by : **S. White** Date : **05/2013**
Drawn by : **S. White** Date : **05/2013**

Drawing Scale 1:20 AT A3

CONTRACTOR MUST VERIFY ALL DIMENSIONS ON SITE

Sheet No:
S-02

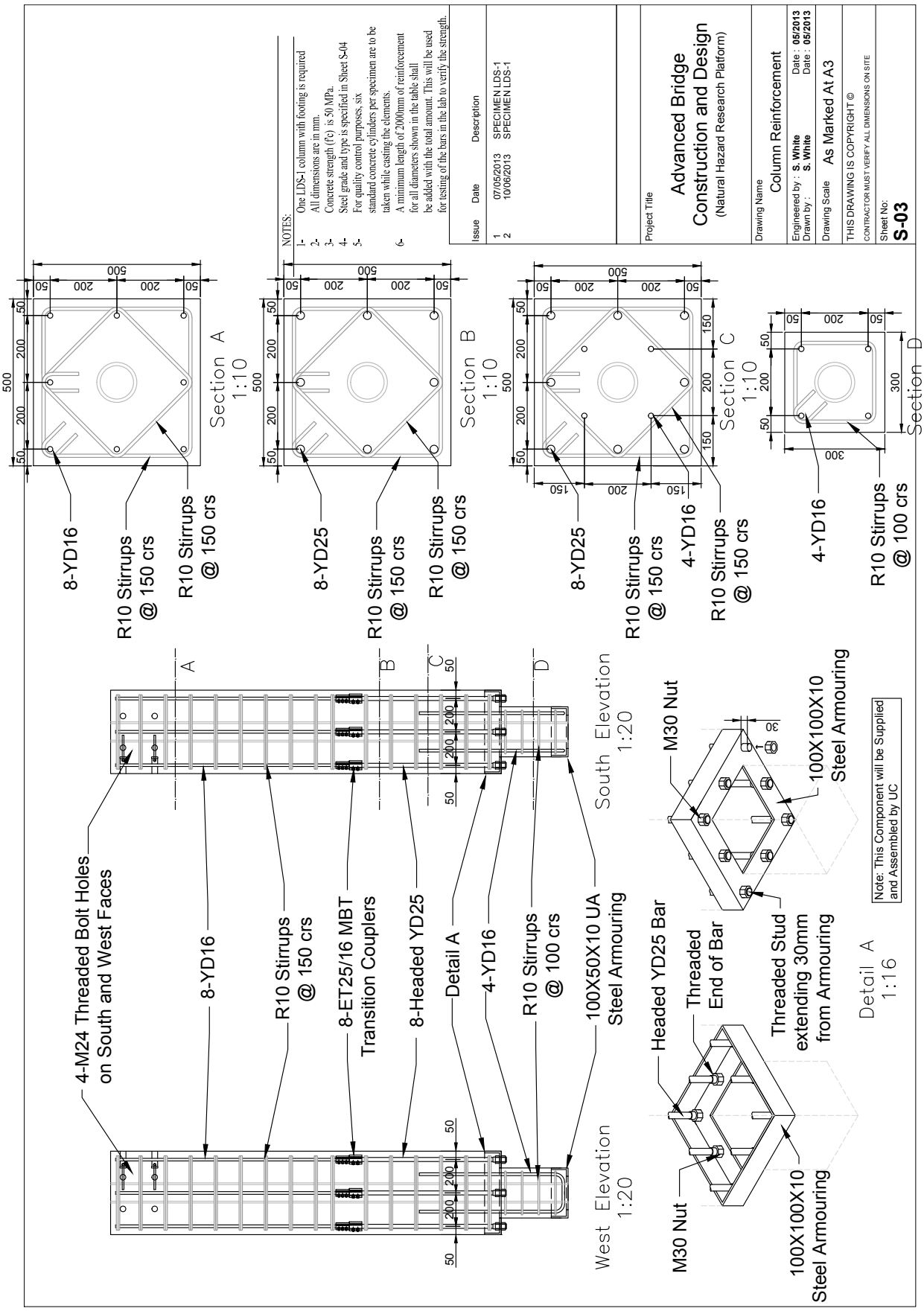

Note: All armouring, headed bars, couplers and nuts will be provided by UC

Reinforcement Summary

Bar ID	No. Required	Diameter	Grade	Type	Notes
A	8	25 mm	500 MPa	Deformed	Supplied by UC
B	8	16 mm	500 MPa	Deformed	
C	2	16 mm	500 MPa	Deformed	
D	16	10 mm	500 MPa	Plain	
E	16	10 mm	500 MPa	Plain	
F	4	10 mm	500 MPa	Plain	
G	8				Supplied by UC

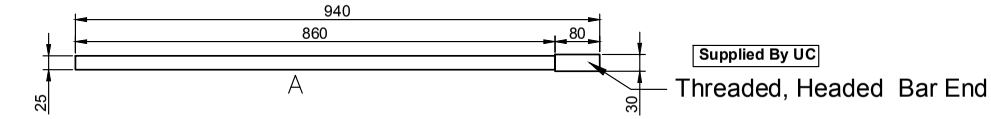

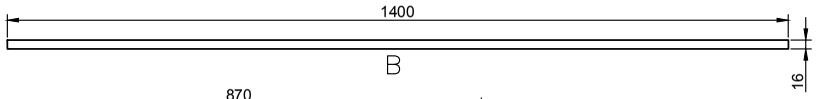

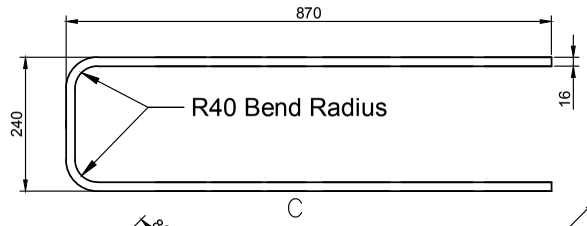

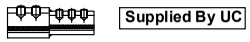

ET25/16 MBT
Transition Couplers
G

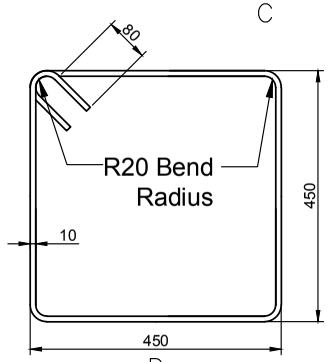

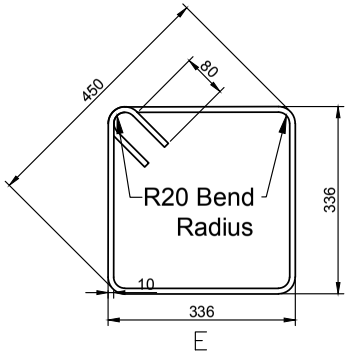

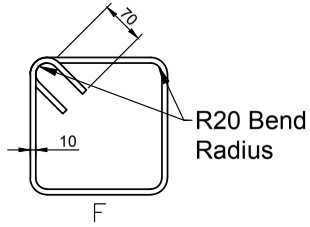

Note: All armouring, headed bars, couplers and nuts will be provided by UC

NOTES:
1- One LDS-1 column with footing is required
2- All dimensions are in mm.
3- Concrete strength (f'c) is 50 MPa.
4- Steel grade and type is specified in Sheet S-04
5- For quality control purposes, six standard concrete cylinders per specimen are to be taken while casting the elements.
6- A minimum length of 2000mm of reinforcement for all diameters shown in the table shall be added with the total amount. This will be used for testing of the bars in the lab to verify the strength.

Issue	Date	Description
1	07/05/2013	SPECIMEN LDS-1
2	10/06/2013	SPECIMEN LDS-1

Project Title

Advanced Bridge Construction and Design
(Natural Hazard Research Platform)

Drawing Name
Column Reinforcement Summary

Engineered by : **S. White** Date : **05/2013**
Drawn by : **S. White** Date : **05/2013**

Drawing Scale

Sheet No:
S-04

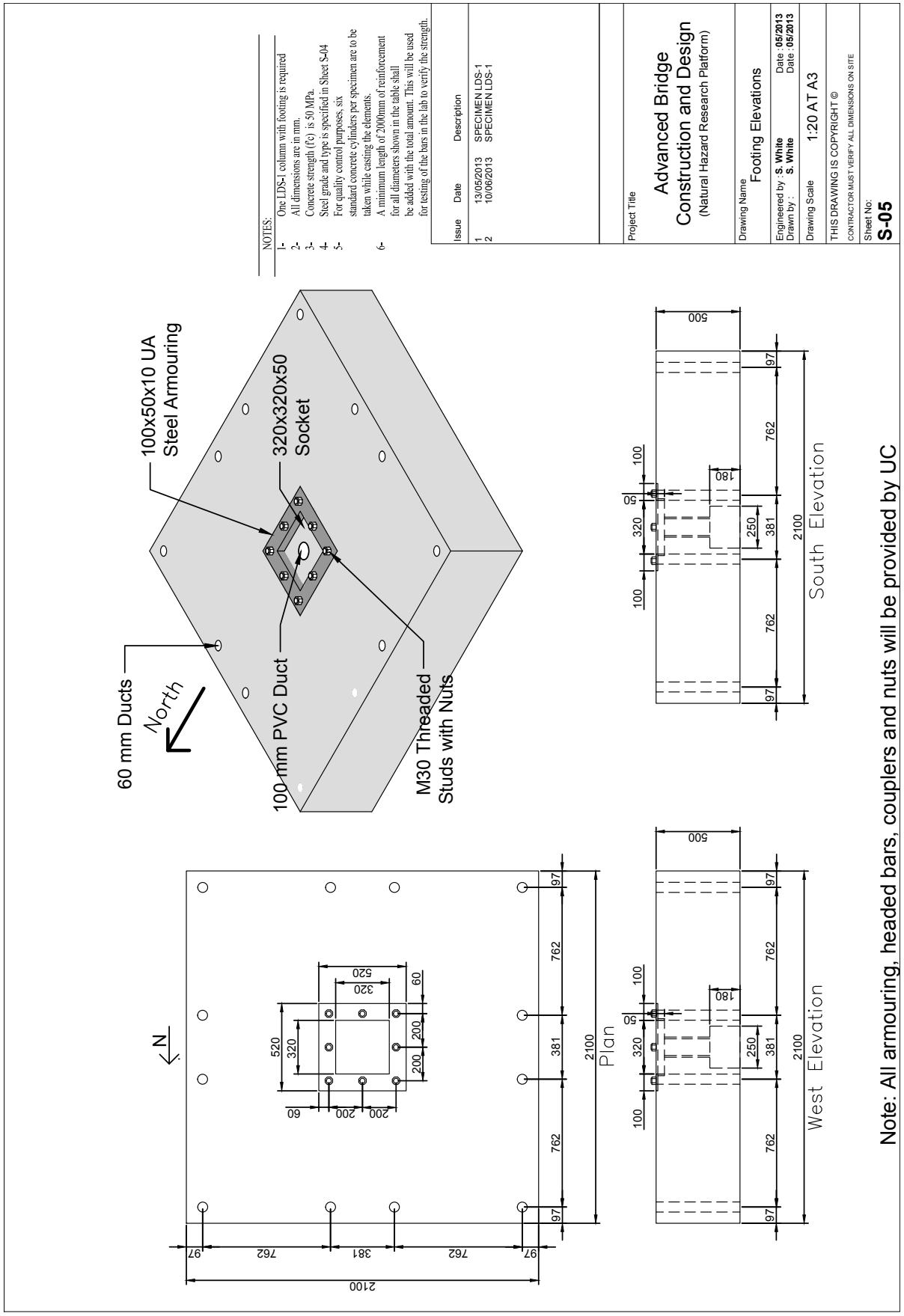
NOTES:
1- One LDS-1 column with footing is required
2- All dimensions are in mm.
3- Concrete strength (f'c) is 50 MPa.
4- Steel grade and type is specified in Sheet S-04
5- For quality control purposes, six standard concrete cylinders per specimen are to be taken while casting the elements.
6- A minimum length of 2000mm of reinforcement for all diameters shown in the table shall be added with the total amount. This will be used for testing of the bars in the lab to verify the strength.
Issue Date Description
1 13/05/2013 SPECIMEN LDS-1
2 10/06/2013 SPECIMEN LDS-1
Project Title
Advanced Bridge Construction and Design
(Natural Hazard Research Platform)
Drawing Name
Footing Elevations
Engineered by : S. White Date : 05/2013
Drawn by : S. White Date : 05/2013
Drawing Scale 1:20 AT A3
THIS DRAWING IS COPYRIGHT ©
CONTRACTOR MUST VERIFY ALL DIMENSIONS ON SITE
Sheet No:
S-05
100x50x10 UA Steel Armouring
320x320x50 Socket
60 mm Ducts
North
100 mm PVC Duct
M30 Threaded Studs with Nuts
N
Plan
South Elevation
West Elevation
Note: All armouring, headed bars, couplers and nuts will be provided by UC

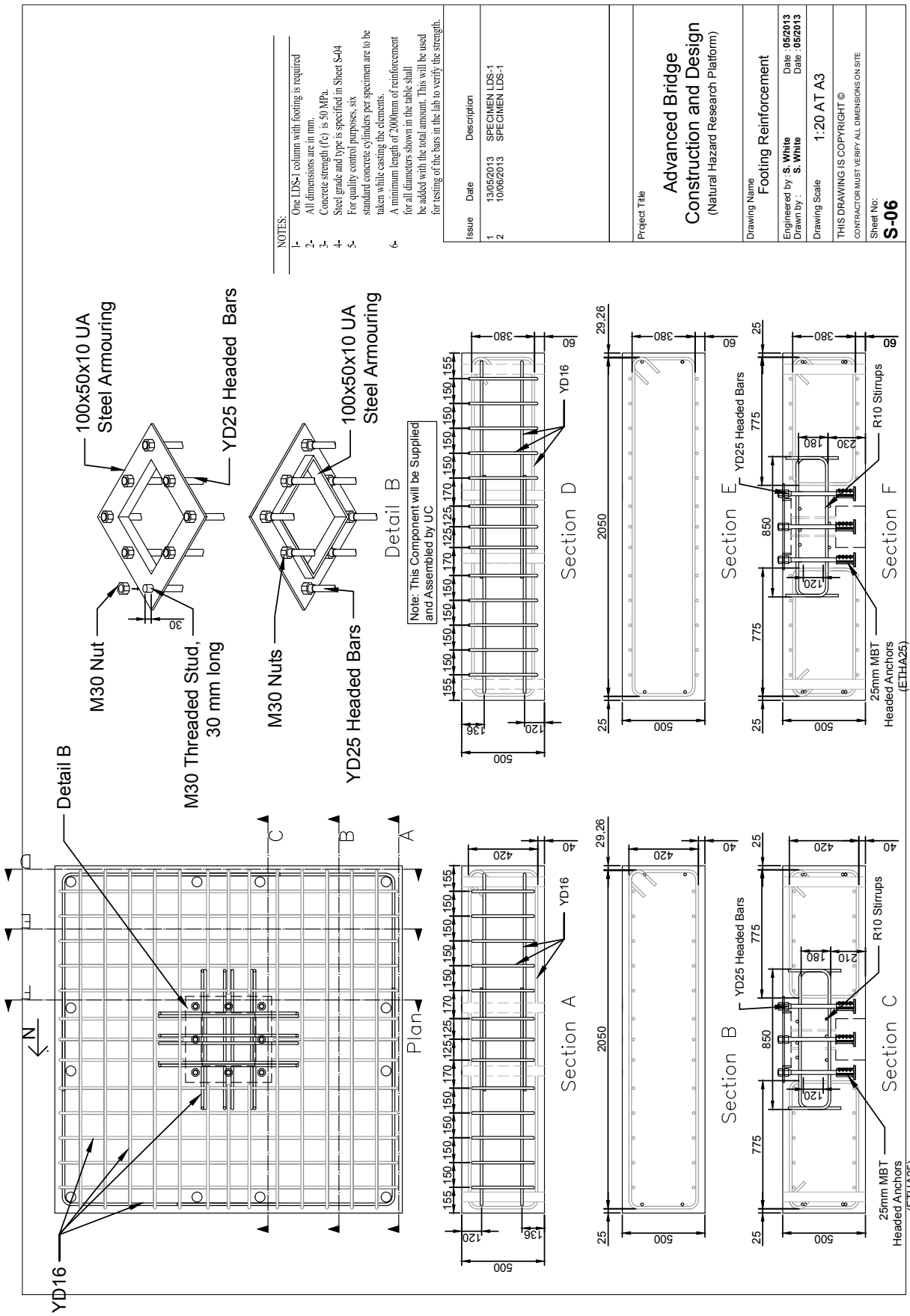
NOTES:
1- One LDS-I column with footing is required
2- All dimensions are in mm.
3- Concrete strength (f'c) is 50 MPa.
4- Steel grade and type is specified in Sheet S-04
5- For quality control purposes, six standard concrete cylinders per specimen are to be taken while casting the elements.
6- A minimum length of 2000mm of reinforcement for all diameters shown in the table shall be added with the total amount. This will be used for testing of the bars in the lab to verify the strength.
Issue Date Description
1 13/05/2013 SPECIMEN LDS-1
2 10/06/2013 SPECIMEN LDS-1
Project Title
Advanced Bridge Construction and Design
(Natural Hazard Research Platform)
Drawing Name
Footing Reinforcement
Engineered by : S. White Date : 05/2013
Drawn by : S. White Date : 05/2013
Drawing Scale 1:20 AT A3
THIS DRAWING IS COPYRIGHT ©
CONTRACTOR MUST VERIFY ALL DIMENSIONS ON SITE
Sheet No:
S-06
Detail B
100x50x10 UA Steel Armouring
YD25 Headed Bars
M30 Nut
M30 Threaded Stud, 30 mm long
M30 Nuts
YD25 Headed Bars
Note: This Component will be Supplied and Assembled by UC
Plan
Section A
Section B
Section C
Section D
Section E
Section F
YD16
R10 Stirrups
25mm MBT Headed Anchors (ETHA25)
Note: All armouring, headed bars, couplers and nuts will be provided by UC

Reinforcement Summary					
Bar ID	No. Required	Diameter	Grade	Type	Notes
H	10	16 mm	500 MPa	Deformed	
I	10	16 mm	500 MPa	Deformed	
J	6	16 mm	500 MPa	Deformed	
K	6	16 mm	500 MPa	Deformed	
L	8	25 mm	500 MPa	Deformed	Supplied By UC
M	12	16 mm	500 MPa	Deformed	
N	8	16 mm	500 MPa	Deformed	
O	8				Supplied By UC

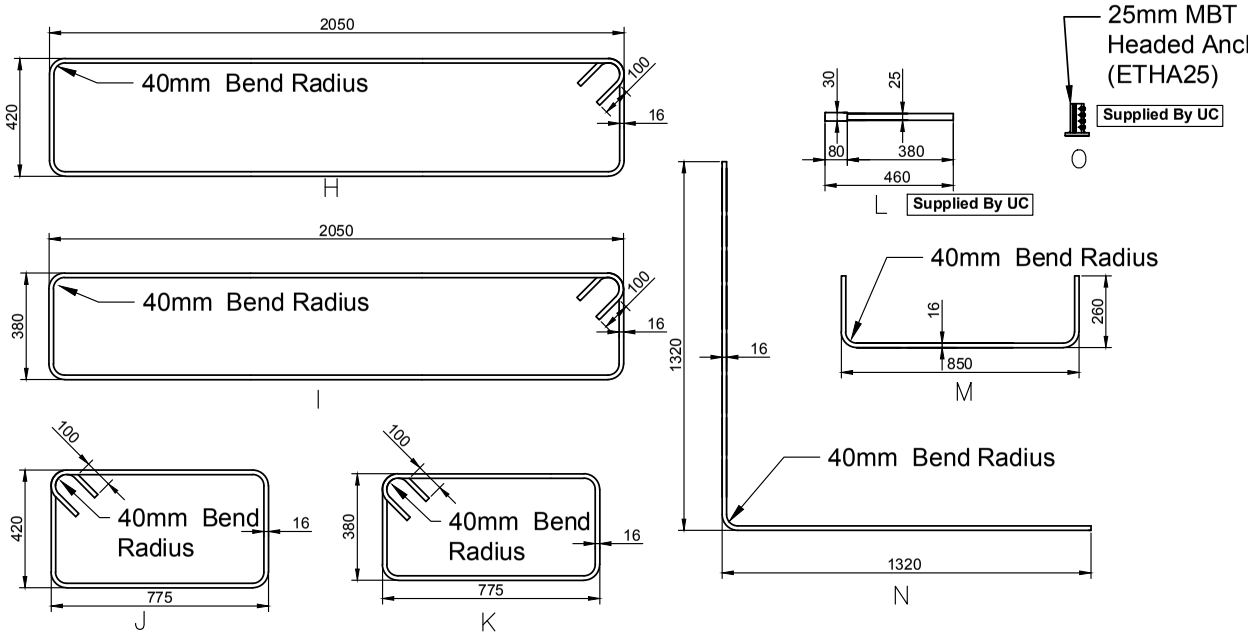

NOTES:

1- One LDS-1 column with footing is required
2- All dimensions are in mm.
3- Concrete strength (f'c) is 50 MPa.
4- Steel grade and type is specified in Sheet S-04
5- For quality control purposes, six standard concrete cylinders per specimen are to be taken while casting the elements.
6- A minimum length of 2000mm of reinforcement for all diameters shown in the table shall be added with the total amount. This will be used for testing of the bars in the lab to verify the strength.

Issue	Date	Description
1	13/05/2013	SPECIMEN LDS-1
2	10/06/2013	SPECIMEN LDS-1

Project Title

Advanced Bridge Construction and Design
(Natural Hazard Research Platform)

Drawing Name
Footing Reinforcement Summary

Engineered by : **S. White** Date : **05/2013**
Drawn by : **S. White** Date : **05/2013**

Drawing Scale

Sheet No:
S-07

Note: All armouring, headed bars, couplers and nuts will be provided by UC

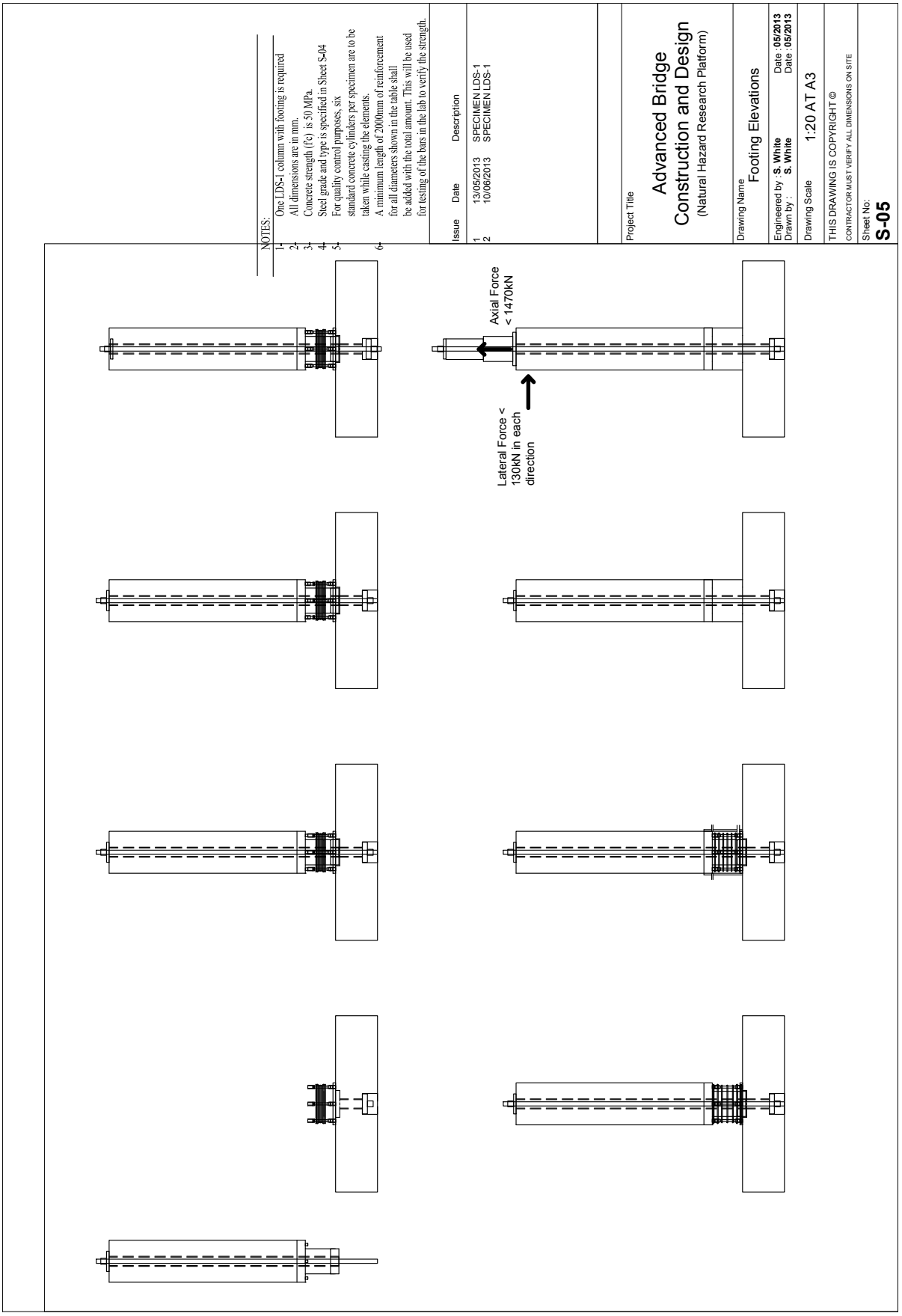
NOTES:
1- One LDS-1 column with footing is required
2- All dimensions are in mm.
3- Concrete strength (f'c) is 50 MPa.
4- Steel grade and type is specified in Sheet S-04
5- For quality control purposes, six standard concrete cylinders per specimen are to be taken while casting the elements.
6- A minimum length of 2000mm of reinforcement for all diameters shown in the table shall be added with the total amount. This will be used for testing of the bars in the lab to verify the strength.
Issue Date Description
1 13/05/2013 SPECIMEN LDS-1
2 10/06/2013 SPECIMEN LDS-1
Project Title
Advanced Bridge Construction and Design
(Natural Hazard Research Platform)
Drawing Name
Footing Elevations
Engineered by : S. White Date : 05/2013
Drawn by : S. White Date : 05/2013
Drawing Scale 1:20 AT A3
THIS DRAWING IS COPYRIGHT ©
CONTRACTOR MUST VERIFY ALL DIMENSIONS ON SITE
Sheet No:
S-05
Axial Force < 1470kN
Lateral Force < 130kN in each direction

Appendix E

Appendix E. Ancon Coupler Engagement Requirements

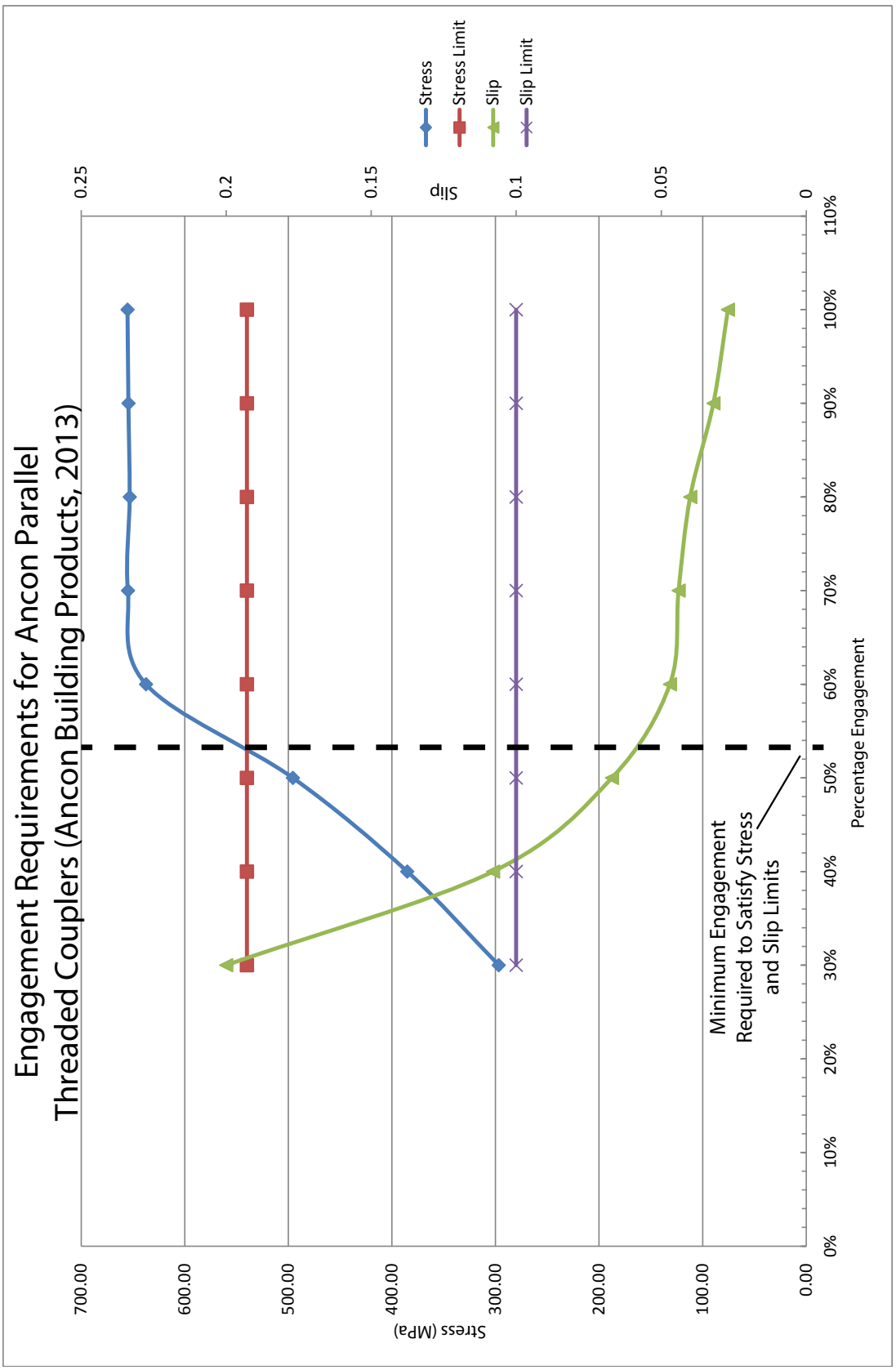
Engagement Requirements for Ancon Parallel Threaded Couplers (Ancon Building Products, 2013)
Stress
Stress Limit
Slip
Slip Limit
Slip
0.25
0.2
0.15
0.1
0.05
0
Stress (MPa)
700.00
600.00
500.00
400.00
300.00
200.00
100.00
0.00
0%
10%
20%
30%
40%
50%
60%
70%
80%
90%
100%
110%
Percentage Engagement
Minimum Engagement Required to Satisfy Stress and Slip Limits

Bibliography

ACI Innovation Task Group 1 (2001). Acceptance Criteria for Moment Frames Based on Structural Testing (T1.1-01) and Commentary (T1.1R-01).

Amaris Mesa, A. D. (2010). *Developments of Advanced Solutions for Seismic Resisting Precast Concrete Frames*. PhD thesis, University of Canterbury.

Ancon Building Products (2013). Reinforcing Bar Couplers for the Construction Industry.

Andisheh, K. (2013). Seismic Performance of Corroded Precast Reinforced Concrete Bridge Piers. *PhD Research Proposal, University of Canterbury*.

Baird, A., Palermo, A., and Pampanin, S. (2013). Controlling Seismic Response using Passive Energy Dissipating Cladding Connections. *2013 NZSEE Conference*.

Beck, J. L. and Skinner, R. I. (1974). The Seismic Response of a Reinforced Concrete Bridge Pier Designed to Step. *International Journal of Earthquake Engineering and Structural Dynamics*, 2:343–358.

Billington, S. L., Barnes, R. W., and Breen, J. E. (1999). A Precast Segmental Substructure System for Standard Bridges. *J. Precast/Prestressed Concrete Inst.*, 44(4):56–73.

Billington, S. L. and Yoon, J. K. (2004). Cyclic Response of Unbonded Posttensioned Precast Columns with Ductile Fiber-Reinforced Concrete. *Journal of Bridge Engineering*, 9(4):353–363.

Bradley, B., Cubrinovski, M., Dhakal, R., and MacRae, G. (2010). Probabilistic Seismic Performance and Loss Assessment of a Bridge-Foundation-Soil System. *Soil Dynamics and Earthquake Engineering*, 30(5):395–411.

Brenes, F., Wood, S., and Kreger, M. (2006). Anchorage Requirements for Grouted Vertical-duct Connectors in Precast Bent Cap Systems.

Buckle, I. G. (1994). The Northridge, California Earthquake of January 17, 1994: Performance of Highway Bridges.

Burkett, W. R., Nash, P. T., Bai, Y., Hays, C., and Jones, C. (2004). Rapid Bridge Replacement Techniques Research Report.

Christopoulos, C. (2004). Frequency Response of Flag-Shaped Single Degree-of-Freedom Hysteretic Systems. *Journal of Engineering Mechanics*, 130(8):894–903.

Christopoulos, C., Filiatrault, A., Uang, C., and Folz, B. (2002). Posttensioned Energy Dissipating Connections for Moment-Resisting Steel Frames. *Journal of Structural Engineering*, 128(9):1111–1120.

Christopoulos, C., Pampanin, S., and Priestley, M. J. N. (2003). Performance-Based Seismic Response of Frame Structures including Residual Deformations. Part I: Single-Degree of Freedom Systems. *Journal of Earthquake Engineering*, 7(1):97–118.

Clifton, G. (2005). *Semi-Rigid Joints for Moments Resisting Steel Framed Seismic Resisting Systems*. PhD thesis, University of Auckland.

Coffin, L. F. J. (1954). A Study of the Effects of Cyclic Thermal Stresses on a Ductile Material. *Trans., American Society of Mechanical Engineers*, 76:931–950.

Constantinou, M. C. and Symans, M. D. (1992). *Experimental and Analytical Investigation of Seismic Response of Structures with Supplemental Fluid Viscous Dampers*. National Center for Earthquake Engineering Research.

Dhakal, R. and Mander, J. (2006). Financial Risk Assessment Methodology for Natural Hazards.

Dwairi, H. M., Kowalsky, M. J., and Nau, J. M. (2007). Equivalent Damping in Support of Direct Displacement-Based Design. *Journal of Earthquake Engineering*, 11(4):512–530.

Filiatrault, A., Tremblay, R., Christopoulos, C., Folz, B., and Pettinga, D. (2013). *Elements of Earthquake Engineering and Structural Dynamics*. Presses Internationales Polytechniques.

Filiatrault, A., Tremblay, R., and Wanitkorkul, A. (2001). Performance Evaluation of Passive Damping Systems for the Seismic Retrofit of Steel Moment Resisting Frames Subjected to Near Field Ground Motions. *Earthquake Spectra*, 17(3):427–456.

Hawkins, N., Wood, S., and Stanton, J. (1994). Performance of Parking Garages in the 1994 Northridge Earthquake. *ASCE Structures Congress XIII, Boston, MA*.

Hewes, J. T. and Priestley, M. J. N. (2002). Seismic Design and Performance of Precast Concrete Segmental Bridge Columns. *State of California Department of Transportation*.

Hieber, D., Wacker, J., Eberhard, M., and Stanton, J. (2005). State-of-the-art Report on Precast Concrete Systems for Rapid Construction of Bridges. Technical report.

Housner, G. W. (1963). The behaviour of Inverted pendulum structures during earthquakes. *Bulletin of the Seismological Society of America*, 53(2):403–417.

Iwata, M. and Murai, M. (2006). Buckling-Restrained Brace Using Steel Mortar Planks; Performance Evaluation as a Hysteretic Damper. *Earthquake Engineering and Structural Dynamics*, 35(14):1807 – 1826. Buckling-restrained brace;Hysteretic characteristics;.

Kam, W. Y., Pampanin, S., Palermo, A., and Carr, A. J. (2010). Self-centering Structural Systems with Combination of Hysteretic and Viscous Energy Dissipations. *Earthquake Engineering & Structural Dynamics*.

Kawashima, K. (2000). Seismic Design and Retrofit of Bridges. *Bulletin of the New Zealand Society for Earthquake Engineering*, 33(3):265–285.

Kawashima, K., Hosoiri, K., Shoji, G., and Sakai, J.-i. (2001). Effect of Unbonding of Main Reinforcements at Plastic Hinge Region for Enhancing Ductility of Reinforced Concrete Bridge Columns. In *Proceedings - Japan Society of Civil Engineers*, pages 45–64. Dotuku Gakkai.

Kawashima, K., MacRae, G., Hoshikuma, J.-I., and Nagaya, K. (1998). Residual Displacement Response Spectrum. *Journal of Structural Engineering*, 124(5):523–530.

Kelly, J. M., Skinner, R. I., and Heine, A. J. (1972). Mechanisms of Energy Absorption in Special Devices for Use in Earthquake Resistant Structures. *Bulletin of N.Z. Society for Earthquake Engineering*, Vol. 5 No. 3:63–88.

Khaleghi, B. (2010). Washington State Department of Transportation Plan for Accelerated Bridge Construction. *Transportation Research Record: Journal of the Transportation Research Board*, 2200(-1):3–11.

Kirkcaldie, D. K. and Lloyd, J. N. (2013). Some Topics Being Addressed in NZTA Bridge Manual Revisions - Shrinkage and Creep in Concrete and Mechanical Coupling of Reinforcing Steel. *New Zealand Concrete Industry Conference 2013*.

Kurama, Y. (1997). *Seismic Analysis, Behaviour, and Design of Unbonded Post-Tensioned Precast Concrete Walls*. PhD thesis, Lehigh University.

Kurama, Y. (2004). A Friction Damper for Post-Tensioned Precast Concrete Moment Frames. *PCI*, 49(4):112–133.

Kurama, Y. C. (2000). Seismic Design of Unbonded Post-Tensioned Precast Concrete Walls with Supplemental Viscous Damping. *ACI Structural Journal*, 97(4):648–658.

Kurama, Y. C., Sause, R., Pessiki, S., and Lu, L. (1999). Lateral Load Behavior and Seismic Design of Unbonded Post-Tensioned Precast Concrete Walls. *ACI Structural Journal*, 96(4).

Lee, W. K. and Billington, S. L. (2011). Performance-Based Earthquake Engineering Assessment of a Self-Centering, Post-Tensioned Concrete Bridge System. *Earthquake Engineering & Structural Dynamics*, 40(8):887–902.

Mackie, K. and Stojadinovic, B. (2004). Residual Displacement and Post-Earthquake Capacity of Highway Bridges. In *Proceedings of the Thirteenth World Conference on Earthquake Engineering*.

Mander, J. and Cheng, C.-T. (1997). Seismic Resistance of Bridge Piers Based on Damage Avoidance Design. *Technical Report NCEER-97-0014*.

Mander, J., Dhakal, R., Mashiko, N., and Solberg, K. (2007). Incremental Dynamic Analysis Applied to Seismic Financial Risk Assessment of Bridges. *Engineering Structures*, 29(10):2662–2672.

Mander, J., Panthaki, F., and Kasalanati, A. (1994). Low-Cycle Fatigue Behaviour of Reinforcing Steel. *Journal of Materials in Civil Engineering.*, 6:453–468.

Mander, J., Priestley, M. J. N., and Park, R. (1988). Theoretical Stress-Strain Model for Confined Concrete. *Journal of Structural Engineering*, 114(8):1804–1826.

Manson, S. S. (1953). Behaviour of Materials Under Conditions of Thermal Stress. *Heat Transfer Symposium, University of Michigan Engineering Research Institute, Ann Arbor, Michigan*, pages 9–75.

Marriott, D. (2009). *The Development of High-Performance Post-Tensioned Rocking Systems for the Seismic Design of Structures*. Phd, University of Canterbury.

Marriott, D., Pampanin, S., Bull, D., and Palmero, A. (2009). A Probabilistic Seismic Loss Assessment of Advanced Post-tensioned Precast Bridge Systems. In *2009 NZSEE Conference*. New Zealand Society for Earthquake Engineering, Inc. Christchurch, New Zealand.

Marsh, M. L., Wenli, M., Garrett, B. E., Stanton, J. F., Eberhard, M. O., and Weinert, M. D. (2011). NCHRP Report 698 - Application of Accelerated Bridge Construction Connections in Moderate-to-High Seismic Regions.

Momtahan, A., Dhakal, R., and Rieder, A. (2009). Effects of Strain-Ageing on New Zealand Reinforcing Steel Bars. *Bulletin of the New Zealand Society for Earthquake Engineering*, 42(2):179–186.

Morgen, B. and Kurama, Y. (2004). A Friction Damper For Post-tensioned Precast Concrete Beam-to-column Joints. *13th World Conference on Earthquake Engineering, Vancouver, Canada*.

New Zealand Standards (2004). NZS1170 - Structural Design Actions.

New Zealand Standards (2006a). Appendix B: Special Provisions for the Seismic Design of Ductile Jointed Precast Concrete Structural Systems.

New Zealand Standards (2006b). NZS 3101 Part1: The Design of Concrete Structures.

NZ Transport Agency (2003). Bridge Manual Second Edition.

NZ Transport Agency (2008). Research Report 364 - Standard Precast Concrete Bridge Beams.

NZ Transport Agency (2010). Roads of National Significance - Economic Assessments Review.

NZ Transport Agency (2013). Bridge Manual Third Edition.

Osanai, Y., Watanabe, F., and Okamoto, S. (1996). Stress Transfer Mechanism of Socket Base Connections with Precast Concrete Columns. *ACI Structural journal*, 93(3).

Ou, Y.-C., Tsai, M.-S., Oktavianus, Y., and Chang, K.-C. (2011). Cyclic Testing of a Tall Precast Segmental Concrete Bridge Column with a Cast-In-Place Plastic Hinge Region. *Earthquake Spectra*.

Palermo, A. (2004). *The Use of Controlled Rocking In the Seismic Design of Bridges*. PhD thesis, Politecnico Di Milano.

Palermo, A. and Pampanin, S. (2008). Enhanced Seismic Performance of Hybrid Bridge Systems: Comparison with Traditional Monolithic Solutions. *Journal of Earthquake Engineering*, 12(8):1267–1295.

Palermo, A., Pampanin, S., and Calvi, G. M. (2005). Concept and Development of Hybrid Solutions for Seismic Resistant Bridge Systems. *Journal of Earthquake Engineering*, 9(6):899–921.

Palermo, A., Pampanin, S., and Marriott, D. (2007). Design, Modeling, and Experimental Response of Seismic Resistant Bridge Piers with Posttensioned Dissipating Connections. *Journal of Structural Engineering*, 133(11):1648–1661.

Pampanin, S., Christopoulos, C., and Priestley, M. J. N. (2003). Performance-Based Seismic Response of Frame Structures Including Residual Deformations. Part II: Multi-Degree of Freedom Systems. *Journal of Earthquake Engineering*, 7(1):119–147.

Pampanin, S., Marriott, D., Palermo, A., and Bolognini, D. (2010). PRESSS Design Handbook.

Podolny, W. and Muller, J. (1982). *Construction and design of prestressed concrete segmental bridges*. Wiley series of practical construction guides. Wiley.

Priestley, M. J. N. (1991). Overview of PRESSS Research Program. *PCI Journal*, 36(4):50–57.

Priestley, M. J. N. (1996). PRESSS Program - Current Status and Proposed Plans for Phase III. *PCI Journal*, 41(2):22–40.

Priestley, M. J. N., Kowalsky, M. J., and Calvi, G. M. (2007). *Displacement-Based Seismic Design of Structures*. IUSS Press, Pavia, Italy.

Priestley, M. J. N., Seible, F., and Calvi, G. (1996). *Seismic Design and Retrofit of Bridges*. A Wiley interscience publication. Wiley.

Priestley, M. J. N., Sritharan, S., Conley, J. R., and Pampanin, S. (1999). Preliminary Results and Conclusions from the PRESSS Five-Story Precast Concrete Test Building. *PCI journal*, 44(6):42–67.

Ralls, M. L., Hyzak, M. D., Medlock, R. D., and Wolf, L. M. (2004). Prefabricated Bridges - Current U.S. Practice and Issues.

Raynor, D. J., Lehman, D. E., and Stanton, J. F. (2002). Bond-Slip Response of Reinforcing Bars Grouted in Ducts. *ACI Structural Journal*, 99(5).

Restrepo, J. I., Mander, J., and Holden, T. J. (2001). New Generation of Structural Systems for Earthquake Resistance . *NZSEE 2001 Conference*.

Restrepo, J. I., Tobolski, M. J., and Matsumoto, E. E. (2011). NCHRP Report 681 - Development of a Precast Bent Cap System for Seismic Regions.

Rodgers, G. (2009). Next Generation Structural Technologies: Implementing High Force-To-Volume Energy Absorbers.

Sarti, F., Smith, T. J., Palermo, A., Pampanin, S., and Carradine, D. (2013). Experimental and Analytical Study of Replaceable Buckling-Restrained Fused-Type (BRF) Mild Steel Dissipaters. In *2013 NZSEE Conference*.

Sideris, P., Anagnostopoulou, M., Aref, A., and Filiatrault, A. (2010). Seismic Performance of Precast Segmental Bridges. In *9th US National and 10th Canadian Conference on Earthquake Engineering: Reaching Beyond Borders*, Toronto, Canada.

Solberg, K., Dhakal, R., Mander, J., and Bradley, B. (2008). Computational and Rapid Expected Annual Loss Estimation Methodologies for Structures. *Earthquake Engineering & Structural Dynamics*, 37(1):81–101.

Solberg, K., Dhakal, R., Mander, J., and Mashiko, N. (2006). Performance of a Damage Protected Highway Bridge Pier Subjected to Bi-Directional Earthquake Attack. pages 437–442.

Stanton, J. (2010). Unbonbed Pretensioned Hybrid Concept. *Presented at the PEER Annual Meeting, San Francisco, CA.*

Stanton, J., Hawkins, N., and Eberhard, M. (1992). Seismic connections for precast concrete structures. pages 4403 – 4403, Madrid, Spain.

Stanton, J., Hicks, T., and Hawkins, N. (1991). PRESSS Project 1.3 - Connection Classification and Evaluation. *PCI Journal*, 36(5):62–71.

Stanton, J., Stone, W. C., and Cheok, G. S. (1997). Hybrid Reinforced Precast Frame for Seismic Regions. *PCI*, 42(2):20–32.

Stanton, J. F., Wacker, J. M., Hieber, D. G., and Eberhard, M. O. (2005). Design of Precast Concrete Piers for Rapid Bridge Construction in Seismic Regions.

Stone, W. C., Cheok, G. S., and Stanton, J. F. (1995). Performance of Hybrid Moment-Resisting Precast Beam-Column Concrete Connections Subjected to Cyclic Loading. *ACI Structural Journal (American Concrete Institute)*, 92(2):229 – 229.

Texas DOT (2008). Accelerated Bridge Construction. *Iowa DOT ABC Workshop.*

Uma, S. R., Pampanin, S., and Christopoulos, C. (2006). A Probabalistic Framework for Performance-based Seismic Assessment of Structures Considering Residual Deformations. *First European Conference on Earthquake Engineering and Seismology, Geneva, Switzerland.*

Uma, S. R., Pampanin, S., and Christopoulos, C. (2010). Development of Probabilistic Framework for Performance-Based Seismic Assessment of Structures Considering Residual Deformations. *Journal of Earthquake Engineering*, 14:1092–1111.

U.S. Federal Highway Administration (2011). Accelerated Bridge Construction Manual.

Utah DOT (2008). Utah Department of Transportation Accelerated Bridge Construction Standards Workshop.